Modelling the long-term impact of modernized irrigation systems on soil water and salt balances, and crop water productivity in semi-arid areas under current and potential climate change conditions.

Integration of agrohydrological model, geographical information system, remote sensing, and climate change model

A thesis presented in partial fulfilment of the requirements for the degree of

Doctor of Philosophy

in

Soil Science

at

Massey University, Palmerston North,

New Zealand.

Muhammad Hamed Khan

2022

MASSEY UNIVERSITY
TE KUNENGA KI PŪREHUROA
UNIVERSITY OF NEW ZEALAND

"*On the earth are tracts adjoining one another, and vineyards, fields of corn and date-palm trees, some forked, some with single trunks, yet all irrigated by the self-same water, though We make some more excellent than the others in fruit. There are sure signs in them for those who understand*"

Al-Quran Chapter 13 (*Al-Ra'd*), verse no 4.

"*We made every living thing from water.*"

Al-Quran Chapter 21 (*Al-Anbiya*), verse no 30.

"He (God) knows whatever goes into the earth and whatsoever issues from it, whatsoever comes down from the sky, and whatsoever goes up to it. He is all-merciful, all-forgiving."

Al-Quran Chapter 34 (*Saba*), verse no 2.

"*He (God) created man from fermented clay dried tinkling hard like earthenware."*

Al-Quran Chapter 55 (*Al-Rahman*), verse no 14.

"*God produced you from the soil like a vegetable growth; He will then return you back to it, and bring you out again"*

Al-Quran Chapter 71 (*Noah*), verses from 17 to 18.

Abstract

Irrigated agriculture plays a key role in ensuring food security and rural livelihoods across semi-arid and arid regions, like in the Indus basin of Pakistan. However, the Indus basin irrigation system of Pakistan is facing serious threats of low crop yields and increasing water scarcity, waterlogging, soil salinity, and overexploitation of groundwater. Considering the irrigation water-management issues, water managers and policymakers in Pakistan are looking into the modernization of the irrigation practices by introducing sprinkler and drip irrigation systems with the intent to save water and enhance crop water productivity. However, such intervention if adopted at a larger scale could seriously affect regional soil water and salt balances, solute leaching, and recharge to groundwaters in semi-arid and arid regions. Therefore, a robust assessment of the long-term potential impacts of modernised irrigation systems, particularly under the potential climate change scenarios, is essential for improving productivity and sustainable irrigated agriculture in semi-arid and arid regions.

Field experiments are practically difficult to quantify the long-term impacts of modernised irrigation practices on soil water and salt balances and crop growths, especially under projected climate change conditions. This thesis developed a modelling framework using local field experiments, and geographical and remote sensing information, combined with a spatially distributed agrohydrological model and climate change projections to analyse the potential impacts of different irrigation application scenarios at the field and canal command scales. This methodology is applied to evaluate the potential impacts of current and proposed modernized irrigation systems on soil water and salt balances, soil salinity build-up, percolation to groundwaters, crop yield and crop water productivity of irrigated crops under long-term contemporary climate (1987-2017)

and potential climate change (2070 -2099) scenarios. The main irrigated crops of wheat, rice, and cotton were studied in the Hakra branch canal command as a case study.

The Hakra branch canal (HBC) command, located in the Indus basin irrigation system of Pakistan, covers 0.21 million ha and is characterised by the typical problems of canal water scarcity, poor groundwater quality, waterlogging and soil salinity, and less-than-optimal crop production. The information collected from local field-scale experiments during the years 2016-2017, GIS, remote-sensing techniques and global climate models are integrated to parametrise, calibrate, and validate the agrohydrological Soil-Water-Atmosphere-Plant (SWAP) model application at both field- and canal command- scales. The SWAP model simulated soil water and salt balances, percolation to groundwaters, and water- and salt-limited crop yields and crop water productivity values of main irrigated crops of wheat, rice, and cotton from field- to canal command- scales in the study area.

The modelling assessment of current irrigation practices revealed significant variation in canal water supplies and over-exploitation of groundwater, resulting in high spatial variability in soil water percolation and salt build-up in the soil at the spatial scale of the head, middle and tail reaches of the canal command. The canal water-inflow is about 19% and 42% higher at the head reaches than at the middle and tail reaches, respectively. The significant seepage from the canal network and the cultivation of high water-consuming crops such as rice are the potential cause of waterlogging at the head reaches. Whereas limited canal inflow and use of poor-quality groundwater (> 3 dS m^{-1}) appear to be potential causes of soil salinity at the tail reaches of the HBC command. The detrimental effects of limited canal inflow and the use of marginal to poor groundwater causes considerable spatial variation in simulated water and salt-limited crop yields. The simulated water and salt-limited crop water productivity values are not only different for

the different crops of wheat, rice and cotton, but also for the same crop across the study area.

The field- and canal-command scale modelling was applied to simulate and assess the potential impacts of the proposed modernized irrigation scenarios, such as

- sprinkler irrigation is defined as a high-efficiency irrigation system with leaching fraction (*HEIS_LF*) and without leaching fraction (*HEIS_noLF*), and
- precision surface irrigation system (*PSIS*) for cotton-wheat cultivation under contemporary climate (1987-2017) and potential climate change (2070-2099) scenarios RCP 2.6 (low emission) and RCP 8.5 (high emission or *business-as-usual*).

The long-term simulation results suggest a saving of about 40% in irrigation water under the *HEIS_noLF* scenario. However, this irrigation water-saving under the *HEIS_noLF* scenario resulted in the risk of an increase in soil salinity due to reduction in soil percolation and its associated salt build-up in the soil profile. Under the *HEIS_noLF* scenario for cotton-wheat cultivation, the soil salinity is simulated to increase from 2.6 to 8.0 dS m^{-1} at the field-scale, and from 2 to >12 dS m^{-1} at the canal command scale, affecting crop yields due to salt stress. The high salt build-up is simulated to reduce crop yields by 38% for cotton, and 48% for wheat under the contemporary climate (1987-2017) at the canal command scale. The soil salinity is simulated to get even worse in poor-quality groundwater areas, resulting in wheat failure of < 1 ton/ha with *HEIS_noLF* under the RCP 8.5 scenario of potential climate change (2070 -2099) conditions.

The modelling analysis suggests a significant leaching fraction is required to maintain acceptable soil salt balance for successful crop production. This leaching fraction could be achieved by a pre-sowing irrigation of 60 mm depth at the start of the season, followed

by an additional 10 mm depth with each irrigation interval using a high-efficiency irrigation application, simulated as *HEIS_LF*. The *HEIS_LF* scenario resulted in 50 to 65% higher average water- and salt-limited crop water productivity values (kg/m^3 ET) of 0.5 for cotton, and 1.87 for wheat. This is compared to the *HEIS_noLF* scenario of 0.25 for cotton, and 0.65 for wheat under potential climate change (2070 -2099) conditions. However, the *PSIS* irrigation scenario resulted in similarly favourable soil water and salt balances, water and salt-limited crop yields and crop water productivity values for the cotton - wheat cultivation. Under the *PSIS* irrigation scenario, the average water-and salt-limited crop water productivity values (kg/m^3 ET) are simulated as 0.50 for cotton and 2.79 for wheat under the contemporary climate (1987-2017), and 0.50 for cotton and 1.92 for wheat in potential climate change (2070-2099) conditions. The modelling analysis simulated the average soil percolation rate as 10 to 20% higher, resulting in the leaching of 20 to 30% more salts from the soil profile under the *PSIS* scenario than the *HEIS_LF* under potential climate change conditions.

The key findings of this modelling assessment suggest that modernisation of irrigation systems as higher-efficiency (*HEIS*) irrigation applications, with no appropriate leaching fraction, would compromise salt build-up in the soil profile. This would potentially reduce crop yields and crop water productivity in the long-term, especially under potential climate change (2070 -2099) conditions. There appears very limited scope for real irrigation water savings using a high-efficiency irrigation system for long-term sustainable crop production in areas making conjunctive use of limited canal water supplies and marginal- to poor-quality groundwaters. Hence, proposed initiatives for implementing high-efficiency irrigation systems should be carefully evaluated in terms of their long-term potential impacts on regional soil water and salt balances, crop yields

and crop water productivity values in areas such as the Indus basin irrigation system in Pakistan, particularly under potential climate-change conditions.

Keywords: High-efficiency irrigation system, Precision surface irrigation system, Soil water and salt balances, Soil Salinity, Crop water productivity, SWAP model, Climate change, Indus basin irrigation system of Pakistan.

Acknowledgements

All the praises be to ALLAH (SWT), the lord of the universes, the Most Beneficent and the Most Merciful, the entire source of knowledge and wisdom bestowed to mankind. Who gave me the courage and potential to pursue this goal and never spoils any efforts of good deeds. The blessings of ALLAH be upon his Prophet MUHAMMAD (PBUH), the city of knowledge and blessing for the entire creations, who guided us to seek knowledge from cradle to grave.

The course of a PhD study is an exciting journey with lots of ups and downs. I have been privileged to receive significant help from many people. I feel indebted and wish to express my sincere gratitude to all those who supported me and helped me directly or indirectly in the completion of this thesis.

First, I would like to express my heartfelt gratitude to my main supervisor Dr. Ranvir Singh for his excellent guidance, encouragement, support and constructive feedback throughout my PhD studies. The development of this thesis would not have been possible without his deep insights, explanations, challenging questions, discussing problems and especially correcting my English in the several drafts of thesis chapters. My discussion with him has been of great benefit to my inexperience scientific writing skills. Ranvir, I will be indebted to you for what I have learnt from you for the rest of my life. Also, I am very grateful to my co-supervisors Dr. Brent Clothier and Dr. Tonny de Vries, for their support, constructive comments, valuable suggestions and advice during the development of this thesis.

The major part of this study included field work and data collection. The practical work involved in this study would never have been possible without support from IWMI Pakistan in terms of facilities and logistics provided by their field office, Haroonabad

(study area). I sincerely thank Dr. Arif Anwar (Principal Researcher and Head, IWMI Pakistan) for his strong support, sharing of available data, access to IWMI technical resources and especially allowing me stay in the IWMI field office throughout my field experiments. I am also very thankful to the staff at IWMI field office Haroonabad, for helping me in my fieldwork. I would like to extend my deepest appreciation to Muhammad Khan, for arranging all preliminary and logistics affairs before and after my arrival at the IWMI field office Haroonabad. Dear Muhammad your readiness to help me to settle down at Haroonabad, the selection of farmer's fields for experiments and the setting up of my fieldwork in HBC command made my life very easy during the data collection process.

I would like to extend my sincere gratitude to the chairman department of Agricultural Engineering, University of Engineering and Technology, Peshawar, for providing laboratory facilities. I would like to appreciate the support of Nazia Arfeen lab engineer for analysing soil samples. I would also like to acknowledge all the support staff of the soil and water laboratory for helping me to set up the analysis apparatus. My profound gratitude to the Dr. Muhammad Javed, Director Punjab Irrigation Department, for providing groundwater data and Dr. Muhammad Riaz, Director Pakistan Metrological Department Lahore, for providing long-term climate data for my case study. My special thanks to Mr Syed Qazafi Anjum for his unconditional support and help in developing the code for modelling analysis used in the thesis.

I would like to express my sincere gratitude to all those who have funded me during my PhD studies; The Higher Education Commission (HEC) of Pakistan for funding my studies; University of Engineering and Technology Peshawar, Pakistan for granting me paid study leave for three years; Helen E Akers Doctoral scholarship and Massey

university Covid 19 Doctoral Student bursary for supporting me during Covid19 lockdown.

I am very thankful to my friends and office mates at Massey university: Ahmad Elwan, Aldrin Rivas, Ainul Mahmud, Atkinson, Gere Geretharan, Khadija Malik, Komahan, May Sasikunya, Nilusha, Stephen Collins, Themba Dumsani, Thi Nguyen, Qinhua Shen, and Yang Li for making this journey enjoyable and memorable. I am also very grateful to Sharon Wright and Fiona Bardell for helping in administrative matters.

I would like to extend my gratitude to all the members of the Massey Muslim Society and the Pakistani community in Palmerston North. Your emotional support and occasional gatherings prevented me and my family from loneliness and homesickness.

Finally, my wholehearted gratitude and thanks to my family. I am so grateful to my parents, and sisters, for their individual love, support and encouragement. I am deeply indebted to my father (Abbajee) for his encouragement and support throughout every situation in my whole life. Dear Abbajee, your support gave me the courage and strength to keep moving in situations when nothing seems to work right. I am also extremely grateful to my wife Sadaf and our beloved children Hasaan, Eshaal and Zohaan. I am quite sure that it would not have been possible to accomplish my PhD studies without their emotional support, good wishes and patience. My dears you always accompanied me and provided a source of happiness throughout the period of our common life. THANK YOU for everything.

Muhammad Hamed Khan
Palmerston North, New Zealand

Table of Contents

List of Figures

List of Tables

Glossary

List of frequently used symbols

Symbol	*Description*	*Dimension*	*SI Unit*
A	Rate of photosynthetic assimilation of CO_2	$M\ L^{-2}\ T^{-1}$	$kg\ m^{-2}\ s^{-1}$
b	Vector containing parameters to be optimised	variable	variable
$\boldsymbol{C}$	*S*olute concentration of soil water	$M\ L^{-3}$	$kg\ m^{-3}$
C	Differential Soil water capacity ($d\theta /dh$)	L^{-1}	m^{-1}
CA	Cropped Area	L^2	m^2
C_{bot}	Salt concentration in percolation	ML^{-2}	Kgm^{-2}
$\Delta\boldsymbol{C}$	Change in salt storage	$M\ L^{-2}$	$kg\ m^{-2}$
C_{air}	Specific heat capacity of moist air per unit mass	$L^{-2}\ T^{-2}\ \Theta^{-1}$	$J\ kg^{-1}\ K^{-1}$
c_{conf}	Vertical resistance of semi-confined layer	T	d
$\boldsymbol{C}$FC	Soil salinity concentration at field capacity	$M\ L^{-3}$	$kg\ m^{-3}$
D_{dif}	Diffusion coefficient	$L^2\ T^{-1}$	$m\ s^{-1}$
e_a	Actual vapour pressure	$M\ L^{-1}\ T^{-2}$	Pa
e_{sat}	Saturation vapour pressure	$M\ L^{-1}\ T^{-2}$	Pa
E	Actual soil evaporation rate	$L\ T^{-1}$	$m\ s^{-1}$
$\boldsymbol{E}$	Actual soil evaporation integrated over time	L	m

E_{emp}	Soil evaporation rate according to an empirical function	L T^{-1}	m s^{-1}
E_{max}	Maximum soil water rate according to Darcy's law	L T^{-1}	m s^{-1}
E_p	Potential soil evaporation rate	L T^{-1}	m s^{-1}
$\boldsymbol{E_p}$	Potential soil evaporation integrated over time	L	m
E_{pan}	Pan evaporation	L	m
$\boldsymbol{E_w}$	Evaporation of ponding water integrated over time	L	m
$EC_{1:5}$ m^{-1}	Electrical conductivity of one part soil mixed with five parts distilled water	-	dS
EC_{FC} m^{-1}	Soil electrical conductivity at field capacity	-	dS
EC_e m^{-1}	Electrical conductivity of the saturated soil paste	-	dS
EC_{gw} m^{-1}	Electrical conductivity of groundwater	-	dS
EC_{obs} m^{-1}	Observed soil salinity in field condition	-	dS
EC_{max} m^{-1}	Critical level of salinity tolerance for a crop	-	dS
EC_{slope} m^{-1}	Decline per unit increase in electrical conductivity beyond EC_{max}	-	% dS
ET	Actual evapotranspiration rate	L T-1	m s^{-1}
ET_p	Potential evapotranspiration rate	L T-1	m s^{-1}

$\boldsymbol{ET_{ref}}$	Reference evapotranspiration integrated over time	L	m
G	Soil heat flux density	$M\ T^{-3}$	$W\ m^{-2}$
h	Soil water pressure head	L	m
h_1	Pressure head below which roots start to extract water from the soil	L	m
h_2	Pressure head below which roots start to extract water optimally from the soil	L	m
h_{3h}	Pressure head below which roots cannot extract optimally anymore, at a high potential transpiration rate	L	m
h_{3l}	Pressure head below which roots cannot extract water optimally anymore, at a low potential transpiration rate	L	m
h_4	Pressure head below which no water uptake by roots is possible ('wilting point')	L	m
$\boldsymbol{I}$	Irrigation integrated over time	L	m
I_{max}	Maximum irrigation	L	m
I_{req}	Irrigation requirement	L	m
I_{int}	Irrigation interval	L	m
I_n	Net irrigation over time	LT^{-1}	ms^{-1}
I_g	Gross Irrigation over time	LT^{-1}	ms^{-1}
$\boldsymbol{I_{cw}}$	Canal water irrigation integrated over time	L	m
$\boldsymbol{I_{gw}}$	Groundwater irrigation integrated over time	L	m
IC_i	Salt concentration in irrigation water	ML^{-2}	kgm^{-2}
J	Solute flux density	$M\ L^{-2}\ T^{-1}$	$kg\ m^{-2}\ s^{-1}$
K	Hydraulic conductivity	$L\ T^{-1}$	$m\ s^{-1}$
$K_{1/2}$	Mean Hydraulic conductivity	$L\ T^{-1}$	$m\ s^{-1}$
k	Crop growing stage	-	-
K_{gr}	Extinction coefficient for global solar radiation	-	-
K_{sat}	Saturated hydraulic conductivity	$L\ T^{-1}$	$m\ s^{-1}$

K_y	Yield response factor	-	-
L_{dis}	Dispersion length	L	m
LAI	Leaf area index	-	-
n	Empirical shape factors in the Van-Genuchten model	-	-
P	Rainfall integrated over time	L	m
P_e	Effective rainfall	L	m
*P*i	Rainfall interception rate	$L\ T^{-1}$	$m\ s^{-1}$
PCP	Precipitation (rainfall)	L	m
q	Water flux density L T-1 m s-1		
q_{bot}	Bottom flux density (positive upward)	$L\ T^{-1}$	$m\ s^{-1}$
$\boldsymbol{Q_{bot}}$	Bottom flux from soil column integrated over time (positive upward)	L	m
$\boldsymbol{Q_{cw}}$	Canal water inflow integrated over time	L	m
$\boldsymbol{Q_{SL}}$	Seepage losses from the conveyance system	$L^3\ T^{-1}$	m^3s^{-1}
r_{air}	Aerodynamic resistance	$L^{-1}\ T$	$s\ m^{-1}$
r_{crop}	Crop resistance	$L^{-1}\ T$	$s\ m^{-1}$
R	Net groundwater recharge integrated over time	L	m
R_n	Net radiation flux density	$M\ T^{-3}$	$W\ m^{-2}$
R_s	Surface Runoff	L	m
RH	Relative Humidity	-	KPa
Slr Rad	Solar Radiation KJ/M^2/Day	-	
S_a	Actual root water extraction rate	T^{-1}	s^{-1}
S_p	Potential root water extraction	T^{-1}	s^{-1}
S_e	Relative saturation	-	-
S_{max}	Maximum root water extraction rate	T^{-1}	s^{-1}
SR	Surface runoff integrated over time	L	m
T_a	Actual transpiration rate	$L\ T^{-1}$	$m\ s^{-1}$
$\boldsymbol{T_a}$	Actual transpiration integrated over time	L	m
T_p	Potential transpiration rate	$L\ T^{-1}$	$m\ s^{-1}$
$\boldsymbol{T_p}$	Potential transpiration integrated over time	L	$m\ s^{-1}$
T_{max}	Maximum Temperature	-	^oC

T_{min}	Minimum Temperature	-	^{o}C
W	Weighting function to account for the relative influence of each data point in objective function, Φ	-	-
ΔW	Change in soil water storage integrated over time	L	m
WS	Wind Speed	LT^{-1}	ms^{-1}
Y	Actual crop yield	$M\ L^{-2}$	$kg\ m^{-2}$
Y_p	Potential crop Yield	$M\ L^{-2}$	$kg\ m^{-2}$
Y_a	Actual observed Yield	$M\ L^{-2}$	$kg\ m^{-2}$
Y_{PDM}	Potential dry matter yield	$M\ L^{-2}$	$kg\ m^{-2}$
Y_{DM}	Actual Dry mater yield	$M\ L^{-2}$	$kg\ m^{-2}$
z	Vertical coordinate (positive upward)	L	m
z_{root}	Rooting depth	L	m
t	time	T	s
ρ_{air}	Air density	$M\ L^{-3}$	$kg\ m^{-3}$
Δv	Slope of the vapour pressure curve	-	$Pa\ K^{-1}$
Φ	Objective function	-	-
φ_{aquif}	Hydraulic head in a semi-confined layer	L	m
φ_{gwl}	Groundwater level in aquifer	L	m
γ_{air}	Psychrometric constant	$L^{-1}M\ T^{-2}\ \Theta^{-1}$	$Pa\ K^{-1}$
α	Empirical parameter in the Van-Genuchten model	L^{-1}	m^{-1}
α_{rs}	Reduction coefficient for salinity stress as used in SWAP	-	-
α_{rw}	Reduction coefficient for water stress as used in SWAP	-	-
α_s	Surface albedo	-	-
ε	Actual light use efficiency of crop	$L^{-2}\ T^{2}$	$kg\ J^{-1}$

λ	Empirical parameter in the Van-Genuchten model	-	-
ρ_w	Density of water	$M\ L^{-3}$	kg m^{-3}
λ_w	Latent heat of vaporization	$L^2\ T^{-2}$	J kg^{-1}
θ	Volumetric soil water content	-	m^3 m^{-3}
θ_{res}	Residual volumetric water content	-	m^3 m^{-3}
θ_{sat}	Saturated volumetric water content	-	m^3 m^{-3}

List of abbreviations

Abbreviation	*Description*
APAR	Actual Photo synthetically Active Radiation absorbed by a plant
BS	Baku Shah Distributary
BCM	Billion Cubic Meter
CanESM2	Canadian Earth System Model second generation
Canal Command	The area under the irrigation domain of a certain canal.
CCCma	Canadian Centre for Climate Modelling and Analysis
CCA	Culturable Command Area: area suitable for agriculture with attached water rights
CGCM4	Coupled Global Climate Model fourth generation
CMIP5	Coupled Model Intercomparison Project Phase 5
CV	Coefficient of Variation
CW1	Cotton-Wheat field 1
CW2	Cotton-Wheat field 2
DGA	Directorate General Agriculture
DLR	Directorate of Land Reclamation
DM	Dry Matter
FESS	Fordwah Eastern Sadqia South
GCM	General Circulation Model
GHGs	Green House Gases
GIS	Geographical Information System
GDP	Gross Domestic Product

GoP	Government of Pakistan
HBC	Hakra Branch Canal
HEIS	High Efficiency Irrigation System
HEIS_LF	HEIS with Leaching Fraction
HEIS_noLF	HEIS with no Leaching Fraction
HKH	Himalayas Karakoram Hindukush
HR	Hakra Right distributary
HL	Hakra Left distributary
IB	Indus Basin
IBIS	Indus Basin Irrigation System
IoA	Index of Agreement
IPCC	Intergovernmental Panel on Climate Change
IWMI	International Water Management Institute
kharif	Summer crop season (April – October)
LULC	Land Use Land Cover
MBE	Mean Bias Error
MODIS	MODerate-resolution Imaging Spectro-radiometer
NCAR	National Centre for Atmospheric Research
NCEP	National Centre for Environmental Prediction
NDVI	Normalized Difference Vegetation Index
NSL	Natural Surface Level
OFWM	On-Farm Water Management
O&M	Operation and Maintenance
PAR	Photo synthetically Active Radiation
PBS	Pakistan Bureau of Statistics

PEST	Parameter ESTimation
PID	Provincial Irrigation Department
PIPIP	Punjab Irrigated agriculture Productivity Improvement Project
PMD	Pakistan Metrological Department
PMIU	Programme Monitoring and Implementation Unit
PSIS	Precision Surface Irrigation System
rabi	Winter crop season (October – April)
RCP	Representative Concentration Pathway
RD	Reduce Distance
RevIIP	Revitalizing Irrigation in Pakistan
RMSE	Root Mean Square Error
rostering	Rotation of water supply among distributary canals
RS	Remote Sensing
RW1	Rice-Wheat field 1
RW2	Rice-Wheat field 2
SAR	Sodium Adsorption Ratio
SCARP	Salinity Control and Reclamation Program
SEBS	Surface Energy Balance System
SEBAL	Surface Energy Balance Algorithm for Land
SD	Standard Deviation
SDSM	Statistical Down Scaling Model
SU	Simulation Unit
SWAP	Soil-Water-Atmosphere-Plant
TSUMEA	Temperature sum from emergence to anthesis
TSUMAM	Temperature sum from anthesis to maturity

Tubewell	A bore (tube) well for pumping groundwater
US-AID	United State Agency for International Development
Warabandi	Available canal water is spread to all farmers in proportion to their land holding
WAPDA	Water and Power Development Authority
WOFOST	WOrld FOod STudies
WMRI	Water Management Response Indicators
WP	Water Productivity
WUA	Water User Association

Chapter 1 : Introduction

1.1 Background

Water is the cornerstone of sustainable development, providing a range of ecosystem services, reducing poverty, supporting economic growth, and maintaining freshwater ecosystems and their benefits for humans and nature (Connor, 2015). From food security to environmental health, water contributes to improved social well-being and affects the livelihoods of billions. Increasing population, economic growth, and climate change put enormous pressure on the world's limited water resources. According to the 2018 edition of the United Nations World Water Development Report, the world population will reach between 9.4 and 10.2 billion by 2050 (Boretti and Rosa, 2019). This will increase demand for water, food and will cause expansion in agricultural land use, which will have a significant impact on the use of world freshwater resources (Thornton and Herrero, 2010). According to Meier *et al.* (2018), about 367 million hectares of agricultural land are irrigated worldwide, seven times more than at the beginning of the 20th century.

Irrigation is an essential contributor to global food security. Most of the expansion of irrigated land has occurred in Asia, where population growth and the demand in water for food production are highest and per capita water availability is relatively lower (Figure 1.1).

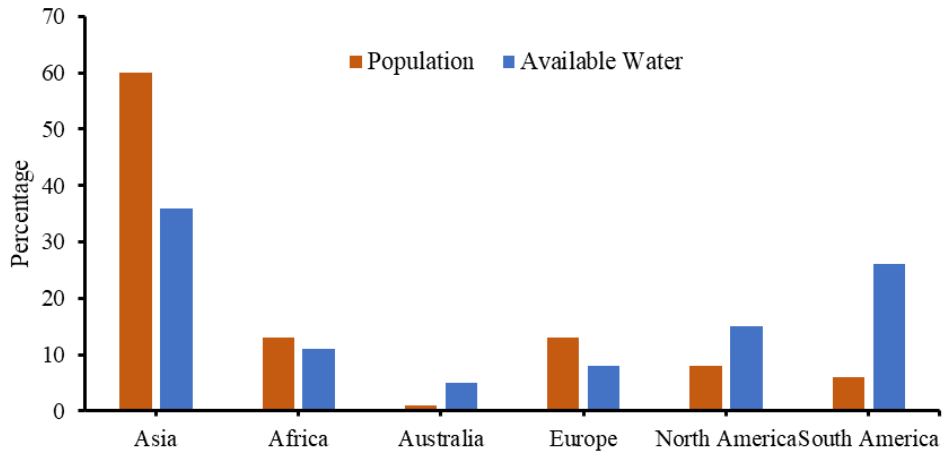

Figure 1.1: Continent wise water availability versus population (Water, 2003).

Agriculture is the largest consumer of the world's water, with up to 70% being used in irrigation (Figure 1.2) (Water, 2003) . The productivity of irrigated land is about three times greater than that of rain-fed land (Connor *et al.*, 2012). Irrigated land produces more than 40% of the world's food and consumes approximately 60 to 80% of the world's freshwater supplies (Connor *et al.*, 2008). However, according to de Loë *et al.* (2008), the global water withdrawal for irrigation is estimated at 2,000 and 2,500 km^3 per year, and on average, only 40% of this water contributes directly to crop production and the rest is lost to evaporation, seepage from conveyance structures, deep percolated, or used by unwanted vegetation.

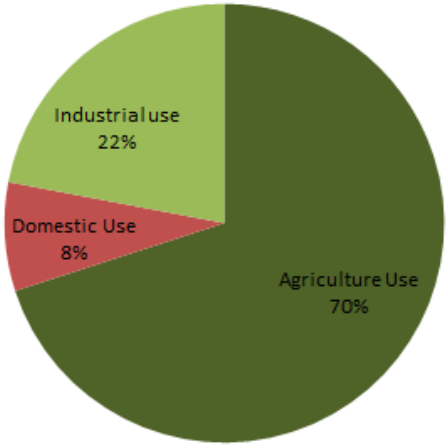

Figure 1.2: World water use by different sectors (Water, 2003).

In many parts of the world, a poor understanding of the physical environment, climatic conditions, and inefficient irrigation practices have been resulting in problems of soil salinisation, waterlogging, degraded soil fertility, reduced surface-water availability, declines in groundwater levels and reduced water quality (Dougherty and Hall, 1995; Rosegrant *et al.*, 2002). Poor drainage and obsolete irrigation practices have caused waterlogging and salinity in about 10% of the world's irrigated land (Connor, 2015). In many regions around the world the groundwater is poorly managed and monitored, most

of the major aquifers in the semi-arid and arid zone are experiencing rapid rates of groundwater decline (Konikow and Kendy, 2005; Wada *et al.*, 2010). The groundwater is being pumped at much greater rates than it can be replenished naturally (Gleeson *et al.*, 2012). Moreover, with the increase in competition for water between industrial, urban, and environmental use, the irrigated agriculture is faced with sever water scarcity particularly in semi-arid and arid regions.

The demand for scarce freshwater supplies is rapidly growing worldwide, but the supplies are not assured. The responses to global water scarcity, specifically in semi-arid to arid regions, are in the form of policy initiatives at the technical, managerial and institutional level to mitigate the impact of water scarcity on irrigated agriculture (Peter, 2004). One technical approach used in the past had focused on developing new infrastructures such as dams for the water storage and expansion of the irrigated area to alleviate water scarcity and ensure food security (Lenzen *et al.*, 2013). However, the development of such colossal irrigation infrastructure projects has been criticised due to growing concerns over environmental degradation (McCartney *et al.*, 2001). Moreover, extension policies have proven inefficient as the demand for water continues to increase (Konar *et al.*, 2012). A managerial level improvement includes switching from supply-based to demand-based irrigation management. Demand management aims to reduce irrigation requirements, leading to water conservation and savings in irrigation (Dziegielewski, 2003; Brooks, 2006). Improvement at the institutional level includes introducing participatory irrigation management by establishing water user associations and farmer organisations, allowing a multi-stakeholder platform for policy making and implementation (Reddy and Reddy, 2005; Uysal and Atış, 2010). The objective of participatory irrigation management is decentralisation and devolution of power to lower levels. There is a consensus that a better understanding and efficient management of

water resources is required to support the needs of the growing population, without degrading the natural environment that sustains the water resources (Pereira *et al.*, 2002; Dziegielewski, 2003; Iglesias *et al.*, 2007; Msangi, 2014; Mancosu *et al.*, 2015). Improvement in irrigation water-use efficiency is considered an effective measure to increase crop water productivity and is a global priority for food production and food security (Esteve *et al.*, 2008). Technical measure includes adopting high-efficiency advanced irrigation systems such as sprinkler, drip irrigation and precision irrigation through computer-control systems. These advanced irrigation technologies are promoted as an effective solution to the prevailing water crises (Bank, 2006; Ward and Darghouth, 2006b; Zhongming *et al.*, 2009; Molden, 2013).

Pakistan is one of the countries that could face severe food and water crises in the near future. Limited water resources and continued population growth have put tremendous pressure on the country's economy. According to the 2017 census, the population of Pakistan is recorded at 208 million, with an annual growth rate of 2.4% (PBS, 2017) (Figure 1.3). With a continuous rise in population, the competition for water by domestic, industrial, and non-agriculture users is also increasing.

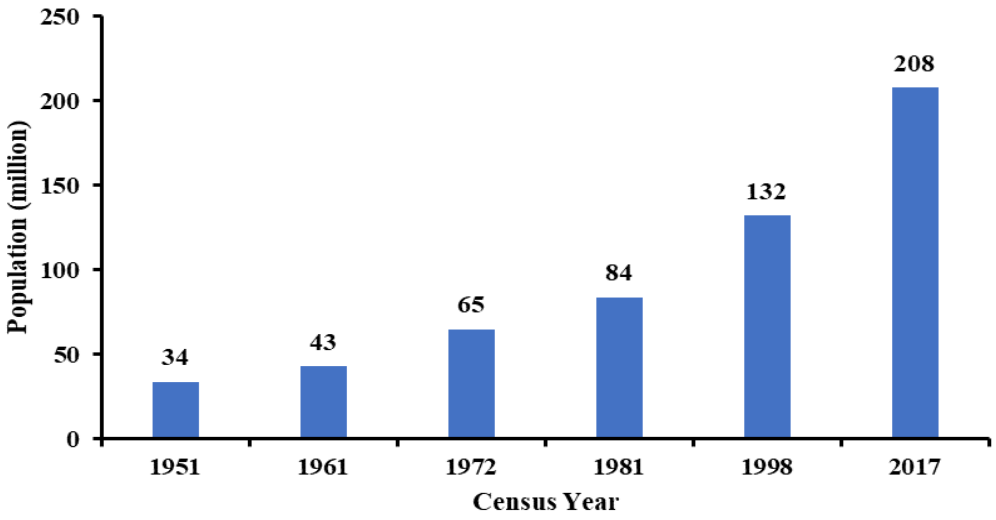

Figure 1.3: Population growth in Pakistan (PBS, 2017).

With the reduction in water storage capacity due to sediment load and the non-availability of additional storage structures, the water availability in Pakistan would reach <1000 m^3 per capita per year by 2035 (Figure 1.4). This is the value below which water availability becomes scarce affecting rural livelihoods, food production, and other economic activities, and environmental health (Rijsberman, 2006). Moreover, agriculture in Pakistan is also threatened by several other factors like soil salinity, waterlogging due to lack of drainage systems, obsolete and inefficient irrigation management systems. Therefore, a multi-dimensional and pragmatic approach is needed to ensure the long-term sustainability of the agriculture production systems.

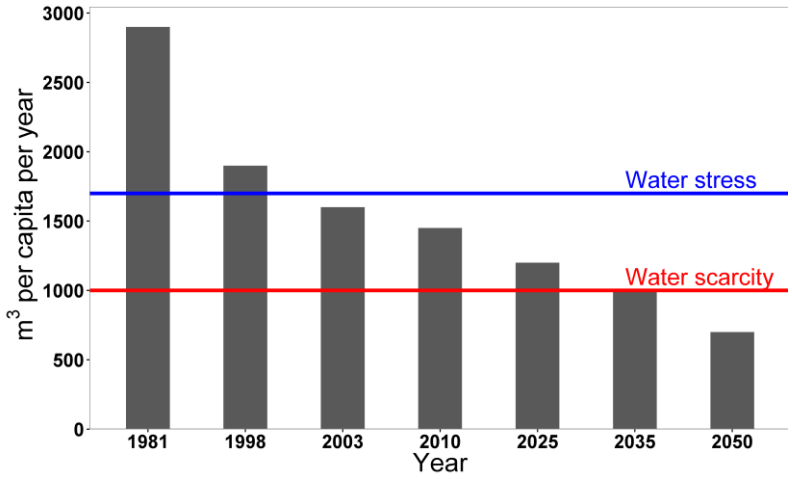

Figure 1.4: Declining per-capita water availability in Pakistan (Briscoe and Qamar, 2008).

Irrigated agriculture in Pakistan is a significant economic contributor, and accounts for 20% of the gross domestic product (GDP), and about 40% of the country's labour force are engaged in the agriculture sector (Briscoe and Qamar, 2008). About 70% of Pakistan's foreign exchange is earned through the export of raw, processed and semi-processed commodities (Raza *et al.*, 2012b). Irrigated agriculture in Pakistan, nationally and specifically in rural areas, is a significant source of income and a major component in poverty alleviation (Bhutto and Bazmi, 2007).

The backbone of irrigated agriculture in Pakistan is the Indus basin Irrigation System (IBIS), which comprises vast networks of canals and associated irrigation systems that tap into the river Indus and its tributaries (Laghari *et al.*, 2012). About 80% of the country's cultivated area are irrigated through IBIS, which provides 90% of the country's food and fibre requirements (Bhatti *et al.*, 2009). Despite its importance, the productivity in the agriculture sector is low and gradually declining (Ringler and Anwar, 2013). Irrigated agriculture in Pakistan suffers from low crop yield, depleting soil fertility through salinisation and waterlogging, plus water scarcity and poor quality of groundwater in many parts. For instance, the average wheat yield in the Indus basin of Pakistan is 2.25 ton ha^{-1}, which is 47% low than the Indian side of the Indus basin (Cai *et al.*, 2010). The primary reason for the low crop yields can be attributed to water and salt stress, mainly caused by the limited availability of good quality surface water supplies (Sharma *et al.*, 2013). The increase in irrigated areas and the unrestricted use of poor-quality groundwater affects crop growth and yields. About 70% of the tubewells of the Indus basin pump sodic or saline-sodic water, which results in about 4.5 million hectares (Mha) of land across the basin being affected by secondary salinisation (Aslam *et al.*, 2006). Another environmental problem that affects crop production and land degradation is waterlogging. According to Qureshi (2011), about 30% of the irrigated area in IBIS is potentially waterlogged due to the water table being less than 3 m from the ground surface. The overall canal network efficiency of the IBIS is estimated about 48% (Hussain *et al.*, 2011), suggesting a huge amount of water lost as non-beneficial evaporation and mainly as seepage, resulting in the rising of the water table (Qureshi *et al.*, 2010). The IBIS of Pakistan has undergone through several interventions for the improvement of irrigation efficiency and sustainability of the irrigated agriculture. For instance, in the 1960s, the Salinity Control and Reclamation Program (SCARP) was

started to control waterlogging and salinity problems in the irrigated areas of IBIS by installation of tubewells for vertical drainage, in addition to subsurface (tile) and surface drains to maintain water table below the root zone (Awan and Latif, 1982; Bhatti, 1987). This also encouraged groundwater use for irrigation using public tubewells, which was soon followed by a boom of private tubewells used by farmers (Bhutta and Smedema, 2007). The number of private tubewells has increased from 0.2 million to 1.2 million over the past five decades (1970 to 2018) (Qureshi and Ashraf, 2019). Though groundwater played a vital role in improving the overall cropping intensity in Pakistan, from about 63% in 1947 to >120% in 2018 (Khan *et al.*, 2016). However, the freely accessible and injudicious groundwater use has resulted in the depletion of groundwater resources, increase in soil salinization, and affect the water and salt balances (Bhutta and Smedema, 2007; Qureshi *et al.*, 2008; Latif and Ahmad, 2009; Bhatti *et al.*, 2017). This indicates that the research conducted for the project implementation was based on limited information and was not tested for their long-term consequences on soil water and salt balances in the project areas.

The Punjab province is considered as the breadbasket of Pakistan. To cope with low crop productivity and low irrigation efficiency, recently, a large-scale project, namely the "Punjab Irrigated agriculture Productivity Improvement Project" (PIPIP), has been initiated (DGA, 2011). According to the project's objectives, the problems of water scarcity and low water productivity can be addressed through the adoption of modernised irrigation, which is referred to in the PIPIP as a High-Efficiency Irrigation System (*HEIS*) (DGA, 2011). The concept of *HEIS* could be applied to all forms of irrigation system that apply water on the surface, or in the root zone, according to crop water requirements, but it is generally associated with a well-managed drip or sprinkler irrigation system. These modern irrigation systems are often considered as a solution to water scarcity and other

problems discussed earlier. The assertion is that this will improve irrigation water use efficiency, save water, and helps to increase crops yield and sustain food production (Kooij *et al.*, 2013).

The component A1 of PIPIP aims to promote the installation of sprinkler and drip irrigation systems throughout the Punjab province (DGA, 2011), in response to the current issues of water scarcity in irrigated agriculture. However, there is lack of knowledge and quantification of the long-term potential impacts of *HEIS* on regional soil water and salt balances, crop yields and crop water productivity particularly in semi-arid regions of Punjab Pakistan. Proposed improvements in irrigation systems could significantly affect soil percolation and soil salinity under current and future climatic conditions. Therefore, a comprehensive understanding of the long-term potential effects of adopting high efficiency irrigation systems on regional soil water and salt balances, crop yields and crop water productivity under current and projected future climatic conditions is essential for the effective management and sustainability of irrigated agriculture in IBIS.

1.2 Rationale of the study

Limited canal water supply and declining groundwater levels are raising concerns of water scarcity to increase productivity and sustainability of irrigated agriculture in Punjab Pakistan (Peña-Arancibia *et al.*, 2021; Kirby and Ahmad, 2022). In response to the current issues of water scarcity and low irrigation efficiency in Pakistan, significant efforts and resources are aimed at modernising irrigation systems such as adopting sprinkler and drip irrigation to improve irrigation efficiency and save water (DGA, 2011). Conventional gravity-flow surface irrigation systems generally have low irrigation efficiency due to several problems such as seepage losses, percolation and fixed irrigation

scheduling, irrespective of crop water requirement. However, surface-irrigation efficiency could be improved by adopting a well-designed, well-managed system and appropriate irrigation scheduling (Anwar *et al.*, 2016). Several studies have compared surface irrigation and modernized sprinkler and drip irrigation systems (Shrivastava *et al.*, 1994; Hassanli *et al.*, 2010; Raza *et al.*, 2020; Babiker *et al.*, 2021). These studies suggest that the modernization of irrigation systems can result in water-saving in irrigation application and improvement of crop water productivity at the field-scale. However, the modernisation of irrigation system could lead to unintended consequences in terms of reduction of groundwater recharge and risks of salt build-up in soil profiles, particularly in the semi-arid and arid-irrigated regions (Raeisi *et al.*, 2019). The potential long-term effects of modern irrigation systems on soil water and salt balances, including crop water productivity, soil salinity, and groundwater recharge, are poorly understood. In a recent review, Perry et al. (2017) found that "there are rather few examples of carefully documented impacts of hi-tech irrigation, while there are many examples of projects and programmes that assume that water will be saved, and productivity increased." For instance, in the Murry-Darling River systems of the irrigated area of Australia, the spatially variable soil salt build-up due to modernizing irrigation through drip and trickle systems has affected around 10% of the irrigated area (Raine et al, 2005). The changes in irrigation practices can considerably impact the soil water and salt balances, and their relationship with crop productivity and local groundwater recharges (Dench and Morgan, 2021). Therefore, programmes focused on improving irrigation efficiency must be evaluated in terms of robust accounting of water flows at the basin-scale, and long-term effects on soil water and salt balances, and crop water productivity, particularly in semi-arid and arid regions (Grafton et al., 2018; Kooij et al., 2013; Perry and Hellegers, 2012). There is currently very limited information available on long-term

potential impacts of high-efficiency irrigation methods on regional soil water balances, soil salinity, and crop water productivity in semi-arid regions of Punjab Pakistan.

Traditionally, field and laboratory experiments are conducted to evaluate and quantify potential effects of different irrigation methods on soil water and salt balance components and crop water productivity (Singh *et al.*, 2006c; Vazifedoust *et al.*, 2008). These studies are essential for understanding the soil-water flow and salt-transport process and detailed crop growth at the field scale. However, field studies are practically limited as time-consuming, laborious and expensive to quantify spatial variability in soil water and salt balance components at a regional scale. It is difficult to extrapolate field-scale assessments at the regional scale due to spatial heterogeneity of climate, surface water, groundwater, soil properties and other agronomic practices at regional scale.

In the past, tools were not available to make a detailed long-term analysis of the irrigation system, especially at the regional scale. However, increased understanding of the soil-water-crop-climate relationships and subsequent development of physical-based agro-hydrological models and global-climate models offers new opportunities for simulation of soil water and salt balance components and crop water productivity at a regional scale, under current and projected climate-change scenarios (Silberstein, 2006; Sood and Smakhtin, 2015; Kour *et al.*, 2016). The simulation models such as Soil-Water-Atmosphere-Plant (SWAP) (van Dam *et al.*, 1997) are effective tools for quantification of complex soil-water-crop-climate interactions in irrigation systems (Singh *et al.*, 2006c; van Dam *et al.*, 2006; Vazifedoust, 2007; Devia *et al.*, 2015). In addition to assessing soil water and salt balance components, simulation models can also help to simulate crop growth in response to varying water and salt stress conditions (Spitters *et al.*, 1989; Supit, 1994; Steduto *et al.*, 2009). Hence models can be used for different scenario analysis to efficiently answer the many "*what if*" questions (Santoso, 2003).

In recent decades, several studies have reported the use of simulation models at the field scale, as well as at regional scale, for quantification of crop water productivity, groundwater recharge, deficit irrigation, drought assessment, and for suggesting alternatives for improvements in irrigated agriculture (D'Urso *et al.*, 1999; Ahmad, 2002; Droogers and Bastiaanssen, 2002; Brisson *et al.*, 2003b; Singh, 2005; Ines *et al.*, 2006; Bastiaanssen *et al.*, 2007; Vazifedoust, 2007; Combalicer *et al.*, 2008; Vazifedoust *et al.*, 2008). However, there has been limited research on the long-term effect of the modernisation of irrigation systems on regional soil water and salt balances, soil salinity, and crop water productivity, particularly under future climate–change scenarios in semi-arid regions. Little is known about potential impacts of project climate change on groundwater recharge, salt build-up and crop water productivity due to adopting modernized high efficiency irrigation systems in semi-arid regions such as Punjab Pakistan. Hence, there is a need to further research and integrate the field experiments with operational knowledge related to crop growth, soil water flow, and salt-transport models and global climatic change projection models. This integration aims to assess potential long-term impacts of modernisation of irrigation methods on soil water and salt balances, soil salinity, and crop water productivity under current and future climate scenarios at field- and canal command- scales.

1.3 Research objectives

The primary research objective of this thesis is to investigate long-term potential impacts of modernized irrigation system on soil water and salt balances, soil salinity, and crop water productivity in semi-arid regions of Punjab Pakistan under current and project climate change scenarios. This thesis focuses on the Hakra Branch Canal (HBC) command that covers in Punjab Pakistan.

The specific research objectives are as follows:

- Calibrate and validate physically based agro-hydrological model Soil-Water-Atmosphere-Plant (SWAP) at field scale using local farmers fields observations in the study area.
- Quantify the long-term potential impacts of modernized irrigation scenarios on soil water and salt balances, soil salinity, and crop water productivity of main crops (wheat-cotton) cultivation at field scale.
- Develop a distributed SWAP model application for quantification of spatially variability in soil water and salt balance components, groundwater recharge, soil salinity, and crop water productivity at canal command scale.
- Integrate projected climatic change scenarios into distributed SWAP modelling and analyse the long-term potential impacts of modernized irrigation scenarios on soil water and salt balances, soil salinity, and crop water productivity of main crops (wheat-cotton) cultivation at canal command scale under current and projected climate change conditions.

1.4 Thesis outline

This thesis comprises eight chapters. The research chapters were formatted as manuscripts for submission to peer-reviewed journals. Therefore, there will be some repetition in the introduction sections, the study area descriptions, and the modelling methodology across the chapters. A brief description of each chapter is provided below:

This Chapter 1 presents an introduction to the entire thesis. It provides the general background, the rationale of this research, and the primary and specific research objectives of this thesis.

Chapter 2 provides a literature review of the Indus Basin Irrigation System (IBIS). An overview is given of the significant challenges in the irrigation system of Pakistan and remedial measures adopted to cope with the problems related to irrigated agriculture. This chapter also reviews the concept of irrigation efficiency, salinity in irrigated agriculture, and soil water and salt balances in semi-arid regions. It focuses on a review of potential impacts of modernisation of irrigation systems on soil water and salt balances, soil salinity, and crop production in semi-arid regions. The chapter identifies and highlights knowledge gaps and informs the need of advance research on the study topic.

Chapter 3 is composed of three sections. In the first section, a detail description of the climate, soil, crop and irrigation of the case study Hakra Branch Canal (HBC) command is discussed. An overview is also provided of the selected farmer's fields for local field observations. The second section briefly introduced soil water flow, salt transport and crop growth process in the Soil-Water-Atmosphere-Plant (SWAP) agro-hydrological model. In the third section, a detail overview is given of the data requirement and its collection at the selected farmer's fields and the canal command scale.

Chapter 4 presents methodology and performance of calibration and validation of SWAP at the local farmer's fields at HBC during the study period 2016-2017. The soil hydraulic parameter estimation through inverse modelling technique is briefly discussed. The calibrated and validated soil water and salt balance components are used to quantify and assess various indicators of irrigation water management effects on soil water and salt balances, and crop water productivity values. The variation of crop water productivity of main crops (cotton, rice, and wheat) is also simulated and analysed at the field scale.

Using the calibrated and validated SWAP model (in Chapter 4), Chapter 5 provides an assessment of the current and *two* modernized irrigation scenarios (i.e. precision surface irrigation system '*PSIS*', and high-efficiency irrigation system '*HEIS*' with or without leaching fractions, referred as '*HEIS_LF*' and '*HEIS_noLF*', respectively) and their long-term potential impacts on the soil water and salt balances, soil salinity, and crop water productivity at the field scale. The current and modern irrigation scenarios are evaluated and assessed in terms of percolation, salt build-up and crop water productivity indicators. The simulation results are analysed and discussed in term of improving productivity and sustainability of irrigation practices for main crops wheat-cotton cultivation at the field scale.

Chapter 6 presents development and application of the distributed SWAP modelling for quantification of spatial variability in soil water and salt balance components, soil salinity, and crop water productivity at the HBC command scale for the agriculture year 2016-2017. The distributed SWAP model is run for all combinations of soil-water-crop-climate in HBC. The aggregation of these combinations and parametrisation of distributed SWAP modelling, using field experiments, land use satellite images and existing geographical information are discussed in detail. The accuracy of the spatial aggregation of input parameters is evaluated by comparing the actual evapotranspiration simulated by the distributed SWAP model with an independent remote-sensing based evapotranspiration data at various spatial and temporal scales. The simulated soil water and salt balance components, crop yield and crop water productivity of the main irrigated crops are analysed at the HBC command scale.

Chapter 7 deals with implementing the distributed SWAP modelling with project climate data for the HBC command. The projected climate data is downscaled through Statistical Down Scaling Model (SDSM) from the CanESM2 GCM model. The analysis of this

chapter addresses the question of whether the adoption of modernised irrigation scenarios can be sustainable for optimum soil water and salt balances and crop water productivity under projected climatic change conditions for the HBC command area.

Chapter 8 summarizes the thesis's key findings and discusses the potential implication of modernisation of irrigation practices on field- and command-scale's soil water and salt balances, soil salinity, and crop water productivity under current and projected climate change conditions in semi-arid regions like HBC. It also provides recommendations for improved irrigation management at the canal command scale and the need for further research to gain greater insight for more effective and specific irrigation management at the field as well as canal command scale in semi-arid regions.

Chapter 2 : Literature Review

2.1 Indus basin

The Indus basin is spread over an area of 1,137,819 km^2 and exists in Pakistan, India, China and Afghanistan (Figure 2.1). The drainage area in Pakistan is 603,044 km^2, which is 53% of the basin area and 85% of the country's total area. The drainage area in India is 3,86,858 km^2 that accounts for 34% of the basin area and 9.8% of the total area of the country (Laghari *et al.*, 2012), Whereas the remaining 13% of the basin lies in China and Afghanistan. This is also called the "Third Pole" as it contains the most significant magnitude of ice cover outside the polar region (Sadoff and Grey, 2002; Archer *et al.*, 2010). The major tributary of the Indus basin is the river Indus which is recharged from the snow melts in the north of the Himalayas mountains (Figure 2.1). Other tributaries of the Indus basin are Sutlej, Ravi, Bias, Chenab and Jhelum, which also originate from the Himalaya-Karakorum-Hindu Kush region. The flooding in the Indus rivers and tributaries brings down rich sediments making this land very fertile. The fertility and the presence of abundant water in this valley caused the creation of the Indus civilization (Mahadevan, 2006). After the Indus Civilization, when this region became under Mughal Empire, the first network of canals was built in the basin. These were ephemeral channels (inundated during high river flows and remain dry when flows were low) (Gilmartin, 1994). Also, there were a few perennial canals, but they only carried water to gardens in imperial forts (Michel, 1967).

The actual development in the Indus basin was initiated in 1849 when the Indian sub-continent came under British Empire. In this period, many canals, weirs, and headworks were constructed across the rivers in the Indus basin (Michel, 1967; Gilmartin, 1994). With the vast infrastructure, thousands of acres of barren land came under cultivation in Punjab and Sindh, as shown in table 2.1.

Table 2.1: Development of irrigated area (in millions of hectares) in the Indus Basin (Gilmartin, 1994; FAO, 2011).

	1880	1918	1940	1947	2009
Punjab	0.58	3.62	5.6	6.31	12.0
Sindh	0.40	1.26	1.80	2.30	5.0

The total irrigated area of the Indus basin is 2,28,694 km^2 (21% of basin area), of which about 60.9% is located in Pakistan, 37.2% in India, 1.9% in Afghanistan and 0% in China because of the rough mountainous character of this part of the basin (Laghari *et al.*, 2012). According to CIESIN (2005), the total population in the Indus basin is 237 million, out of which 61% is in Pakistan, 35% in India and 4% in Afghanistan. Thus, water demands are highest for Pakistan, followed by India.

The amount of water withdrawal by Pakistan is 180 $km^{3,}$ out of which 128 km^3 (71%) is used as surface water and 52 km^3 (29%) as groundwater (Briscoe and Qamar, 2008). The amount of water withdrawals in India is 98 km^3 of which 96% is used for irrigated agriculture (Gupta and Deshpande, 2004; Amarasinghe *et al.*, 2009). The geography and the climate of the Indus basin ranging from alpine mountainous region in the north to flat deserted costal region in the south. Based on this diversity the basin can be divided in to three geographical and climatic regions such as upper, middle and lower Indus basin. The upper Indus basin consists of Himalayan and Karakorum mountainous regions having highest mountains and large volume of snow cap after polar regions. It receives a mean annual rainfall of more than 1000 mm and comes under humid climatic zone. The middle Indus basin consists of flat topography with mean annual rainfall ranges from 800 mm in the northern part to 300 mm in the southern part and exhibit sub humid to semi-arid climate with the mean annual temperature ranges from 29 to 33 ^oC. The mean annual rainfall in the lower Indus basin is less than 200 mm and is therefore comes under arid

climate zone. This indicates significant difference in the climatic patterns in upper, middle and lower part of the Indus basin. The potential evapotranspiration in the middle and lower Indus basin ranges from 2 to 6 mm/day (Waqas *et al.*, 2020), this demonstrates the need of supplemental irrigation for successful crop production.

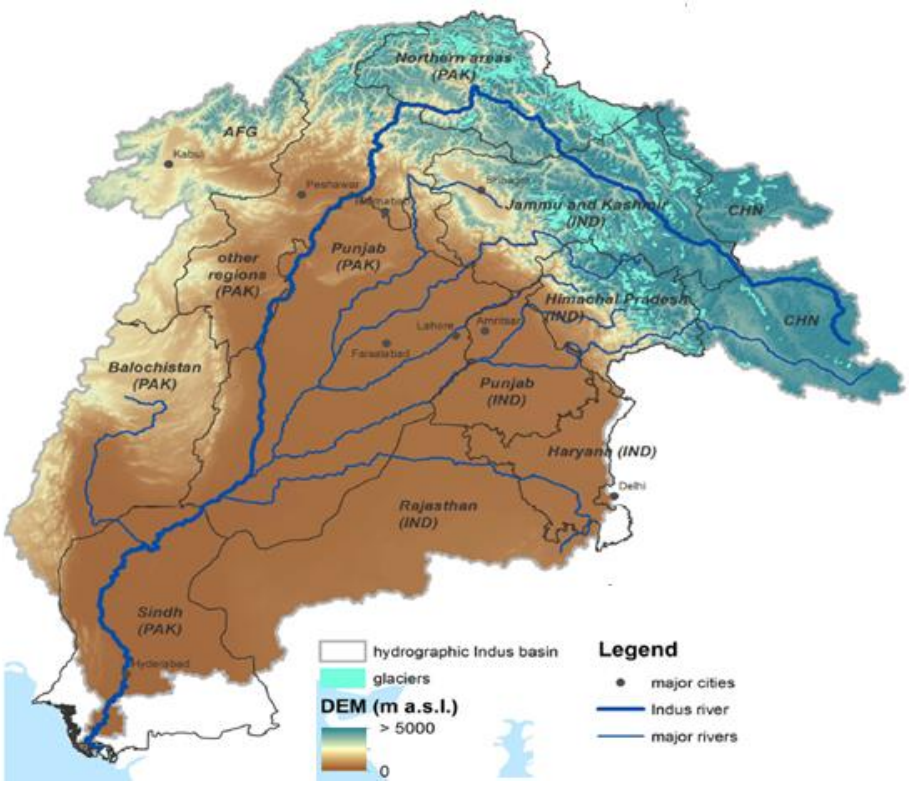

Figure 2.1: Boundaries of the Indus Basin (Country code according to UN: AFG=Afghanistan, CHN=China, IND=India, PAK=Pakistan) Laghari et al. (2012).

2.1.1 Indus Basin Irrigation System of Pakistan

Pakistan is located in South Asia and is bounded by India in the east, Iran and Afghanistan in the west, China in the north and the Arabian Sea in the south (Figure 2.2). The country lies between 22.5º and 35º north and 60º and 75º east, covering a total area of 796,096 km^2. Pakistan is divided into four provinces Baluchistan, Khyber Pakhtunkhwa, Punjab, and Sind, and federally administrated tribal areas in the west and north of the country (Figure 2.2). The topography of Pakistan is blessed with diverse features ranging from

the world's second highest peaks (K 2) in the north to the coastal plains in the south. This makes the climate of the country vary from temperate sub-humid in mountainous alpine highland in the north to the subtropical arid and semi-arid in the south (Hewitt, 2011). Alpine climatic conditions are experienced in the north due to mountainous ranges and are characterised by lengthy, cold and snowy winters with very short and mild summer (Archer, 2003). The climate of the centre of the country experiences hot and dry summer with temperature exceeding 45^{o}C and varies from north to south. The coastal strip in the southern part of the country experiences a coastal climate with the sea breeze blowing all year round, maintaining a moderate temperature (Mahar and Zaigham, 2010).

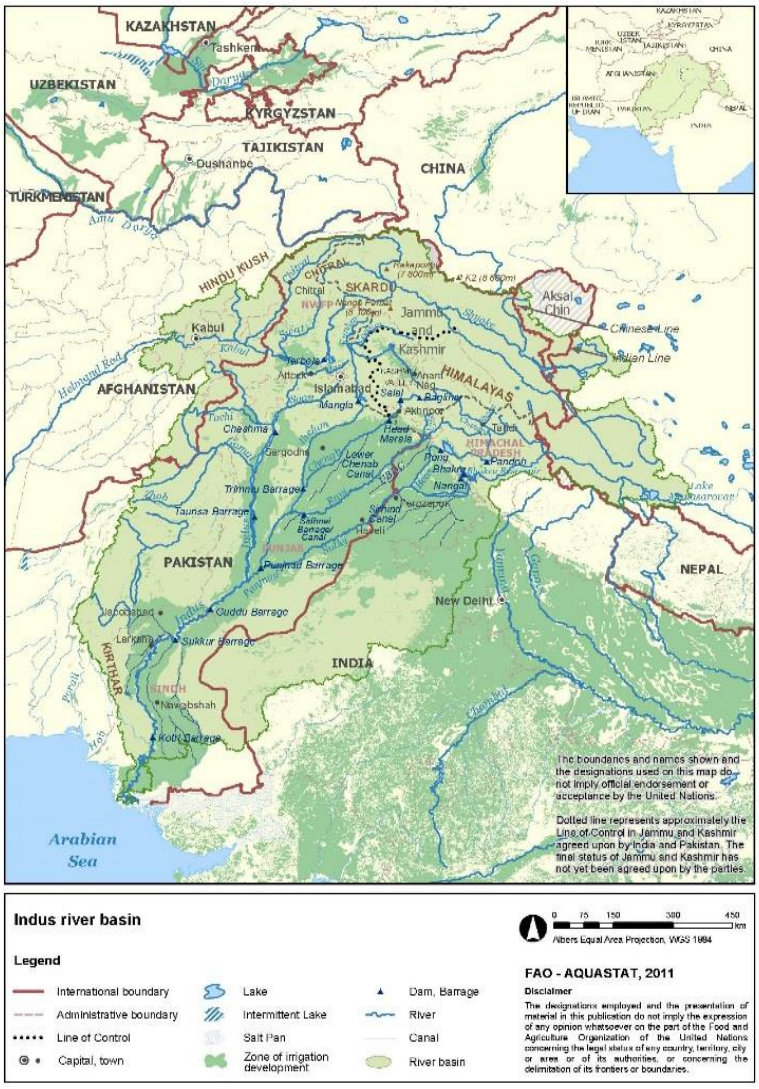

Figure 2.2: Location of Pakistan, Indus basin and its tributaries (FAO, 2011).

The economy of Pakistan is agriculture based and contribute 21% to the Gross Domestic Production (GDP) of the country (Farooq, 2013). About 45% of the labour force is employed in the agricultural sector, which supports 75% of the population and accounts for more than 60% of foreign exchange earnings (Qureshi, 2011). Irrigation is used on all the arable land of Pakistan and produce 90% of the food and fibre of the country (GoP, 2009).

According to FAO (2015), 95% of irrigated land of Pakistan is located in the Indus basin river system, of which Punjab province accounts for 69% of the total crop area. The Indus Basin Irrigation System (IBIS) of Pakistan is one of the largest contiguous gravity flow irrigation networks of the world, which consists of 3 main reservoirs (i.e., Terbela on the Indus river, Mangla on Jehlum river, and Chashma on the Indus river), 19 barrages, 12 interlink canals, 45 main canal commands, and about 107000 outlets (Latif, 2007). It also consists of 7,321 km branch canals, 307, 056 km of secondary canals (distributaries/minors), and 1.6 million km of tertiary canals (watercourses) (Figure 2.3) (Bhatti and Kijne, 1990; Latif, 2007). Nearly 85% of all arable land in Pakistan is irrigated. Crops are grown in two seasons, summer cropping called *kharif* season from May to October, winter cropping, also called *rabi* season, from November to April. Cotton and rice are the major crops of the *kharif* season, whereas wheat is the only major crop of *rabi* season; other crops are sugar cane, oilseeds and fodder, which are mostly grown in both seasons (Tahir and Habib, 2001).

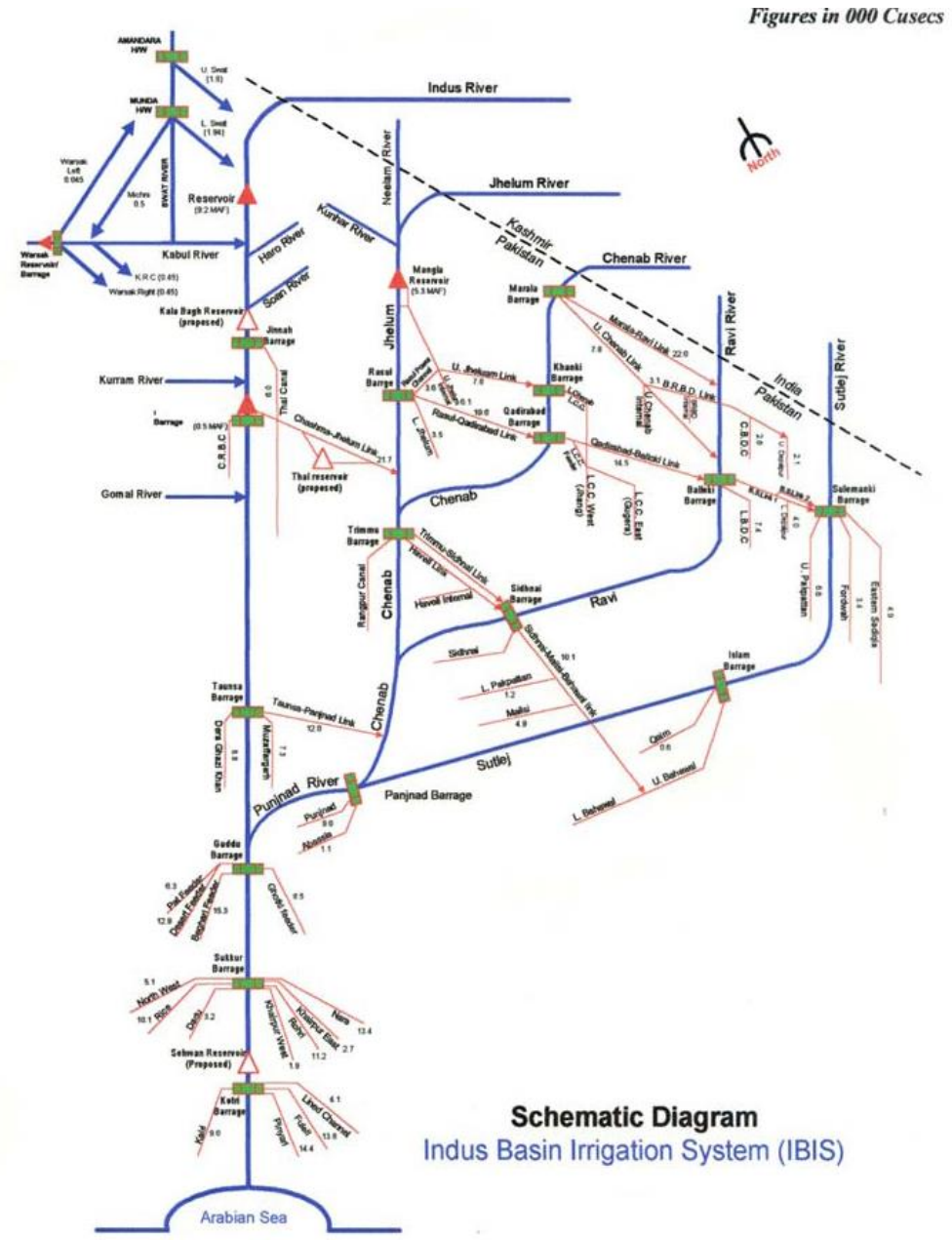

Figure 2.3: Indus basin irrigation system of Pakistan (Ahmad *et al.*, 2013).

Most of the canals in the Indus basin are run-of-the-river system, in which the discharge in the canal depends on the flow in the river. Figure 2.4 shows a typical schematic view of the irrigation infrastructure (Latif, 2007). The main canals off-take from the river through diversion headworks (weirs or barrages), which are divided into several branch canals called the primary system. The branch canals are further divided into several distributaries/minors called the secondary system. The distributaries/minors are further

divided into watercourses that divert water to the fields through Nakka. This is called the tertiary system of the canal networks. The primary and secondary systems are managed by the provincial irrigation department (PID), whereas the tertiary systems are controlled by the farmers.

Figure 2.4: Typical irrigation distribution network in Pakistan (Latif, 2007).

2.1.2 Water allocation procedure in IBIS

As part of building extensive hydraulic infrastructure by the British, they also introduced the framework for water allocation called "*Warabandi"* (Condon *et al.*, 2014). The *Warabandi* is a combination of two words, i.e, "*wahr",* which means turns and "*bandi"* means fixed. It is essentially a periodic rotation of water distribution within a watercourse with a fixed volume and duration proportional to the size of the farmer's field

(Bandaragoda, 1998). This system of water allocation was implemented by the 1873 Act and is still used in Pakistan and the northern part of India. According to Malhotra (1982), the reason behind the implementation of the *Warabandi* system is due to the fact that the water supply from the rivers of Indus basin are highly erratic and varying from season to season and year to year. As no past experience were available for managing the canal system, two options were proposed to adopt, each one with its own pros and cons (Malhotra, 1982). The first was to restrict the canal irrigation to such limited area that could be fully irrigated even with the lowest available water supply. This would lead to maximum production per unit of land but not per unit of water available. The option one could not be beneficial for assurance against famine and would not have been optimum as substantial amount of water remained unutilized during the time of high flow. The second option was to spread the irrigation to as much larger area as possible that could be supported by the lowest available supply thereby creating a perpetual scarcity condition. This option would lead to maximum production per unit of water available and not per unit of land covered and would provide protection against famine. This second option also minimize chance of water remained unutilised. The second option was selected for implementation. The principal of this option was *Protective irrigation* that is to spread water over large area in equitable manner (Malhotra, 1982; Jurriëns *et al.*, 1996). The idea is to reach as many farmers as possible and to protect them against famine and crop failure.

According to Bandaragoda and Rehman (1995) the *Warabandi* rotational cycle lasts for seven days, each famer in the water course command receives one turn in the cycle for an already fixed duration. The turn begins at the head proceeds to the tail until the last farmer gets water. This completes one cycle of *Warabandi*, the farmer has the right to use all of the water flowing in the watercourse. Every year the Warabandi roster is rotated

by twelve hours to give compensation to those famers who had turns at night in the preceding roster.

According to Malhotra (1982) *Warabandi* is an integrated water management system that aims to achieve *high efficiency* and *equity* in water use. The efficiency is to be achieved by imposition of water scarcity on each farmer and equity through distribution of equal share of water per unit area. Studies conducted to evaluate the performance of the *Warabandi* system revealed that if the method is correctly applied, it can produce yields comparable with the output of perfect demand system (Narayanamurthy, 1985) . However, the limited water supply due to water scarcity is generally augmented with freely accessible groundwater pumping for potential crop yield. The successful application of *Warabandi* system also requires a well-maintained physical infrastructure and good understanding among the water users.

However, in Pakistan with variation in water flow, increased in cropping intensities and non-adherence to the standard operation procedures had affected the true spirit of *Warabandi* system. Studies conducted on *Warabandi* system in Pakistan revealed that, in actual practice, most of the theoretical features of official *Warabandi* had been eroded and no longer hold (Bandaragoda and Rehman, 1995). Latif (2007) analysed spatial variation of water flow along the irrigation canals in Pakistan. Results of his study revealed that there is a significant inequity in the distribution of canal water from head to tail reaches, with the tail reaches receiving less water than the head reaches. As Pakistan's canal irrigation system operates in a water scarce environment. There is a need to revisit and modify the system according to the present-day requirements to use the scarce water resources of the country judiciously and efficiently.

2.2 Challenges in the IBIS

The agriculture in Pakistan is highly dependent on irrigation perhaps more than anywhere else in the world. However, the IBIS of Pakistan is under pressure and threatened due to several challenges. Some of the major challenges are discussed in the following sections.

2.2.1 Waterlogging and salinity

According to Bhutta and Smedema (2007), the time when the irrigation system was developed for the Indus basin the water tables were deep enough and irrigation supplies were low to recharge the groundwater. However, with increase in the irrigated area and cropping intensity, more irrigation water was supplied causing continuous water table rise due to percolation from irrigated fields and seepage from irrigation network (Qureshi and Fatima, 2012). Moreover, given the alluvial geo-morphological setting and arid zone climate conditions, the occurrence of large-scale waterlogging and salinity of the irrigated lands was evident. To monitor the groundwater level, observation wells were installed across the doabs of the Punjab in 1882 (Mohammad, 1964). The historically irrigation induced groundwater rise across the Punjab irrigated area was recorded since 1886 (Figure 2.5).

According to Revelle (1964), by the end 1960s 30% of the irrigated area of the Indus basin was affected by the twine menace of water logging and salinity (Figure 2.5) and another 30% had risen water table and adverse signs of soil salinity (Mohammad, 1964; Revelle, 1964). In Indus basin of Pakistan most extensive irrigated areas are in the province of Punjab and Sindh which are being severely threatened by waterlogging and soil salinity. As these regions are characterized by arid to semi-arid climate, flat topography and having no adequate drainage system to discharge excessive water from the fields (Datta and De Jong, 2002).

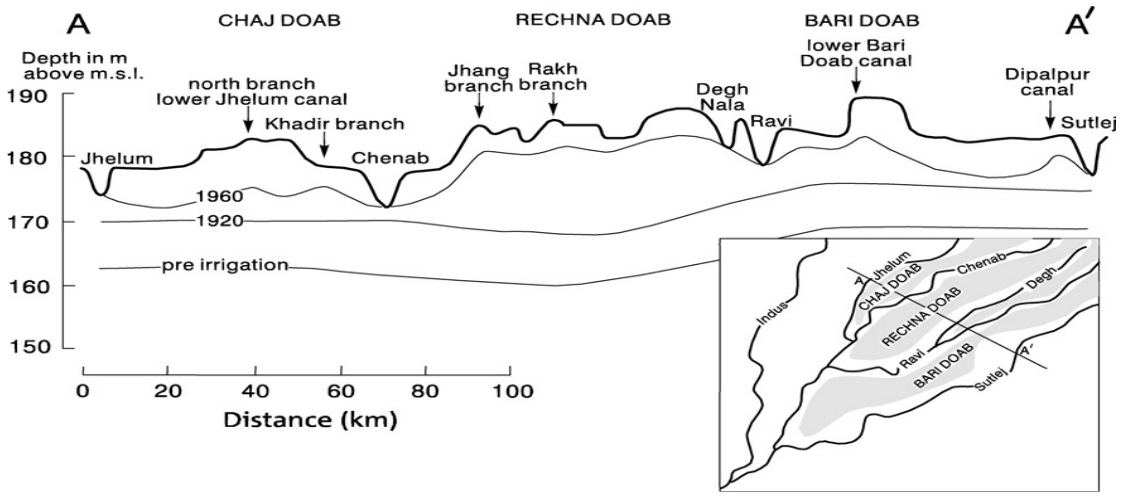

Figure 2.5: Change in water table after introduction of canal irrigation in Punjab Pakistan. (Wolters and Bhutta, 1997).

The other major causes are the seepage from unlined earthen irrigation channels, low irrigation application efficiency, and unrestricted use of poor quality groundwater (Qureshi *et al.*, 2008). Recurrent floods due to limited storage capacity have further aggravated the twin menace of waterlogging and soil salinity (Shah, 1988; Alam and Bhutta, 2004; Mustafa and Wrathall, 2011). Waterlogging and soil salinity is a major threat to the sustainability of irrigated agriculture in Indus basin. The intensity of waterlogging is higher at the head reaches of the canal due to extensive seepage loses from the unlined canal network and over irrigation by the farmers (Qureshi *et al.*, 2008). The famers at the head of canal have access to good quality surface as well as groundwater which is recharged through seepage from canal networks (Latif, 2007; Awan *et al.*, 2016). Whereas intensity of soil salinity is comparatively higher at the tail reaches of the canal system. According to Latif and Ahmad (2009), reduced canal water supply at the tail reaches of the canal irrigation system lead the downstream farmers to pump poor quality groundwater, thereby risks of increasing soil salinity.

Kahlown and Azam (2002) quantified the combined effects of waterlogging and soil salinity on the yield of major crops (cotton, wheat, rice and sugarcane) at the canal

command of Fordwah Eastern Sadqia South (FESS) canal. According to their findings the extent of yield loss varied from 27 to 33% for wheat and sugarcane crops, and from 11 to 60% for rice and cotton at water table depth < 2 meters (below ground level) and soil salinity between 4 to 12 dS m^{-1}, and a complete crop failure with soil salinity levels beyond 12 dS m^{-1}. According to Qureshi and Perry (2021) extensive groundwater pumping adds 45 million tons of salts annually affecting about 4.5 million hectare irrigated land by various level of soil salinity. These salt affected soils also adversely affect the socioeconomic conditions of the farmer's community with low living standards and health problems (Malik *et al.*, 2021).

2.2.2 Water scarcity and climate change

The water scarcity is constantly growing as the demand of water continue to increase and the supply of water is declining due to depletion of natural resources and alteration of hydrological cycles (Lenzen *et al.*, 2013). The major sources of fresh water (Glaciers and snow caps) in Indus basin are drying and melting, causing serious water shortage within agriculture, industrial and domestic sectors (McCartney *et al.*, 2022). The hydrology of Indus basin is based on the rivers that are originated from the Himalayas Karakoram Hindukush (HKH) mountains dominated by snow and glaciers. The Water and Power Development Authority (WAPDA) of Pakistan monitoring the glaciers in northern part of Pakistan since 1980. Their measurements indicates that runoff from glaciers and snowmelts from the HKH ranges contributes around 50 to 80% to the Indus basin rivers. According to Soncini *et al.* (2015) and Ikram *et al.* (2016) the glaciers of the HKH region are retreating faster than those in other parts of the world. Ageta and Kadota (1992) and Solomon (2007) also reported rapid decline in glacier volume in HKH region and attributed this decline to global warming. According to World Bank Report 2013 such rapid decline of the glacier volume decreases flow of the Indus basin rivers from 30 to

40% (Winston *et al.*, 2013). The accelerated glacier and snow melting may lead to increased risk of avalanches and floods over the first half of the 21st century and the by the end of the century the extent of glacier is expected to have significantly decreased, reducing the contribution of glacial and snow melts which reduces overall flow across the Indus basin (Winston *et al.*, 2013).

The surface water resources of Pakistan are insufficient to meet the demand of agriculture, industrial and domestic sector. Pakistan is already in the list of water stressed countries of the world (Figure 1.4), a situation which is, if further degraded will leads to serious water scarcity. The limited water resources and high population growth (Figure 1.3) has put enormous pressure on the water economy of Pakistan. The hydrological budget of the Indus river system is dominated by monsoonal rainfall and snowmelts of the Himalaya and adjacent Tibetan Plateau (Bookhagen and Burbank, 2010). According to Hussain *et al.* (2011) the predicted mean annual flow in the Indus basin are around 175 Billion cubic meter (BCM). The annual estimated losses in the river system are about 12 *BCM*. On average, nearly 33 *BCM* flows to the sea per year, leaving only 130 *BCM* for the canal diversion per annum. Most of the canals are unlined (Qureshi *et al.*, 2008) which results in seepage loss of 25% (33 BCM), furthermore around 30% (29 BCM) are lost in tertiary system leaving only 68 *BCM* at the farm gate canal supplies. This means that out of 130 BCM available at canal head works about 62 *BCM* are lost in the conveyance. However, the losses in the conveyance system help recharge the groundwater (Ahmad and Majeed, 2001).

The use of groundwater in the Indus basin has a long history. Earlier the groundwater was abstracted from open wells through Persian wheel, rope and bucket (Qureshi *et al.*, 2010). However, large scale extraction and use of groundwater started in 1960s (Qureshi *et al.*, 2008). Currently there are 1.2 million public and private tubewells operating in the

Indus basin, 90 percent of which are for irrigation purpose. According to a report "Facts about Groundwater usage" by National Groundwater Association of the United State of America, Pakistan is the fourth largest user of the groundwater (NGWA, 2016). The report shows that India is the largest consumer of the ground water and extract about 251 km^3/year, followed by China and USA both extract 111 km^3 $year^{-1}$ and then Pakistan which extract 65 km^3/year (NGWA, 2016). The estimated groundwater contribution to the annual water budget is 60 BCM (Ahmad and Majeed, 2001). This unregulated extraction of groundwater in excess of freshwater recharge cause the decline of groundwater table at a rate of 1.5 to 3 m $year^{-1}$, making groundwater inaccessible in 15 to 20% of irrigated areas (Qureshi and Perry, 2021). This high rate of groundwater level decline suggests that there is little potential for groundwater exploitation (Watto and Mugera, 2016). Pakistan is currently close to using all of the available surface and groundwater resources, yet it is projected that over 30% more water will be required to meet the agriculture, industrial and domestic demands over the next 20 years (Habib, 2021)

2.2.3 Low crop yields and crop water productivity

The crop production in Pakistan had increased significantly over the past decades (1960s – 1980s) during the era of green revolution by increasing the cropping intensities from 70% to more than 150% as well as improved inputs and other farming practices (Hussain *et al.*, 2003; Briscoe and Qamar, 2008). However, in recent years the growth rate of major crops have slowed. According Qureshi and Perry (2021), despite the same agro-metrological conditions, the average wheat yield in the Indian Punjab is 4.2 ton ha^{-1} as compared to 3.2 ton ha^{-1} in Pakistani Punjab. The average water productivity for wheat is 0.5 kg m^{-3} in Pakistan as compared to 1.0 kg m^{-3} in India (Hussain *et al.*, 2003; Usman, 2012). The substantial increase in crop water productivity and overall profitability can

be achieved by improved water management practices at the farm and irrigation system levels (Jehangir *et al.*, 2002). The rapid increase in population and competition of water demand for domestic and industrial uses has reduced water availability to agriculture sector in Punjab Pakistan (Jehangir *et al.*, 2007). Less efficient irrigation system, poor management at farm, poor quality of groundwater, and soil salinity and high cost of farm inputs has led to reduction in crops yield (Mudasser *et al.*, 2001; Raza *et al.*, 2012a). Despite of huge investments in water management and research, food security is threatened mainly due to less focus on improving resource use efficiency, like irrigation system efficiency, efficiency in genotype and water use efficiency (Raza *et al.*, 2012a). In the "business as usual" scenario, the shortfall of water is predicted to result in serious food shortage in the years to come which will severely effect the economy and livelihood of the people (Qureshi and Fatima, 2012). Given the present water resources situation it is impossible for Pakistan to increase the cultivated area. Therefore, the only way to achieve food security is to increase crop water productivity by efficient irrigation management and improved agronomic practices (Ahmad *et al.*, 2004; Bakhsh *et al.*, 2018).

2.3 Remedial approaches and measures

The twin problem of waterlogging and soil salinity was observed soon after the introduction of irrigation in the Indus basin. In 1870 the observation wells were first time installed to monitor the groundwater level (Mohammad, 1964). There were also some other measures to control waterlogging and salinization like closure of canal during monsoon season, construction of surface drains and lowering of canal flow (Goldfarb and Adams, 1960). However, these measures provide only temporary or local reliefs, whereas the severity of waterlogging and soil salinity was continue to increase regionally. In 1958, the Water and Power Development Authority (WAPDA) was established to

control waterlogging and soil salinity through a large-scale Salinity Control and Reclamation Project (SCARP) (Rahimtoola, 1965; Alam, 2015). This project aimed to lower watertable and reclaim the salt affected soil through surface and sub-surface drainage system. These projects are briefly discussed below.

2.3.1 Vertical drainage system

The WAPDA, in collaboration with United States Geological Survey Department, conducted their first detailed survey of groundwater level and soil salinity in late 1950s to identify the waterlogged and salinized regions (Goldfarb and Adams, 1960). As a result, about 14 thousand public tubewells with an average capacity of 80 l s^{-1} were installed for vertical drainage in the affected areas covering about 2.6 million ha during 1960s and 1970s (Mundorff *et al.*, 1976). The main objective of the vertical drainage project was to lower the groundwater level and increase irrigation supplies to the farmer fields by using the pumped groundwater directly or mixed with canal water. This additional supply of irrigation water at the farm gate has increased the cropping intensity. However, this demonstration has led to proliferation of private tubewells with an average pumping capacity of up 28 l s^{-1} by farmers during the years from 1970 to 1980. Since then, the private tubewells numbers are increasing with an average annual growth rate of 9.6 percent (Qureshi and Perry, 2021). Currently, there are estimated 1.3 million public and private owned tubewells operating across the IBIS of Pakistan of which more than one million are in the Punjab province (PBS, 2017).

The implementation of vertical drainage projects was moderately successful and initially the problem of water logging and soil salinity was somewhat controlled (Briscoe and Qamar, 2008). However, the uncontrolled and unregulated exploitation of groundwater has created serious consequences of depletion of the fresh groundwater resources and leads to lowering of groundwater level and subsequent intrusion of saline groundwater

into fresh groundwater aquifers (Qureshi and Perry, 2021). This has not only deteriorated the quality of groundwater but also increased the pumping cost.

2.3.2 Horizontal drainage system impasse

According to Mundorff *et al.* (1976) it was soon realized that re-circulating the saline water through vertical drainage system, further aggravated the soil salinity problem. Therefore, in saline groundwater areas the vertical drainage system was replaced by horizontal subsurface (tile) drainage system, in which saline water from the fields were diverted to the surface drains and onward discharged to the rivers. However, under Pakistani economic conditions the horizontal (tile) drainage systems were 10 times more expensive than the tubewell system (Bhatti, 1987). Despite the high cost, the main reason of introducing tile drainage system was the assumption that the long-term drainage water quality would be better under the tile drainage system than the tubewell drainage. This in turn would reduce the drainage water disposal problem by producing better drainage water quality that can be reused for irrigation (Bhatti, 1987). The horizontal subsurface drainage project was initiated in three provinces Khyber Pakhtunkhwa, Punjab and Sindh having moderately to high level of waterlogging and soil salinity.

Over the past 5 decades WAPDA has completed 63 SCARP projects that includes installation of 16950 number of tubewells, construction of 14361 kilometers length of surface drains and 12612 kilometers length of horizontal tile drains (Bhutta and Smedema, 2007). The potential impact of these SCARP project was positive in controlling waterlogging and salinity problems. This helps in increasing the cropping intensities from 84 to 115% in most of the SCARP areas (Bhutta and Smedema, 2007). However, over the time, increased maintenance and operation cost and waterlogging in surrounding areas due to seepage from the unlined surface drains and increasing salinity

due to pumping saline groundwater affected the efficiency and the intended objectives of the SCARP projects (Bhatti, 1987; Qureshi, 2016).

2.3.3 On-farm water management

According to Byrnes (1992) the main focus of the agricultural policies of the government of Pakistan (GoP) from 1950s to 1970s was mainly construction of large dams, barrages, main canals, link canals, salinity control and drainage projects. However, other agricultural development requirements, including on-farm water management (OFWM) and operation and maintenance (O&M) were largely neglected. In Pakistan irrigation system, the primary and secondary canals are managed by the provincial irrigation department (PID), whereas the tertiary channels (watercourses) maintenance and operation are the sole responsibility of the farmers. Because of inadequate knowledge and limited financial resources, the century old watercourses have deteriorated causing excessive conveyance losses. Realizing these huge conveyance and application losses at the farm level, the Government of Pakistan (GoP) initiated a pilot project called On-Farm Water Management (OFWM) in the selected regions during 1976-77 in collaboration and assistance from US-AID (O'Mara and Duloy, 1984). The project include lining of water courses to reduces seepage losses, precision land levelling to reduce field application losses, and application of biotech and chemical measures to reclaim salt affected soils. In addition to the engineering aspect of the project, the farmers were organized as water user association (WUA) at watercourse level for the operation and maintenance of the watercourses. However, these efforts are confined to field and farm level, and no serious attempt was made to translate the implication of these project at regional level (Noorka, 2011). The problem of water logging and soil salinity still widely persist in a large tract of irrigated areas.

2.3.4 Modernization of irrigation system

Recently, the policy makers in Pakistan have suggested to shift from the conventional surface irrigation to High Efficiency Irrigation System (*HEIS*) (sprinkler and drip irrigation) to address inefficient irrigation system, low crop water productivity and dwindling water resources. The *HEIS* is implemented in Punjab province with financial assistance from World Bank as a pilot project aka Punjab Irrigated-agriculture Productivity Improvement Project (*PIPIP*) (2012-2018). This project is designed to introduce drip and sprinkler irrigation system on 50,000 ha of the farmer fields across the Punjab province. The *PIPIP* promotes *HEIS* amongst the farmers for enhancement of crop water productivity and optimal utilization of resources and invite farmers to high value agriculture. According to Punjab Agricultural Department (2018), *HEIS* has been installed on 18350 ha all over the Punjab province. Out of the total installation of *HEIS* 58% were installed for the orchards, 23% installed for the field crops (wheat, oil-seeds etc), 19% installed on vegetables and row crops (cotton, maize etc). The project was extended for further 3 years with additional financing to ensure completion of *HEIS* on 50,000 ha. Many researchers revealed the benefits of adoption *HEIS*. For example, Ashraf and Yasin (2012) reported 50% saving of water and improvement of 39 and 105% in crop water productivity (crop yield per m^3 of irrigation water applied) for sugarcane and citrus, respectively. Asif *et al.* (2016) reported 65% reduction in fertilizer use, 19% reduction in pesticide use, 24% increase in crop yield, and 64% increase in crop water productivity (crop yield per m^3 of irrigation water applied) as compared to conventional surface irrigation at multiple field trials in District Toba Tek Singh. The increase in crop yield as high as 100% is reported by the World Bank Monitoring and Evaluation unit in their annual assessment report (Stutley *et al.*, 2018). Qureshi *et al.* (2015) evaluated 56%

saving of irrigation water and 26% increase in crop yield (sun flower) under *HEIS* as compared to conventional farrow irrigation system at farmers' fields at district Jamshoro.

Similarly, other studies have revealed the benefits of *HEIS* in terms of irrigation water savings, reduced farm inputs, enhancement in crop yield and crop water productivity at the farmers' fields on the short term basis (Khan *et al.*, 2013; Bakhsh *et al.*, 2015; Yasin *et al.*, 2021; Shahid *et al.*, 2022). However, the adoption of *HEIS* is the paradigm shift from centuries old conventional surface irrigation system to modernize pressurized irrigation system, which will potentially impact the regional water and salt balances, crop yields and water productivity of the Pakistan irrigated agricultural system.

2.4 Irrigation efficiency paradox

The irrigation efficiency is an engineering term used to quantify the performance of irrigation system and the response of crops to irrigation (Howell and Stewart, 2003). Although irrigation efficiency has been adopted in water resource management to preserve water and increase crop yield (Batchelor *et al.*, 1996; Deng *et al.*, 2006; De Pascale *et al.*, 2011). However, the definition of irrigation efficiency is still not unanimous and evolving due to complex water accounting in irrigated areas (Bos, 1979; Jensen, 2007). The irrigation efficiency was first defined by Israelsen and Blaney (1946) as the ratio of the amount of water used beneficially by crop (evapotranspiration) to the amount of water delivered to the cropped area. However, according to Molden (1997) the classification of beneficial and nonbeneficial water use is a controversial point in defining irrigation efficiency. The direct and major beneficial use of irrigation is to satisfy crop evapotranspiration. The other beneficial use of irrigation is maintaining the soil productivity, frost protection and providing optimum moisture for seed germination. Jensen (1967) also suggested the amount of water used to control salt build up in the soil profile as a beneficial use because sustainable crop production requires acceptable salts

concentration in the soil profile (Maas and Hoffman, 1977). However, Jensen (2007) did a comprehensive review of irrigation efficiency concept, and he argued that researcher often did not consider water stored in the root zone and water used for removing salts from the soil as beneficial use. For instance, Burt *et al.* (1997) argued that it is inappropriate to consider the water stored in root zone or use for deep drainage as beneficial before it has been actually consumed by crop (crop evapotranspiration). However, in actual water management practices the water stored in root zone is often counted beneficial regardless, if it is actually consumed or not. Hence according to Jensen (2007), the term irrigation efficiency could be misleading if the water applied and not stored in the root zone is considered "wasted". Since the only water lost in the system during an irrigation event is the portion that is evaporated during the time of application of water until the soil became at field capacity (after 2 to 3 days). The water that is stored or percolated or flowed to an open drain is still part of the system and can be used beneficially (Jensen, 2007).

According to Macneil (2018) the modernize irrigation technologies are the tools to save water and maximize irrigation efficiency. The notion is that modernize/efficient irrigation system save water and improve crop water productivity. However, according to Grafton *et al.* (2018), there is a paradox, in which improving irrigation efficiency through modernize irrigation system could fail to improve and even reduce the amount of water available to other sectors. Scheierling *et al.* (2006) reported that annually, governments around the world spend huge capital on subsidizing modernisation of irrigation systems such as introducing sprinkler or drip irrigation systems. Their goal is to increase irrigation efficiency and conserve water with the understanding that this will allow water to reallocated to other sector such as industries, domestic or the environment, maintaining or increasing agricultural productivity (Flörke *et al.*, 2018).

Efficient irrigation technologies can significantly improve on-farm irrigation efficiencies such as irrigation application efficiency, distribution uniformity and reduce deep percolation (Playán and Mateos, 2006; Berbel *et al.*, 2019). However, the resulting long-term decrease in soil percolation may contributes to reduction in leaching of salts and recharge to groundwater (Raine *et al.*, 2007; Grafton *et al.*, 2018).

Policy makers often support increase in irrigation efficiency, promote modernize advance irrigation technologies to save water and improve crop water productivity. However, scientific evidence has shown that increasing irrigation efficiency through advanced irrigation technologies has rarely delivered the intended benefits of water saving and increased water availability (Burt *et al.*, 1997). The importance of soil water and salt balances, and water accounting at the basin scale has often been underestimated while implementing the advanced irrigation technologies (Grafton *et al.*, 2018). The increase in irrigation efficiency must be accompanied by robust water accounting, assessment of uncertainties, and good understanding of long-term effects of soil water and salt balances and their effect on crop yields and water productivity under current and future climatic conditions.

2.5 Salinity in irrigated agriculture

Historically, irrigated agriculture has faced challenges of sustaining its productivity due to geochemical factors and natural hazards as well as irrigation induced activities, soil salinity and waterlogging that continue to affect agriculture (Shahid *et al.*, 2013; Sharma and Singh, 2017).

Soil salinity has been identified as a major cause of land degradation affecting crop cultivation (Bhardwaj *et al.*, 2019). According to Hossain (2019) annually 1 – 2% of the global irrigated land has been lost due to soil salinization. Currently, the global salinity

affected area is about 1125 million hectares of which one fifth are irrigated land (Cicek *et al.*, 2022). With this pace of soil salinization it is estimated that 50% of cultivable land will be lost by 2050 (Hossain, 2019). The major regions with significant soil salinity are Murray-Darling basin in Australia (Jolly *et al.*, 2001), the Yellow river basin in China (Fan *et al.*, 2012), the Amu-darya basin in Uzbekistan (Ibrakhimov *et al.*, 2004), the Indo -Ganga basin in India (Bhardwaj *et al.*, 2019) and the Indus basin in Pakistan (Bhutta and Smedema, 2007).

The sustainability of irrigated agriculture cannot be achieved without adequate accounting of soil water and salt balances (Zaman *et al.*, 2018). The accumulation of salt in soil depends on the salinity of irrigation water and the amount of the irrigation applied (van Schilfgaarde *et al.*, 1974). Therefore, sustainability of irrigated agriculture requires a sound understanding of long-term effects of irrigation practices on soil water and salt balances, crop yields and crop water productivity under current and future climatic conditions.

2.5.1 Salinity

Soil salinity is the indicator of the concentration of all dissolved mineral salts present in the soil and water on a unit volume or mass basis (Ghassemi *et al.*, 1995; Zaman *et al.*, 2018). The major salinity constituents are dissolved cations sodium (Na^{+}), calcium (Ca^{+2}), magnesium (Mg^{+2}), potassium (K^{+}) and the anions chloride (Cl^{-}), sulphate (SO_4^{-2}), carbonates (CO_3^{-2}), bicarbonate (HCO_3^{-}) and nitrate (NO_3^{-}). Some hyper saline soils also contain boron (B), selenium (Se), lithium (Li) and aluminium (Al) which are highly toxic to plants and human as well as animals (Wallender and Tanji, 2011). The ratio of different salinity constituents in soil-water to the chemical reaction that takes place between soil-water-plant system at different spatial and temporal scale (Bresler and Hoffman, 1986). Generally, soil salinity is usually predicted in soil-water as total salts

irrespective of its constituents. However, chemical analysis can provide full details of salinity and its specific ion concentration.

Electrical conductivity (*EC*) is used as a quick method to quantify soil and water salinity (Letey *et al.*, 2011). The presence of charged anions and cations in the soil-water solution allow the electric current to pass between two electrodes (i.e. with standardised solution and temperature) (Tanjii, 1990). The higher the concentration of ions in a soil water solution the higher is the electrical conductivity. The *EC* is expressed in Siemens per meter, but in agriculture *EC* is often low thus deciSiemens per meter is commonly used.

2.5.2 Sodicity

Sodicity refers to the level of sodium present in soil or water. The presence of sodium influences the structural stability of soil minerals particularly clay minerals and the potential of drainage, erosion and dispersion problems (Shahid *et al.*, 2018). The sodicity of water or soil is usually described as proportion of sodium (*Na*) cation, compared to the divalent cations i.e. magnesium (*Mg*) and calcium (*Ca*) in soil water solution (Sepahvand *et al.*, 2021). It is expressed as sodium adsorption ratio (SAR), as follows:

$$SAR = \frac{Na}{\sqrt{\frac{Ca + Mg}{2}}} \qquad \text{Eq 2.1}$$

The salinity problems are apparent in the environment in a number of ways i.e. presences of natural salts deposits or geological formation due to chemical weathering of earth materials, saline water irrigation, soil and water amendments, chemical fertilizers, drainage water for irrigation and sea water intrusion (Oster, 1994; Ghassemi *et al.*, 1995; Fan *et al.*, 2012).

2.5.3 Fertilizer effects on soil salinity

Saline soils contain an excess amount of soluble salts mostly Na^+, Ca^+, Mg^+, Cl^-, SO^-_4, CO^-_3 and HCO^-_3 (Shahid *et al.*, 2013). The presence of these elements (anions and cations) affect the osmotic pressure of soil solution causing low physiological availability of water and poor plant growth (Dregne and Mojallali, 1969). In addition to poor aeration due to waterlogging and use of poor quality of irrigation water may further aggravate plant's ability to uptake nutrients in required amount (Bhutta and Smedema, 2007). The application of fertilizers alleviates the effects of low to moderate soil salinity. It has also been demonstrated that addition of plant nutrients interact positively with soil salinity (Hassan *et al.*, 1970). The positive effects of added fertilizers are generally observed at low to medium level of soil salinity normally from 2 to 10 dS m^{-1} (Hassan *et al.*, 1970; Esmaili *et al.*, 2008), however, at higher salinity levels crop yields are poor even with the application of fertilizers.

The increase in salt concentration in the root zone have a complex effect on the minerals and nutrients of plants. Hassan *et al.* (1970) demonstrated in greenhouse study that in saline soils, barley plants showed increased uptake of *Na*, *Mg*, *Mn*, and *Zn* but decreased uptake of *P, K, Ca* and *Fe*. In an experimental study under large lysimeter in Tehran, Iran by Esmaili *et al.* (2008) reported that the concentration of *Na*, *Ca*, *Mg*, and *Cl* in sorghum plant tissue increased with increasing salinity whereas the concentration of *N*, *P*, and *K* decreased.

The effects of the major nutrients elements (*NPK*) in saline soils are discussed as follows:

Nitrogen (N):

Irshad *et al.* (2008) reported a reduction in nitrogen use efficiency and crop yield (maize) under saline soil conditions due to high leaching of nitrogen losses as NO_3. Reduction in

nitrification of ammonia due to high soil salinity and direct toxic effects of *Cl* (Agarwal *et al.,* 1971) and poor aeration due to anaerobic conditions restrict the availability and absorption of nitrogen by plants (Woodruff *et al.,* 1984). According to Chhabra (2017) most of the semi-arid to arid regions of the world like India, Pakistan, Egypt and some part of California USA, used saline groundwater to fulfil crop water requirement containing significant amount of NO_3. Though it can meet the nitrogen requirement to a certain limit, however, continuous use of such water for irrigation become toxic to plants and delays maturity and vegetative growth that affect grain filling adversely (Esmaili *et al.,* 2008).

Phosphorus (P):

Ryden and Syers (1975) observed that with increase in soil salinity, the retention of *P* increased. Shambat (1980) reported that saline soils adsorb more *P* than non-saline soils and thus require more *P* fertilizers to produce good crops. Under saline conditions the mobility of *P* is restricted and thus for its uptake the plant roots must mine through the soil. However, soil salinity restricts root growth which in turn decreases the surface area of the plant roots in contact with phosphorus and thus reduces the uptake of phosphorus (Hassan *et al.,* 1970). As a result, there is an increase in the requirement of phosphorus application in saline soils. Ferguson and Hedlin (1963) observed the effects of the phosphorous application on the relative yield of wheat grown in saline soils with *ECe* (electrical conductivity of saturated paste extract) 6.2 dS m^{-1} and non-saline soils 0.6 dS m^{-1} (fig 2.6). The results show that the response of *P* is higher on saline soils then on non-saline soils of comparable available *P* status. The higher plant response to applied *P* occured on moderately saline soils. The application of *P* fertilisers in saline soils helps increase in the crop yield and decrease the absorption of toxic elements such as *Cl* (Singh *et al.,* 1979).

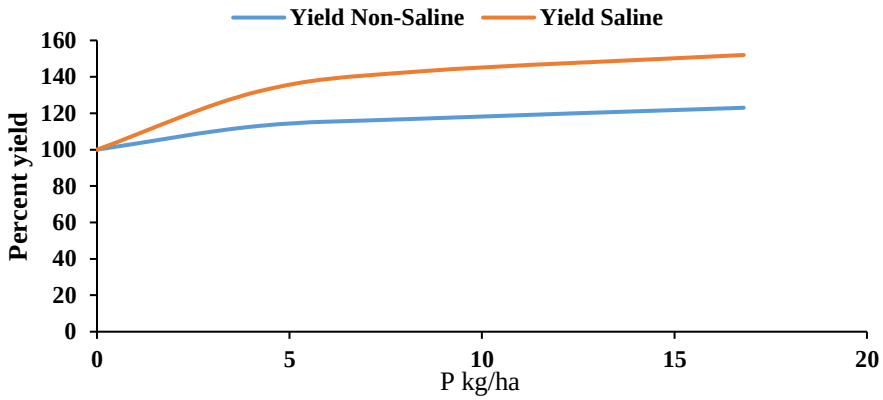

Figure 2.6: Effect of phosphorous fertilization on wheat relative yield under saline and non-saline condition.

Potassium (K):

Saline soils often contain medium to high amount of potassium (Sharma *et al.*, 1968), but during reclamation of saline soil through leaching significant amount of potassium is lost (Bingham, 1973). Plant grown under high soil salinity generally shows potassium deficiency due to adverse effects of *Na* and *Ca* on *K* absorption (Bingham, 1973). The presences of excess *Na* cause reduction of *K* within plant, which leads to reduction in crop yield. However, Bar-Tal *et al.* (1991) showed in a pot experiment that with the increasing soil salinity the concentration of *Na*, *Ca* and *Mg* content of corn plant increased without affecting the *K* concentration, but the *K*:*Na* ratio and *K*: (*Ca* +*Mg*) ratio imbalance became a limiting factor for the cotton yield. On low to moderately saline soils the application of potassium fertiliser may increase crop yield (Dregne and Mojallali, 1969; Thomas and Langdale, 1980).

It is evident that inherent deficiency of the main nutrients is also responsible for reduction in the productivity of saline soils. According to Chhabra (2017) the factors that affects nutrients availability in saline soils are the uptake and absorption of nutrients by plant roots due to ionic imbalance and root growth restrictions and disturbing the metabolism

of nutrients with in plant, mainly through water stress and thus reducing the effectiveness of fertilizers.

Howvere, Esmaili et al. (2008) also argue that while fertilizer application improved plant nutrient status, it may also increase salinity in the soil solution. (Lunin and Gallatin, 1965) also observed an increase in salt concentration of the soil with increased application of fertilizers.

2.5.4 Salts distribution within Root Zone

In agricultural fields the major source of salts accumulation is the irrigation water which are applied frequently as per crop requirement (Oster, 1994). The factors that affect salt distribution in the soil profile depends on climate and soil conditions and the level of salinity in irrigation water and management practices such as leaching fraction, sub-surface drainage, and percolation (Bernstein and Francois, 1973; Bresler and Hoffman, 1986; Hoffman *et al.,* 1990). The surface irrigation like basin, border and sprinkler irrigation systems produce predominantly one dimensional vertical soil water flow, leaching most of the salts from the root zone and accumulating in the lower part of the soil profile (Burt, 1995) provided the depth of water flow is sufficient to fulfil the leaching requirement (Tanji and Kielen, 2002). Reduction of water flow depth reduces the capacity to flush salts from root zone. The salt distribution is different under shallow water table conditions because the capillary rise plays a vital role in redistributing the salt within the root zone (Scherer *et al.,* 1996).

According to Smith (2011) the irrigation practices can be divided into three temporal hierarchies i.e. past, present and future irrigation. The past irrigation practices, which are also termed as '*traditional irrigation*', simply apply water to crops like surface flooding. The current practices are considered more precise that ensure efficient and uniform

application of water as per crop water requirements. The future prospect of irrigation includes accurate, precise, and spatially variable application of water to meet the requirements of individual plants (Zhu *et al.*, 2018). Such type of future irrigation is termed as the precision irrigation. New developments in both design and management of irrigation systems can provide differential delivery of optimal irrigation quantities over the irrigated field with variable soil type, crop yield potential, and topography (Dennis, 2002). However, under these modern irrigation systems more attention should be given to the root zone salinity effects and other environmental impacts (Raine *et al.*, 2005).

2.5.5 Crop responses to salinity

Different crops have different response under varying soil salinity conditions; however, the result is the same, i.e. reduction in crop yield (Katerji, 1995). According Tanji (1990) the soil salinity effects can be distinguished into osmotic effects and toxic effects (Figure 2.7). Under osmotic effects, plant losses energy required for its physiological processes and the crop roots suffer dehydration under low soil osmotic potential (Katerji *et al.*, 2003). The toxicity effect is the result of rise of certain ion level above plant threshold cause crop to reach the wilting point early (Van Genuchten and Gupta, 1993). The situation can be worse at low moisture content in the soil. In addition, the salinity also has a strong effect on the chemical properties of the soil that can hamper the absorption of important crop nutrients (Läuchli and Epstein, 1990) (*see section 2.5.2 above*).

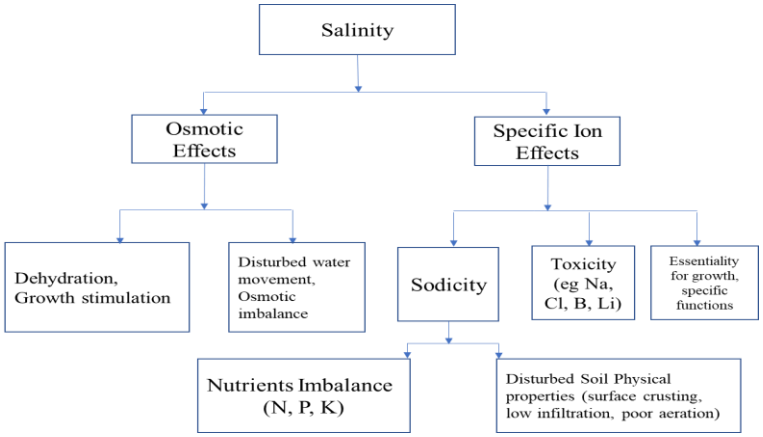

Figure 2.7: Effects of salinity on plants and soil properties (Läuchli and Epstein, 1990).

Management of soil salinity requires a sound understanding of crop salinity tolerances thresholds, type of irrigation system and scheduling, depth of applied irrigation applied, and quantification of solute movement in different soil-water-atmosphere-plant conditions (Rhoades, 1990). Many experimental studies have been conducted to determine salt tolerance of crops (Bingham, 1973; Van Bakel *et al.*, 2009; de Vos *et al.*, 2016). However, there are difficulties in determining the soil solution variables related to crop response that can be measured in the field (Smith and Hancock, 1986). As a result, a number of studies proposed empirical methods to determine root zone salinity as an indicator of crop response to salinity. Bernstein (1961) suggested that salt concentration in drained water can be equal to the crop salinity thresholds at which the yield decrease to 50 percent for field, forage and vegetable crops. van Schilfgaarde *et al.* (1974) mentioned the crop salinity threshold should be equal to the soil salinity level at which plant roots cannot extract water. However, Hoffman and Van Genuchten (1983) provided experimental evidence that Bernstein (1961) method overestimate the crop salt tolerance threshold, and van Schilfgaarde *et al.* (1974) method underestimate crop salt threshold and relate crop response to the linearly averaged salt concentration of the root zone. Bernstein and Francois (1973) and Minhas *et al.* (1990) consider the effects of spatial

variation of soil salinity and recommend using a weighted average root zone salinity. However, Hoffman (2006) argued that "*plant response is better correlated with average root zone salinity, but the problem is determining that average*". This clarifies that the effect of spatial variation of salinity within the root zone requires a good prediction of distribution of salts in soil profile.

Maas and Hoffman (1977) carried out a comprehensive analysis in which crop yield reduction is related to electrical conductivity of the soil saturated paste (EC_e) and list threshold values for crop salt tolerance which was later updated by Tanjii (1990). These crop salinity tolerance threshold values are based on assumption that plant responds to uniform root zone salinity and crop tolerance is defined as function of crop yield reduction across a range of soil salinity (Maas and Hoffman, 1977). According to this function, the threshold value of soil salinity for a certain crop is evaluated below which no significant loss occurs to the crop yield due to soil salinity and above which the crop yield decreases linearly with increase in soil salinity. To quantify decrease in the crop yield a least-square linear equation is fit to the data for each experimental value beyond the threshold soil salinity. The reduction in the crop yield for any given soil salinity beyond the threshold limit can be calculated by the equation, as follows:

$$Y = 100 - B(EC_e - A) \qquad \text{Eq 2.2}$$

Where, Y is the relative yield (%), A is the soil salinity threshold, and B is the percent crop yield decrease per unit soil salinity increase.

The Maas and Hoffman (1977) data set of different crops response to salinity were developed by analysing more than 60 crops using two parameters : 1) the crop salt tolerance threshold value, and 2) the percent of crop yield decrease per unit increase in salinity in excess of the threshold value. Maas and Hoffman (1977) proposed soil salinity

response function (Eq.2.2) to provide the technical and scientific grounds for irrigation management guidelines globally (Feinerman *et al.*, 1982; Van Genuchten and Gupta, 1993; Letey *et al.*, 2011). However, Van Bakel *et al.* (2009) conducted a review of crop salt tolerance in the Netherlands, and according to their findings the Maas and Hoffman function to estimate crop yield reduction due to soil salinity is not sufficiently reliable to define salinity norms under the Netherlands conditions. This could be because the Maas-Hoffman (1977) experiments were performed in California USA, where different climate conditions prevails, crops are irrigated with surface water dominated by *Ca*, *Mg* and carbonates whereas Dutch water are dominant by *Na* and *Cl*. Also, in Dutch conditions applied water through sprinkler irrigation system may cause uptake of *Na* and *Cl* through plant leaf tissues, which may cause burning of leaves (Van Bakel *et al.*, 2009). However, a recent study reported by de Vos *et al.* (2016) performed experiments at the open-air laboratory of Salt form Texel in the Netherlands, in which through its unique design and reliable field trials under highly controlled environment evaluated the crop salt tolerance of several different species and varieties using Maas-Hoffman model. They also compared the results of Maas-Hoffman function with (Van Genuchten and Gupta, 1993) model. According to their findings, the Van Genuchten and Gupta (1993) model does not assume a threshold value, but the values of 90% yield were compared with Maas-Hoffman model. It shows that EC_e values with 90% and 50% crop yield are comparable and shows comparatively similar results (de Vos *et al.*, 2016). This shows the capability of using Maas-Hoffman model for the assessment of crop salt tolerance. However, de Vos *et al.* (2016) also concluded that "salt tolerance also depends on many variables like plant variety, soil type, water quality and environmental condition". These interacting variables should be taken into consideration while conducting salt tolerance investigation.

2.5.6 Modelling Crop Response to Salinity

The quantification of crop response to soil salinity and its effects on crop yield is a complex phenomena due to dynamism of soil water and solute movement in the soil profile, spatial variation in soil properties and temporal changes in climatic conditions (Molz, 1981). This requires extensive experimental work to determine the effects of soil salinity on the Soil-Water-Plant-Atmosphere interaction. However, field experiments are very laborious, time consuming and require sophisticated equipment (Ferrer-Alegre and Stockle, 1999). Agrohydrological models are helpful tools to integrate these factors and for assessing potential impacts of different management practices on soil water and salt balances and their effects on crop growth (Ferrer and Stockle, 1996). They are particularly practical to assess long-term effects of different management practices under current and future projected climatic conditions.

Agrohydrological models vary from very simple to high sophisticated, from crop specific to soil based (Molz, 1981; Ritchie and Alagarswamy, 1989). According to Hoffman *et al.* (1990) agrohydrological models can be broadly classified in to Seasonal models and Transients models. Seasonal models such as one developed by Letey *et al.* (1985) relate crop yield to the amount of irrigation water applied of a given salinity. This relationship is based on the combination of relationship between crop yield and evapotranspiration, crop yield and average root zone salinity, average soil salinity and leaching fraction (Letey *et al.*, 1985). According to Bresler and Hoffman (1986) seasonal models assume a steady state condition and do not include the effects of spatial and temporal variation of soil salinity on the crop response. Letey *et al.* (1985) reported crop water production functions based on steady state conditions that is in line with the field data. However, Bresler and Hoffman (1986) demonstrated that steady state conditions are not suitable for irrigation management under saline conditions. According to Katerji (1995) the main

advantage of seasonal models is their simplicity in computation and the major disadvantage is the assumption of steady state conditions, the results of such models cannot be generalized.

Transient models such as SWAP (van Dam *et al.*, 1997) simulate changes in soil water and solute flows in the soil profile caused by irrigation and rainfall in addition to root water uptake (Ferrer-Alegre and Stockle, 1999). These models differ in their conceptual approach, complexity, formulation for root water uptake and crop response to soil water stress and salinity (Wagenet and Hutson, 1989). These models relates the crop yield and crop water use in relation with the osmotic potential and matric potential that occur in root zone (Oster, 1994; Qadir *et al.*, 2007). According to Majeed *et al.* (1994) the effectiveness of transient models in salinity management requires a mechanistic approach of relevant processes in soil-water-plant-atmosphere system and interaction of these processes with crop growth.

Recently Oster *et al.* (2012) conducted a comparative review of five well established transient agrohydrological models. These are HYDRUS (Šimunek *et al.*, 2012), UNSATCHEM (Šimůnek *et al.*, 1996), SALTMED (Ragab, 2002) ENVIRO-GRO (Pang and Letey, 1998) and SWAP (van Dam *et al.*, 1997). These models apply Richard's equation for soil water flow and conversion-dispersion equation for solute flow and different plant function for relating crop response to osmotic and matric stress. They concluded that HYDRUS and SWAP simulate similar results in terms of solute transport, whereas the results from UNSTCHEM follow similar trends of crop growth as HYDRUS and SWAP. ENVIRO-GRO simulated high crop yield when the salinity in irrigation water is less than 2.0 dS m^{-1} as compared to other models. However, ENVIRO-GRO simulated a sharp decline in relative crop yield for soil salinity greater than 2 dS m^{-1}, as compared to other models except for SALTMED. Relative crop yield simulated by

SALTMED are significantly less as compared to other models even at low salinity of 0.5 dS m^{-1}. According Oster *et al.* (2012) this could be the use of additive water and salt stress function whereas other models (HYDRUS, SWAP and UNSATCHEM) uses multiplicative stress function to account for water and salt stress on crop growth.

The SWAP van Dam *et al.* (1997) is an existing multi-year, multi-crop, daily time step and physical based model with a process-oriented approach to the modelling of soil-water-plant atmosphere system. The model includes a variety of agronomic management options such as crop growth, irrigation management and environmental impact analysis capability (water and salt balances). The physically based SWAP model (van Dam *et al.*, 1997) offers opportunity to conduct long-term simulations of soil water flow and salt transport processes, and crop growth at field scale as well as at regional scale (Singh *et al.*, 2006b; Singh *et al.*, 2006c). In combination with field experiments, SWAP provides detailed insight and potential effects of various irrigation scenarios on soil water and salt flows in interaction with crop (Singh *et al.*, 2006a; van Dam *et al.*, 2008; Vazifedoust *et al.*, 2008). Woldegebriel (2011) demonstrated application of SWAP model to simulate salt accumulation under drip irrigation system in Gediz basin of Turkey. Xue and Ren (2016) demonstrated the SWAP capability to evaluate crop water productivity under sprinkler irrigation at regional scale in Hetao irrigation China. The built-in crop response to soil salinity function in SWAP results in an excellent tool for comprehensive soil salinity management.

2.6 Research needs

Farmers in the Indus basin irrigation systems of Pakistan, like in many other semi-arid regions, are faced with challenges of declining irrigation water supply, increasing waterlogging and soil salinity, and low crop yields. It is evident from the above reviewed studies that the adoption of modernized irrigation systems such as sprinkle and drip

irrigation aim to improve irrigation efficiency and increase crop yields and crop water productivity in irrigated agriculture. However, our understanding and knowledge is limited regarding the long-term impacts of modernised irrigation systems on soil water and salt flows, soil salinity build-up, and crop water productivity in semi-arid and arid regions. We are yet to comprehensively investigate the long-term potential impacts of modernised irrigation systems at the regional soil water and salt balances, crop yields and crop water productivity in semi-arid irrigated lands of Indus basin in Pakistan, particularly under projected climate change conditions. A sound understanding of the spatial and temporal variation of soil water and salt balances and their effects on crop growth are key for effective management and sustainability of irrigated agriculture under current and future climate change in Indus basin in Pakistan. The modernised irrigation systems are being gradually introduced in Pakistan. Hence there is a need for further studies to quantify the feasibility of adoption of modernised irrigation systems, taking in to account the impact of future climate change scenarios on regional soil water and salt balances, crop yields, and crop water productivity of main irrigated crops in semi-arid regions of Indus basin in Pakistan. Agrohydrological models such as SWAP offers a practical tool to simulate spatial and temporal dynamics in soil-water-atmosphere-plant continuum from field- to regional scale. This can facilitate modelling long-term potential impacts of different irrigation management practices on soil water and salt balances, crop yields and crop water productivity under current and future projected climatic conditions.

Chapter 3 : Case Study, SWAP model and Database

This chapter is divided in to three sections. The first section briefly introduces the case study Hakra Branch Canal command with an overview of its general physical environment, soil condition, cropping pattern and irrigation systems. The second section introduces the Soil-Water-Atmosphere-Plant (SWAP) model and its soil water and salt flows and crop growth processes involved in the model simulations. The third section gives an overview of the SWAP modelling data requirements and its collection at the selected farmers' fields and at canal command scale.

3.1 Hakra Branch Canal command

3.1.1 Introduction

The case study for this research is the Hakra Branch Canal (HBC) command which is located between 29º 3` 35`` N to 29º 56` 3`` N latitude and 72º 14` 35`` E to 73º 26` 17`` E in the Bahawalnagar district of province Punjab of Pakistan (Figure. 3.1). The HBC off-take from the left bank of the Fordwah canal, which starts at the Sulemanki head works on the Sutlej river (Jehangir *et al.*, 1998). The canal water flow, cropping pattern and soil salinity conditions of HBC reflects most of the canal commands in Punjab Pakistan.

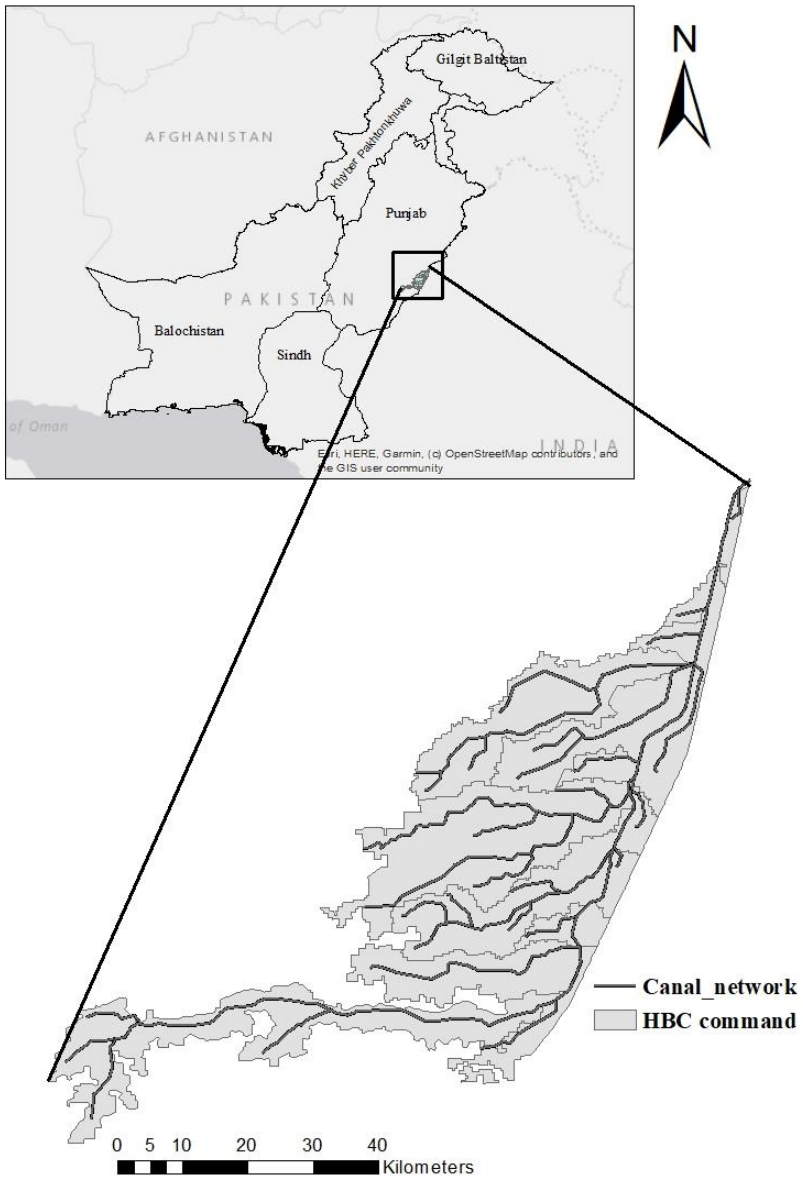

Figure 3.1: Location map of Hakra branch canal command in Punjab Pakistan.

3.1.2 Climate

The climate of the HBC command is characterized as being semi-arid with a large seasonal fluctuation in temperature and rainfall. Summer is hot and long, lasting from April to October. June is the hottest month, when the average maximum temperature over the recent 39 years (1979 to 2017) is recorded at 42 ^{o}C (Figure 3.2). The temperature frequently exceeds 48 ^{o}C in the month of May and June. Based on the mean monthly

records, January is the coldest month of the year, with the mean minimum and maximum temperature being recorded at 5.8 ^{o}C and 25.6 ^{o}C, respectively (Figure 3.2).

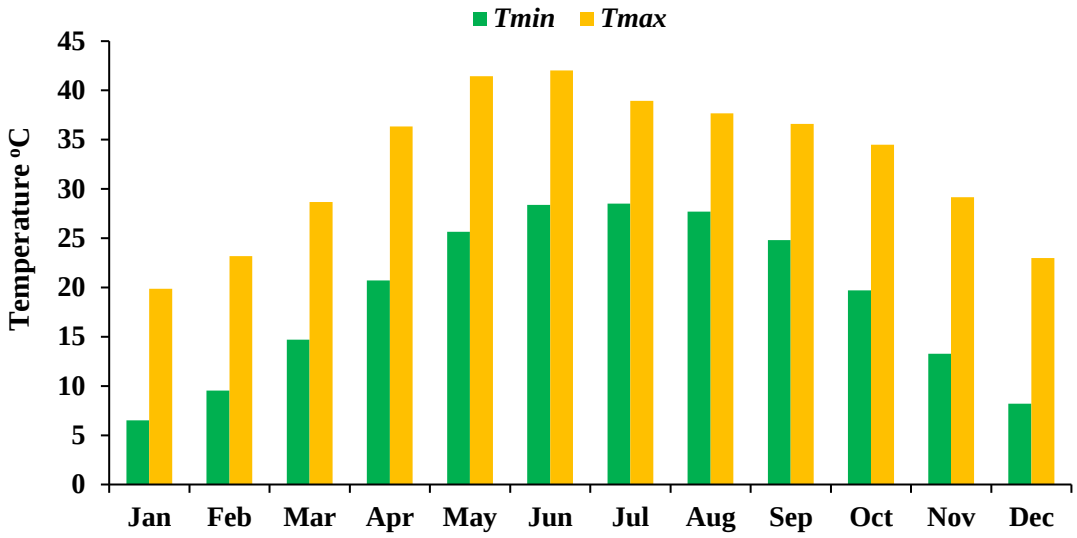

Figure 3.2: Monthly average minimum and maximum temperature in Hakra branch canal (HBC) command during the period from 1979-2017.

The mean annual rainfall in the HBC command area is recorded at 250 mm per year over period 1979 - 2017. The rainy season occurs from July to September and accounts for two-third of the total annual rainfall. One third of the annual rainfall falls in winter from January to March as low intensity frontal rain. A very dry period prevails from October to December. A comparison of rainfall P and reference evapotranspiration ET_o calculated with the FAO ET_o calculator model (Raes and Munoz, 2009) for period of 39 years (1979 to 2017) is presented in Figure 3.3. The months of May to August represents the maximum rates of ET_o, with the estimated values ranging on average from 200 (i.e., 6.5 mm per day) to 260 mm (8.4 mm per day).

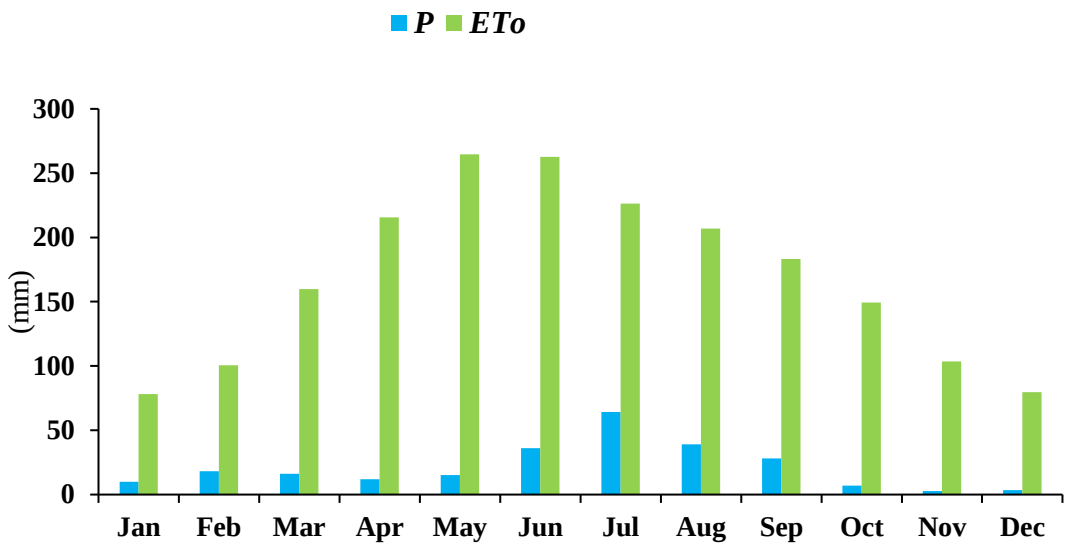

Figure 3.3: Monthly average rainfall (*P*) and reference evapotranspiration (ET_o) in Bahawalnagar (located in the HBC) during the period from 1979-2010.

In summary, the climate of the HBC command is characterized as being dry with extremes of temperature and very low rainfall. The average monthly rainfall is only 5 to 28% of ET_o in HBC (Figure 3.3). Crop production is not possible without adequate irrigation, even in the rainy season.

3.1.3 Soil

As with most of the soils in Indus basin, the soils of the HBC command are composed of alluvial materials carried from the Himalayan ranges by the Sutlej River and other tributaries of the Indus basin river system (Kahlown *et al.*, 1998). These soils comprise a high percentage of fine to very fine sand and silt. The soil texture varies from sandy to sandy clay loam, with a dominance of loam soils except a narrow strip of sandy clay loam along the tail reaches of the HBC. The surface soil is underlain by loamy sand to sandy loam subsoil layers. The soil is high to moderately permeable and has a low water holding capacity. The soil organic matter is extremely low (< 1%) and the bulk density ranges from 1.4 to 1.7 g cm^{-3} (Aamer *et al.*, 2015; W. Ahmad, 2017). The surface elevation varies from 130 m to 165 m above mean sea level and has a moderate slope along the

direction from northeast to southwest. Moreover, extensive areas of sand dunes are also found in Hakra branch canal command area.

The soils are in general intrinsically fertile and have a high potential for crop productivity. But due to water scarcity, poor farm management and the limitations of waterlogging and soil salinity the productivity of most of the land in the command area is adversely affected.

3.1.4 Crops and cropping pattern

The climatic conditions in HBC command allow two crops per year, that is the *kharif* (summer) crops and *rabi* (winter) crops. The HBC command is part of the cotton-wheat agro-climatic zone of the Indus basin, where the cotton-wheat combination is grown on more than 60 percent of the area (Figure 3.4). It is regarded as one of the top cotton producing regions of the Indus basin. The introduction of high yielding crop varieties coupled with intensive irrigation and increased use of fertilizers over recent years has increased the crop yields, especially for cotton (Sajjad Ali, 2013). Rice is also planted across about 10 percent of the area, specifically in the head reaches of the canal (Figure 3.4). Lower yielding and less water demanding crops such as mustard (rapeseed), gram (chickpea), and millet are also cultivated in rainfed, or in areas with limited irrigation supplies. However, cotton and rice are the main crops during the *kharif* (summer), and these are followed by wheat and mustard during the *rabi* (winter) season. The planting dates for the major crops are generally as follows:

Crop	**Planting time**	**Harvest time**
Cotton	April to mid-June	October to mid-November
Rice	May to July	October
Fodder	April	July
Gram	November	April
Mustard	November	Mid-March
Wheat	Mid-November to Mid-Dec	April to mid-May

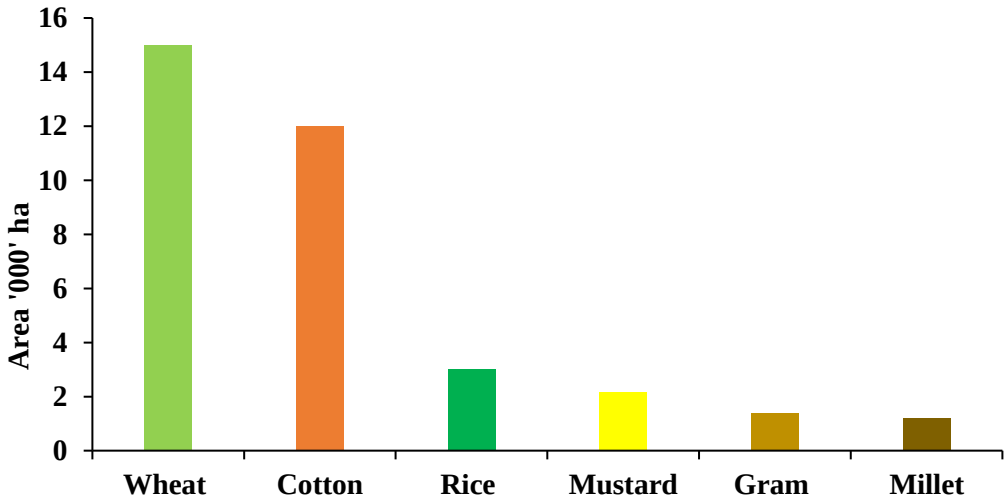

Figure 3.4: The crop area of major crops grown in Hakra command during the agricultural year 2016-2017 (CRS, 2017).

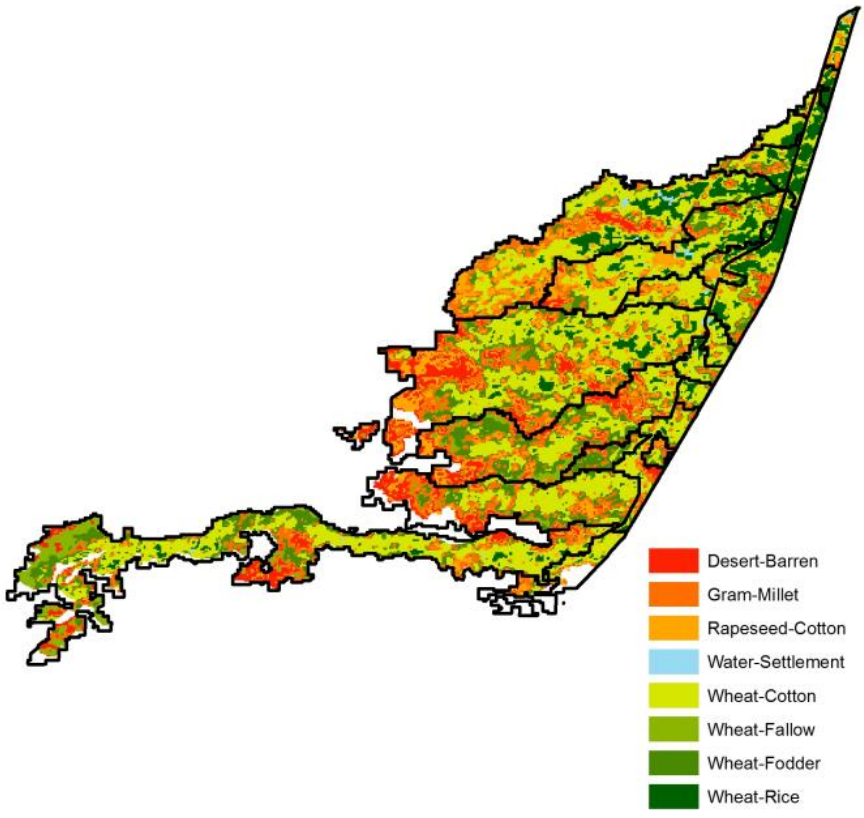

Figure 3.5: Spatial distribution of the cropping pattern in Hakra canal command in Punjab Pakistan (2014-2015) (Liaqat *et al.*, 2016)**.**

3.1.5 Canal water

The climate of the HBC command makes irrigation a prerequisite for intensive agriculture. As with most of the canal systems in the Indus Basin Irrigation System (IBIS) of Pakistan, the HBC is a run-off-river system where the main canal (Fordwah-Eastern Sadqia main canal) off-take directly from the river (here the Sutlej River) through headworks (here, the Sulemanki headworks) and divides into two or more branch canals (Malik and Hakra). Hence, the discharge in the canal system fluctuates with the discharge in the river. As a result of often limited and fluctuating water supply, the distributary canals are operated on a canal roster, where under any given *warabandi* interval, a group of distributaries are closed, and others are opened. According to Anwar and Ul Haq (2013) canal rostering help to operate the distributary at its full capacity at least once fortnightly. This ensures water flow to the field by gravity, which establish equity in terms supplying the rated discharge into the field channel and maintaining a non-silting and non-scouring flow velocity.

The total cultivable area of the HBC command is 203,616 hectares, which is further divided into 16 perennial and one seasonal distributary commands also called flood channel, that gets flow only during the *kharif* season. The distributaries are numbered sequentially with suffix L if the distributary falls to the left side of the HBC, and R for the right side of the HBC. Table 3.1 shows the name, design discharge and command area of each distributary in the HBC command area. The distributaries are managed by Farmer Organizations (FOs). However, the water delivery, measurement and canal rostering remain responsibility of the Provincial Irrigation Department (PID) of Punjab Pakistan. Table 3.2 shows typical canal roster for the HBC command for the agriculture year 2016–2017, as prepared and disseminated by the Provincial Irrigation Department. As per the roster (Table 3.2), the 17 distributaries are divided

into three groups (A, B and C), with each group further divided into two subgroups (A1, A2, B1, B2, C1 and C2). Each subgroup receives the approximately full-design depth (highest priority) after every two *warabandi* interval i.e., every fortnight to ensure equitable distribution of water among the distributaries.

Table 3.1: Characteristics of the distributaries supplied by the Hakra branch canal in Punjab, Pakistan (de Vries and Anwar, 2015).

Reach	Distributary Name	Discharge m^3s^{-1}	Area Hectares
Head	Baku Shah	0.17	609
	1L	2.35	6918
	1R	0.54	2009
	2L	0.54	1769
	2R	0.62	2147
	3R	10.00	29443
	4R	6.40	17586
Middle	3L	0.28	703
	4L	0.25	682
	5R	1.01	4270
	6R	15.5	41206
	7R	7.73	21795
	8R	0.68	2573
Tail	9R	6.00	19909
	Flood channel	2.00	6684
	Hakra Left	0.65	2418
	Hakra Right	14.00	42895

The canal water is distributed among the farmers at watercourse level according to the weekly fixed rotation *warabandi* for a specified time per week which is proportional to the landholding. The farmer decides to apply the allocated amount of canal water, usually through surface flooding to irrigate their fields. (Anwar and Ul Haq, 2013) used the Gini and Theil indices as measures of inequity for HBC command during the *rabi* of 2010-11. The application of these inequity indices showed that the average canal distributaries operation discharge is less than the design discharge, even under a high priority. Further

if the distributaries fall into the low, or lowest, priority in a given *warabandi* interval, the canals are generally operated below their design capacity. This results in command issues like the outlet not flowing at the rated discharge, the water level in the distributary below the field level, resulting in inequity between the canal outlets and low water velocities causing sedimentation problems.

Table 3.2: Canal roster for Hakra branch canal distributaries during the growing seasons of 2016-17 (Source: https://irrigation.punjab.gov.pk/).

Group A		1L, 4R, Hakra Right, Hakra Left
	SubGroupA1	Hakra Right, Hakra Left
	SubGroupA2	1L, 4R
Group B		BS, 1R, 2R, 3R, 5R, 2L, 7R, 3L, 4L, 8R, Flood Channel
	SubGroupB1	BS, 1R, 2R, 3R
	SubGroupB2	5R, 2L, 7R, 3L, 4L, 8R, Flood Channel
Group C		6R, 9R
	Subgroup C1	6R
	Subgroup C2	9R

Date		Group Priority			Subgroup Priority					
From	To	Highest	High	Low	Highest		High		Low	
16/04/2016	23/04/2016	A	B	C	A2	A1	B2	B1	C2	C1
24/04/2016	1/05/2016	C	A	B	C1	C2	A1	A2	B1	B2
2/05/2016	9/05/2016	B	C	A	B2	B1	C2	C1	A2	A1
10/05/2016	17/05/2016	A	B	C	A1	A2	B1	B2	C1	C2
18/05/2016	25/05/2016	C	A	B	C2	C1	A2	A1	B2	B1
26/05/2016	2/06/2016	B	C	A	B1	B2	C1	C2	A1	A2
3/06/2016	10/06/2016	A	B	C	A2	A1	B2	B1	C2	C1
11/06/2016	18/06/2016	C	A	B	C1	C2	A1	A2	B1	B2
19/06/2016	26/06/2016	B	C	A	B2	B1	C2	C1	A2	A1
27/06/2016	4/07/2016	A	B	C	A1	A2	B1	B2	C1	C2
5/07/2016	12/07/2016	C	A	B	C2	C1	A2	A1	B2	B1
13/07/2016	20/07/2016	B	C	A	B1	B2	C1	C2	A1	A2
21/07/2016	28/07/2016	A	B	C	A2	A1	B2	B1	C2	C1
29/07/2016	5/08/2016	C	A	B	C1	C2	A1	A2	B1	B2
6/08/2016	13/08/2016	B	C	A	B2	B1	C2	C1	A2	A1
14/08/2016	21/08/2016	A	B	C	A1	A2	B1	B2	C1	C2
22/08/2016	29/08/2016	C	A	B	C2	C1	A2	A1	B2	B1
30/08/2016	6/09/2016	B	C	A	B1	B2	C1	C2	A1	A2
7/09/2016	14/09/2016	A	B	C	A2	A1	B2	B1	C2	C1
15/09/2016	22/09/2016	C	A	B	C1	C2	A1	A2	B1	B2
……..	……..	……..	……..	……..	……..	……..	……..	……..	……..	……..
……..	……..	……..	……..	……..	……..	……..	……..	……..	……..	……..
……..	……..	……..	……..	……..	……..	……..	……..	……..	……..	……..
……..	……..	……..	……..	……..	……..	……..	……..	……..	……..	……..
……..	……..	……..	……..	……..	……..	……..	……..	……..	……..	……..
……..	……..	……..	……..	……..	……..	……..	……..	……..	……..	……..
10/03/2017	17/03/2017	B	C	A	B1	B2	C1	C2	A1	A2
18/03/2017	25/03/2017	A	B	C	A2	A1	B2	B1	C2	C1
26/03/2017	2/04/2017	C	A	B	C1	C2	A1	A2	B1	B2
3/04/2017	10/04/2017	B	C	A	B2	B1	C2	C1	A2	A1

Furthermore, the canal water is allocated on a constant time per unit area without taking

in to account the seepage losses along the channel which causes another issue of inequitable water distribution at the secondary and tertiary levels (Hamid *et al.*, 2000). The rate of seepage losses from the canal increases with the increase in the length of the canal. Thus, farmers in the tail reaches get much less water as compared to those in the head reaches. According to Qureshi (2014), the tail enders get 20% less water than the farmers in the head reaches.

3.1.6 Groundwater

The deficit in the canal water supply is supplemented by using groundwater in the HBC command. The groundwater in HBC command is shallow (< 3m) in the head reaches and gradually becomes deeper in the tail reaches (> 20 m). The seepage and percolation losses over the years from the canal networks have established a shallow watertable of relatively good water-quality in areas along the canal networks. This encourages the farmers to install shallow tube-wells along the HBC and its distributaries. According to Awan *et al.* (2016), in the head reaches of the canal, about 45% of irrigation supply dependence comes from groundwater. It is estimated 37% in the middle reaches, and 18% in the tail reaches. They further suggested that the reason for low abstraction of groundwater in the tail reaches is due to greater depth of the water table which increases pumping cost, and that the quality of water is poor due to high salinity (EC > 12 dS m^{-1}). There are no official estimates of the number of tube wells in the HBC command, however, Bhatti *et al.* (2017) quantified the tube well density as about 24 tube wells per thousand hectares in the HBC command. The tube wells are usually concentrated in good groundwater areas. On average every fourth farmer has a tube well and a large number of non-owners purchase groundwater from the locally fragmented market (Qureshi *et al.*, 2003).

The groundwater quality deteriorates from the head to tail reaches of the system (Latif, 2007). The use of this poor quality of groundwater creates the problem of secondary

salinization, which is the major threat to the low productivity and food security of the area. Conjunctive use of canal water and groundwater is also practised, particularly in poor groundwater quality areas of the canal command. According to Qureshi (2014) about 33% of the head reaches of the command area have depths to the water table that fluctuate around 1 meter below soil surface. In the middle reaches it is between 2 to 4 m and >4 meters in the tail reaches.

3.1.7 Waterlogging and Soil Salinity

Waterlogging and soil salinity is highly variable in the HBC command. The extent of waterlogging is higher at the head reaches whereas the soil salinity is relatively high at the tail reaches of the canal command. This is mainly due to inequitable and insufficient supply of good quality canal water (Awan *et al.*, 2016). The high rate of seepage losses due to unlined canal network and cultivation of high-water consuming crops such as rice causes the rise of water table. Most of the head reaches of the HBC command have water table ranges from <1 m to 2 m (Qureshi, 2014). The groundwater quality is relatively better (< 2 dS m^{-1}) at the head reaches as compared to the tail reaches of the canal command. The limited supply of canal water compels the farmers at the tail reaches to use poor quality groundwater. According to Qureshi (2014) more than 80% of the HBC command area has soil salinity between 2 to 4 dS m^{-1}, whereas the rest of the command area has soil salinity level higher than 15 dS m^{-1} particularly in the tail reaches.

3.2 Soil-Water-Atmosphere-Plant (SWAP) Model

To improve soil water management and increase crop water productivity, the cause-effect relationship between soil hydrological components such as soil evaporation, crop transpiration, percolation, salt build-up and biophysical components such as crop yield and dry matter production must be quantified in a soil-water-plant-atmosphere continuum. The spatial and temporal quantification of these complex soil hydrological and biophysical variables is a complicated process due to expensive, laborious and time-consuming field experiments, especially at canal command scales. However, with the development of computer-based simulation models the required soil hydrological and biophysical variables can be quantified from field- to canal-command scales. In the next section a detail description of the selected agrohydrological model, Soil-Water-Atmosphere-Plant (SWAP) is discussed.

3.2.1 Introduction

The SWAP is a physically-based agrohydrological simulation model that simulates transport of water, solutes and heat in a variably saturated topsoil and considers interactions with plant growth in the soil-water-plant-atmosphere continuum (Figure 3.7). The development of SWAP was started by Feddes (1971) as SWATR as part of his PhD dissertation at Wageningen University in the Netherlands. It was further developed by Feddes *et al.* (1978) as SWATRE with extended boundary conditions and improved numerical solutions. After 1990 there have been further developments and applications of SWATRE. New modules like solute transport (Smets *et al.*, 1997), generic crop-growth modules, soil heterogeneity and heat flow (van Dam *et al.*, 1997) were added, and the model was renamed as SWAP (Kroes *et al.*, 2008). The SWAP program is written in the standard FORTRAN language and is designed for integrated modelling of Soil-Atmosphere-Water-Plant system. It can be downloaded free of cost from

www.swap.alterra.nl. The simulation of solute and water transport processes are considered at the field scale level across the entire growing season.

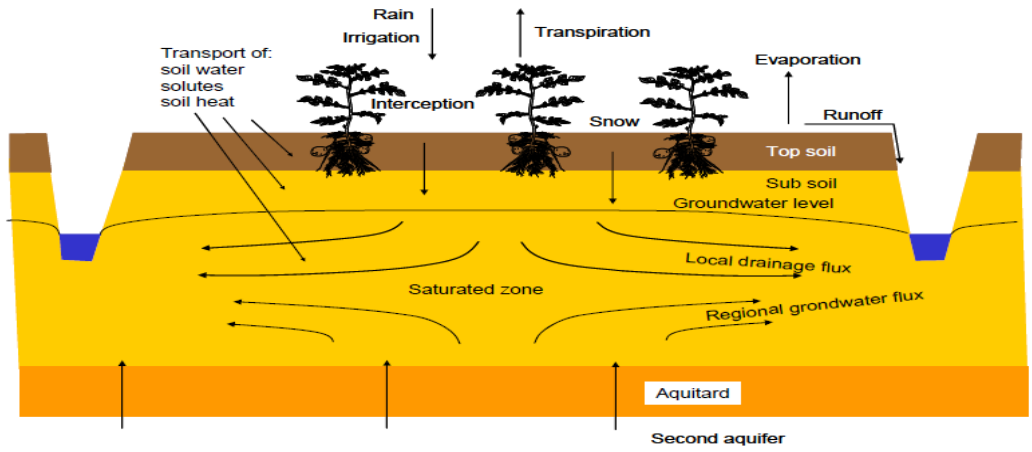

Figure 3.6: SWAP model domain and transport (Kroes *et al.*, 2008).

The crop growth model, *World Food STudies* (*WOFOST*) (Spitters *et al.*, 1989; Supit, 1994) is fully integrated with SWAP. Soil surface and atmospheric conditions are defined as the upper boundary condition, and unsaturated zone down from the soil surface to the ground water level is the lower boundary condition (Figure 3.6). The SWAP model simulates physical processes related to soil-water flow, solute flow, crop growth, surface water management, evapotranspiration and rainfall, and irrigation scheduling (van Dam *et al.*, 1997; Singh *et al.*, 2006a; Kroes *et al.*, 2008). Modelling concepts of these processes are briefly summarized below:

3.2.2 Soil water flow

Gravity and the spatial variation in the soil water potential causes the flow of soil water. To quantify these fluxes SWAP solves Richards' equation in combination with Darcy's law and the well-known continuity equation. To compute transient water flow, Richards' equation is:

$$C(h)\frac{\partial h}{\partial t} = \frac{\partial}{\partial z}\left[K(h)\left(\frac{\partial h}{\partial z} + 1\right)\right] - S(z) \qquad \text{Eq. 3.1}$$

where, C is the differential soil water capacity (the rate of change of moisture content θ with soil water pressure head h) [L^{-1}], K the hydraulic conductivity [$L\ T^{-1}$], h is the soil-water pressure head [L], t is the time [T], z is the vertical coordinate [L] positive upward, and S is the root water extraction rate [T^{-1}].

The SWAP model solves Richards' equation (3.1) numerically, using an implicit finite difference scheme, subjected to specified initial and soil profile's upper and lower boundary conditions, and known relationships between soil hydraulic variables such as soil moisture content θ, pressure head h, and hydraulic conductivity K for the unsaturated soil zone (van Dam and Feddes, 2000). The expression for analytical characteristic function $\theta(h)$ is described by (van Genuchten, 1980) as:

$$\theta(h) = \theta res + (\theta sat - \theta res)(1 + |\alpha h|^{n})^{-m} \qquad \text{Eq. 3.2}$$

where, θres is the residual soil moisture content [$L^3\ L^{-3}$], θsat is the saturated soil moisture content [$L^3\ L^{-3}$], α [L^{-1}], n and m are the empirical shape factors. The m factor is set equal to:

$$m = 1 - \frac{1}{n} \qquad \text{Eq. 3.3}$$

The above $\theta(h)$ relation is applied to the (Mualem, 1976) model of the unsaturated hydraulic conductivity function, which results in the following $K(\theta)$function:

$$K(\theta) = K_{sat}\, S_e^{\lambda}[1 - (1 - S_e^{-m})^{m}]^2 \qquad \text{Eq. 3.4}$$

where, $K_{sat}$is the saturated hydraulic conductivity [$L\ T^{-1}$], λ is the shape parameter depending on $\frac{\partial K}{\partial h}$, and S_e is the relative saturation defined as:

$$S_e = \frac{\theta - \theta_{res}}{\theta_{sat} - \theta_{res}}$$ Eq. 3.5

The upper boundary conditions of the unsaturated soil zone are described by the reference evapotranspiration rate ET_p, irrigation I, and rainfall P. The SWAP model uses Penman-Monteith equation (Allen *et al.*, 1998a) for calculation of ET_p from daily meteorological data of air temperature, solar radiation, relative humidity, and wind speed. The upper boundary conditions are important for accurate simulation of rapidly varying soil water fluxes near the soil surface. This situation occurs with infiltration, or runoff, events during intensive rain, or when the soil gets flooded by irrigation (van Dam *et al.*, 1997).

Under actual field conditions where the soil surface is partly covered by the crop canopy, the ET_p is partitioned into potential soil evaporation E_p and potential transpiration T_p using leaf area index (LAI) as function of crop development stage, as follows:

$$E_p = ET_p \, e^{-K_{gr} LAI}$$ Eq. 3.6

where, K_{gr} is the light extension coefficient for global solar radiation [-].

When the soil is wet the actual soil evaporation E is controlled by atmospheric demand and equals to E_p. Whereas under dry soil conditions, E is controlled by the maximum soil water flux E_{max} [L T^{-1}] in the topsoil and is computed by Darcy's law as follows:

$$E_{max} = K_{1/2} \left(\frac{h_{atm} - h_1 - z_1}{z_1} \right)$$ Eq. 3.7

where, $K_{1/2}$ is the mean hydraulic conductivity [LT-1] between surface and the top node, h_{atm} is the soil-water pressure head [L] in equilibrium with air humidity, and h_1 and z_1 are the soil water pressure head [L] and the soil depth [L], respectively of first node of soil profile.

However, rain splashing, dry crust formation, root growth and other cultural practices, may affect the soil hydraulic function of the topsoil layer. Consequently, Darcy's law may overestimate the actual soil evaporation flux *E* (van Dam and Feddes, 2000). To overcome such affects in SWAP, in addition to Eq. 3.7, the empirical function of Black *et al.* (1969) can be used to compute soil evaporation rate E_{emp} and limits the actual soil evaporation rate *E* to the minimum value of E_p, E_{max} and E_{emp}.

The potential transpiration flux T_p [LT^{-1}] is computed as

$$T_p = \left(1 - \frac{P_i}{ET_{p0}}\right) ET_p - E_p \qquad \text{Eq. 3.8}$$

where, P_i is the intercepted rainfall [LT^{-1}] by vegetation, ET_{p0} is the potential evapotranspiration of wet crop assuming zero crop resistance. Here $\frac{P_i}{ET_{p0}}$ represents the daylight fraction of intercepted water evaporation.

The actual transpiration *T* is controlled by root-water extraction and depends on the rooting depth, root distribution and soil water pressure heads across the root zone. For practical reasons, a homogeneous root distribution over the rooting depth is assumed. The maximum root water extraction rate is computed by distributing T_p over the rooting depth as follows:

$$S_p(z) = \frac{T_p}{D_{root}} \qquad \text{Eq. 3.9}$$

where, $S_p(z)$ is the potential root water extraction [T^{-1}] and D_{root} is the rooting depth.

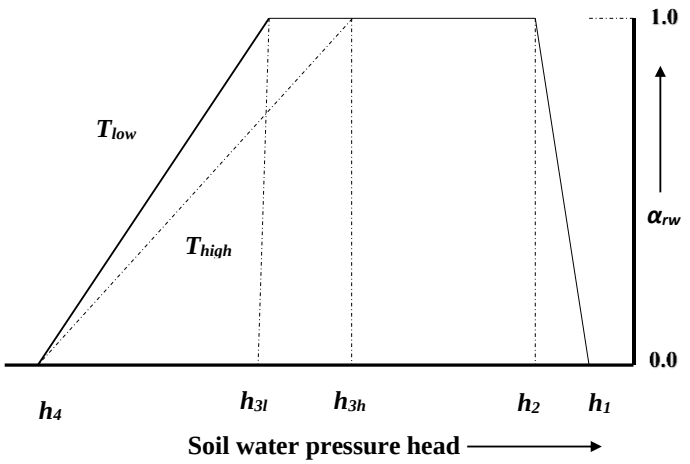

Figure 3.7: Root water extraction reduction coefficient α_{rw} as function of soil water pressure head h and potential transpiration rate T_p (Feddes *et al.*, 1978)

Under non-optimum conditions the stresses either due to being too dry or too wet (water stress) and high salinity concentrations (salt stress), $S_p(z)$ reduces to the actual root water extraction $S_a(z)$ (Eq. 3.10). In case of water stress, SWAP incorporates the water stress reduction function proposed by (Feddes *et al.*, 1978) as shown in Figure 3.7. For dry conditions, the critical soil water pressure head h_3 depends on T_p. The soil water pressure head variables of h_1, h_2, h_{3l}, h_{3h} and h_4 are crop specific and can be found from the literature (Taylor and Ashcroft, 1972; Doorenbos and Kassam, 1979; Smith, 1992).

For salt stress, the Maas and Hoffman (1977) response function is used in SWAP. According to this function the crop yield can be linearly related to the salinity (measured as the electrical conductivity) of the soil profile. Crops tolerate salt stress up to certain threshold limit, after which the yield reduces linearly with the increasing salt concentration in the soil (Figure. 3.8).

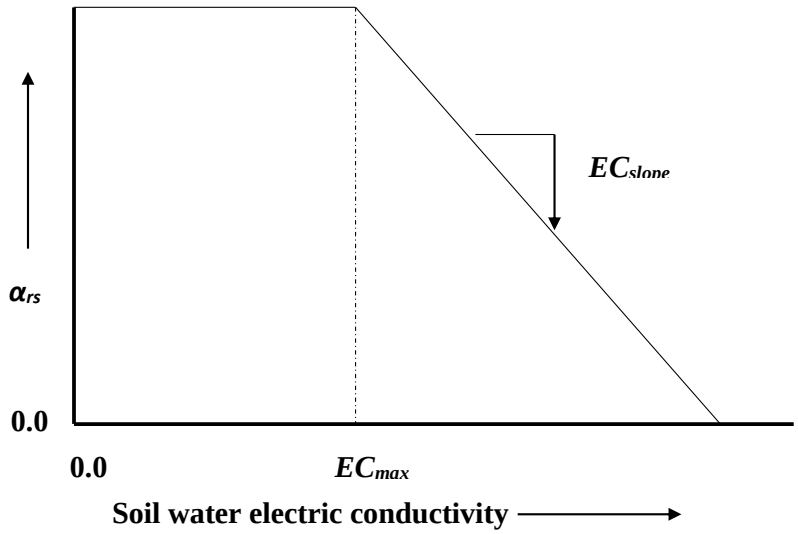

Figure 3.8: Root water extraction reduction coefficient α_{rs} as a function of soil water electrical conductivity *EC* (Maas and Hoffman, 1977).

According to Cardon and Letey (1992), the SWAP model computes the actual root water extraction rate $S_a(z)$ [T^{-1}] as the product of both the water and salt stress and potential water extraction rate $S_p(z)$, as follows:

$$S_a(z) = \alpha_{rw}\, \alpha_{rs}\, S_p(z) \qquad \text{Eq. 3.10}$$

where, α_{rw} is the reduction coefficient due to water stress [-], and α_{rs} is the reduction coefficient due to salt stress [-]. Finally, the actual transpiration is computed from the integration of $S_a(z)$ over the rooting depth.

The bottom boundary condition of SWAP can either be the bottom of the unsaturated zone, or the upper part of the saturated zone. These define the fluxes at the bottom of the soil profile. In case of a deep groundwater level (> 3 m) a free drainage condition is applied by assuming the pressure head gradient equal to be zero so that the bottom flux is:

$$q_{bot} = -K(h)\left(\frac{\partial h}{\partial z} + 1\right) = -K(h)(0+1) = -K(h) \quad \text{Eq. 3.11}$$

In case of shallow groundwater level (< 3m) the measured groundwater level as function of time can be specified as the bottom boundary condition (Kroes *et al.*, 2008).

3.2.3 Solute transport

The SWAP model is designed as one-dimensional to simulate soil water and salt transport processes at field scale. The SWAP model focuses on the transport of solutes that can be described by the physical processes of convection, diffusion, and dispersion in the soil profile.

Solute transport through diffusion is caused by a solute gradient. The solute flux density J_{dif} is described by Fick's law:

$$J_{dif} = -\theta D_{dif} \frac{\partial c}{\partial z} \quad \text{Eq. 3.12}$$

where, D_{dif} is the diffusion coefficient [$L^2\ T^{-1}$], c is the solute concentration in soil water]M L^{-3}]. The D_{dif} is very sensitive to the actual soil water content as it provides the effective solute transport path and effective cross sectional transport area.

The solute transport through the convective flux J_{con} [M $L^{-2}\ T^{-1}$] is given by:

$$J_{con} = qc \quad \text{Eq. 3.13}$$

where, q is Darcy's water flux density [L T^{-1}]

The dispersion flux J_{dis} [M $L^{-2}\ T^{-1}$] of the solute transport is given by:

$$J_{dis} = -\theta D_{dis} \frac{\partial c}{\partial z} \quad \text{Eq. 3.14}$$

where, D_{dis} is the dispersion coefficient [$L^2\ T^{-1}$]. Under laminar flow conditions D_{dis} is proportional to pore water velocity of $v = {}^{q}/_{\theta}$ (Bolt, 1979), and

$$D_{dis} = L_{dis}|v| \qquad \text{Eq. 3.15}$$

where, L_{dis} is the dispersion length [L].

The total solute flux J [M L^{-2} T^{-1}] is described as follows:

$$J = J_{dif} + J_{con} + J_{dis} = qc - \theta\left(D_{dif} + D_{dis}\right)\frac{\partial c}{\partial z} \qquad \text{Eq. 3.16}$$

Under irrigated field conditions the diffusion process is much slower than the dispersion and convective processes and is neglected in this study. Hence, in this study, salt transport is simulated as Eq. 3.16 reduces to:

$$J = qc - \theta D_{dis}\frac{\partial c}{\partial z} \qquad \text{Eq. 3.17}$$

The continuity equation for solute transport can be derived by considering conservation of mass in an elementary soil volume:

$$\frac{\partial X}{\partial t} = -\frac{\partial J}{\partial z} - S_s \qquad \text{Eq. 3.18}$$

where, X is the total solute concentration in the soil profile (θC) [M L^{-3}], S_s is the solute sink term [M L^{-3} T] that accounts for transformations and root uptake. Neglecting transformations in the case of salt and root uptake Eq. 3.18 takes the form, as follows:

$$\frac{\partial \theta c}{\partial t} = \frac{\partial}{\partial z}\left[\theta D_{dis}\frac{\partial c}{\partial z}\right] - \frac{\partial qc}{\partial z} \qquad \text{Eq. 3.19}$$

Eq. 3.19 is the one dimensional, dynamic, convective-dispersive salt transport equation that simulates salt balance and salt stress on root water uptake in saturated and unsaturated soils (Van Genuchten and Cleary, 1979; Boesten and Van der Linden, 1991). To solve Eq 3.19, SWAP requires the solute concentration in the irrigation water, rainwater and groundwater.

To calculate the electrical conductivity of the saturation extract, EC_{sat} (dS m^{-1}) from the soil water solute concentration c (mg cm^{-3}) the following equation is applied (Kroes *et al.*, 2008):

$$EC_{sat} = 1.492\, c_i \frac{\theta_i}{\theta_{sat}} \qquad \text{Eq. 3.20}$$

where θ_i is the simulated water content (cm^3 cm^{-3}) and θ_{sat} is the saturated water content (cm^3 cm^{-3}).

Soil Water and Salt balances

The SWAP model applies, the above described physically based processes, to quantify different components of soil water and salt balances of a soil profile, in close interactions with the vegetation growth. The soil water balance components simulated by SWAP for a vertical soil column with vegetation accumulated over a certain time period is given by:

$$\Delta W = P + I - R_s - P_i - T - E - E_w \pm Q_{bot} \qquad \text{Eq. 3.21}$$

where, ΔW [L^{-1}] is the change in soil water storage, P [L] is the rainfall, I [L] is the irrigation, R_s [L] is the surface runoff, P_i [L] is the rainfall intercepted by vegetation, T [L] is the actual transpiration, E [L] is the actual evaporation from the soil surface, E_w [L] is the evaporation from the ponding water surface, and Q_{bot} [L] is the water percolation from soil profile bottom (positive upward).

The salt balance of the soil profile over the given time interval can be expressed as:

$$\Delta C = PC_p + IC_i + Q_{bot}C_{bot} \qquad \text{Eq. 3.22}$$

where, ΔC is the change in soil salt storage [M L^{-2}], $PC_p$is the salt concentration in the rainwater [M L^{-2}], IC_i is the salt concentration in the irrigation [M L^{-2}], and $Q_{bot}C_{bot}$ [M L^{-2}] is the salt concentration in the bottom flux.

3.2.4 Crop growth

The SWAP model includes both simple and detailed crop growth modules. The simple module prescribes crop growth independent of soil water and salt conditions. The simple model is useful when crop growth is measured, and focus is on simulation of soil water and salt flows in the soil profile. In this module, the measured leaf area index, crop height and rooting depth are prescribed as a function of the crop development stage, that is either controlled by the temperature sum, or it can be linear with time. When the simple crop module is used, the effect of soil water and salt stress on crop production can be quantified using a simple linear relationship between relative yield and relative transpiration (de Wit, 1958; Hanks, 1974; Feddes, 1985) and this is described as:

$$\frac{Y}{Y_p} = \frac{T}{T_p} \qquad \text{Eq. 3.23}$$

where, Y and Y_p are the actual and potential crop yields [M L^{-2}], and T and T_p are the actual and potential transpiration [L].

The simple crop module does not compute the crop potential and actual yield. However, the yield response factors (Doorenbos and Kassam, 1979) may be defined for growing stages as a function of crop development stages. The simple crop module does not simulate any interaction between the crop growth, and the water and salt stress conditions.

The detailed crop module in SWAP implements the complex generic crop growth model *WOFOST* (Spitters *et al.*, 1989; Supit, 1994) for simulation of crop growth in close interactions with the dynamics of soil water and salt flows in the soil profile. The *WOFOST* model has the advantage of simulating potential and actual crop production,

by relating crop growth to water and salt stress. Figure 3.9 shows the main processes incorporated in *WOFOST*. The potential crop production depends on air temperature, solar radiation, and crop characteristics. The radiation energy absorbed by the crop canopy is the function of incoming solar radiation and the specific crop leaf area. About 50% of the incoming solar radiation is photo-synthetically active radiation (*PAR*) which are used in plant photosynthesis processes (Supit, 1994; Singh, 2005). Under optimal conditions of no water and salt stresses and in the absence of any pest, weed and nutrient deficiency, the potential photosynthesis determines the maximum level of crop production. The gross CO_2 assimilation rate is simulated by *WOSOST* and is based on the absorbed *PAR* by crop canopy and on the leaf characteristics. This potential CO_2 assimilation rate is reduced by water and salt stress under given field conditions and is quantified by the relative transpiration ratio of the actual to potential transpiration.

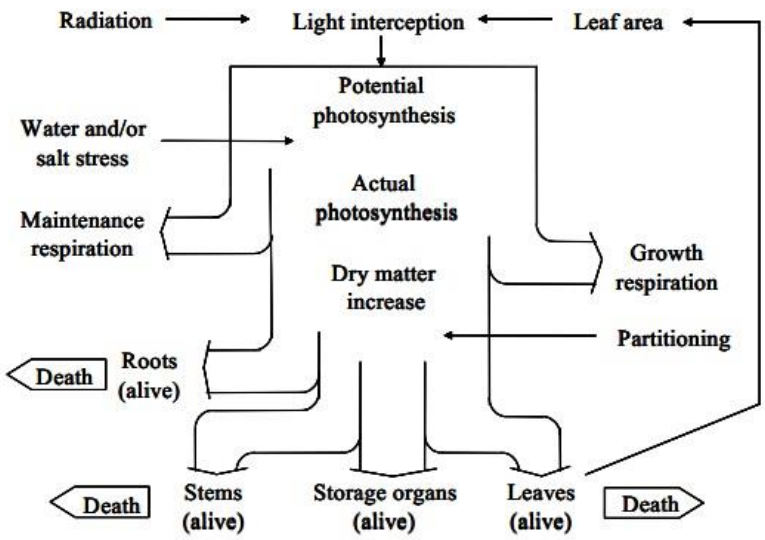

Figure 3.9: Schematisation of crop growth process involved in the WOrld FOod STudies (*WOFOST*) model (Spitters *et al.*, 1989) integrated in the Soil-Water-Plant-Atmosphere (SWAP) model (van Dam *et al.*, 1997; Kroes and van Dam, 2003)**.**

The light interception and CO_2 assimilation are the main driving forces in the crop growth processes that produce carbohydrates for biomass, maintenance respiration, and dry matter production. The dry matter produced is partitioned into root, leaves, stem and

storage organs as function of crop phenological development stage (Spitters *et al.*, 1989). Figure 3.10 represents the three-level hierarchies of productivity of crop growth that are growth defining, limiting and reducing factors (van Ittersum *et al.*, 2003). Growth defining factors determine the potential production that can be achieved without any stresses. These factors include radiation intensity, carbon dioxide concentration and crop growth characteristics like phenology, physiology and canopy architecture. The management of growth-defining factors depends on the decisions like sowing dates, sowing density and breeding. Growth-limiting factors consists of water, salt, nutritional, pest/disease, and weeds stresses under actual field conditions. The abiotic water and salt stress factors reduce the potential crop production due to water- and salt-limited crop production. Any growth-reducing factors due to biotic factors such as nutrient deficiency, weeds, pests and diseases reduce further reduces the water- and salt-limited crop production to actual crop production. The effective management of these growth factors help in developing sustainable crop production practices. The combination of all these growth factors results in prediction of crop productivity under actual conditions (van Ittersum *et al.*, 2003). However, the effects of nutrients deficiency, pest, weeds and diseases on crop growth have not been incorporated into SWAP, hence SWAP simulates only water- and salt-limited crop production. Also, current version of SWAP model did not consider any potential effects of changes in atmospheric CO_2 levels (due to climate change) on crop growth dynamics. Further details of the crop growth model can be found in (van Dam *et al.*, 1997; Kroes and van Dam, 2003).

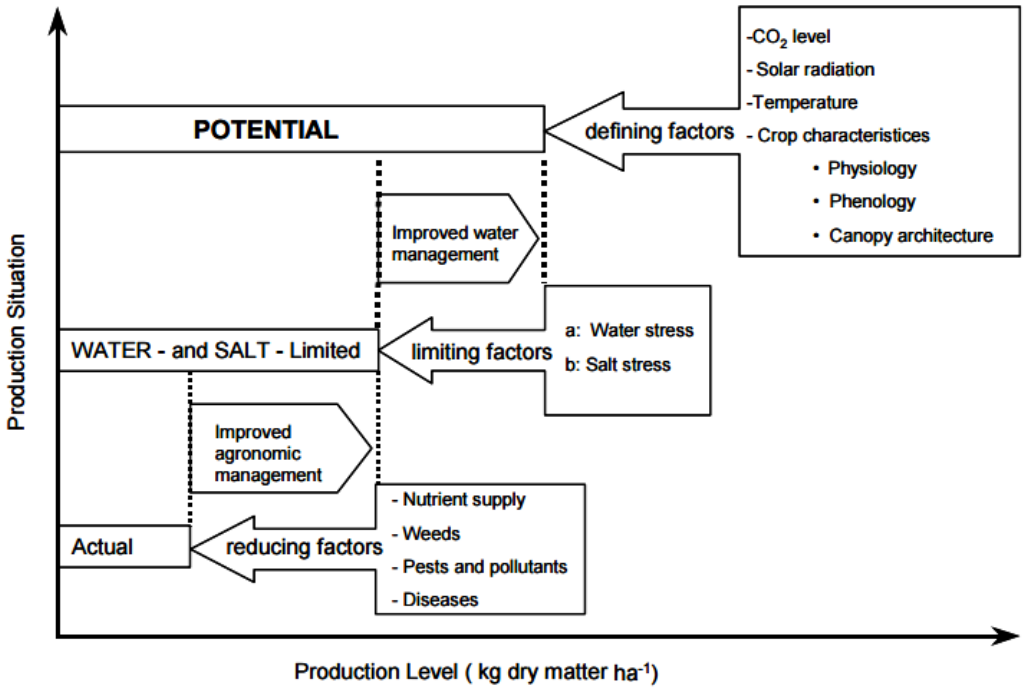

Figure 3.10: A hierarchy of crop production function. Adapted after (Lovenstein *et al.*, 1995) in (Singh, 2005).

3.2.5 Irrigation scheduling

Irrigation practices affect soil water flow and salt dynamics, that in turn affects crop growth and its yield in field conditions. The SWAP model has the capability to design efficient irrigation scheduling criteria based on several flexible options. Irrigation strategies may be applied with a fixed irrigation regime, or a scheduled irrigation regime. The fixed regime is defined by the fixed depth of irrigation at a given interval irrespective of the crop requirement. Whereas the scheduled regime defined by several criteria related to time and depth of irrigation application. A combination of fixed and schedule regime is also possible and that allows the evaluation of crop growth and crop water productivity in relation to various stages of water and salt stresses in the soil profile.

3.2.5.1 Fixed irrigation

In the fixed regime, a user-defined fixed application depth at defined dates is applied as a gross irrigation depth. Interception (losses) of irrigation water may occur depending

upon application type such as surface irrigation or sprinkling. The net irrigation depth is evaluated by:

$$I_n = I_g - E_i \qquad \text{Eq. 3.24}$$

where, I_n is the net amount of irrigation water [L T^{-1}], I_g is the gross supplied fixed irrigation water [L T^{-1}], and E_i is the interception loss of irrigation water [L T^{-1}]. The interception (losses) of irrigation water is assumed to evaporate on the same day of irrigation event.

3.2.5.2 Schedule irrigation

The irrigation scheduling criteria define the type of irrigation, either surface or sprinkler, and the time when irrigation should take place, as well as how much depth of irrigation to apply. A specified combination of time and depth criteria as function of crop development stage can be defined during the cropping season until the end of crop growth.

According to the rate of soil water depletion through evapotranspiration and percolation, the timing of the next irrigation interval is automatically calculated by taking account of the given weather, groundwater conditions, root water uptake and water flow through capillary rise. Five different timing criteria that can be used to generate the irrigation schedule include:

- Allowable daily stress (i.e., relative transpiration) on the crop
- Allowable depletion of readily available water in the root zone
- Allowable depletion of total available water in the root zone
- Allowable depleted amount of water in the root zone
- Critical pressure head or moisture content at sensor depth

In the application depth criteria two options are used to schedule the irrigation, as described below.

Back to field capacity

A certain depth of irrigation water is applied as per the defined time criteria to bring the soil moisture back to field capacity. An additional amount of irrigation can be defined to leach salts. This option is useful in case of sprinkler and micro irrigation, which allows variation in application depth according to the crop water requirement.

Fixed irrigation depth

A specified amount of fixed irrigation depth is applied to the field according to the defined time criteria. This option applies to most gravity surface irrigation systems, which allows little variation in irrigation application depth.

3.3 Overview of data collection

The accurate simulations by well-defined agrohydrological models such as SWAP requires calibration and validation of their input parameters with existing environmental conditions. A comprehensive data collection at field and command scale is executed at the case study (HBC) for the calibration and validation of the SWAP model. This section provides description of the data required, and sources and methodology used for the data collection in HBC area. The data used in this study are derived from two different sources: field experiments at selected farmers' fields and from existing secondary sources such as literature, and from allied research organizations. Moreover, the required data and information have been classified into two main categories: field- and canal command-scale.

3.3.1 Field scale

Field observations were conducted for the two main crop combinations of cotton-wheat and rice-wheat at selected farmers' fields in the HBC command during the agricultural year 2016-2017. In total four farmers' fields, with two cotton-wheat being denoted as CW1 and CW2 and the two rice-wheat fields denoted as RW1 and RW2, were selected in the HBC command (Figure. 3.11). The selection of the farmer's fields was based on the location within the irrigation system (head, middle and tail), crop rotation, soil, water sources, and groundwater conditions and the extent of salinity and waterlogging problems. The fields RW1 and RW2 were located (Figure 3.11) at the head reach of the 4R distributary canal with sufficient access to canal and groundwater. Here, the soil texture varies from silt loam to sandy loam, and this provides suitable growing conditions for rice-wheat cultivation. However, the RW1 field was affected with waterlogging and saline conditions with no significant drainage system and the groundwater level < 1m below ground level.

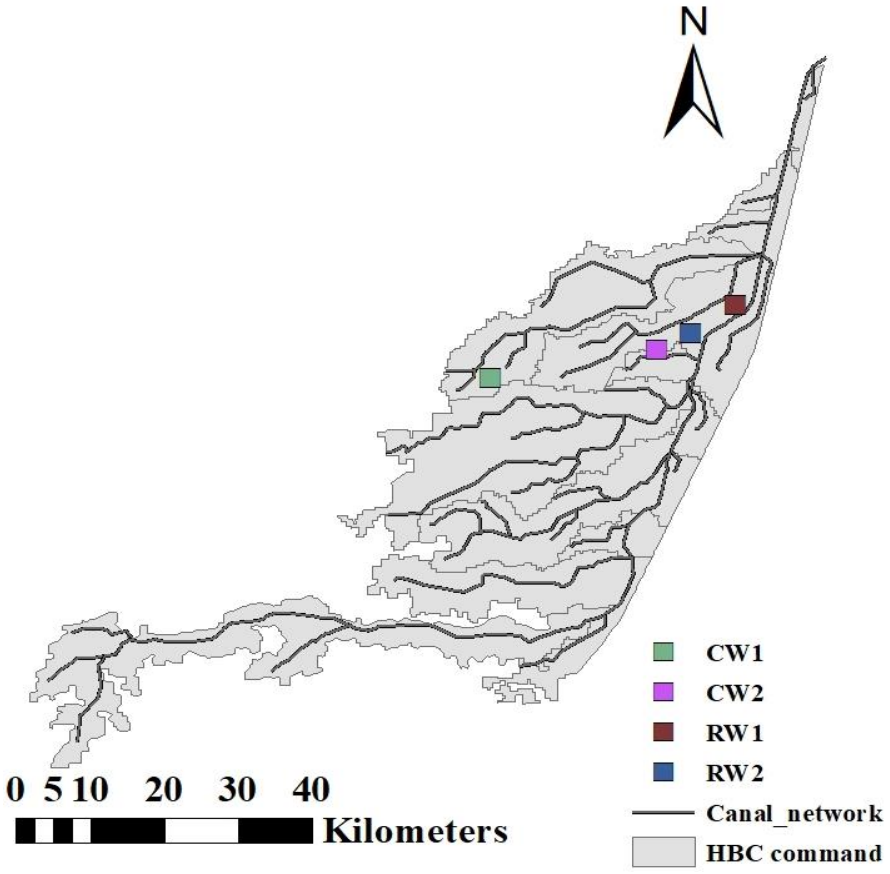

Figure 3.11: Location of the selected farmers' fields in the Hakra Canal Command in Punjab Pakistan. CW denotes cotton-wheat fields and RW denotes rice-wheat fields.

The dominant cotton-wheat combination is grown on a light textured soil such a sandy loam to loamy sand. The field CW1 was located (Figure 3.11) at the tail reach of the 3R distributary with no supply of canal water in the *kharif* (summer) season. The main source of irrigation at CW1 was groundwater. The quality of the groundwater was poor (> 3 dS m^{-1}) and at a greater depth (> 3m). The CW2 field was located (Figure 3.11) at the middle reach of the 5R distributary. The good supply of canal water and high-quality groundwater provides suitable growing conditions for cotton-wheat cultivation at this field.

The selected fields were intensively monitored for detailed soil, water and crop growth parameters. An overview of the data collected at the selected farmers' fields in HBC command is presented in Table 3.3. The collected data were used for the input parameters to the SWAP model for calibration and validation and these were categorized into climate, soil, water, and crop parameters. The daily climate data was used by SWAP to calculate the reference evapotranspiration rate. The climate data includes daily maximum, and minimum temperature, solar radiation, relative humidity, wind speed, rainfall and these were sourced from the meteorological station installed at the International Water Management Institute's (IWMI) field office at Haroonabad, in the district of Bahawalnagar located in the study area. In the case missing data and errors, then data from Pakistan Metrological department (PMD) station district Bahawalnagar are used.

For the soil parameters, soil samples were obtained from the depths of 0-15, 15-30, 30-60, 60-90 and 90-120 cm in the selected farmer's fields. The soil samples were analysed for basic physio-chemical properties such as, soil texture, bulk density, saturation percentage, hydraulic conductivity, pH, electrical conductivity and organic carbon. Moreover, soils samples were frequently taken before and after irrigation, plus any rainfall events, for soil moisture and electric conductivity determinations for the SWAP calibration and validation.

For the irrigation regime, the source (canal/groundwater), timing, amount and quality of each irrigation were recorded. At the rice-wheat RW1 and RW2 fields, the major source of irrigation was from canal water. However, due to limited canal water, tubewell-water supplements the canal water in the *kharif* season depending on canal rostering. The discharge of the canal water was measured by an electronic flow meter, where a volumetric method was used to measure the discharge of the tubewells. The timings of

irrigation events were recorded to calculate the amount of irrigation water applied at each field.

Table 3.3: Overview of the data collected at the selected farmer's fields for calibration and validation of SWAP model in HBC command area.

Data	Collection method	Frequency	Purpose
Metrological data			
Max, Min Temperature, Relative Humidity, Solar Radiation, Wind Speed, Rainfall	Pakistan Metrological department (PMD) and International Water Management Institute (IWMI) Met station in Haroonabad Field office (Study area)	Daily	Input data
Soil physio-chemical properties			
Texture	USDA Classification	Once	Input data
Bulk Density	Core method	Once	Input data
Saturated hydraulic conductivity	Constant water head method	Once	Input data
Organic carbon	Wet digestion method	Once	Input data
Saturation percentage	Saturation past method	Once	Input data
Soil moisture	Gravimetric method	Before and after Irrigation	Calibration and validation
pH	Soil-water suspension (1:5) by pH meter	Once	General
Electric Conductivity	Soil-water suspension (1:5) by Conductivity meter	Before and after Irrigation	Calibration and Validation
Irrigation			
Discharge of irrigation source i.e canal water or groundwater	current meter/ volumetric method	At each irrigation	Input data
Duration of irrigation	Warabandi/Field observation	At each irrigation	Input data
Irrigation depth	Discharge * Flow Duration/Field Area	At each irrigation	Input data
Irrigation quality	Conductivity meter/Field observation	At each irrigation	Input data
Crop growth parameters			
Crop development stage after sowing i.e emergence, panicle initiation, anthesis, maturity and harvest	Field observation	4-5 times	Input data
Plant density and tiller	Field observation	4-5 times	Input data
Plant height	Field observation	4-5 times	Input data
Dry matter partitioning	Field observation	4-5 times	Calibration and Validation
Rooting depth	Auger method	3-4 times	Input data
Crop yields	Field observation	At harvest	Calibration and Validation

The crop growth parameters such as the dates of the main phenological stages of sowing, emergence/transplanting, panicle initiation, anthesis, maturity and harvest were recorded. In addition, the plant density, number of tillers, crop height, rooting depth, dry matter production were also recorded at different stages depending on the crop growth period. All these observations were performed from randomly selected plants at three locations over the entire field.

The collected information from the selected farmers' fields was used to calibrate and validate SWAP at the field scale. The saturated soil moisture content ranges from 31 to 45% in the rice-wheat fields and 29 to 40% in the cotton-wheat fields. The bulk density varied from 1.47 to 1.89 g cm^{-3} for the rice-wheat fields, and from 1.58 to 1.76 g cm^{-3} for the cotton-wheat fields. The organic carbon was low all the fields (<0.5%) and the soil is sodic in nature with *pH* ranging from 75 to 9.0. The ground water at RW1 field was shallow (< 1 m, below ground level), whereas at the cotton-wheat it was deep (>3m, below ground level). The observed soil moisture and salinity before and after each irrigation intervals were used for calibration and validation of soil hydraulic parameters in SWAP at the field scale.

3.3.2 Canal command scale

At the canal-command scale, a substantial amount of spatial and temporal information on climate, land use, soil, irrigation and groundwater were acquired to develop a distributed application of SWAP model at the canal-command scale (Table 3.4). The long-term climate data (1979 to 2017) were obtained from the Pakistan metrological department for the district of Bahawalnagar. The data include maximum and minimum temperature, relative humidity, wind speed and rainfall. However, the data of solar radiation was downloaded from NASA website using R package '*nasapower*' (Sparks, 2018).

Table 3.4: Overview of the data collected for Hakra branch at the canal command scale.

Data	Source	Purpose	Availability
Climate data: Daily minimum and maximum temperature, Humidity, wind speed and Rainfall	Pakistan metrological department (PMD) and IWMI Metrological station at Haroon Abad and Lahore	Reference Evapotranspiration and Effective Rainfall	Available from 1979- 2017
Solar radiation	https://power.larc.nasa.gov	Reference Evapotranspiration	
Land use:	Satellite image, ground truth points	Cropping pattern and Land use map	(Liaqat *et al.*, 2016)
Canal inflow: Daily discharge diverted to the Hakra canal from head works	Irrigation department Bahawalnagar circle	Canal water supply	*https://irrigation.punjab.gov.pk/channel-line-diagram*
Canal network characteristics : Canal design dimensions, design discharge, area served (CCA)	Irrigation department Bahawalnagar circle	Canal water supply	IWMI database (2015-2016)
Ground water: Depth and quality	Provincial irrigation department. Ground water survey as part of this study	Groundwater (2016-2017)	*https://irrigation.punjab.gov.pk/*
Canal boundaries	Irrigation department Bahawalnagar circle	Distributary command map	IWMI database. (2015-2016)

The land-use information at the canal command scale is an important component for accurate distributed SWAP modelling of irrigation systems (Singh, 2005). Liaqat *et al.* (2016) performed satellite remote sensing analysis for producing a land use classification map of the HBC command. The map was developed at a spatial resolution of 250 m by

using the Normalized Difference Vegetation Index (NDVI) that is available from Moderate Resolution Imaging Spectro-radiometer (MODIS). The classification was based on the ISODATA clustering technique. In addition, a record of around 200 ground-truth points is used to check the accuracy and reliability of the land-use classification map (Liaqat *et al.*, 2016). According to the land-use map wheat was the single main crop during the *rabi* season, and cotton and rice are the main crops in the *kharif* season in HBC command area. The Programme Monitoring and Implementation Unit (PMIU) of the Provincial Irrigation Department (PID) was responsible for maintaining an online database of water flow in the canal networks of all the major canal system in the province of Punjab, including HBC. The daily discharge of all the distributaries of the HBC during the agricultural year 2016-2017 is sourced from the PMIU website. The area-related canal-water rights, called Culturable Command Area (CCA)were available at distributary canal level. The information on the groundwater level and water quality were obtained from the Directorate of Land Reclamation (DLR) of PID. The groundwater level and its quality was measured at 84 piezometers spread over the HBC command twice a year in June (pre monsoon) and in October (post monsoon). This groundwater information was collected for the year 2016 (pre and post monsoon) and the map of the groundwater level and quality was developed using kriging spatial-corelation technique in ArcMap. Most of the information at the canal command scale in HBC was available at the distributary command level. The boundary map of HBC distributaries command was obtained from IWMI database. The collected information was aggregated and processed at the distributary command map level and subsequently used in the aggregation of homogeneous units for simulations of their soil water and salt balances (*see* Chapter 6).

Chapter 4 : Calibration and validation of the SWAP model to quantify and assess soil water and salt balances, and crop water productivity at the field-scale

4.1 Introduction

In many arid and semi-arid regions, the productivity and sustainability of irrigated agriculture is threatened by a combined effects of climate change, soil degradation, limited water supplies, low irrigation efficiency and the over exploitation of groundwater (Marlet *et al.*, 2009). The Hakra Branch Canal (HBC) command, located in semi-arid areas of Punjab Pakistan (Figure.3.1) also suffers from problems of both rising and declining groundwater levels, waterlogging and secondary soil salinization and low crop yields (Kahlown and Azam, 2002; Latif and Pomee, 2003; Phuong *et al.*, 2015; Awan *et al.*, 2016). Current irrigation methods and practices at HBC significantly affect soil water and salt balances, and ultimately the crop water productivity. The recently conducted Revitalizing Irrigation in Pakistan (RevIIP) project funded by Kingdom of the Netherlands, in collaboration with International Water Management Institute (IWMI), carried out several studies on improved management of main canal water adequacy, and equity of canal water supply in the secondary canals of HBC. These studies provide insights into hydrology, equity in canal water distribution and system performance at canal command scale in HBC (Ahmad *et al.*, 2013; Bell *et al.*, 2014; de Vries and Anwar, 2015). However, there is limited research available on the long-term potential effects of current irrigation practices on soil water and salt balances, crop growth, and crop water productivity under limited canal water supplies and variable groundwater quality conditions in the study area.

According to Kijne (1996), a robust understanding of soil water and salt balances in planning and management of irrigation system is often been under estimated, especially on a long-term basis. A robust assessment of long-term effects of different irrigation practices requires quantification and analysis of soil water and salt balance components such as soil-water evaporation, transpiration, percolation, changes in soil water and salt

storages, and water- and salt-stress on crop growth under different soil water-crop-climate combinations.

Field experiments are expensive, practically limited and time consuming in the quantification of all the required soil water and salt-balance components, and crop growth parameters, especially for diverse soil-water-climate conditions, and on the long-term basis (Singh *et al.*, 2006a). However, well-developed agro-hydrological models, such as the Soil-Water-Atmosphere-Plant (SWAP) (van Dam et al., 1997), are useful tools to integrate field observations to evaluate the difficult-to-measure soil water and salt balances components, and crop water productivity (Mostafazadeh-Fard *et al.*, 2009). The physically based SWAP model (van Dam *et al.*, 1997), informed by the local field observations, offers a robust tool to conduct long-term simulations of soil water flow and salt transport processes, in interaction with crop growth dynamics at field scale (Singh *et al.*, 2006c), as well as at the regional scale (Singh *et al.*, 2006b). Woldegebriel (2011) demonstrated the application of SWAP model to simulate salt accumulation under drip irrigation system in Gediz basin of Turkey. Xue and Ren (2016) used SWAP to evaluate crop-water productivity under sprinkler irrigation at regional scale in Hetao irrigation China. SWAP provides detailed insights into the potential effects of various irrigation scenarios on soil water and salt balances, crop growth and its yields, and crop water productivity (Singh *et al.*, 2006c; van Dam *et al.*, 2008; Vazifedoust *et al.*, 2008). However, a robust application of agrohydrological models such as SWAP requires their calibration and validation using the local field observations of key input parameters (Singh *et al.*, 2006c; van Dam *et al.*, 2008; Vazifedoust *et al.*, 2008).

The research described in this chapter sought to analyse and use local farmer field observations to calibrate and validate SWAP model to simulate soil water and salt balances, and crop water productivity of main crops in HBC Command area, Punjab

Pakistan. The SWAP model was calibrated and validated for the main crops (cotton-wheat and rice-wheat) using observations from four local farmer's fields in the HBC. Most of the input parameters for SWAP were measured directly at the farmers' fields, whereas the unknown parameters such as soil hydraulic parameters are determined indirectly through an inverse modelling technique. A non-linear Parameter ESTimation program (PEST) (Doherty, 1994) is linked with SWAP for calibration and validation of key soil hydraulic parameters using the observed soil moisture and soil salinity in the experimental fields. The simulated water and salt balance components and crop yields were analysed to quantify key soil water management response indicators (WMRI) to assess the water stress, percolation, salt build up, relative yield, and the water productivity values of wheat, cotton, and rice crops during the agriculture year 2016-17. This provides the quantitative information and insights on the performance of current irrigation practices on crop water productivity and their sustainability in the semi-arid areas of Punjab Pakistan, and other similar regions elsewhere.

4.2 Field experiments and SWAP model input parameters

Two cotton-wheat fields (denoted as CW1 and CW2) and two rice-wheat fields (denoted as RW1 and RW2) located in HBC (Figure 3.11) were monitored for their crop cultivation and irrigation practices including detailed soil moisture, soil salinity and crop parameters during the agriculture year 2016-17. The sowing and harvesting dates for rice-wheat fields were defined from May 1st, 2016 to Oct. 31st, 2016 for rice (*kharif* season), and from Nov. 1st, 2016 to Apr 30th, 2017 for wheat (*rabi* season), Similarly, the sowing and harvesting dates for cotton-wheat fields were defined from May 1st, 2016 to Nov. 30th, 2016 for cotton (*kharif* season), and from Dec. 1st , 2016 to April 30th , 2017 for wheat (*rabi* season).

Soil samples were taken at the sowing from each field for the basic soil physio-chemical properties of texture, bulk density, hydraulic conductivity, electric conductivity, organic carbon and saturation percentage. The soil samples were taken from 0-15, 15-30, 30-60, 60-90 and 90-120 cm depth from the cotton-wheat fields and 0-15, 15-30 and 30-60 cm from the rice-wheat fields. The soil moisture, on a dry mass basis, was determined using gravimetric method before and after each irrigation event and after any major rainfall event and finally at the harvest of crop. The soil salinity ($EC_{1:5}$) before, and after each irrigation event was also determined with help of electrical conductivity meter in a soil suspension of 1:5 (one part soil five-part distilled water). The detail of field observations and experiment are discussed in Chapter 3. SWAP simulate salinity as solute concentration in soil water (EC_{sw}). Therefore, for comparison of observed and simulated soil salinity the observed $EC_{1:5}$ was converted in EC_{sw} using the following expression:

$$EC_{sw} = EC_{1:5}\frac{5\rho_b}{\theta_{sw}} \qquad \text{Eq. 4.1}$$

where, θ_{sw} is the volumetric soil water content (cm3 cm^{-3}) and ρ_b is the soil bulk density (g cm^{-3})

The SWAP model requires input parameters to define upper boundary conditions of climate and irrigation, crop parameters, soil parameters, the lower boundary condition of free drainage or shallow groundwater, and initial soil water and salinity conditions. The local climatic data and soil-water-crop observations at the local farmers' fields (CW1, CW2, RW1 & RW2) (Figure 3.11) are used to develop the input parameters for SWAP as follows:

4.2.1 Upper boundary

The SWAP model requires inputs of daily reference evapotranspiration (ET_p), rainfall, and any irrigation applied, to define the upper boundary conditions. The ET_p was

calculated by the Penman-Monteith model (Allen *et al.*, 1998a) using the daily weather data of the minimum and maximum temperature, relative humidity, vapour pressure, solar radiation, wind speed, and rainfall. The local weather data were obtained from a metrological station operated by the International Water Management Institute (IWMI) field office in Haroonabad, located within HBC area. Figure 4.1 shows the variation of daily maximum and minimum temperatures, solar radiation, vapour pressure, and rainfall measured in HBC during the agriculture year 2016-17. The maximum temperature reached 48^{o}C on 140th Julian day during *kharif* (summer) season and the minimum temperature reached 2^{o}C on 12th Julian day during the *rabi* (winter) season. The total annual rainfall was measured at 115 mm only, out of which 98 mm occurred during the *kharif* (monsoon) season. The daily solar radiation ranged from 1.89 to 27 MJ m^{-2} day^{-1} with an average value of 17.56 MJ m^{-2} day^{-1}. The daily vapour pressure varied from 0.39 kPa to 3.95 kPa with an average value of 1.74 kPa.

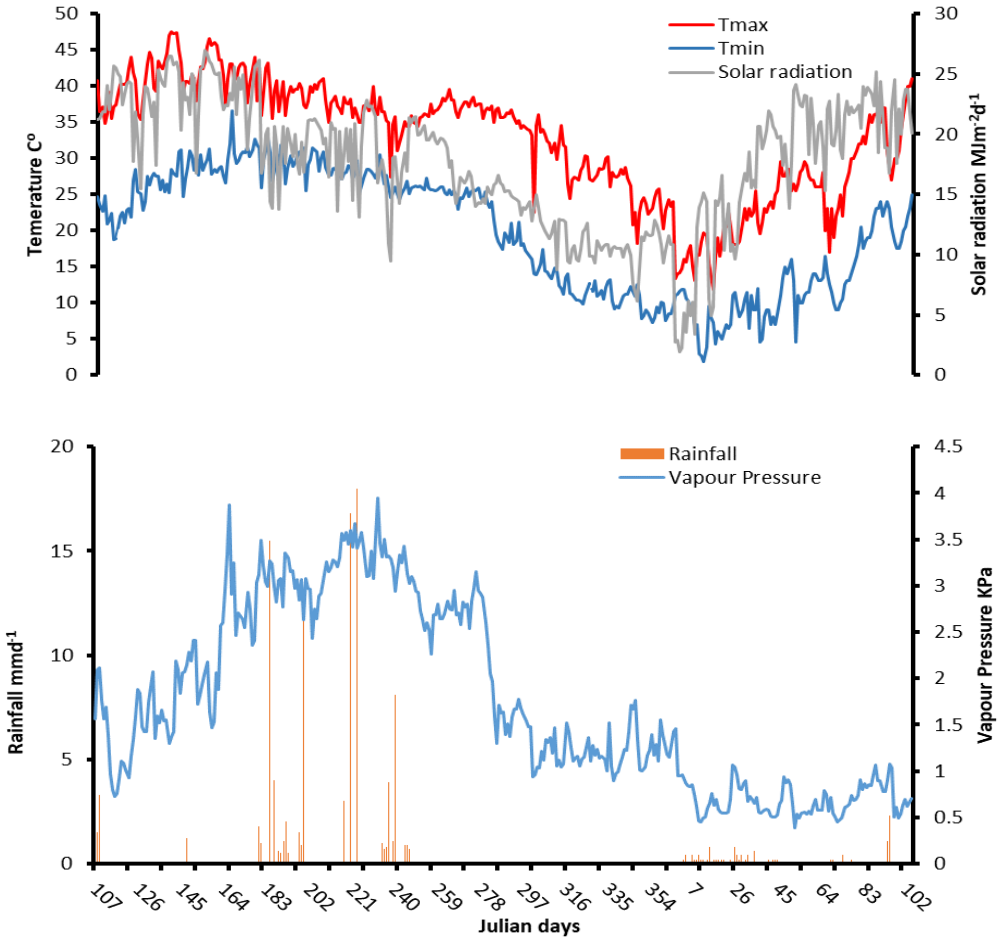

Figure 4.1: Variation of weather conditions in the Hakra Branch Canal command, Punjab Pakistan during the agricultural year 2016-17.

Table 4.1 summarizes irrigation and rainfall received to the selected farmer's fields in both seasons (*kharif* and *rabi*) during the agricultural year 2016-17. The coefficient of variation in irrigation applications was relatively low for the cotton as compared to rice, and higher for the wheat in the cotton-wheat fields as compared to the rice-wheat fields. The low coefficient of variation for wheat in the rice-wheat fields was due to smaller depth of irrigation being applied during *rabi* season. The Cotton received the highest irrigation (830-1102 mm) and the wheat received the lowest irrigation (112 – 489 mm) at the study fields (Table 4.1). The wheat received less irrigation in the wheat-rice fields as compared to the wheat-cotton fields. The reason for the low irrigation for wheat in the rice-wheat fields was the intense irrigation during rice crop which left higher soil

moisture in the root zone and was also due to shallow water table conditions in the rice-wheat fields area. The amount of rainfall contribution was very low only 17 mm in *rabi* (winter) season, while the rainfall contribution was mostly occurred (98 mm) in *kharif* (monsoon) season during the entire agricultural year of 2016-17.

Table 4.1: A summary of irrigation and rainfall depths received in four experimental farmers' fields in HBC command, Punjab Pakistan during the agricultural year 2016-2017.

Field	Crop	Irrigation (mm)					Rainfall (*mm*)
		Total depth	No of irrigation	Mean	*SD*	*CV* (%)	
CW1	Cotton	830	7	118	15	13	98
	Wheat	275	4	69	26	37	17
CW2	Cotton	1102	12	92	12	13	98
	Wheat	489	5	98	13	13	17
RW1	Rice	964	18	53	27	50	98
	Wheat	117	3	39	3	8	17
RW2	Rice	786	18	50	23	47	98
	Wheat	112	3	37	3	7	17

4.2.2 Crop parameters

The SWAP model offers both a simple and a detailed crop growth module to simulate crop growth in the soil-water-plant-atmosphere continuum (van Dam *et al.*, 1997). The detailed crop module, as used in this study, simulates the crop growth in interactions with water and salt flows in the soil profile. The detailed crop module is based on the WOrld FOod STudies (*WOFOST)* model, which simulates a potential crop growth in terms of its phenological development, light interception, CO_2 assimilation, and dry matter formation along with its partitioning between root growth, leaves, stems and the yield of the storage organs (Spitters *et al.*, 1989; Supit, 1994). The potential crop growth was reduced by soil water- and salt-stress to predict water- and salt-limited crop yields.

Further details of SWAP and its crop growth simulation modules are explained in Chapter 3.

Table 4.2: Input parameters of the detailed SWAP model used in crop growth simulation in HBC Command, Punjab Pakistan.

Parameters	Cotton	Rice	Wheat*
Temperature sum from emergence to anthesis, *TSUMEA* (°C)	2690	2230	1393
Temperature sum from anthesis to maturity, *TSUMAM* (°C)	880	655	897
Specific leaf area, S_{la} (ha kg^{-1})	0.0018	0.014	0.0022
Minimum canopy resistance, r_{crop} (s m^{-1})	70	70	70
Light use efficiency $\grave{\varepsilon}$ (kg ha^{-1} hr^{-1} / J m^2 s^{-1})	0.45	0.45	0.45
Maximum CO_2 assimilation rate, A (kg ha^{-1} hr^{-1})	56	40	40
Salinity			
Critical level, EC_{max} (dS m^{-1})	7.7	5.0	6.0
Decline per unit EC, EC_{slope} (% dS m^{-1})	5.4	9.0	7.1

*For wheat at the rice-wheat fields, *TSUMEA* = 1692 °C and *TSUMAM* = 935 °C (The difference in values is due to early sowing at the rice-wheat fields)

The detailed crop module requires input parameters of crop height, temperature sums required for the crop development stages, light use efficiency $\grave{\varepsilon}$ (kg ha^{-1} hr^{-1} / J m^2 s^{-1}), CO_2 assimilation rate A (kg ha^{-1} hr^{-1}), dry matter partitioning, and crop water uptake and salinity stress threshold values (Table 4.2). The crop parameters such as crop developmental stages (sowing, emergence, panicle initiation, anthesis, maturity and harvest), plant height, dry matter partitioning, and rooting depth were based on observations at the local famers' fields during the agricultural year 2016-17. Crop input parameters such as assimilation, light use efficiency, conversion of assimilation into biomass, pressure head for crop water use, salt stress limit at which root water uptake decline and root density distribution were not measured in the local farmers field. These

parameters are estimated based on experimental data and relevant information from existing studies for wheat and cotton crops under similar conditions in Sirsa district, Haryana (India) located nearby the study area (Bessembinder *et al.*, 2003). Crop growth was relatively sensitive to the crop-specific CO_2 assimilation rate, light use efficiency and specific leaf area (van Dam *et al.*, 1997; Singh *et al.*, 2006c). In this study, these crop input parameters were adjusted by running the model with several combination of their values within a realistic range (Table 4.2), and by comparing the simulated crop growth variables such as crop yield and above ground biomass with the observations at the local farmers' fields.

4.2.3 Soil parameters

A soil profile of 160 cm is defined as being the effective root zone of the wheat, rice and cotton crops simulated. The soil profile was further divided into two or three soil layers according to the soil texture description of each farm field soil profile (Table 4.3). As most of the hydrological processes prevailed in the upper layers, the soil profile was further discretized spatially into 30 compartments with a nodal distance of 1 cm for the top 10 compartments, followed by 5 cm for the next 10 compartments and 10 cm for the remaining soil profile (van Dam *et al.*, 1997). Using the defined soil hydraulic variables, the SWAP model applies Richards' equation to simulate soil water flow in the soil profile, subjected to specified initial and soil profile's upper and lower boundary conditions (van Dam and Feddes, 2000) (see to Eqs 3.1 to 3.5 in Chapter 3). In this study, a coefficient of 0.35 cm d^{-1} was used to limit the soil evaporation rate from the top soil layer (Black *et al.*, 1969). The SWAP model simulates salt transport as dynamic, convective-dispersive transport, using specified initial salt conditions and influxes of

salts in the irrigation water (refer to eqs 3.12 to 3.19 in Chapter 3). According to Nielsen *et al.* (1986), the dispersion length is set to 5 cm for salt transport.

The observed soil profile characteristics (Table 4.3) were used to define soil input parameters including the soil hydraulic parameters (Eqs 3.2 & 3.4) to simulate soil water flows in the soil profile. The derived soil hydraulic parameters were then calibrated and validated using observations of soil moisture and soil salinity during crop growth seasons at each of the farmer's fields (see Section 4.3 below).

Table 4.3: Soil properties of the selected farmer fields. The symbol *C* for clay, *Si* for silt, *BD* for bulk density and *OC* is organic carbon. Soil texture *SL* means sandy loam, *L*S is loamy sand, *SiL* is silty loam and *SL* sandy loam.

Fields	**Soil physical properties**					
	Layer (cm)	**Soil Texture**	***C* (%)**	***Si* (%)**	***BD* (g cm^{-3})**	***OC* (%)**
CW1	0-90	*SL*	8	19	1.58	0.36
	>90	*LS*	4	20	1.58	0.26
CW2	0-90	*SL*	6	24	1.70	0.34
	>90	*SiL*	19	55	1.76	0.27
RW1	0-30	*SiL*	8	55	1.61	0.35
	30-60	*L*	12	42	1.78	0.32
	>60	*SL*	7	33	1.78	0.26
RW2	0-30	*SiL*	9	50	1.47	0.33
	30-60	*L*	11	40	1.89	0.32
	>60	*SL*	6	39	1.84	0.31

In the case of rice cultivation, under actual field conditions, the farmers puddle the soil before rice transplant in-order to reduce percolation below root zone, and thereby maintain a ponding on the soil surface for optimum rice growing condition. To capture

this management practice during simulation of soil water flow in rice growing period, the saturated hydraulic conductivity of the top 30 cm soil layer of rice fields was reduced by 20% (Singh *et al.*, 2001). The empirical function of Black *et al.* (1969) for reducing soil evaporation is also set off during rice growing period.

4.2.4 Lower boundary and initial conditions

The SWAP model simulates eight different criteria to define lower boundary conditions, each have a specific scale of application (van Dam *et al.*, 1997). In this study, the wheat-rice fields (RW1 and RW2) were located in shallow groundwater conditions (< 1.5m), while the wheat-cotton fields (CW1 and CW2) were located in a deeper groundwater condition (> 3 m). The water table depth was measured at 0.80 and 1.20 m (below ground level) at the RW1 and RW2, respectively. Accordingly, considering the farmer's field conditions, a measured water table depth for shallow groundwater conditions (< 3 m below ground level) was defined as a bottom boundary condition for the wheat-rice fields (RW1 and RW2), and a free drainage condition for the wheat-cotton fields (CW1 and CW2) with a deeper groundwater level (> 3 m below ground level).

The initial soil conditions for the *kharif* season were not measured, therefore SWAP was run one year in advance with the same inputs, and the end of the year soil moisture and salinity profiles were used as the initial soil condition. This is a commonly used modelling practice to define initial soil conditions in absence of field observations (Singh *et al.*, 2006c).

4.3 Calibration and validation of soil hydraulic parameters

Soil moisture and salinity dynamics are highly sensitive to the soil hydraulic parameters (refer to Eqs 3.2 and 3.4 in Chapter 3) used in the simulation of soil water flow and salt

transport processes in soil-water-plant-atmosphere continuum (van Dam and Feddes, 2000; Jhorar *et al.*, 2004; Singh *et al.*, 2006c). In this study, several parameters describe the soil hydraulic function, e.g., the saturated soil hydraulic conductivity and the saturated soil moisture contents. These were determined based on the observations at the farmers' field (Table 4.4). However, the other soil hydraulic function variables, such as the residual soil moisture content and the empirical shape factor are difficult to measure directly in the field. They are derived by the pedotransfer functions (Wösten *et al.*, 1998) using the inputs of soil texture, bulk density and organic carbon for each soil layer (Table 4.3). The pedotransfer functions derived soil hydraulic variables were then calibrated and validated by comparing observations of soil moisture and soil salinity in the local field conditions (Singh *et al.*, 2006c; Vazifedoust *et al.*, 2008; Yuan *et al.*, 2019). In this study, the two sensitive and uncertain soil parameters of the empirical shape factors, α and n (Table 4.4) were calibrated and validated using the soil moisture and salinity profiles observed during the field experiments. In an automatic calibration procedure, called inverse modelling, the non-linear *parameter estimation program*, PEST (Doherty, 1994) was linked with SWAP to calibrate the soil parameters ($\boldsymbol{\alpha}$ and $\boldsymbol{n}$) for each soil layer, using the objective function *O(b)*, as follows:

$$O(b) = \sum_{i=1}^{N} \left[\left\{ W_\theta \left(\theta_{obs}(t_i) - \theta_{sim}(b, t_i) \right) \right\}^2 + \left\{ W_{EC} \left(EC_{obs}(t_i) - EC_{sim}(b, t_i) \right) \right\}^2 \right] \quad \text{Eq. 4.2}$$

where, N is the number of observations, $\theta_{obs}(t_i)$ and $EC_{obs}(t_i)$ are the observed soil moisture and salinity at time t_i, and $\theta_{sim}(b, t_i)$ and $EC_{sim}(b, t_i)$ are the simulated soil moisture and salinity using an array with the parameter value b. Here, W_θ and W_{EC} are the weight associated with the observed soil moisture and soil salinity, respectively. The

weight are associated with different observation types in the objective function (Eq. 4.2) to overcome any undue preference to an observation due to its magnitude differences with others. Gribb (1996) suggested the weight of each different data type by taking the inverse square of the mean values. However, Singh *et al.* (2006c) accounted for observation differences of θ and EC by using W_θ = 1 and W_{EC} = 10% of average $\frac{\theta_{obs}}{EC_{obs}}$ in the calibration of soil hydraulic parameters for SWAP simulations of cotton-wheat and rice-wheat cultivation in the Sirsa district of India, located closer to the study area. The latter method of the observations' weight was applied here, which gave relatively more weight to the soil moisture observations in the calibration of soil hydraulic parameters. Optimization of the soil empirical shape factors, α and *n* for different soil layers of the stratified soil profile were performed simultaneously. The optimization process was repeated with different initial values of α and *n* to test uniqueness of the optimisation solutions (Singh *et al.*, 2006c). The optimized values of $\boldsymbol{\alpha}$ and $\boldsymbol{n}$ with other soil hydraulic parameters are listed in Table 4.4.

The Root Mean Square Error *(RMES)* is quantified between the observed and simulated soil moisture and salinity profiles during both the calibration and validation periods, as follows:

$$RMSE = \sqrt{\frac{\sum_{i=1}^{N}[Obs(t_i) - Sim(t_i, b)]^2}{N}} \qquad \text{Eq. 4.3}$$

where, $Obs(t_i)$ and $Sim(t_i, b)$ are the observed and simulated values of output variable (i.e., soil moisture or soil *EC* in this study) at time t_i and *N* is the total number of observations. The *RMSE,* considered among the 'best' overall measures of the model performance, quantified the average absolute error in the simulated and observed soil moisture and salinity profiles.

4.4 Irrigation performance assessment

4.4.1 Water management response indicators

The concept of irrigation efficiency has been generally used to evaluate the performance of irrigation system (Wolters, 1992) and can be defined in terms of irrigation system performance, uniformity of water application and response of the crop to irrigation (Howell, 2003). However, it does reveal limited information and insights into soil water and salt balances, and processes that lead to waterlogging and soil salinity. These factors affect crop growth and its productivity (Molden and Gates, 1990). Therefore, a combination of several water-management response indicators (*WMRI*) (Bastiaanssen *et al.*, 1997) was implemented in this study to evaluate the water and salt stress on crops, percolation and salt build in the soil profile. The quantified *WMRI* indicators were evaluated to help assess irrigation water management performance under water- and salt-limited conditions. These indicators are:

- Relative transpiration (defined as a ratio of actual transpiration to potential transpiration, i.e. T_a/T_p), this ratio quantifies the intensity of water and salt stress on the crop.
- Water supply index (defined as a ratio of irrigation or rainfall to actual evapotranspiration, i.e. I/ET_a *and* P/ET_a) helps in estimating how much water inputs (irrigation and rainfall) to crops has effectively been used as actual evapotranspiration by crop.
- Percolation Index (defined as a ratio of percolation to irrigation, i.e. Q_{bot}/I) quantifies the fraction of water applied are lost as percolation.
- Salt storage index (defined as a ratio of changes in salt storage to salt storage in the soil profile, i.e. $\Delta C/C$) indicates amount of salt build up in the root zone

Here, T_a and T_p are the actual and potential transpiration, I is the irrigation, P is the rainfall, ET_a is the actual evapotranspiration, Q_{bot} is the percolation, and ΔC is the change in salt storage and C is the initial salt concentration in the soil profile.

4.4.2 Crop water productivity

The concept of water productivity is increasingly being used to evaluate the productivity benefits derived from the application and consumption of water in farm management strategies under arid and semi-arid regions (Molden, 1997; Molden *et al.*, 2003; Fernández *et al.*, 2020a). Crop water productivity can be expressed in different ways referring to different types of crop yield, such as dry matter or grain yield, and the amount of water used or consumed by crop transpiration, evapotranspiration, evapotranspiration plus percolation, and irrigation (Molden, 1997; Molden *et al.*, 2003; Rodrigues and Pereira, 2009). This variation in defining crop water productivity is useful to quantify crop water utilization and to identify when and where water can be saved in on-farm practices. The following definitions of crop water productivity are used here and evaluated to assess irrigation performance as follows:

$$WP_T = \frac{Y(kg\ ha^{-1})}{T(m^3\ ha^{-1})} \qquad \text{Eq. 4.4}$$

where, WP_T is water productivity expressed as crop yield Y (dry matter or grain) per unit of actual transpiration and indicates the physiological performance of a certain crop. The WP_T is also known as transpiration efficiency and relates CO_2 and H_2O through diffusion process and varies directly with size of stomatal opening of leaves (Flexas *et al.*, 2010).

In actual field conditions it is difficult to distinguish between plant transpiration and soil evaporation. The loss of water through evaporation reduces crop water productivity from WP_T to WP_{ET} and is expressed as:

$$WP_{ET} = \frac{Y(kgha^{-1})}{ET(m^3\ ha^{-1})} \quad \text{Eq. 4.5}$$

where ET is the actual evapotranspiration from crop and soil surface.

This WP_{ET} represents actual amount of water used in crop production (Kijne *et al.*, 2003). Since part of the soil water content is also percolated (Q_{bot}) which further reduced WP_{ET} to WP_{ETQ} (Singh et al., 2006c). However, depending on the groundwater quality of the region the Q_{bot} can be considered as water loss if the groundwater quality is poor, or as a recharge to the groundwater if the groundwater quality is good which can then be reused through groundwater pumping. Accounting for the percolated (Q_{bot}) the WP_{ETQ} is

$$WP_{ETQ} = \frac{Y(kg\ ha^{-1})}{ETQ(m^3\ ha^{-1})} \quad \text{Eq. 4.6}$$

expressed as follows:

To quantify the performance of the irrigation system it is preferable to assess the *WP* in terms of irrigation (*I*) water applied during crop period and is termed as irrigation water productivity (WP_I) (Rodrigues and Pereira, 2009) as follows:

$$WP_I = \frac{Y\ (kg\ ha^{-1})}{I\ (m^3\ ha^{-1})} \quad \text{Eq. 4.7}$$

The *WP* indicator provides an insight of where and when water could be saved. Quantification of *WP* is therefore important to plan an efficient irrigation management

under water- and salt-limited conditions. A robust quantification of different soil water and salt balance components and crop yields will certainly enhance our ability to improve crop water productivity under water scarce and soil salinity conditions in the study area and other similar semi-arid conditions elsewhere.

4.5. Results and discussion

4.5.1 Simulation of soil moisture and salinity profiles

The SWAP model input parameters (Table 4.2 and 4.4) are calibrated and validated by comparing SWAP simulations of soil moisture, soil salinity and crop growth with their observations at the local farmers fields during the agricultural years 2016-17. The start date of simulation is set May 1st, 2016 and the end date April 30th, 2017. The calibration of soil hydraulic parameters at the cotton-wheat fields (Table 4.4) is performed using the first sub-set of the field observations over three months from June 2016 to August 2016, and the validation is performed using the second sub-set of the field observations over eight months from September 2016 to April 2017. For the rice-wheat fields, the calibration is performed from November 2016 to February 2017 and validation from March to April 2017 using the field observations of soil moisture and salinity levels during only the wheat (*rabi*) season from November 2016 – April 2017. In rice fields, the field observations of soil moisture and salinity during rice crop were not conducted due to surface water ponding in rice cultivation in *kharif* season from May 2016 – October 2016.

Table 4.4: Soil hydraulic parameters derived for different soil layers at the farmer fields in HBC Command, Punjab Pakistan. The symbol $\boldsymbol{\theta_{res}}$is residual moisture content, $\boldsymbol{\theta_{sat}}$ is the saturated moisture content, $\boldsymbol{K_{sat}}$ is the saturated hydraulic conductivity, λ is the empirical coefficient, α and n are the empirical shape factor. Parameter $\boldsymbol{\alpha}$ and $\boldsymbol{n}$ were optimized.

Field	Soil layer (cm)	Texture	Soil hydraulic parameters					
			θ_{res} (cm^3cm^{-3})	θ_{sat} (cm^3cm^{-3})	K_{sat} (cm d^{-1})	α (cm^{-1})	n [-]	λ [-]
CW1	0-90	*SL*	0.01	0.29	59.12	0.069	1.21	-0.12
	90-160	*LS*	0.01	0.34	48.24	0.015	1.90	1.13
CW2	0-90	*SL*	0.01	0.34	31.0	0.026	1.41	0.31
	90-160	*SiL*	0.01	0.39	8.54	0.053	1.10	-0.83
RW1	0-30	*SiL*	0.01	0.45	11.8	0.025	1.79	0.77
	30-60	*L*	0.01	0.42	12.42	0.024	1.62	-0.72
	60-160	*SL*	0.01	0.32	14.75	0.005	1.27	-0.79
RW2	0-30	*SiL*	0.01	0.47	10.8	0.020	1.80	0.45
	30-60	*L*	0.01	0.41	9.05	0.018	1.79	-0.67
	60-160	*SL*	0.01	0.31	8.17	0.006	1.40	0.77

Comparing the simulations and field observations, the root mean square error (*RMSE*) values varied between 0.03 and 0.05 $cm^3\ cm^{-3}$ for the soil moisture content, and from 0.07 to 0.17 dS m^{-1} for the soil salinity $EC_{1:5}$ during the calibration period (Table 4.5). The *RMSE* ranged from 0.02 to 0.07 $cm^3\ cm^{-3}$ for soil moisture and from 0.06 to 0.20 dS m^{-1} for the soil salinity $EC_{1:5}$ during the validation period (Table 4.5). The *RMSE* values for the soil moisture and salinity are similar between the calibration and validation periods, supporting effective calibration and application of the soil hydraulic parameters (Table 4.4).

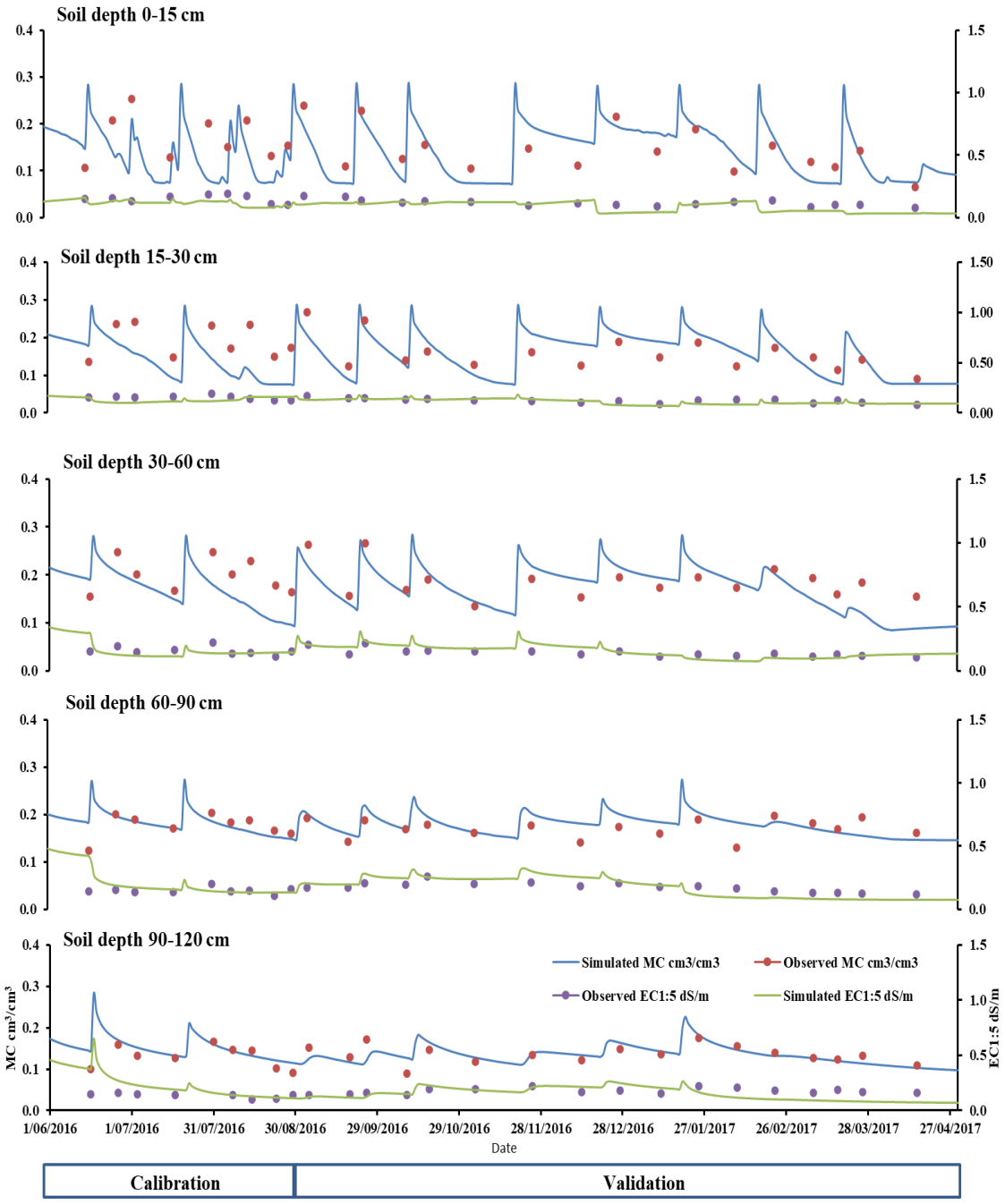

Figure 4.2: The observed and simulated soil moisture and salinity profile at a local farmer field (CW2) under cotton-wheat cultivation in HBC command, Punjab Pakistan. (refer to appendix A for CW1, RW1 and RW2 former fields)

The lower *RMSE* values (Table 4.5) and absence of any systematic under- or over-prediction of soil moisture content and $EC_{1:5}$ values (Figure 4.2) suggest an acceptable simulation of the soil water flow and salt transport dynamics at the study fields. Hence,

the calibrated and validated SWAP could be used with a degree of confidence for further simulations of different soil water and salt balance components in the study area.

Table 4.5: SWAP model performance in simulation of soil moisture and salinity levels at the farmer fields in HBC Command, Punjab Pakistan. The *RMSE* quantifies the root mean square error and *N* is the number of observations of soil moisture content θ and soil electrical conductivity $EC_{1:5}$ (one part soil five part water) compared for both calibration and validation periods in the cotton-wheat (CW) and the rice-wheat (RW) fields during the agricultural year 2016-2017.

Field	Calibration				Validation			
	θ (cm^3cm^{-3})		$EC_{1:5}$ dS/m		θ (cm^3cm^{-3})		$EC_{1:5}$ dS/m	
	N	***RMSE***	***N***	***RMSE***	***N***	***RMSE***	***N***	***RMSE***
CW1	50	0.05	50	0.12	70	0.07	70	0.17
CW2	45	0.04	45	0.07	75	0.04	75	0.06
RW1	18	0.03	18	0.11	15	0.02	15	0.20
RW2	18	0.03	18	0.17	15	0.02	15	0.12

4.5.1 Soil water and salt balances

The calibrated soil hydraulic parameters (Table 4.4) along with other inputs (Table 4.2 and 4.3) are used to simulate soil water and salt balance components at the selected farmers' fields (Table 4.6). The SWAP simulated seasonal potential evapotranspiration (ET_p) varied from 933 mm to 1075 mm during *kharif* (cotton and rice) season and 450 mm to 519 mm during *rabi* (wheat) season (Table 4.6). The ET_p for wheat at the rice-wheat fields is simulated to be higher than ET_p for wheat at the cotton-wheat field (Table 4.6). This is mainly due to one month longer growing period for wheat crop at the rice-wheat fields, namely from Nov 1, 2016 to Apr 30, 2017 as compared to wheat at the cotton-wheat fields from Dec 1st, 2016 to Apr 30th, 2017. Liaqat *et al.* (2016) quantified potential and actual *ET* on both a seasonal and annual basis for HBC command using

surface energy balance system (SEBS) model over period from 2008 to 2014. Their results showed seasonal average ET_p ranged between 906 mm (*kharif*) and 485 mm (*rabi*) with an annual average value of 1391 mm. These estimates correspond well with the SWAP simulated ET_p values for the rice-wheat (RW1 and RW2) and cotton-wheat (CW1 and CW2) fields in this study (Table 4.6).

Table 4.6: SWAP simulated water and salt balance components for the main agricultural crops at farmer's fields in the HBC command area, Punjab Pakistan during the agricultural year 2016-17. The symbol P_e is effective precipitation, I irrigation, I_{cw} is canal water irrigation, I_{gw} is groundwater irrigation, T_p is potential transpiration, T_a is actual transpiration, ET_p is potential evapotranspiration, ET_a is actual transpiration, Q_{bot} is percolation, ΔW is change in water storage in the soil profile, IC_i is salt concentration in irrigation water, Q_{bot} C_{bot} is salt concentration in percolated water, ΔC is change in salt storage in the soil profile.

Components	Fields							
	CW1		CW2		RW1		RW2	
	Cotton	Wheat	Cotton	Wheat	Rice	Wheat	Rice	Wheat
	Water balance (mm)							
P_e	98	17	98	17	98	17	98	17
I	830	275	1102	489	964	117	886	112
I_{cw}	0	170	780	410	503	117	612	112
I_{gw}	830	105	320	80	461	0	274	0
T_p	598	208	783	297	325	310	480	331
T_a	478	164	580	288	304	180	412	229
ET_p	997	450	1075	489	933	518	952	519
ET_a	545	222	671	347	632	224	720	314
Q_{bot}	-364	-172	-509	-193	-157	183	-133	120
ΔW	19	-102	20	-34	274	94	131	-65
	Salt balance (mg cm^{-2})							
IC_i	172	25	67	38	91	4	72	3
$Q_{bot}C_{bot}$	-122	-114	-68	-47	-49	65	-59	30
ΔC	50	-89	-1	-9	42	69	12	33

*Height of soil column considered 160 cm

The potential evapotranspiration is reduced to actual evapotranspiration (ET_a) due to water and salt stress under actual field conditions (Singh *et al.*, 2006a). Awan *et al.* (2016) estimated that annual ET_a, based on the surface energy balance algorithm for land (SEBAL), varied significantly within all distributaries of HBC command with a

minimum of 460 mm to a maximum of 939 mm. Liaqat *et al.* (2016) also estimated, again using the Surface Energy Balance System (SEBS) model, a seasonal average ET_a of 641 mm during *kharif* season and 322 mm during *rabi* season with annual average ET_a of 963 mm for HBC command from 2008 to 2014. In this study, the SWAP simulated seasonal ET_a varied from 545 mm to 671 mm at the cotton fields, from 632 mm to 720 mm in the rice fields and from 222 mm to 314 mm at the wheat fields (Table 4.6).

The variation in ET_a of the similar crops in different fields is caused by several factors such as the quality and quantity of irrigation, soil salinity and crop period. The average seasonal ET_a is simulated at 642 mm in *kharif* (cotton and rice) season and 263 mm during *rabi* (wheat) season with an average annual value of 905 mm during the year 2016-2017. These SWAP-simulated annual ET_a values are in good agreement with annual average ET_a values of 939 and 963 mm reported by Awan *et al.* (2016) and Liaqat *et al.* (2016), respectively in the study area.

The SWAP-simulated annual percolation Q_{bot} ranged from -536 mm to -778 mm in the cotton-wheat fields, and from -13 mm to 27 mm in the rice-wheat fields (Table 4.6). The percolation Q_{bot} is higher during the *kharif* season in the cotton-wheat fields than in the *rabi* season which results in significant amount of irrigation water percolation during the *kharif* season in both cotton fields. This is clear sign of over irrigation in the cotton fields (Table 4.6). This is due to heavy irrigation applications and the sandy soil texture in cotton fields. Despite of high depth of irrigations, the percolation is simulated relatively less in the rice fields (RW1 and RW2) as compared to the cotton fields (CW1 and CW2) (Table 4.6). This is due to relatively lower soil hydraulic conductivity (Table 4.4) and simulation of soil-puddling effect during the rice cultivation. This leaves behind a saturated soil profile after the rice harvest. As a result, for the rice-wheat fields, the wheat

irrigation *I* during the *rabi* season is only about 12% to 14% of the rice irrigation during *kharif* (rice) season. Also, the wheat irrigation is 2 to 4 times more in the cotton-wheat fields (CW1 and CW2), as compared to the rice-wheat fields (RW1 and RW2) (Table 4.6). This is due to the saturated soil profile left after rice cultivation and shallow water table condition in the rice-wheat fields.

There are risks of soil salinity build-up and secondary soil salinization due to the shallow water table and use of poor-quality groundwater which threaten the productivity and the sustainability of irrigated agriculture in the Hakra Branch Canal Command. In this study, the annual change in salt storage ΔC at both the rice-wheat fields is simulated to be relatively higher (45 to 111 mg cm^{-2}) than for the cotton-wheat fields (-10 to -39 mg cm^{-2}) (Table 4.6). This is due to the high irrigation applied during the *kharif* (rice) season but reduced percolation for creating the puddled conditions of topsoil surface during rice cultivation. The soil puddling restricts the downward flux of salts. However, on the cotton-wheat field CW1 during *kharif* (cotton) season, the change in salt storage is simulated to be high at 50 mg cm^{-2}, despite significant Q_{bot} of -364 mm (Table 4.6). This is due to the use of 830 mm of poor-quality groundwater (3.28 dS m^{-1}), which added large amounts of salts (172 mg m^{-2}) to the soil profile at the CW1 during *kharif* (cotton) season. However, for the same field CW1, the conjunctive use of good quality canal water I_{cw} (170 mm) and poor-quality groundwater I_{gw} (105 mm) during the *rabi* (wheat) season resulted in a leaching (-89 mg cm^{-2}) of the accumulated salt from the soil profile. This indicates the importance of appropriate leaching fractions in terms of restricting a salt build up in the root zone.

4.5.2 Crops yields under current conditions

The calibrated detailed crop module of SWAP (Tables 4.2 and 4.3) was used to simulate the potential, and water- and salt-limited crop dry matter and grain yield of the study fields. The SWAP model simulates the potential crop dry matter yield (Y_{PDM}) and grain yield (Y_P) reduce into water- and salt-limited dry mater (Y_{DM}) and grain yield (Y) due to water and salt stress experienced by the crop. Under actual field conditions factors such as seed quality, nutrient deficiency, and pests will also affect crop yield. However, these factors are not considered in SWAP which assumes optimum agronomic conditions without pest stress and nutrients deficiency. Hence, the SWAP simulated crop dry matter yield (Y_{PDM}) and grain yield (Y_P) are referred as the water- and salt-limited crop dry matter and grain yield (refer to figure 3.10 in Chapter 3). Table 4.7 reports the simulated potential, water- and salt-limited and observed crop dry matter and grain (or seed) yield at the study fields during agricultural year 2016-2017.

Table 4.7: SWAP simulated potential, water- and salt-limited, observed fresh dry matter yield, grain (or seed) yields of main crops at farmer's fields in the HBC Command, Punjab Pakistan during 2016-17.

Field	Crop	Simulated (ton ha^{-1})				Observed (ton ha^{-1})	
		Potential		Water- and salt-limited		Y_{DM}	Y_a
		Y_{PDM}*	Y_P*	Y_{DM}**	Y**		
CW1	Cotton	23.64	2.65	17.22	1.89	10.9	1.3
	Wheat	15.30	6.93	11.27	4.49	9.1	3.4
CW2	Cotton	24.49	4.16	20.57	2.79	15.3	2.4
	Wheat	14.96	6.07	14.22	6.00	10.6	4.2
RW1	Rice	13.84	6.73	11.60	5.37	11.8	4.1
	Wheat	16.29	7.69	15.43	4.68	9.2	3.9
RW2	Rice	18.19	6.62	17.39	6.02	13.2	4.7
	Wheat	17.90	7.96	17.41	6.70	9.5	4.5

*Moisture in air-dry fresh matter:12% for wheat and rice and 18% for cotton

**Simulated water- and salt-limited yield $\boldsymbol{Y}$ considering 44% seed (or grain) in the simulated storage organs $\boldsymbol{Y_{SO}}$ for cotton, 81% for rice and 80% for wheat. The simulated yield include 15, 16 and 14% moisture in grain (or seed) for cotton, rice, and wheat, respectively.

The potential yield for cotton is simulated 30% higher, for rice 15% higher and for wheat 25% higher, as compared to the water- and salt-limited yield. Whereas the potential simulated yields are 30% to 50% higher than the observed yields. The observed crop yields varied from 1.3 to 2.4 ton ha^{-1} for cotton, 4.1 to 4.7 ton ha^{-1} for rice, and 3.4 to 4.5 ton ha^{-1} for wheat at the study fields (Table 4.7). The statistical data as reported by the crop reporting services of Punjab (CRS, 2017) records average actual yield of 2.0 ton ha^{-1} for cotton, 3.02 ton ha^{-1} for rice, and 3.31 ton ha^{-1} for wheat in HBC Bahawalnagar district during the agricultural year 2016-2017.

The SWAP simulated potential yield of cotton varied from 2.65 ton ha^{-1} (CW1) to 4.16 ton ha^{-1} (CW2) (Table 4.7), which is about 2 times higher than the observed yield. The SWAP simulated water- and salt-limited cotton yields are about 14% to 31% higher than the observed cotton yields at the study fields. Similarly, the average potential yield of rice is simulated at 7.35 ton ha^{-1} (Table 4.7), which is about 40% higher than the observed average rice yield. The average water and salt-limited rice yield is simulated 28% higher than the observed rice yields. Wheat is the major crop of *rabi* season which account for about 90% of the cultivated area of HBC. The average potential yield for wheat is simulated at 7.2 ton ha^{-1}, which 1.4 times higher than water- and salt-limited yield and 1.8 times higher than the observed yield at the study fields (Table 4.7). The lowest wheat yield of 3.4 ton ha^{-1} observed at the field CW1 with optimum irrigation supplies and a relative transpiration of 0.59 indicates in addition to water and salt stresses, the presence of nutritional deficiency, diseases and pest stress causes the lower yield. Furthermore, the average actual observed wheat yield at the rice-wheat fields is higher than the cotton-wheat fields. This is because of sufficient moisture availability and early sowing at rice-wheat fields.

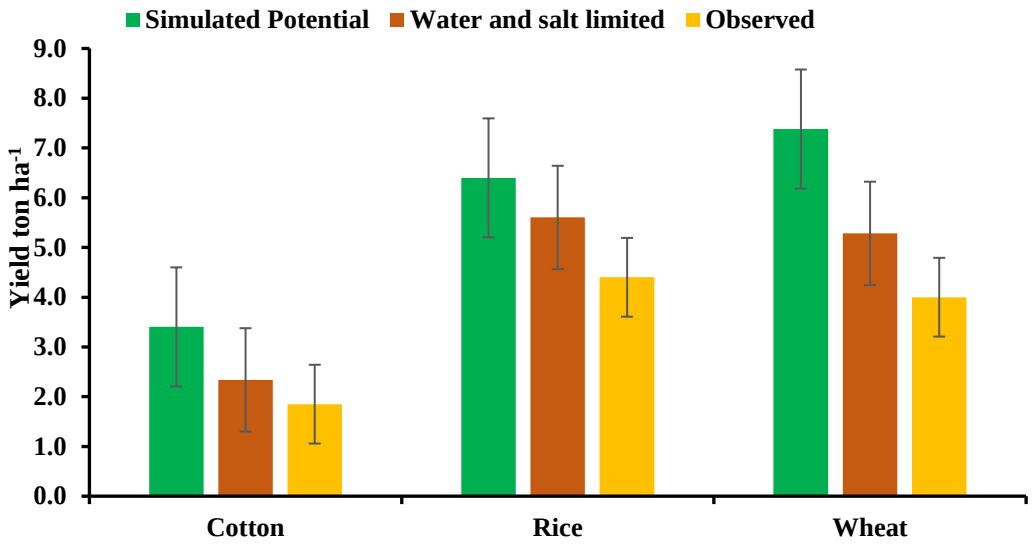

Figure 4.3: Simulated potential, water- and salt-limited, and observed yields of main crops at farmer's fields in Hakra branch canal command area, Punjab Pakistan during the agricultural year 2016-17.

The relative comparison of SWAP simulated potential crop yields as 10% to 35% higher than the simulated water- and salt-limited yields (Figure 4.3) suggests a significant impact of water- and salt-stress on the crop yields. Furthermore, the water- and salt-limited crop yields are simulated 14 to 33% higher than the actual observed yields (Figure 4.3), indicating a combined effects of pest and nutrient deficiency in addition to water and salt stress on the observed crop yields. This suggest that ensuring efficient irrigation supplies and improved crop management could potentially increase crop yields by 30 to 50% at HBC command.

4.5.3 Analysis of irrigation performance indicators

The SWAP simulated soil water and salt balance components (Table 4.6) allowed quantification and assessment of a range of irrigation water management response indicators for each crop combination (Table 4.8 and 4.9). The relative transpiration (T_a/T_p) is quantified to evaluate comparative performance of a crop across the study fields. In this case, the potential transpiration (T_p) of the best developed crop, i.e., 783 mm for cotton at the field CW2, 480 mm for rice at the field RW2, 297 mm for wheat at

the field CW2 at wheat-cotton fields, and 331 mm for wheat at the field RW2 at rice-wheat fields (Table 4.6), is used to quantify the T_a/T_p for cotton, rice and wheat crops at the study fields (Table 4.8and 4.9). The high T_p of wheat in the rice-wheat fields is due to the longer crop period (Nov-Apr) as compared to wheat at the cotton-wheat fields (Dec-Apr).

4.5.3.1 Cotton-wheat combination

Table 4.8 summarizes various irrigation water management response indicators quantified for the cotton-wheat cultivation. The cotton crop at the field CW1 resulted into a low T_a/T_p of 0.61 (Table 4.8) mainly due to use of only poor quality (3.28 dS m^{-1}) groundwater during the *kharif* (cotton) season. Whereas the relatively higher irrigation and a higher canal-water contribution resulted into a slightly higher T_a/T_p of 0.74 for cotton at the field CW2 (Table 4.8). The wheat T_a/T_p is simulated to be high (0.80) at the field CW2, and this is attributed to higher application of good-quality canal water for irrigations. Whereas the wheat T_a/T_p is simulated to be very low (0.57) at the field CW1, indicating a high salt stress due to higher salts build up (0.53) during the *kharif* season (Table 4.8).

As expected, the contribution of rainfall to crop evapotranspiration is quantified to be very low (0.05 to 0.18), as compared to the irrigation supplies. Moreover, the rainfall contributes mainly during the *kharif* (cotton) season. The contribution of canal water is quantified high at the field CW2. The cotton at the field CW1 received only groundwater for irrigation. Overall, the water supply index, that is the ratio of rainfall plus irrigation to crop evapotranspiration, is simulated to be from 1.32 for wheat at the CW1 field, to 1.79 for cotton at the CW2 field. This indicates higher soil percolation during the cotton crop. The seasonal percolation index, defined as the ratio of percolation to irrigation applied, is simulated to be high (> -0.4) for both cotton-wheat fields. This suggests a

significant amount of percolation, namely recharge to groundwater, occurring under the current irrigation practices at the study fields.

Table 4.8: Computed irrigation water management response indicators for cotton-wheat cultivation at farmer's fields in HBC command, Punjab Pakistan during the agricultural year 2016-17.

Field	Crops	Water management response indicators						
		Relative transpiration (T_a/T_p)	Rainfall Contribution (P/ET_a)	Irrigation Contribution (I/ET_a)		Water Supply Index ($P+I/ET_a$)	Percolation index	Salt storage index
				Canal	Tubewell			
CW1	Cotton	0.61	0.18	0.00	1.52	1.70	-0.44	0.53
	Wheat	0.57	0.08	0.77	0.47	1.32	-0.63	-0.26
CW2	Cotton	0.74	0.15	1.16	0.48	1.79	-0.46	-0.02
	Wheat	0.97	0.05	1.18	0.23	1.46	-0.39	-0.12

Despite this high percolation, the salt storage index is simulated to be higher (0.53) at the field CW1 during *kharif* (cotton) season (Table 4.8). This is caused by use of only poor quality (3.28 dS m^{-1}) groundwater during the *kharif* (cotton) season. The same field, when irrigated with conjunctive use of canal and groundwater during the *rabi* (wheat) season resulted into a reduction in the salt storage (-0.26). This indicates that conjunctive use of canal and groundwater can help to control a salt build up in the soil profile, albeit with consequences to groundwater quality.

4.5.3.2 Rice-wheat combination

Table 4.9 summarizes various irrigation water management response indicators quantified for the rice-wheat cultivation. The rice-wheat fields are located within close proximity to the canal and in the head-reaches of the HBC, where sufficient supplies from the canal are available. At the fields RW1 and RW2, the water supply index is

quantified higher (from 1.37 to 1.68) during the *kharif* (rice) season, compared to 0.41 to 0.60 during the *rabi* (wheat) season due to saturated soil profile left after the rice crop (131 mm and 274 mm) (Table 4.6). This is because comparatively high irrigation applications and rainfall during the *kharif* (rice) season. In most of the rice-wheat fields the ground water is less than 3 meters, which provides a conducive environment for rice growth. Despite sufficient access to the good quality of canal water, the relative transpiration T_a/T_p showed significant variations in the RW1 and RW2 fields (Table 4.9). For instance, the T_a/T_p ranges from 0.63 to 0.86 for rice and 0.54 to 0.86for wheat This is because these field are under waterlogged conditions with the water-table at under one meter below natural surface level. This causes no significant downward flux to drain excess water and leach out the salts. The percolation index was positive during the *rabi* (wheat) season at both RW1 and RW2 fields. This showed high capillary rise due to shallow watertable that contributes to salt build-up as indicated by the positive salt storage index (Table 4.9).

Table 4.9: Computed irrigation water management response indicators for two rice-wheat -cultivation at farmer's fields in the HBC command, Punjab Pakistan during the agricultural year 2016-17.

Field	Crops	Water management response indicators						
		Relative transpiration	Rainfall Contribution P/ET_a	Irrigation Contribution I/ET_a		Water Supply Index ($P+I/ET_a$)	Percolation index	Salt storage index
				Canal	Tubewell			
RW1	Rice	0.63	0.17	0.80	0.73	1.68	-0.16	0.28
	Wheat	0.54	0.09	0.52	0.00	0.60	1.57	0.51
RW2	Rice	0.86	0.13	0.85	0.38	1.37	-0.15	0.07
	Wheat	0.81	0.05	0.36	0.00	0.41	1.07	0.27

4.5.4 Crop water productivity under current conditions

Table 4.10 summarizes the simulated water- and salt-limited crop water-productivity values for cotton, rice and wheat crops at the study fields. These values are quantified using Equations 4.3 to 4.6 and SWAP simulated soil water balance components of T, ET_a, and Q_{bot} (Table 4.6), plus the *SWAP* simulated water and salt-limited grain (or seed) yield Y_{sim} , and the actual grain (or seed) yield Y_{obs} at the selected farmers' fields (Table 4.10). The average WP_T expressed as Y_{sim}/T ($kg\ m^{-3}$) is quantified to be 0.44 for cotton, 1.92 for rice, and 2.76 for wheat. Similarly, the average WP_T based on observed yield (Y_{obs}) is quantified to be 0.34 for cotton, 1.25 for rice, and 1.91 for wheat. The reduction in WP_T based on the observed yields is due to the effects of nutrient deficiency, pest and diseases that cannot be simulated by SWAP.

According to Zwart and Bastiaanssen (2004), the global WP_{ET} values ($kg\ m^{-3}$) were quantified as 0.63 for cotton, 1.09 for rice, and 1.08 for wheat. Usman (2012) estimated WP_{ET} ($kg\ m^{-3}$) values of 0.26 for cotton and 1.12 for wheat in the cotton-wheat zone of Punjab Pakistan. Cai *et al.* (2010) gave a WP_{ET} ($kg\ m^{-3}$) value of 0.69 for rice in the Indus basin of Pakistan. Singh *et al.* (2006c) also evaluated WP_{ET} using the SWAP model at the selected farmer fields at the Sirsa Irrigation Circle India, and they reported the average water- and salt-limited WP_{ET} ($kg\ m^{-3}$) values of 0.31 for cotton, 0.86 for rice, and 2.01 for wheat. In this study, the SWAP simulated the average water- and salt-limited WP_{ET} ($kg\ m^{-3}$) are quantified as 0.38 for cotton, 0.84 for rice, and 2.07 for wheat (Table 4.10). Similarly, the average WP_{ET} ($kg\ m^{-3}$) based on the actual observed crop yields is quantified to be 0.29 for cotton, 0.66 for rice, and 1.52 for wheat (Table 4.10).

It appears that traditional flood-irrigation practices in HBC command causes substantial amount of water lost due to percolation (Tables 4.8 and 4.9). This further reduces the

WP_{ET} to WP_{ETQ} at the field scale. The average water- and salt-limited WP_{ETQ} $Y/(ET+Q)$ was 0.22 for cotton, 0.69 for rice, and 1.23 for wheat (Table 4.10). The average WP_{ETQ} based on the actual observed crop yields was 0.17 for cotton, 0.54 for rice, and 0.89 for wheat (Table 4.10).

Table 4.10: SWAP simulated water- and salt-limited crop water productivity of main crops at farmer's fields in Hakra command area, Punjab Pakistan during the agricultural year 2016-17.

Fields	Crop	WP_T		WP_{ET}		WP_{ETQ}		WP_I	
		Y_{sim}/T	Y_{obs}/T	Y_{sim}/ET	Y_{obs}/ET	$Y_{sim}/(ET+Q_{bot})$	$Y_{obs}/(ET+Q_{bot})$	Y_{sim}/I	Y_{obs}/I
CW1	Cotton	0.39	0.27	0.35	0.24	0.21	0.14	0.23	0.15
	Wheat	2.74	2.05	2.02	1.51	1.14	0.85	1.63	1.22
CW2	Cotton	0.48	0.41	0.42	0.35	0.24	0.2	0.25	0.22
	Wheat	2.62	1.81	2.05	1.42	1.07	0.74	1.23	0.85
RW1	Rice	1.77	1.36	0.85	0.65	0.68	0.52	0.56	0.43
	Wheat	2.6	2.14	2.09	1.72	1.15	0.95	4.01	3.3
RW2	Rice	1.46	1.15	0.84	0.66	0.71	0.56	0.68	0.54
	Wheat	2.49	1.65	2.13	1.42	1.54	1.03	5.98	3.97
Mean	Cotton	0.44	0.34	0.39	0.30	0.23	0.17	0.24	0.19
	Rice	1.62	1.93	0.85	0.66	0.70	0.54	0.62	0.49
	Wheat	2.61	1.91	2.07	1.52	1.23	0.89	3.21	2.34

Compared to the average WP_{ET} values, the average WP_{ETQ} values are 18% less for rice, 42% less for cotton, and 41% less for wheat (Table 4.10). The reduction from WP_{ET} to WP_{ETQ} for wheat at the cotton-wheat fields (CW1 and CW2) represents over-irrigation at these fields. The reduction in WP_{ETQ} for rice was relatively less due to less percolation in the rice fields (Table 4.6), caused by low hydraulic conductivity to maintain surface ponding. The average water- and salt-limited WP_I was 0.24 for cotton, 0.62 for rice, and 3.21 for wheat, and based on the actual observed crop yields is quantified to be 0.19 for cotton, 0.48 for rice, and 2.34 for wheat (Table 4.10).

Whereas for wheat on rice-wheat fields, the WP_I was approximately 2 times higher than the WP_{ET}. Also, the WP_I ($kg\ m^{-3}$) values for wheat are much higher at the rice-wheat

(RW1 and RW2) fields, compared to the cotton-wheat fields (CW1 and CW2). This is due to lower amount of irrigation application in wheat at the rice-wheat fields (Table 4.6) and the presence of large amount of moisture left after the rice crop. This indicate that wheat is the highest efficient crop in terms of physical crop production, specifically in the rice-wheat crop rotation in HBC command. However, the economic water productivity of these crops (wheat, rice, and cotton) would be different due to different input costs and value of the crop yields.

4.6 Conclusions

To explore the effects of on-farm irrigation practices through soil water and salt balances and crop water productivity, a physically based agro-hydrological model, Soil-Water-Atmosphere-Plant (SWAP) was calibrated and validated using the observed data from four farmers' fields of cotton-wheat and rice-wheat crop rotation at HBC command during the agriculture year 2016-2017. Good agreement between the simulated and observed soil moisture (*RMSE* = 0.03 – 0.07), soil salinity (*RMSE* = 0.07 – 0.20 dS m^{-1}), and crop yields provided confidence to use the calibrated and validated SWAP model to evaluate the potential effects of different irrigation practices on soil water and salt balances, crop yields, and crop water productivity at the study farmer's fields.

The simulated low relative transpiration of 0.6 for cotton at the CW1 field, 0.63 for rice at the RW1 and 0.54 for wheat at the RW1 revealed that water- and/or salt-stress on the cultivated crops. This is also evident from relatively higher positive value of salt storage index simulated for the CW1 and RW1 fields (Table 4.8 and 4.9). This was due to using of poor-quality groundwater (3.28 dS m^{-1}) at the CW1 field, and saline and waterlogged conditions at the RW1 field. The positive value of the percolation index of both rice-wheat fields reveals capillary rise which is sign of waterlogging in these fields.

Using the calibrated and validated SWAP, a robust simulation of soil water balance components like transpiration, evapotranspiration, percolation, and water- and salt-limited crop yields enabled quantification of the crop water productivity values of the main crops cotton, rice and wheat at the study fields. This covered different forms on crop water productivity values, including WP_T, WP_{ET}, WP_{ETQ} and WP_I (Table 4.10). The high temperature and vapour pressure deficit during the *kharif* (summer) season result in significant amount of water loss in terms of evaporation. Consequently, this causes WP_T, WP_{ET}, WP_{ETQ} and WP_I of the *kharif* crops (cotton and rice) to be lower than the *rabi* crop (wheat). Furthermore, due to traditional flood surface irrigation of the study fields, a significant proportion of applied water is percolated from the root zone or stored in the root zone. This results in a reduction of WP_{ET} to WP_{ETQ}. Usually in irrigated areas the percolation helped to recharge the groundwater, which can then be recycled through groundwater pumping. Moreover, percolation also contributes to leaching of excessive salt built-up in the soil profile. However, in area of poor groundwater quality percolation is a loss of water. The leaching of salts limits the utility of re-pumping for irrigation.

It can be concluded that the analysis from the agro-hydrological model SWAP, in combination with field experiments, is useful approach to quantify and evaluate the soil water and salt balances, and water- and salt-limited crop yields at field scale. Moreover, this modelling approach is helpful in quantifying the potential effects of different irrigation practices on soil percolation, groundwater recharge, and salt build up in the soil profile, and their combined impacts on crop yields and crop water productivity values in the study area.

Chapter 5 : Potential effects of modern irrigation systems on soil-water and salt balances, and crop-water productivity of wheat-cotton cultivation at field scale

5.1 Introduction

Irrigated agriculture in Pakistan, nationally and specifically in rural areas, is a significant source of livelihoods, food security, and a major component in poverty alleviation (Bhutto and Bazmi, 2007). However, the growing population and projected climatic changes are putting increasing pressure on limited water supplies for irrigated agriculture in Punjab Pakistan (Ringler and Anwar, 2013; Sharma *et al.*, 2013), as well as in other semi-arid and arid regions worldwide (Dehghanisanij *et al.*, 2006; Connor *et al.*, 2012). Irrigated agriculture in many semi-arid and arid regions suffers from low crop yields, limited surface water supplies, and is at risk of soil salinization and waterlogging in areas of poor groundwater quality, and declining groundwater levels (Ragab and Prudhomme, 2002; Foster *et al.*, 2018). As a response, modernization of irrigation systems is considered to be able to improve irrigation water use efficiency in water-scare semi-arid and arid regions of Pakistan (DGA, 2011; Latif *et al.*, 2016) and elsewhere (Varela-Ortega and Sagardoy, 2002; Ward and Darghouth, 2006a; Sanchis-Ibor *et al.*, 2017; Huang *et al.*, 2020). Adoption of new technologies and high-efficiency irrigation systems such as sprinkler and drip irrigation is suggested to improve irrigation efficiency, save water, and increase crop yields (DGA, 2011).

However, modernisation of irrigation practices can lead to unintended consequences in terms of reduction of groundwater recharge, and the risk of salt build-up in the soil profile, particularly in semi-arid and arid-irrigation systems. Significant effort and resources are aimed at modernisation of irrigation practices in Punjab Pakistan (DGA, 2011). However, there have been hardly any studies that have comprehensively analysed the long-term effects of modern irrigation practices on soil-water and salt balances, and crop water productivity in the semi-arid areas of Punjab Pakistan. This chapter integrates local field observations into the agrohydrological model, Soil-Water-Atmosphere-Plant

(SWAP) to predict the long-term potential effects of modern irrigation practices on soil water and salt balances, and crop water productivity of the two main crops of wheat and cotton grown in the Hakra Branch Canal (HBC) command, located in Punjab Pakistan. In Chapter 4, the SWAP model was calibrated and validated for simulation of soil water and salt balances, and crop growth of the main crops of cotton-wheat and rice-wheat at four farmer fields in the study area. In this chapter, the calibrated and validated SWAP model is further developed to simulate longer-term (10 years, 2007-2017) effects of surface flood and high-efficiency sprinkler irrigation systems on soil-water and salt dynamics and crop water productivity of the cotton-wheat cultivation at the field-scale. This approach is tested by analysing the simulated soil water and salt balances, and crop growth in relation to different water and salt stress levels as function of different irrigation water applied. This investigation aims to quantify the longer-term potential effects of improved irrigation efficiency and its management in semi-arid regions of Punjab Pakistan. This will help to develop productive and sustainable crop production systems not only in the semi-arid regions of Punjab Pakistan, but also in other similar semi-arid and arid regions globally.

5.2 Irrigation Scenarios

The calibrated and validated SWAP model is applied to simulated two different irrigation options, either a fixed pre-defined schedule, or a calculated irrigation schedule (van Dam *et al.*, 1997). In the fixed irrigation mode, the day and depth of irrigation application, the quality of irrigation water, and the type of irrigation system are needed as inputs into SWAP. However, in the calculated irrigation application, SWAP calculates the irrigation scheduling according to the type of irrigation (surface or sprinkler), the time of irrigation (allowable daily crop stress, *Ta/Tp)*, and irrigation depth criteria of either fixed depth, or

back-to-field capacity. Using these options, we defined and simulated three irrigation scenarios as described below. These were simulated for cotton-wheat cultivation.

5.2.1 Current (*reference*) irrigation scenario*:*

The reference irrigation-scenario is the current fixed rotation (Warabandi) system in the HBC. In this reference scenario, as per the local field observations, a conjunctive use of canal and groundwater is used to simulate a total of 1100 mm irrigation depth applied in 12 irrigation intervals with an average irrigation depth of 92 mm for the cotton crop; and a total of 480 mm irrigation applied in 5 irrigation intervals with an average irrigation depth of 98 mm for the wheat crop (Table 4.1). The electrical conductivity of conjunctive irrigation water is specified as 0.96 dS m^{-1} based on the field observations. The reference scenario is simulated over a period of 10 years from May 1st, 2007 to April 30th, 2017 (sourced from Pakistan Metrological Department) and serves as a basis for further analysis and comparisons with modern irrigation scenarios as follows.

5.2.2 Precision surface irrigation system (*PSIS*):

Laser-based land levelling and flexible water supplies are recommended to help improve water-use efficiency of surface irrigation applications in cropping systems (Clemmens *et al.*, 1999; Ahmad *et al.*, 2007; Maqsood and Khalil, 2013; Shahani *et al.*, 2016; Miao Q, 2017; Rizwan *et al.*, 2018). This is defined and simulated as a modernised gravity-fed surface irrigation system, also known as 'precision surface irrigation system (*PSIS*)', by using irrigation scheduling with a fixed irrigation depth criterion in the SWAP model. The timing of irrigation is based on the relative transpiration (the ratio of actual transpiration to potential transpiration, T_a/T_p) as the crop stress criterion for flexible irrigation applications. A fixed depth irrigation is applied when the crop reached a pre-

defined level of T_a/T_p due to the crop water and/or salt stress levels. In this scenario, a total of six irrigation scheduling criteria, notably *I0.5*, *I0.6*, *I0.7*, *I0.8*, *I0.9*, and *I0.95*, are set corresponding to different targeted crop T_a/T_p ratios of 0.5, 0.6, 0.7, 0.8, 0.9 and 0.95, respectively. In surface irrigation-systems, the depth of irrigation application ranges from 50 to 150 mm depending upon size of fields and their levelling, the number of border strips, the soil texture affecting the infiltration rate, the irrigation discharge rate, and climatic conditions (Lecina *et al.*, 2005; Laghari *et al.*, 2010; Chen *et al.*, 2013; Mohan Reddy, 2013; Anwar *et al.*, 2016). In the *PSIS* scenario, two fixed irrigation depth scenarios, 60 mm and 80 mm for each irrigation event, are simulated representing surface irrigation depths that are assumed when the field is properly levelled and water is uniformly distributed as improved surface irrigation (Wagan *et al.*, 2015; Anwar *et al.*, 2016; Shahani *et al.*, 2016; Ashraf *et al.*, 2017).

5.2.3 High-efficiency irrigation system (*HEIS*):

Modern pressurized irrigation systems that include sprinkler and drip irrigation are promoted as highly efficient irrigation-systems that can apply a specific amount of irrigation when required by a crop. To quantify the potential effects of the shift from conventional surface irrigation to the high efficiency 'sprinkler' irrigation system (*HEIS*), the irrigation scheduling with a sprinkler irrigation system are based on "back to field capacity" irrigation depth criterion as adopted in SWAP model. In this *HEIS* scenario, a total of six irrigation scheduling criteria, namely *I0.5*, *I0.6*, *I0.7*, *I0.8*, I0.9, and *I0.95* corresponding to different targeted crop T_a/T_p ratios of 0.5, 0.6, 0.7, 0.8, 0.9 and 0.95, respectively, are specified to trigger an irrigation event and bring the soil condition back to field capacity at each irrigation event. To explore the effects of changes in the irrigation system on the salinity level in soil profile, the *HEIS* irrigation scenario is simulated first without a leaching fraction (*HEIS_noLF*), and then with a leaching fraction (*HEIS_ LF*).

In case of *HEIS_ LF* an additional irrigation depth (60 mm) is applied before the crop sowing, and the subsequent irrigations also received 10 mm of additional irrigation to the calculated 'back to field capacity' irrigation depths.

The quality of the irrigation water is assumed the same, as in the *reference baseline*, with an electrical conductivity of 0.96 dS m^{-1}, as based on the local field observations for the *PSIS* and *HEIS* irrigation scenarios, representing a conjunctive use of canal and marginal quality groundwater.

5.3 Irrigation Performance Indicators

The long-term simulations over the 10 years from May 1st, 2007 to April 30th, 2017 of the three irrigation scenarios are analysed using the following irrigation performance indicators:

5.3.1 Percolation (Q_{bot}): This is the amount of water percolating below the crop root zone and quantifies the water exchange between unsaturated and groundwater zones. It quantifies the potential effects of irrigation practices on groundwater, where a negative value represents recharge to groundwater system. Percolation occurs when the infiltrated water exceeds the storage capacity of the soil profile. Using the simulated soil water balance components, the soil percolation can be quantified as follows:

$$Q_{bot} = -(P + I - R_s - P_i - T - E - E_w \pm \Delta W) \qquad \text{Eq. 5.1}$$

Where, Q_{bot} is the water percolation from the soil profile lower boundary (positive upward, negative downward) [L], P is the rainfall [L], I in the is the irrigation [L], R_s is the surface runoff [L], P_i is the rainfall intercepted by vegetation [L], T is the actual transpiration [L], E is the actual evaporation from the soil surface [L], E_w is the evaporation from the ponding water surface [L], and ΔW is the change soil storage [L].

Under free-drainage conditions, as simulated in this study, SWAP simulates the lower percolation flux by assuming the pressure head gradient equals zero at the bottom of soil profile. This implies that the bottom flux equals the hydraulic conductivity of the lowest soil compartment (van Dam *et al.*, 1997). In this study, the SWAP-calculated daily percolation values are accumulated to quantify the average seasonal and annual percolation (Q_{bot}) under the different irrigation scenarios.

5.3.2 Change in salt storage (ΔC): Salt storage in a soil profile is affected by the balance of all salt inputs and outputs over a specified time period. The fluxes of soil salt inputs and outputs are through rainfall, irrigation water, and percolation from the soil profile. In this study, the salt input via rainfall is assumed negligible. Via irrigation it is set at 0.96 dS m^{-1} as per the local field observations (see Section 5.2 above). The difference between the salt inputs and outputs equals to the changes in salt storage (ΔC) of the soil profile. If the amount of salt input exceeds the amount of salt output, then salt accumulates and increases the salinity of the soil profile. Therefore, the change in salt storage (ΔC) can be used to quantify the soil salinity trends and helps in understanding soil salinity problems at the field scale, as well as at the regional scale. In this study, SWAP quantified ΔC (per unit area) by solving the salt balance equation:

$$\Delta C = PC_p + IC_i + Q_{bot}C_{bot} \qquad \text{Eq. 5.2}$$

where, ΔC is the change in salt storage [M L^{-2}], C is the solute concentration [M L^{-3}], P is the precipitation [L], I is the irrigation [L], Q is the percolation [L] and subscript 'p' refer precipitation, 'i' refers to irrigation and *bot* refers to lower boundary flux.

5.3.3 Crop Water productivity : A crop water productivity (*WP*) analysis has been suggested to be a useful indicator for assessing on-farm irrigation practices of a crop production system (Singh *et al.*, 2006c; Fernández *et al.*, 2020b). According to Molden

et al. (2003), crop water productivity accounts for crop dry-matter produced per unit amount water used. From a biophysical perspective, the numerator of *WP* is the crop yield, but the definition of denominator, such as transpiration, evapotranspiration, or total water applied, varies according to the purpose, scale and domain of the analysis (Singh *et al.*, 2006c; Fernández *et al.*, 2020b). From an agronomic perspective, the crop evapotranspiration *ET* represents the actual amount of water consumed in crop production systems and *WP* can here be expressed as follows:

$$WP_{ET} = \frac{Y_g}{ET_a} \qquad \text{Eq. 5.3c}$$

where, Y_g crop grain (or seed) yield [ML^{-2}], ET_a is the actual evapotranspiration from crop and soil surface [L].

In terms of the actual amount of irrigation water used, the denominator in the *WP* equation is replaced by total irrigation depth applied and can be expressed as:

$$WP_{Irr} = \frac{Y_g}{I} \qquad \text{Eq. 5.4}$$

where, WP_{Irr} is the water productivity in terms of irrigation water applied during the entire crop period [ML^{-3}], Y_g crop grain (or seed) yield [ML^{-2}], and I is the irrigation depth applied [L].

5.4 Results and discussion

5.4.1 Reference (baseline) scenario

Table 5.1 summarizes the modelled effects of current irrigation practices on soil water and salt balances, crop yields and crop water productivity values as simulated for the

cotton-wheat cultivation over the period of 10 years (2007-2017). The seasonal rainfall varied from 98 mm to 460 mm with an average of 231 mm during the *kharif* (cotton) season, and from 7 mm to 104 mm with an average of 51 mm during the *rabi* (wheat) season. Rainfall is significantly less than the crop water demands in the study area. The long-term SWAP simulated ET_p (E_p + T_p) varied from 1011 mm to 1144 mm with an average of 1078 mm during the *kharif* (cotton), and from 389 mm to 490 mm with an average of 451 mm during the *rabi* (wheat) season (Table 5.1). The long-term SWAP simulated ET_p values show a close agreement with the ET_p values of 906 mm during *kharif* season and 485 mm during *rabi* season calculated by Liaqat *et al.* (2016) in HBC command.

The seasonal rainfall received contributes only 21% to the ET_p during the *kharif* season, and 11% to the ET_p during the *rabi* season (Table 5.1). The average irrigation under the *reference* irrigation scenario was applied at 1100 mm during the *kharif* (summer) season and 490 mm during the *rabi* (winter) season based on the observations at the local farmers' fields (Table 5.1). As a result, SWAP simulated seasonal actual evapotranspiration (ET_a) from 684 to 818 mm, with an average value of 760 mm for cotton crop during the *kharif* season, and from 282 to 357 mm with an average value of 327 mm for wheat crop during the *rabi* season. Applying the surface energy balance system (SEBS) model, Liaqat *et al.* (2016) estimated seasonal average ET_a of 641 mm during the *kharif* season, and 322 mm in the *rabi* season with an annual average ET_a of 963 mm for HBC over the period from 2008 to 2014. These ET_a values are in close agreement with the simulated ET_a values in this study (Table 5.1).

The average annual water-supply of 1872 mm yr^{-1}, accounting for both the average annual rainfall (282 mm yr^{-1}) and irrigation (1590 mm yr^{-1}), amounts to 1.2 times of the average annual reference evapotranspiration ET_p predicted to be 1529 mm yr^{-1} (Table

5.1). About 42% of the average annual water supply is simulated to percolate Q_{bot} (-779 mm yr^{-1}) to groundwater, including an average of about -557 mm during the kharif season, and about -222 mm during the *rabi* season (Table 5.1). This high percolation rate could be attributed to the high irrigation applications (Table 5.1) and the sandy texture of the soil (Table 4.3). Liaqat *et al.* (2016) also reported seasonal groundwater recharge of 330 mm during the *kharif* season, and of 235 mm during the *rabi* season, with an average annual groundwater recharge of 565 mm across the whole command of HBC during period from 2008-2014. Liaqat *et al.* (2016) also reported an average annual groundwater abstraction of 680 mm yr^{-1} for irrigation in the HBC during the same period. In the selected farmers' fields, the annual average contribution of groundwater is 668 mm of the total annual-average irrigation of 1348 mm for the cotton-wheat cultivation (Table 4.6). Considering this, groundwater contributes about 50% of annual irrigation supply for cotton-wheat cultivation in the study fields. This highlights that groundwater abstraction is an integral part of irrigation in the HBC, which varies in its quality from less than 1 up to 20 dS m^{-1}. Furthermore, this stresses the role played by percolation in sustaining the groundwater resource.

In arid and semi-arid areas, the high use of marginal- and poor-quality groundwater with high levels of salts can lead to a salt build-up in the soil profile (Datta and De Jong, 2002; Smedema and Shiati, 2002; Garg and Hassan, 2007; Mukherjee *et al.*, 2015). The salinity levels in the soil profile must be maintained below the crop-specific threshold level (EC_{max}) (Maas and Hoffman, 1977) beyond which crop yields are reduced due to salt stress on crop growth (van Dam *et al.*, 1997). We used a mixture of good quality canal water (EC = 0.57 dS m^{-1}) and marginal quality groundwater (EC = 1.66 dS m^{-1}) to simulate a representative conjunctive use of canal and groundwater (EC = 0.96 dS m^{-1}) for a cotton-wheat rotation over period of 10 years in the study area. This resulted in a

salt balance from -26 mg cm^{-2} (2600 kg ha^{-1}) to +28 mg cm^{-2} (2800 kg ha^{-1}) during the *kharif* season, and from -1500 kg ha^{-1} to +2000 kg ha^{-1} during the *rabi* season (Table 5.1). This variation in the salt balance can be attributed to variations in the rainfall received. This causes significant salt leaching during high rainfall years such as 2010-2013 and 2015-16 (refer Table B.1 in the appendix B). The results showed that high applications of irrigation (1100 mm yr^{-1}) resulted in an average of salt-leaching of -38 kg ha^{-1} yr^{-1} during the *kharif* season, and a negligible salt build-up of 100 kg ha^{-1} yr^{-1} during the *rabi* season (Table 5.1). There was no significant change in soil salinity (62 kg ha^{-1} yr^{-1}) on an average annual basis under the *reference* irrigation scenario (Table 5.1). At the end of 10-year simulation period, the average soil salinity in the soil profile is simulated as being 1.76 dS m^{-1}, significantly lower than the crop threshold salinity levels of 7.7 dS m^{-1} for cotton and 6.0 dS m^{-1} for wheat (Table 4.2). Overall, this suggests that negligible salinity stress should be observed by the cotton-wheat crops under the *reference* scenario. This could be due to a significant percolation Q_{bot} that was simulated from -532 mm yr^{-1} to -1043 mm yr^{-1} (refer Table B.1 in the appendix B), with an average of -780 mm yr^{-1} (Table 5.1) This means about 50% of the irrigation serves a leaching fraction under the *reference* irrigation practices (Table 5.1).

The SWAP model combined effects of water and salt stresses reduces the relative transpiration of the crop. The simulated relative transpiration (T_a/T_p) varied from 0.90 to 0.95 with an average of 0.92 for the cotton crop, whereas it varied from 0.96 to 0.98 with an average of 0.98 for the wheat crop (Table 5.1). These high T_a/T_p values reveal no significant water and salt stress on the cotton-wheat crops simulated under the *reference* irrigation practices. The predicted water- and salt-limited crop yields varied from 2.4 to 4.07 ton ha^{-1}, with an average of 2.98 ton ha^{-1} for cotton, and from 3.55 to 6.69 t ha^{-1}, with an average of 5.70 ton ha^{-1} for wheat (Table 5.1).

The predicted crop water productivity based on the simulated water- and salt-limited crop yields (*Y*) and actual evapotranspiration (*ET*), WP_{ET} (Eq. 5.3) varied from 0.30 to 0.55 kg m^{-3} with an average value of 0.39 kg m^{-3} for cotton, and from 1.10 to 2.13 kg m^{-3} with average value of 1.75 kg m^{-3} for wheat over the 10 years (2007-2017) (Table 5.1). Whereas the crop water productivity based on irrigation WP_{Irr} varied from 0.22 to 0.37 kg m^{-3} with an average value of 0.27 kg m^{-3} for cotton and from 0.73 to 1.37 kg m^{-3} with average value of 1.17 kg m^{-3} for wheat (Table 5.1).

Table 5.1: SWAP simulated mean soil water and salt balance components of cotton-wheat crops under 'business-as-usual' reference (baseline) irrigation scenario for 10 years (2007-2017) in Hakra canal command, Punjab Pakistan. (refer to Table B.1 in the appendix B for annual based soil water and salt balance components)

Soil water and salt balances, and crop water productivity	*Kharif* Season (Cotton)		*Rabi* Season (Wheat)	
	Mean	*CV*	Mean	*CV*
Rain(mm)	231	0.42	51	0.63
Irrigation (mm)	1100	-	490	-
E_p (mm)	354	0.04	186	0.09
T_p (mm)	724	0.08	265	0.11
T (mm)	665	0.08	259	0.11
T_a/T_p (mm)	0.92	0.02	0.98	0.01
ET_a (mm)	760	0.06	327	0.08
Q_{bot} (mm)	-557	-0.24	-222	-0.16
ΔW (mm)	16	3.04	-9	-2.22
IC_i (mg cm^2)	73	-	31	-
C_{bot} (mg cm^2)	-73	-0.21	-30	-0.3
ΔC (mg cm^2)	-0.38	-40.4	1	10.01
Yield (kg ha^{-1})	2978	0.18	5707	0.16
WP_{ET} (kg m^{-3})	0.39	0.2	1.75	0.18
WP_{Irr} (kg m^{-3})	0.27	0.18	1.17	0.16

The symbols *E* is evaporation, *T* is transpiration *ET* is evapotranspiration, *Q* is percolation, ΔW change in water storage, *I* is irrigation, *C* is solute concentration, ΔC is change in solute concentration, *WP* is water productivity. Subscripts *p* is potential, *a* is actual, *bot* is bottom, *ET* is evapotranspiration, *Irr* is irrigation, CV is the coefficient of variation.

Combining field observations and SWAP predictions, Singh *et al.* (2006c) quantified the average WP_{ET} values of 0.31 and 2.01 kg m^{-3} for cotton and wheat, respectively, and

found the average WP_{Irr} values of 0.26 and 1.67 kg m^{-3} for cotton and wheat, in the Sirsa Irrigation Circle of Haryana state of India, an irrigation area very close to the study area. These indicative WP_{ET} and WP_{Irr} values show a close agreement with the

predicted results in this study (Table 5.1) and provide further evidence that the model simulations were merited further scenario analyses. Interestingly, the average WP_{Irr} values were simulated about 2/3rd (~65-68%) of the average WP_{ET} values for both cotton and wheat crops (Table 5.1). This suggests a potential to improve irrigation applications in the *reference* irrigation scenario practices.

5.4.2 Precision surface irrigation scenario

Figure 5.1 shows the predicted effects of 'precision surface irrigation scenario, noted as *PSIS*'. This involves a comparison of the fixed irrigation depths of 60 mm and 80 mm on average annual irrigation amounts, percolation, and soil salt storage in the soil profile under the cotton-wheat cultivation. Over the long-term, the cotton-wheat cultivation irrigation under the *PSIS* scenario required an average annual irrigation from 618 mm yr^{-1} under *I0.5* irrigation scheduling, up to 900 mm yr^{-1} under *I0.95* irrigation scheduling with a fixed irrigation depth of 60 mm (Figure 5.1). It required from 664 mm yr^{-1} under *I0.5*, to 920 mm yr^{-1} under *I0.95* with a fixed irrigation depth of 80 mm (Figure 5.1). This suggests potential savings of the cotton-wheat irrigation amount from 3% under *I0.95*, to 8% under *I0.5* with a fixed irrigation depth of 60 mm, as compared to 80 mm. However, under the *PSIS I0.5* irrigation scheduling, the salt storage in the soil profile is predicted to be at 35 mg cm^{-2} (~ 3.5 ton ha^{-1}, with a soil salinity of 8.54 dS m^{-1}) using a 60 mm irrigation depth, as compared to 37 mg cm^{-2} (~ 3.7 ton ha^{-1}, with a soil salinity of 8.87 dS m^{-1}) with 80 mm irrigation depth (Figure 5.1). Under the *PSIS I0.80* irrigation scheduling, the salt storage increased linearly from 35 to 43 mg cm^{-2} (~ 4.3 ton ha^{-1}, a

soil salinity of 10 dS m^{-1}) with the 60 mm irrigation depth, but reduced from 37 to 31 mg cm^{-2} (~ 3.1 ton ha^{-1}, a soil salinity of 7.43 dS m^{-1}) with the 80 mm irrigation depth (Figure 5.1).

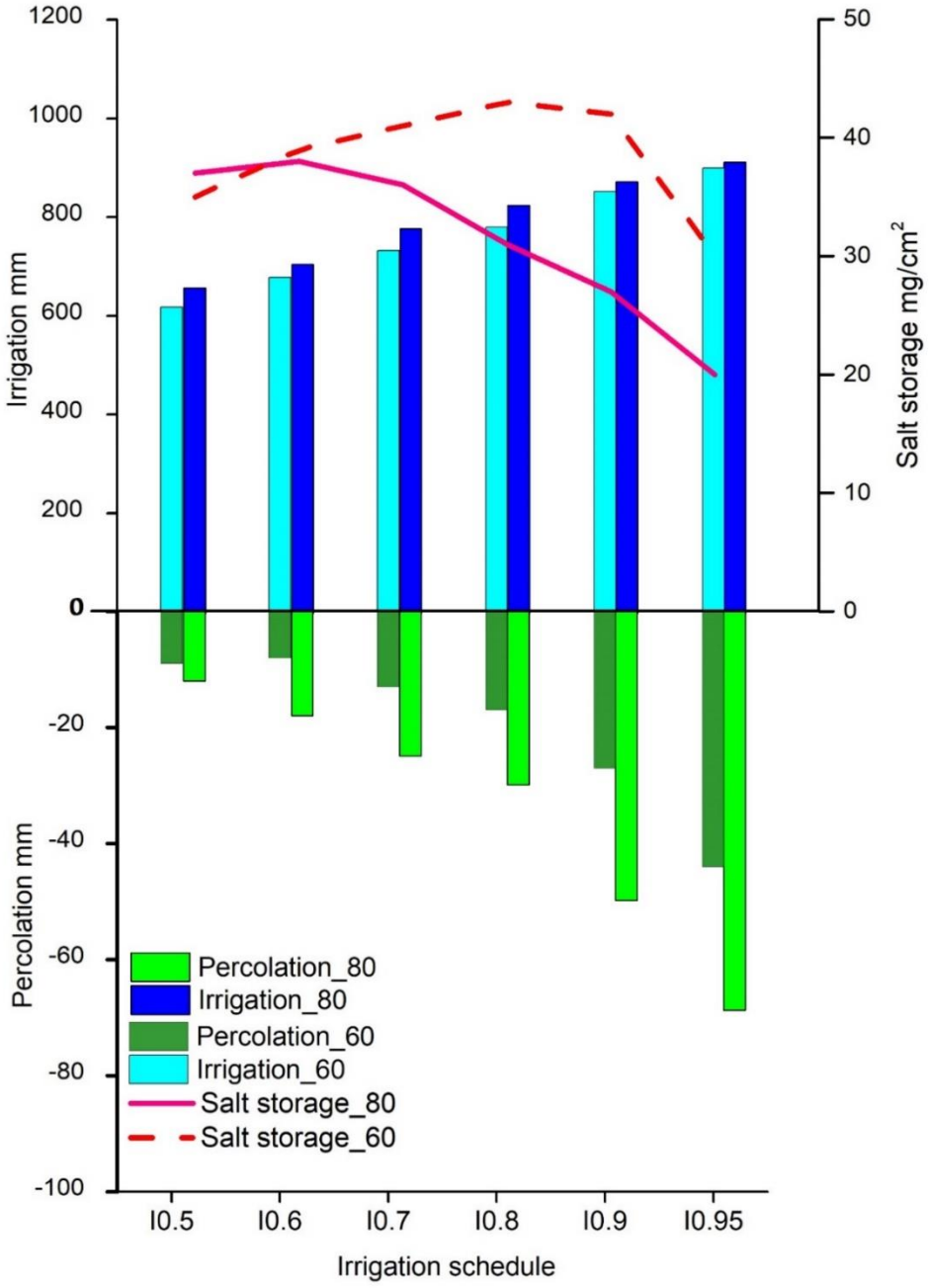

Figure 5.1: Simulated effects of 'precision surface irrigation system *(PSIS)*' scenario with a fixed irrigation depth of 60 mm (*PSIS_60mm*) and 80 mm (*PSIS_80mm*) on the long-term (10 years, 2007 - 2017) average irrigation applied, percolation and salt storage in the soil profile under cotton-wheat cultivation in Hakra canal command, Punjab Pakistan.

Under the *PSIS I0.95* irrigation scheduling, the salt storage is predicted to be at 30 mg cm^{-2} (~3.1 ton ha^{-1}, a soil salinity of 6.65 dS m^{-1}) with a 60 mm irrigation depth, whereas it is predicted to be at 20 mg cm^{-3} (2.0 ton ha^{-1}, salinity 5.7 dS m^{-1}) with the 80 mm irrigation depth (Figure 5.1). The simulated soil salinity values with the 60 mm irrigation depth, particularly under the *PSIS I0.5 to I0.80* irrigation scheduling, are higher than the critical thresholds EC_{max} of 6.0 and 7.7 dS m^{-1} for wheat and cotton crops, respectively (Table 4.2). It is evident from these results that the *PSIS* with 80 mm of fixed depth irrigation resulted into relatively lower salt storage in the soil profile, particularly under the least daily crop-stress criterion of the *I0.95* irrigation scheduling (Figure 5.1).

Figures 5.2 and 5.3 show the predicted effects of changes in irrigation amounts and salt storage, with respect to the setting of the daily crop stress of the transpiration ratio criterion under different scenarios, over the long-term crop yields (Figure 5.2a & 5.2b), and the seasonal transpiration (Figure 5.2c & 5.2d) for cotton and wheat crops, respectively. However, the lesser irrigation amounts applied and relatively high soil salinity levels under the *I0.5* and *I0.6* criteria for irrigation scheduling (Figure 5.1) affected the crop water uptake (Figure 5.2c & 5.2d) and resulted in relatively lower crop yields (Figure 5.2a & 5.2b). In case of the *PSIS* scenario, the seasonal average T_a/T_p with fixed irrigation depth of 60 mm is achieved for cotton crop from 0.83 under *I0.5* irrigation scheduling, to 0.98 under *I0.95* irrigation scheduling (Figure 5.2c), and for wheat crop from 0.80 under *I0.5*, to 0.97 under *I0.95* (Figure 5.2d). Whereas the seasonal average T_a/T_p with fixed irrigation depth of 80 mm is achieved for cotton from 0.86 under *I0.5* irrigation scheduling, to 0.99 under *I0.95* irrigation scheduling (Figure 5.2c). And, for wheat crop this was from 0.85 under *I0.5* to 0.98 under *I0.95* (Figure 5.2d).

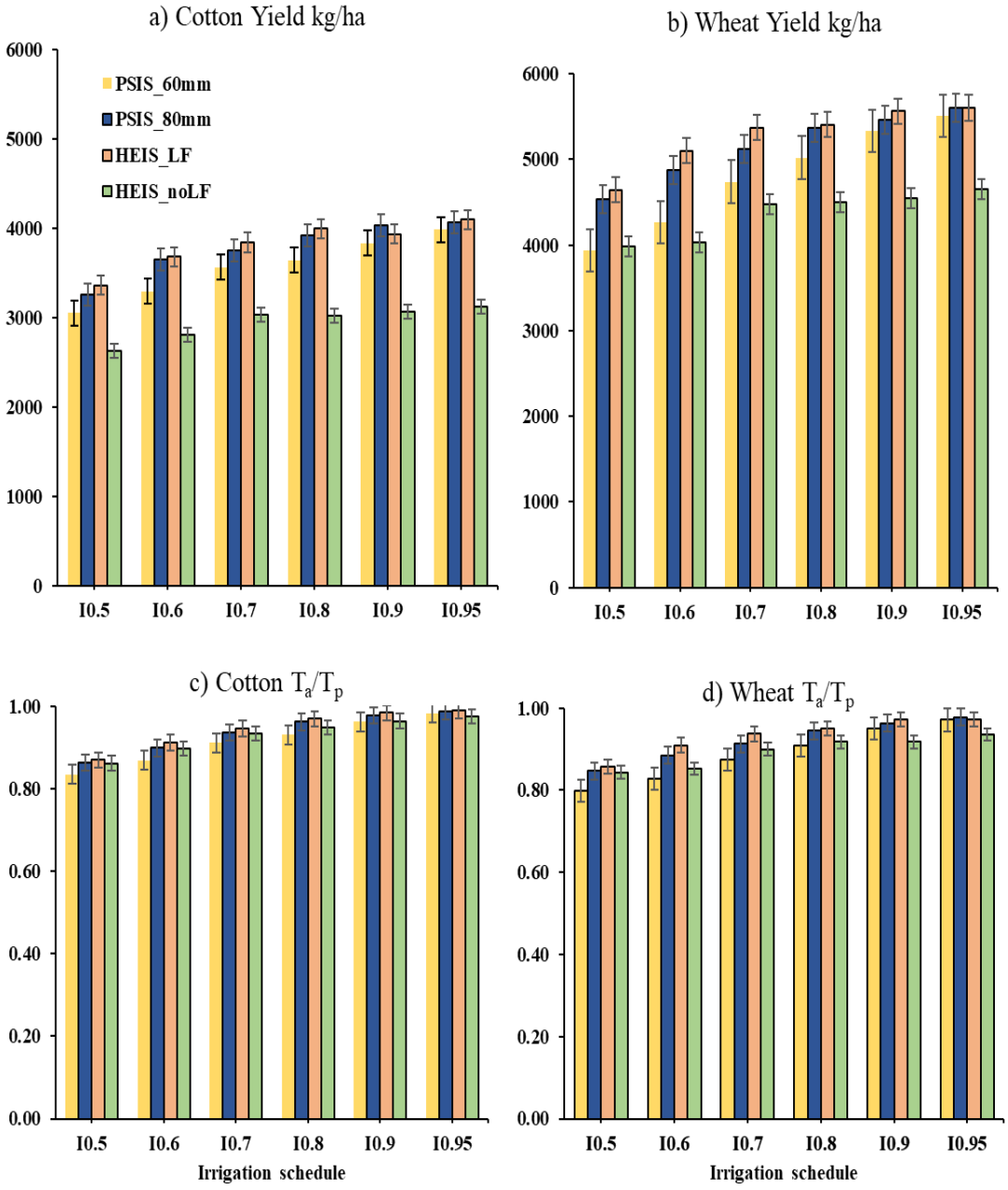

Figure 5.2: Simulated effects of the 'precision surface irrigation system (*PSIS*) with a fixed irrigation depth of 60 mm (*PSIS_60mm*) and 80 mm (*PSIS_80mm*), and the the 'high efficiency irrigation system (*HEIS*)', with a leaching fraction (*HEIS_LF*) and without a leaching fraction (*HEIS_no LF*), on the long-term (10 years, 2007 – 2017) average crop yields (a and b) and seasonal average crop relative transpirations (c and d) of cotton-wheat cultivation in Hakra canal command, Punjab Pakistan.

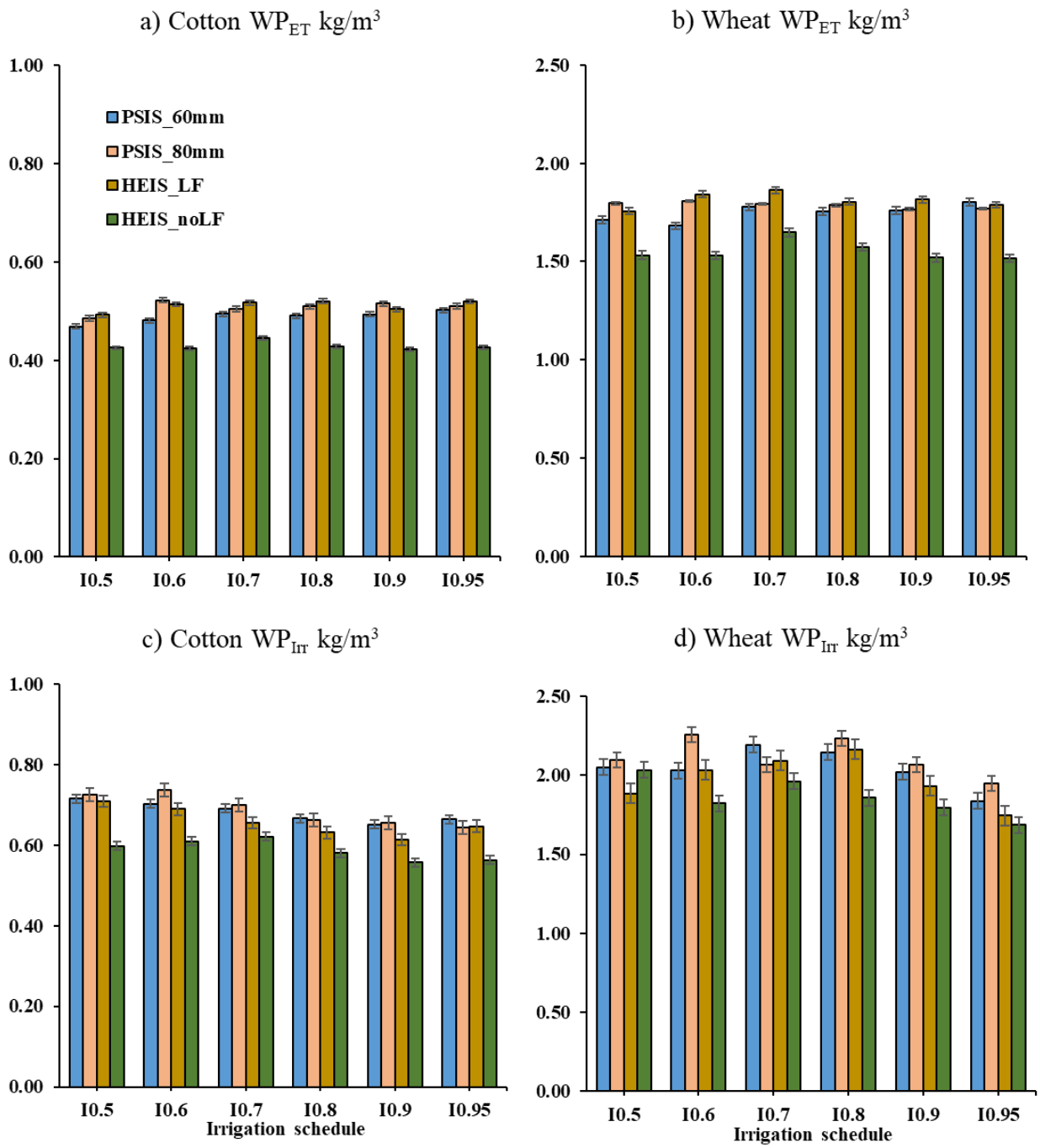

Figure 5.3: Simulated effects of the 'precision surface irrigation system (*PSIS*) with a fixed irrigation depth of 60 mm (*PSIS_60mm*) and 80 mm *(PSIS_80mm*), and the 'high efficiency irrigation system (*HEIS*)', with a leaching fraction (*HEIS_LF*) and without a leaching fraction (*HEIS_no LF*), on the long-term (10 years, 2007 - 2017) average crop water productivity of cotton-wheat cultivation in Hakra canal command, Punjab Pakistan.

The simulation results show, as expected, generally a positive relationship by which the crop yields increased with an increase in the crop relative transpiration (figure 5.2). From the seasonal average T_a/T_p analysis (Figs. 5.2c and d) it is evident that there would be no significant water and salt stress experienced by the wheat and cotton crops, even at the low fixed irrigation depth of 60 mm, particularly for the > *I0.7* criterion. In case of the *PSIS* scenario, the average wheat yield showed an increase of 40%, from 3.9 ton ha^{-1} under *I0.5* irrigation scheduling, to 5.5 ton ha^{-1} under *I0.95* irrigation scheduling with 60 mm irrigation depth. This is an increase of 23% from 4.5 ton ha^{-1} under *I0.5*, to 5.6 ton ha^{-1} under *I0.95* with 80 mm irrigation depth (Figure 5.2b). Similarly, the average cotton yield increased by 25% and by 20% when the irrigation scheduling increased from *I0.5* to *I0.95* with an irrigation depth 60 mm and 80 mm, respectively (Figure 5.2a). However, the average crop yields are predicted to be relatively lower for both the wheat and cotton crops with the *PSIS_60mm* as compared to the *PSIS_80mm*, particularly for under the *I0.5* and *I0.6* criteria for irrigation scheduling (Figure 5.2a & b). The *PSIS_60mm* and *PSIS_80mm* irrigation at > *I0.9* criteria had resulted into a higher percolation facilitating salt leaching (lower salt storage) (Figure 5.1), causing minimal water and salt stress and average higher crop yields (Figure 5.2).

However, the average WP_{ET} and WP_{Irr} values showed no significant variation for both the wheat and cotton crops when the irrigation schedule increased from *I0.5* to *I0.95* (Figure 5.3). Also, the changes in the fixed irrigation depth from 60 mm to 80 mm showed no significant effect on the average WP_{ET} and WP_{Irr} values for both the wheat and cotton crops (Figure 5.3). This could be attributed to almost a linear increase in the crop *ET* with the associated increase in the crop yields, as expected. Overall, the wheat and cotton yields and WP_{ET} values under the *PSIS* scenario are, however, achieved highest with the *I0.95* irrigation scheduling with 80 mm irrigation depth (Figs. 5.2 and 5.3). The analysis

of the *PSIS* scenario (Figs. 5.1-5.3) suggests that a precise application of surface irrigations with a fixed irrigation depth of 80 mm using a lower daily crop stress criterion (*>10.90*) would be beneficial in terms of maintaining soil salinity (Figure 5.1), and relatively higher wheat and cotton yields (Figure 5.2) and water productivity values (Figure 5.3) in the study area.

5.4.3 High-efficiency irrigation scenario

Figure 5.4 shows the predicted effects of using a 'high-efficiency irrigation system (*HEIS*)' with a leaching fraction (*HEIS_LF*), and without a leaching fraction (*HEIS_noLF*), on the long-term average of annual irrigation amounts, percolation, and soil salt storage in the soil profile for the cotton-wheat cultivation in the study area. Under *HEIS_noLF*, the cotton-wheat average annual irrigation is predicted to be from 635 mm yr^{-1} under *I0.5*, to 830 mm yr^{-1} under *I0.95*, while under *HEIS_LF* it is predicted to be from 720 mm yr^{-1} under *I0.5* to 955 mm yr^{-1} under *I0.95* (Figure 5.4). This results in savings of irrigation water from 12% to 15% under *HEIS_noLF* irrigations, but at the risks of an adverse salt build up in the soil profile, and a significant reduction in percolation as recharge to the groundwater system (Figure 5.4).

The average salt storage is simulated from 10% to 67% higher, the average annual percolation from 61 to 73% lower under *HEIS_noLF* irrigations as compared to *HEIS_LF* irrigations (Figure 5.4). Under *HEIS_noLF* scenario, the salt storage is simulated at 35 mg cm^{-2} (~ 8.8 dS m^{-1} soil *EC*) under *I0.5*, and to be at 34 mg cm^{-2} (~ 8.1 dS m^{-1} soil *EC*) under *I0.95* (Figure 5.4). These soil salinity levels are higher than the critical thresholds EC_{max} of 6.0 and 7.7 dS m^{-1} for wheat and cotton crops (Table 4.2). This suggests potentially adverse effects on the soil salinity on crop water uptake and yields of the cotton-wheat cultivation in the study area. This is supported by the results of

seasonal average T_a/T_p for both wheat and cotton crops predicted to be relatively lower under *HEIS_noLF* irrigations compared to *HEIS_ LF* irrigations (Figure 5.2 c&d).

Under the *HEIS_noLF* scenario, the seasonal average T_a/T_p is simulated for wheat crop from 0.84 under *I0.5*, to 0.94 under *I0.95* (Figure 5.2d). And for the cotton crop from 0.86 under *I0.5* to 0.97 under *I0.95* (Figure 5.2c). As a comparison, under the *HEIS_ LF* scenario, the seasonal average T_a/T_p is simulated for wheat crop from 0.86 under *I0.5* to 0.97 under *I0.95* (Figure 5.2d), and for cotton crop from 0.87 under *I0.5* to 0.99 under *I0.95* (Figure 5.2c). The average wheat and cotton yields are predicted to be from 17% to 24% lower under *HEIS_noLF* irrigations as compared to *HEIS_ LF* (Figure 5.2 a&b). This results in a reduction of 3% to 12% in the wheat and cotton WP_{Irr} values (Figure 5.3 c&d), and a reduction of 13% to 18% in the wheat and cotton WP_{ET} values under *HEIS_noLF* irrigations (Figure 5.3 a&b).

The analysis of the *HEIS* scenario (Figures 5.2 -5.4) suggests that high-efficiency irrigation systems such as sprinklers, without an appropriate leaching fraction (*HEIS_noLF*), poses a risk of salt build-up in the soil profile. Additional irrigation applications would be required to leach any excess salts and minimize soil salt build-up and its potentially adverse effects on crop yields and their water productivity. This is evident from the analysis of *HEIS_LF* scenario that resulted in relatively less salt storage (Figure 5.4), and higher crop yields (Figure 5.2) and water productivity values for the cotton-wheat cultivation (Figure 5.3).

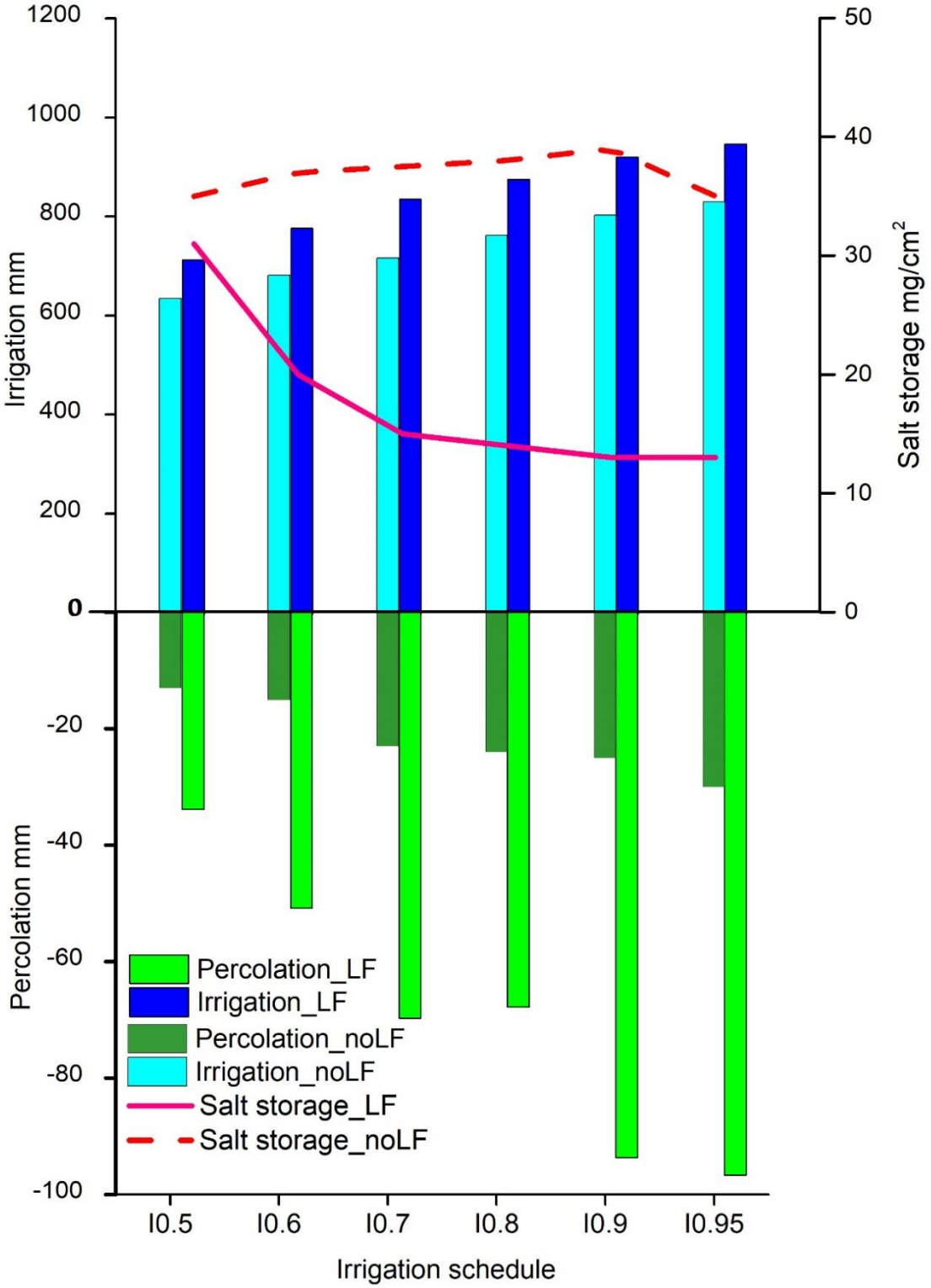

Figure 5.4: Simulated effects of 'high efficiency irrigation system (*HEIS*)', with a leaching fraction (*HEIS_LF*) and without a leaching fraction (*HEIS_noLF*) scenario on the long-term (10 years, 2007-2017) average irrigation applied, soil water percolation and salt storage under cotton-wheat cultivation in Hakra canal command, Punjab Pakistan.

5.4.4 Comparison of different irrigation scenarios

A comparison of the *reference*, *PSIS_80mm* and *HEIS_LF* at *I0.95* scenarios (Table 5.2) suggest a scope of >40% savings in irrigation amounts under the *PSIS_80mm* and *HEIS_LF*, compared to the *reference*. Also, *PSIS_80mm* and *HEIS_LF*, as compared to the *reference* resulted into similar average crop yields and WP_{ET} values for wheat crop, but an increase of ~ 30% in average crop yields, and WP_{ET} values for cotton crop (Table 5.2). The WP_{Irr} values are simulated to be >60% and >40% higher, respectively for the wheat and cotton crops under the *PSIS_80mm* and *HEIS_LF* as compared to the *reference* (Table 5.2). The high crop yield and water productivity values under *PSIS_80mm* and *HEIS_LF* irrigation scenario could be attributed to flexible irrigation scheduling according to crop water requirement instead of fixed irrigation irrespective of crop water requirement under reference irrigation scenario.

Table 5.2: SWAP simulated effects of different irrigation scenarios on long-term (10 years, 2007 - 2017) average soil water and salt balances, and water- and salt-limited crop yields and water productivity values of cotton-wheat cultivation in Hakra canal command, Punjab Pakistan. The *PSIS* stands for 'precision surface irrigation system with 80 mm fixed irrigation depth' (*PSIS_80mm*), and the *HEIS* stands for 'high efficiency irrigation system' with a leaching fraction (*HEIS_LF*) or without a leaching fraction (*HEIS_noLF*).

Water and Salt balance, crop performance		***Reference (baseline)***	***PSIS_80mm***	***HEIS_LF***	***HEIS_noLF***
Irrigation *(mm yr^{-1})*		1590	920	955	830
Percolation, Q_{bot} *(mm yr^{-1})*		-779	-69	-97	-30
Salt storage, ΔC *(mg cm^{2})*		0.51	20	13	35
Relative transpiration, T_a/T_p	*Cotton*	0.92	0.99	0.99	0.97
	Wheat	0.98	0.98	0.97	0.94
Crop Yield (ton ha^{-1})	*Cotton*	2.98	4.06	4.09	3.12
	Wheat	5.70	5.61	5.61	4.65
WP_{ET} *(kg m^{-3})*	*Cotton*	0.39	0.51	0.52	0.43
	Wheat	1.75	1.77	1.79	1.52
WP_{Irr} *(kg m^{-3})*	*Cotton*	0.27	0.64	0.65	0.56
	Wheat	1.17	1.95	1.79	1.69

This suggests a significant scope of improving the *reference* scenario representing current irrigation practices observed at the local farmers' fields. The analysis also clearly suggests that savings in irrigation amounts and improvements in the cotton-wheat yields (Figure 5.2, Table 5.2) and their water productivity values (Figure 5.3, Table 5.2) are possible, as long as the irrigation depths are supplemented by a sufficient depth of leaching fraction to prevent a salt build-up in the soil profile (Figure 5.1 and 5.4). A highly efficient irrigation system with minimum percolation (*HEIS_noLF*) poses a risk of salt build-up with its potentially adverse effects on crop yields and their water productivity (Figure 5.4, Table 5.2). This is demonstrated by the predictions of relatively lower crop yields and water productivity WP_{ET} values, particularly for the wheat crop under *HEIS_noLF* which results in a relatively lower percolation and higher salt-build-up in the soil profile (Table 5.2).

Irrigation with marginal to high salinity waters over a long periods of time could result into salt build-up and affect crop yields in arid and semi-arid regions (Kahlown *et al.*, 1998; Horneck *et al.*, 2007; Esteve *et al.*, 2008). Raine *et al.* (2007) reported that the long-term use of high-efficiency irrigation systems has potentially increased the root zone salinity in Australia. They considered that 10% of the irrigated area in Australia, which could produce 40% of the total annual revenue from irrigated lands, are potentially adversely affected due to increases in root-zone salinity resulting from the adoption of high efficiency irrigation systems. This could be mitigated by providing an appropriate leaching fraction to maintain, or reduce salt build-up, if no other alternate irrigation source available to replace the poor quality irrigation water.

In this study, the three irrigation scenarios; the *reference*, and the *PSIS_80mm* and *HEIS_LF* irrigation at *I0.95* irrigation scheduling, maintained the soil salinity levels between 0.51 – 20 mg cm^{-2}, ~ 1.76 - 5.66 dS m^{-1} (Table 5.2) which are below the critical

thresholds EC_{max} of 6.0 and 7.7 dS m^{-1} for wheat and cotton crops, respectively (Table 4.2). whereas the *HEIS_noLF* at *I0.95* irrigation scheduling added 35 mg cm^{-2}, ~ 8.0 dS m^{-1} (Table 5.2) which is higher than crop threshold EC_{max}.

The depth of percolation in the *reference* scenario is predicted to be significantly higher by 8 to 11 times as compared to *PSIS_80mm* and *HEIS_LF*, due to very high depths of 1590 mm irrigation applied under the *reference* scenario as observed in the farmers' fields (Table 4.6). This is because in the HBC command the water is currently allocated to farmers' fields using Warabandi, irrespective of crop water requirements. Also, farmers potentially consider that more irrigation is better for soil moisture and crop growth. This could be helpful in leaching the salts out from the root zone in areas with deeper groundwater levels. However, under shallow groundwater level conditions, this high percolation rate could cause waterlogging and secondary salinization, and then potentially affect the crop growth.

Interestingly, both the *PSIS_80mm* and *HEIS_LF* irrigations at *I0.95* irrigation scheduling resulted into similar long-term average soil water and salt balances, and cotton-wheat crops yields and water productivity values (Table 5.2). This suggests there is a potential for improved 'precision' surface irrigations to help maintain appropriate soil water and salt balances, and improved crop yields and water productivity values for cotton-wheat cultivation. However, any further gains in water savings by high-efficiency irrigation systems would be constrained by its potential risks to increase the soil salinity, and its adverse effects on the cotton-wheat crop yields and their water productivity values. This is demonstrated in the *HEIS_noLF* scenario (Table 5.2). Instead, a gravity-fed precision surface irrigation system (represented by *PSIS_80mm*), with significantly less cost to the farmers, could help achieve similar water-savings and improvements in the cotton-wheat crop yields and their water productivity values, as demonstrated in the

PSIS_80 mm scenario (Table 2). Anwar *et al.* (2016) showed that if fields are maintained well-graded, then surface irrigation in the context of *Warabandi* has potentially an efficiency as high as 80% without any infrastructural changes.

5.5 Conclusions

Use of local field-observations, combined with agrohydrological and crop growth modelling, offered a robust tool to assess long-term potential effects of different irrigation systems on the irrigation requirements, soil water balances including percolation, soil salinity, and crop yields and water productivity of cotton-wheat cultivation in Hakra Branch Canal command in Punjab Pakistan. The calibrated and validated agro-hydrological model, *SWAP-WOFOST* was applied to perform long-term analyses over 10 years, from 2007 to 2017, for three representative irrigation systems; the *reference* irrigation, precision surface irrigation system (*PSIS*); and a high-efficiency irrigation system (*HEIS*), with appropriate leaching fraction (*HEIS_LF*) and without leaching fraction (*HEIS_noLF*).

The modelling suggests a scope of over 40% savings in irrigation amounts, an increase of about 30% in the average crop yield and evapotranspiration-based water productivity WP_{ET} value for the cotton crop. This is an increase of >50% in the irrigation-based water productivity WP_{Irr} values for both the wheat and cotton crops. Interestingly, both the *PSIS* and *HEIS_LF* irrigation scenarios resulted into similar gains in long-term average savings in irrigation water, and crop yields and their water productivity values for the cotton-wheat cultivation in the study area.

The expected higher benefits of irrigation water savings associated with the *HEIS_noLF* irrigations appear to be constrained by the potential risks of increase in soil salinity. As a result, there are adverse effects on the cotton-wheat crop yields and water productivity values. To avoid the salt build-up and avoid the critical thresholds for the crops requires provision of appropriate leaching fraction, if no other alternate good-quality irrigation source available to replace marginal or poor-quality irrigation water from groundwater

resources. The modelling results obtained here suggest a limited scope for saving of irrigation water by modernisation to very high-efficiency irrigation systems, such as sprinkler, for using marginal quality (> 0.96 dS m^{-1}) irrigation waters for cotton-wheat cultivation. This is due to the need for a significant leaching fraction to avoid further salt-build up in the soil profile, and to minimise its adverse effects on crop yield and its water productivity.

The modelling suggests that the traditional gravity-fed surface irrigation system, when improved with flexible irrigation supplies and precise uniform applications, as simulated in the *PSIS* scenario, could deliver similar results in terms of irrigation requirements, crop yields and water productivity values for the cotton-wheat cultivation. Likewise, this could be achieved under a modern pressurized high-efficiency irrigation system such as sprinkler but with appropriate leaching fraction, as simulated as *HEIS_LF*.

However, this modelling was limited in scope to field-scale simulations, with homogeneous soil, irrigation water quality and crop rotation assumptions. Further research is suggested to conduct long-term field experiments that are focused on monitoring the potential effects of different irrigation systems on the long-term soil water and salt balances, crop yields and water productivity values. Also, further research is suggested to assess the potential long-term effects of precision irrigation applications at the canal-command scale. This should account for heterogeneous soil, irrigation water quality, and crop rotation to determine if these findings apply over larger scales.

Chapter 6 : Calibration and validation of a distributed agro-hydrological model to quantify and assess soil water and salt balances, and crop water productivity at the canal-command scale

6.1 Introduction

A sound understanding of spatial and temporal variations of soil water and salt balances provides key information for formulating balance irrigation strategies to improve water productivity and sustainability of irrigated crop systems from field to canal command scale. In Chapter 4, a field-scale agro-hydrological (SWAP) modelling approach was calibrated and validated to quantify soil water and salt balances, and crop water productivity at wheat-cotton and wheat-rice fields in the Hakra Branch Canal (HBC) command. The calibrated and validated field-scale SWAP model was then applied to evaluate long-term effects of different irrigation systems, namely precision surface irrigation and high-efficiency sprinkler irrigation with and without appropriate leaching fractions, on soil water and salt balances, and crop water productivity of wheat-cotton cultivation at the field scale in the HBC command (see Chapter 5). However, the field-scale analysis is limited to isolated fields and thus is not representative of spatial and temporal variations in soil water and salt balances, and crop water productivity at the canal command scale. This is because of the spatial variability in climatic conditions, soil types, crop types, and irrigation quality and quantity at the canal command scale. It is practically difficult and time-consuming to directly measure and quantify soil water and salt balances, and crop water productivity components under spatial heterogeneity of soils, crops, irrigation waters, and climatic conditions at a canal command scale. Therefore, the application of distributed agro-hydrological modelling offers an effective tool to account for spatial and temporal heterogeneities of climatic conditions, soil types, crops, and irrigation practices, and quantify spatial and temporal variations in soil water and salt balances, and crop water productivity at the canal-command scale (Singh *et al.*, 2006a; Singh *et al.*, 2006b; Feddes, 2007; Xie and Cui, 2010; Noory *et al.*, 2011; Aghdam *et al.*, 2013; Xue and Ren, 2017; Wang *et al.*, 2019).

The deterministic agro-hydrological model SWAP has been effectively used in a distributed mode to evaluate the effects of irrigation strategies on soil water and salt balances, and crop water productivity in semi-arid regions (Droogers *et al.*, 2000; Singh *et al.*, 2006a; Singh *et al.*, 2006b; Noory *et al.*, 2011; Xu *et al.*, 2012; Bellot and Chirino, 2013). In this context, spatial aggregation of all combinations of climatic conditions, soil types, land use and irrigation quantity and quality into the representative model input parameters is performed in a GIS environment by overlaying the thematic maps of crops, soils, irrigation water supplies, and groundwater level and quality to generate homogeneous simulation units (Singh *et al.*, 2006a). However, a robust application of distributed agro-hydrological modelling requires its calibration and validation to accurately represent spatially heterogeneity of climate conditions, soil, crop, and irrigation practices at the canal command scale. The agro-hydrological models are calibrated and validated using in-situ observed information of key soil-water-crop parameters such as soil moisture, soil salinity and crop biomass, groundwater recharge (Wesseling and Feddes, 2006; Feddes, 2007; Xie and Cui, 2010; Noory *et al.*, 2011; Kamyab-Talesh *et al.*, 2015; Xue and Ren, 2017). However, in-situ observations are generally based upon point sources and thus cannot be represents a canal command scale due to spatial and temporal variation of parameters like soil texture, crop phenology, groundwater level and quality and other allied components. Furthermore, gathering such information at a canal command scale is difficult, time consuming and requires sophisticated equipment (Singh *et al.*, 2006b). However, satellite remote sensing technologies now hold the capability to provide extensive amount of spatially and temporally distributed hydrologically data such as actual evapotranspiration, crop biomass and land use / land cover that can be implemented to calibrate and validate the

distributed hydrological models (Singh *et al.*, 2006a; Vazifedoust, 2007; Minacapilli *et al.*, 2009; Sánchez *et al.*, 2010; Wanders *et al.*, 2012; Xu *et al.*, 2014; Berbel *et al.*, 2019).

The Indus Basin irrigation-systems of Pakistan remains a research laboratory for many researchers focusing on the use of remote-sensing techniques as an input data sources to quantify rivers flow dynamics (Tahir *et al.*, 2011), irrigation management (Ahmed *et al.*, 2021), groundwater use (Cheema *et al.*, 2014), and land use/land cover and crop evapotranspiration (Liaqat *et al.*, 2015). However, there is a lack of using remote sensing-based information such as land use and crop evapotranspiration to parameterise and calibrate/validate distributed agro-hydrological modelling approaches to quantify soil water and salt balances, and crop water productivity in Indus basin irrigation systems.

This chapter aimed to develop a distributed SWAP model to simulate spatial and temporal variations in soil water and salt balances, and crop water productivity across the Hakra Branch Canal command (HBC) (*see* Chapter 3 for the study area description). The spatial and temporal input parameters and boundary conditions for distributed simulation units are obtained through spatial aggregation of existing geographical data including soil types, remote sensing-based crop maps, irrigation information, groundwater quality and depth. These agro-hydrological variables in the HBC are quantified and aggregated for different crop combinations at the simulation-unit level. The spatial accuracy of the distributed SWAP modelling is evaluated by comparing the modelling-based evapotranspiration with the independent remote sensing-based evapotranspiration at different spatial and temporal scales. The calibrated and validated distributed SWAP results are then analysed to quantify the spatial and temporal variations in soil water and salt balances, including net groundwater recharge, salt build-up in the soil profile, and crop water productivity of the main crops of cotton, rice, wheat, and mustard in the HBC command.

6.2 Methods and materials

6.2.1 Aggregation of spatial data for distributed modelling

The distributed SWAP modelling requires spatial aggregation of all combinations of climatic conditions, soil types, land use, and irrigation quantity and quality into the representative model input parameters for different simulation units in the study area. These variables were collected and aggregated in the HBC command during the agriculture year 2016-17. Chapter 3 provides the details of the SWAP modelling and overview of the sources of collated geographical data used in this study.

6.2.1.1 Climate Variables

The distributed SWAP requires daily climatic variables including maximum and minimum temperature, solar radiation, relative humidity, wind speed and rainfall, to define the upper boundary of the simulation units of soil-water-plant combinations. The required daily climatic variables (Figure 4.1) were obtained from a metrological station installed at IWMI field office, Haroonabad, located in district Bahawalnagar of Punjab, Pakistan, which comes under the command area of HBC. The recorded annual rainfall during the study period of 2016-17 was only 115 mm. It was low as compared to the mean annual rainfall recorded at 280 mm over a period of 1979 to 2017.

6.2.1.2 Crop types

The climatic conditions of HBC command allow two cropping seasons, defined as *kharif* (May-October) and *Rabi* (November-April). Liaqat *et al.* (2016) developed a land use/land cover (LULC) classification map of HBC command at a spatial resolution of 250 m using the Moderate Resolution Imaging Spectroradiometer (MODIS) Normalized Difference Vegetation Index (NDVI) over an 8-day time step for the year 2014-2015 (Fig 3.6). They identified and mapped cotton, rice, bare soil, water pond, and some other crops

such as millet, fodder during the *kharif* season, and early wheat, late wheat, mustard, bare soil and other crops and fodder during the *rabi* season. In this study, this LULC map (Liaqat *et al.*, 2016) was reclassified to produce a major crop combination map for the study area. The local crop growth data were available mainly for cotton, rice, wheat and mustard crops. The limited availability of crop data and minor land-use classes like water ponds and other crops affected the reclassification of the map. Therefore, in reclassification, the early and late wheat classes are combined to represent wheat during *rabi* season, and minor areas of water ponds and other crops, identified as only 3% of the total area, are merged with a nearby land use class. Finally, the reclassified crop maps of both seasons are combined to derive the crop combinations map with four main classes, namely cotton-wheat, rice-wheat, cotton-mustard and desert-barren (Figure 6.1). The cotton-wheat combination covered about 118 thousand ha (48%), followed by the cotton-mustard over ~45 thousand ha (18%) and the rice-wheat over ~21 thousand (9%). Approximately 61 thousand ha (25% of the total command area) is classified as desert-barren land.

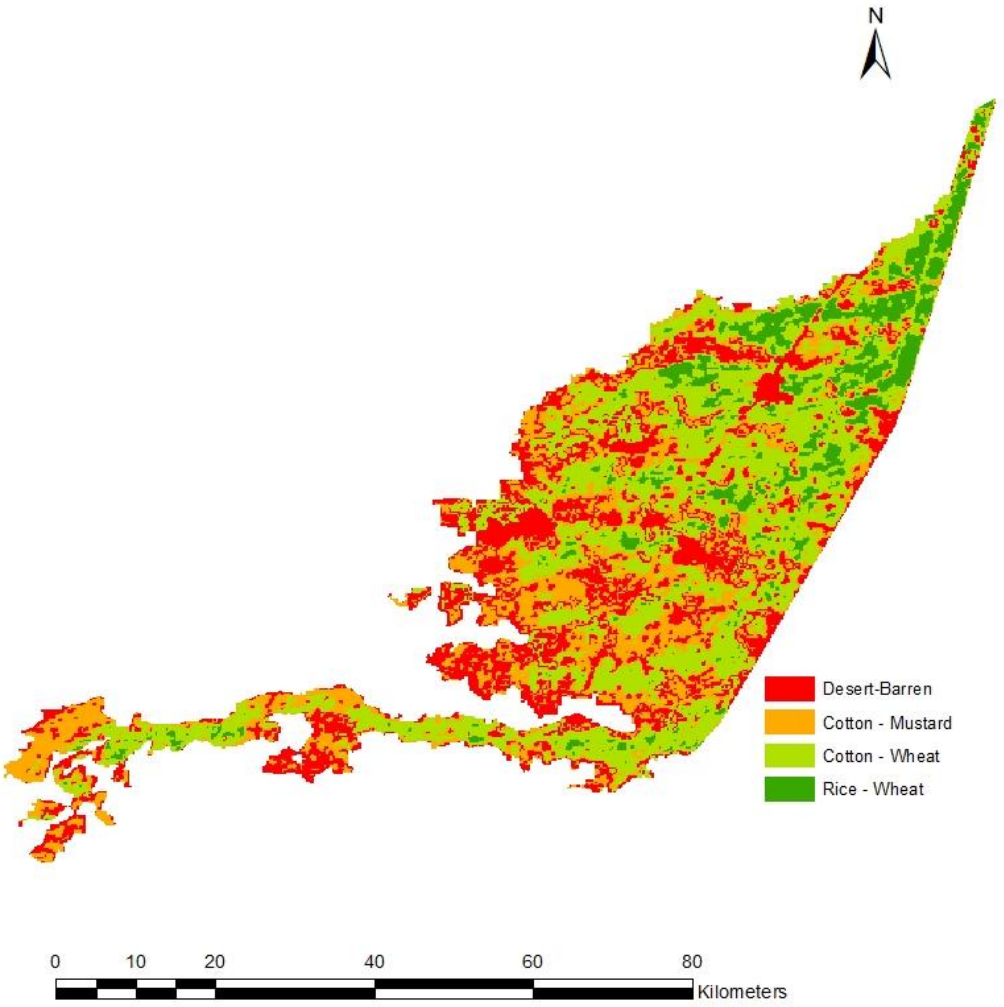

Figure 6.1: Reclassified crop combination map of the Hakra Branch Canal (HBC) command during the year 2014-2015. Based on the land use and land cover map produced by (Liaqat *et al.*, 2016) (Figure 3.6).

6.2.1.3 Soil types

The soil map of the HBC command is sourced from the Punjab Soil Survey Department (PSSD) and covered four major types of soil textural classes, namely sand, loam, sandy loam, and sandy clay loam (Fig. 6.2). The soil profile of each soil type was reduced to two soil layers: topsoil (0 – 30 cm) and subsoil (30 – 160 cm) based on the proportion of sand, silt clay, bulk density and carbon content. In the HBC command the soil texture varies mainly from sand to loam covering about 193 thousand ha (68% of total command

area), except in the tail Hakra right distributary (Fig 6.2) where it varies from sandy loam to sandy clay loam covering about 83 thousand ha (32% of total command area).

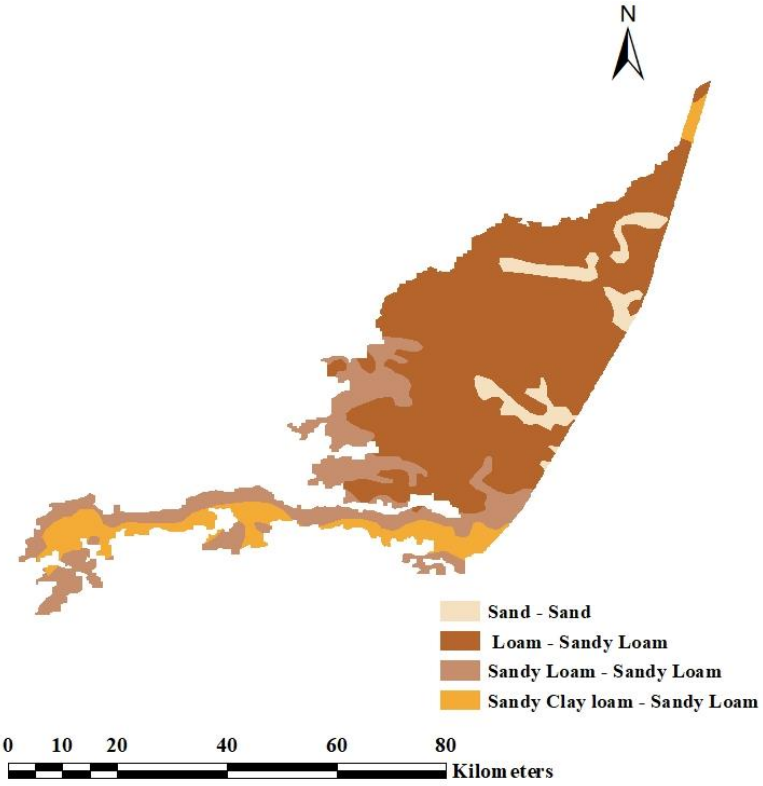

Figure 6.2: Soil map of Hakra Branch Canal command with four major soil textural classes (Source: Soil Survey of Punjab, Pakistan).

6.2.2 Groundwater quality and depth

The spatial information on the groundwater quality and depth (Figure 6.3) was developed from existing 84 piezometers spread over the HBC command during the study period (2016-2017). The existing piezometers were monitored pre- and post-monsoon in June 2016 and October 2016, respectively by the Land Reclamation Division (LRD) of Punjab Irrigation Department (PID). The groundwater quality varied highly from less than 3 dS m^{-1} to as high as 19.5 dS m^{-1} (Figure 6.3a).

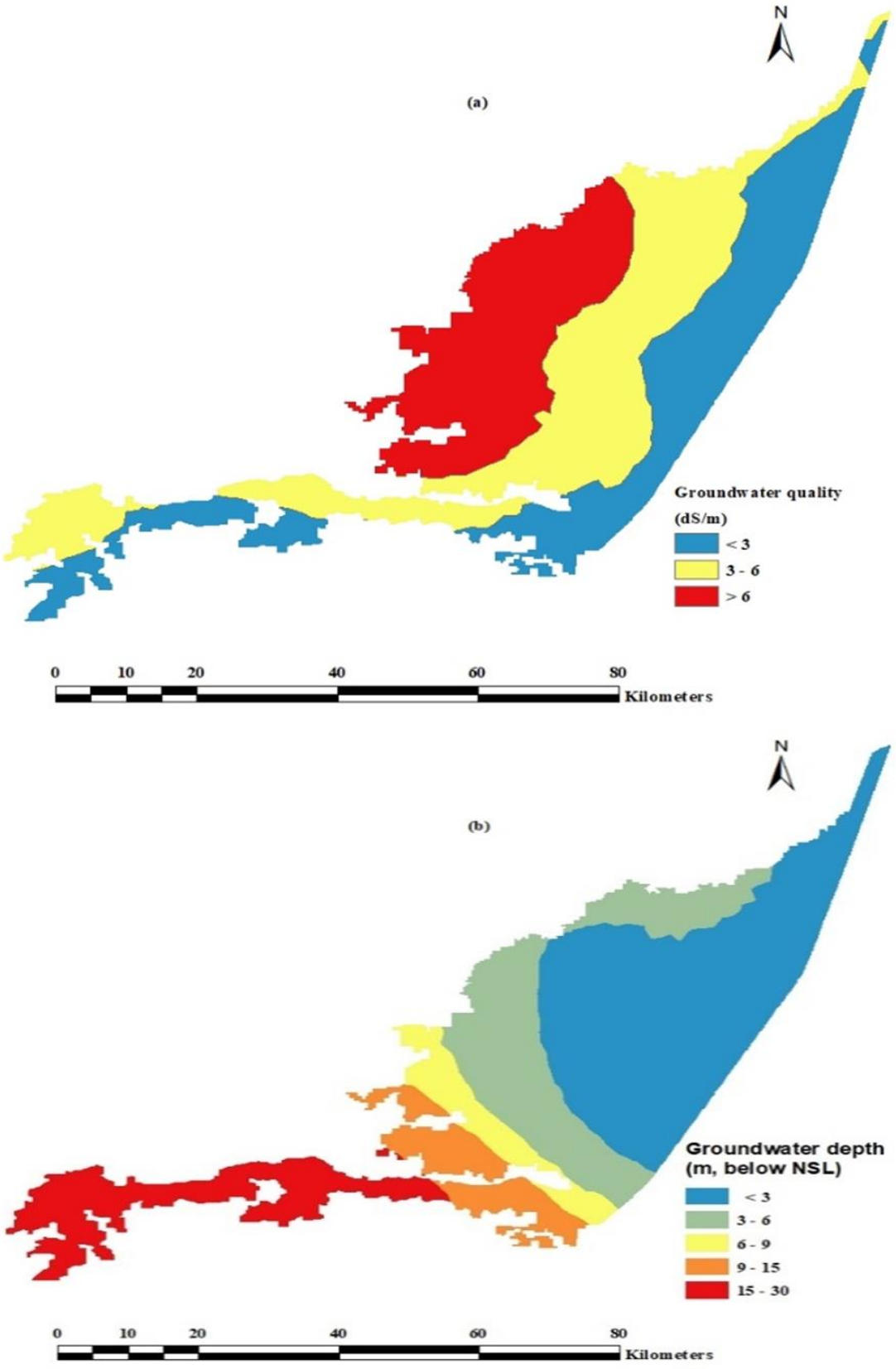

Figure 6.3: Groundwater condition in the HBC command (a) groundwater quality (dS m^{-1}) October 2016, (b) groundwater depth (m) below natural surface level (NSL) October 2016.

The groundwater with low salinity values (<3 dS m^{-1}) along the HBC was mainly due to relatively low salinity water seepage from the canal. The groundwater quality was relatively poor in the western part of the HBC command which also receives less canal water supply and is located at tails of the canal distributaries (Figure 6.3b). Interestingly, the groundwater quality appears good at the southern tail reach of the HBC command area. This is possibly affected by the Ghaggar river flood plain closer of the southern boundary of the command area. The groundwater depth varied from < 3 m below the natural surface level (NSL) mostly in the head reaches of the HBC command, to as much as up to 30 m below NSL at the tail reaches (Figure 6.3b)

6.2.3 Irrigation network and its supplies

The HBC comes under Eastern Sadqia canal command (main canal), which off takes from Sulemanki head works on the River Sutlej. Like other canal systems in the IBIS of Pakistan, the HBC is a run-of-river system where the canal water supply fluctuates with the river flow. The limited canal water supply in the HBC is supplemented by the groundwater use. Approximately 5 thousand tubewells are installed at a density of 24 tubewells per thousand hectares in the HBC command area (Bhatti *et al.*, 2017). The canal water-supply and estimates of groundwater pumping were analysed and aggregated at the distributary canal command level. This follows a similar irrigation aggregation analysis by (Singh *et al.*, 2006b) who developed and applied distributed SWAP modelling in the semi-arid region of Sirsa irrigation circle, Haryana, Northern India.

In order to quantify the irrigation supply, the crop water requirement was represented by the reference evapotranspiration ET_p [L] estimated using daily weather data by Penman-Monteith equation (Monteith, 1965; Allen *et al.*, 1998b). The depth of irrigation required I_{req} [L] for a specific crop during the specified irrigation interval I_{int} were calculated by subtracting the effective rainfall P_{eff}, that contributes to the crop water requirement,

from ET_p [L]. Several methods have been established to estimate the effective rainfall (Abishek *et al.*, 2017; Ali and Mubarak, 2017; Kumar *et al.*, 2017). However according to Adnan and Khan (2009), effective rainfall is 80% to 100% of the total rainfall exceeding 150 mm in the study area. Since the study year had a very low rainfall of 115 mm hence it is assumed as effective rainfall. The irrigation requirement I_{req} [L] is restricted by a maximum irrigation depth I_{max} [L] and specified at 80 mm for cotton, wheat and mustard, and 100 mm for rice. The high ET_p rates particularly during *kharif* (summer) season could result in unrealistic high I_{req} [L]. Therefore, the I_{req} [L] is estimated as follows:

$$I_{req} = min\left[\sum_{t=1}^{I_{int}}\left(ET_p - P_{eff}\right)(t), I_{max}\right]. \quad \text{Eq. 6.1}$$

Here, I_{int} is the irrigation interval in days of a crop. The I_{req} is partly supplied through the limited and unreliable canal water supply, and partly through groundwater pumping in the study area.

6.2.3.1 Canal water supply

The HBC supply to 16 perennial distributary canals and one flood channel which only operates during summer (*kharif)* season. However, in this study, only 16 perennial distributary canals commands are considered (Figure 6.4).

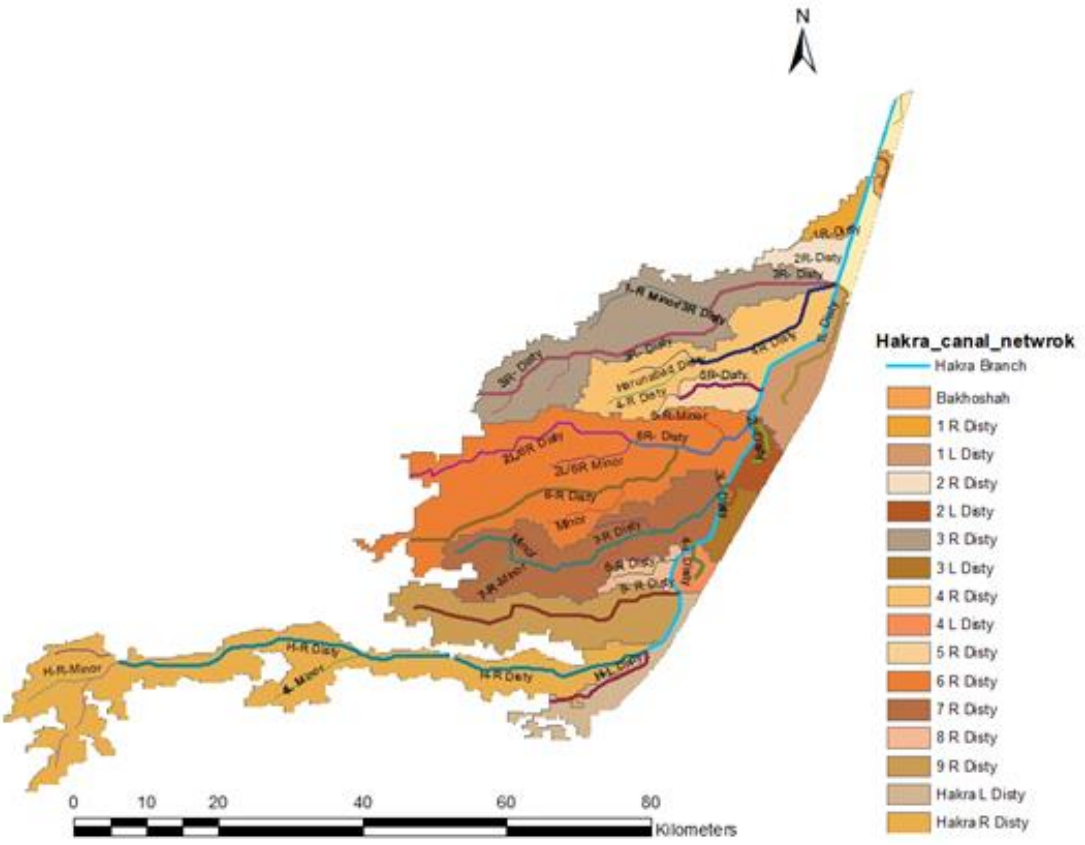

Figure 6.4: Hakra branch canal and its distributaries commands in the study area.

The limited canal water supply is rotated over a group of distributaries according to *canal rostering* (Table.3.2) and then allocated to farmers' fields through a network of watercourses for a specified interval per week proportional to size of the farm. As per this *Warabandi* (fixed rotation schedule) system, during any given *Warabandi* interval, the distributaries with highest priority are operated at their full allocation capacity, while others are either operated at a low allocation capacity or closed. The canal water supply is based on the agriculture area under the canal water rights, known as Culturable Command Area (CCA). The Punjab Irrigation Department (PID) is responsible for regulating the canal roster and discharge measurement using stream-gauging technique. Staff-gauges were installed at the head of each distributary to measure the depth of water. For any depth, the corresponding canal discharge is determined from the calibrated

depth-discharge rating curves. Typically, the canal discharge is recorded twice a day by the Programme Monitoring and Implementation Unit (PMIU) of the PID and uploaded to their online database. The daily canal discharge at the head of each distributary during the agricultural year 2016-2017 was downloaded from the PMIU online database *(https://irrigation.punjab.gov.pk/channel-line-diagram)*. In each distributary command area, the measured canal discharge Q_{dc} [L^3 T^{-1}] was converted to the daily canal water depth $I_{cw,dc}$ [L T^{-1}] over the cropped area (CA_{dc}) of the distributary command, as follows:

$$I_{cw,dc} = \frac{\left(Q_{dc} - Q_{SL,(dc+wc)}\right)}{CA_{dc}} \qquad \text{Eq. 6.2}$$

Here, $Q_{SL,(dc+wc)}$ is the seepage losses [L^3 T^{-1}] from the distributary canal and the watercourses in the command area. The results from a study conducted by Hussain *et al.* (2011) are used to estimate seepage losses from the distributary canal and watercourses. According to their findings, irrigation efficiency of the distributary canals and watercourses is about 70 and 75%, respectively in IBIS of Pakistan, including the HBC. This suggested a combined seepage losses of about 48% in the distributary and watercourses of the study area.

6.2.3.2 Groundwater supply

The limited canal water-supply in HBC is supplemented by the groundwater pumping for crop irrigation. The irrigation deficit I_{def} [L] during an irrigation interval I_{int} is therefore calculated by subtracting the $I_{cw,dc}$ [L] (Eq. 6.2) from the I_{req} [L] (Eq. 6.1) and that is supplied through groundwater pumping. Further, the supply of I_{def} through groundwater pumping depends on the maximum groundwater pumping capacity, which

is a function of pumping discharge, hours of operation, and groundwater quality. Hence, the daily maximum groundwater capacity is calculated by:

$$Q_{gw\,max}(t) = RF_{gw} \text{ x } N_{tw} \text{ x } Q_{tw} \text{ x } H_{tw} \text{ (t)} \qquad \text{Eq. 6.3}$$

Here, $Q_{gw\,max}$ [L^3 T^{-1}] is the maximum groundwater capacity, RF_{gw} is the reduction factor accounting for the quality EC_{gw} of groundwater, as groundwater pumping is limited in poor groundwater quality areas. To restrict the groundwater pumping the value of RF_{gw} is specified at 1.0 for EC_{gw} < 3 dS m^{-1}, 0.75 for 3 dS m^{-1} < EC_{gw} < 6 dS m^{-1} and 0.5 for EC_{gw} > 6 dS m^{-1} (Qureshi *et al.*, 2010). The N_{tw} is the number of tubewells in a distributary command and aggregated through the tube density (Bhatti *et al.*, 2017). Q_{tw} is the mean tubewell discharge [L^3 T^{-1}] and is estimated using the methodology defined by (Ullah *et al.*, 2016). The H_{tw} is the mean hours of operation of the tubewell per day [T], which is specified at 8 hours per day (Qureshi *et al.*, 2003).

The daily maximum groundwater capacity $Q_{gw\,max}$ [L^3 T^{-1}] of the distributary command could provide the maximum groundwater irrigation capacity $I_{gw,max}$ over the crop area of distributary command CA_{dc}:

$$I_{gw,max}(t) = \frac{Q_{gw,max}}{CA_{dc}}\ (t) \qquad \text{Eq 6.4}$$

However, the actual groundwater irrigation depth I_{gw} [L] during each irrigation interval is restricted to the minimum of the irrigation deficit I_{def} [L], subtracting the $I_{cw,dc}$ [L] (Eq. 6.2) from the I_{req} [L] (Eq. 6.1), and the maximum groundwater pumping capacity $I_{gw,max}$ [L] (Eq. 6.4), as follows:

$$I_{gw} = min\left[I_{def}, \left(I_{gw,max} \text{ x } I_{int}\right)\right] \qquad \text{Eq. 6.5}$$

The irrigation I [L] for different crops at each irrigation interval is then determined by adding supply from the canal $I_{cw,dc}$ [L] (Eq. 6.2) and from the groundwater pumping I_{gw}[L] (Eq. 6.5) in each distributary.

Finally, the quality of irrigation water is calculated as the weighted mean and is based on the depth and quality of canal and groundwater supply. Generally, the water quality is expressed in dS m^{-1}, while in SWAP the water quality it is simulated as the concentration of solutes, C [M L^{-3}] as follows:

$$C_i = \frac{C_{cw}I_{cw} + C_{gw}I_{gw}}{I_{cw} + I_{gw}}. \qquad \text{Eq 6.6}$$

Here, C_i [M L^{-3}] is the solute concentration at each irrigation interval, C_{cw} and C_{gw} [M L^{-3}] are the solute concentrations in canal water I_{cw} and groundwater I_{gw}, respectively. The unit conversion is carried out using the relation 1 dS m^{-1} = 0.64 mg cm^{-3} (Kroes *et al.*, 2017).

6.2.4 Schematization into homogenous units

The distributed SWAP modelling required schematization of the HBC command into homogeneous simulations units of unique soil-water-crop combinations. The homogeneous simulation units are aggregated through a process referred to as stratification in a GIS environment by overlaying the thematic maps of crops, soil, irrigation, groundwater level and quality (Singh et al., 2006b).

The spatial information on irrigation, groundwater depth and its quality are aggregated at distributary canal level of the HBC. The stratification of homogeneous simulation units is performed by overlaying the thematic maps of crop combination (Figure 6.1), soil (Figure 6.2), groundwater depth and groundwater quality (Figure 6.3), distributary canal command boundary (Figure 6.4), using the geo-processing technique in Geographic

Information System (GIS) (Figure 6.5). A number of relatively small simulation units (<50 ha) generated are merged to the adjoining areas. Overall, the aggregation of maps resulted 142 simulation units across the HBC command (Figure 6.5).

6.2.5 Parametrization of distributed SWAP modelling

The distributed SWAP modelling requires the parameter assigned to each homogeneous simulation unit for running the SWAP model in a distributed manner. This process is referred as parametrization and includes the defining of the upper boundary conditions, including climatic variables and irrigation fluxes, crop and irrigation calendars, detail crop growth parameters, soil profile description including soil hydraulic functions (Singh et al., 2006b). It also requires definition of the lower boundary conditions, and the initial soil profile status in terms of soil moisture and soil salinity levels.

A pre-processing Visual Basic.Net programme was developed to link simulation units from GIS with SWAP and to write the input files in batch for a SWAP run of the individual simulation unit. A post-processing R code was developed to process the SWAP simulation results of the individual simulation units and join them with the GIS simulation units map to analyse further spatial and temporal variations of soil water and salt balances, and crop water productivity at canal command scale.

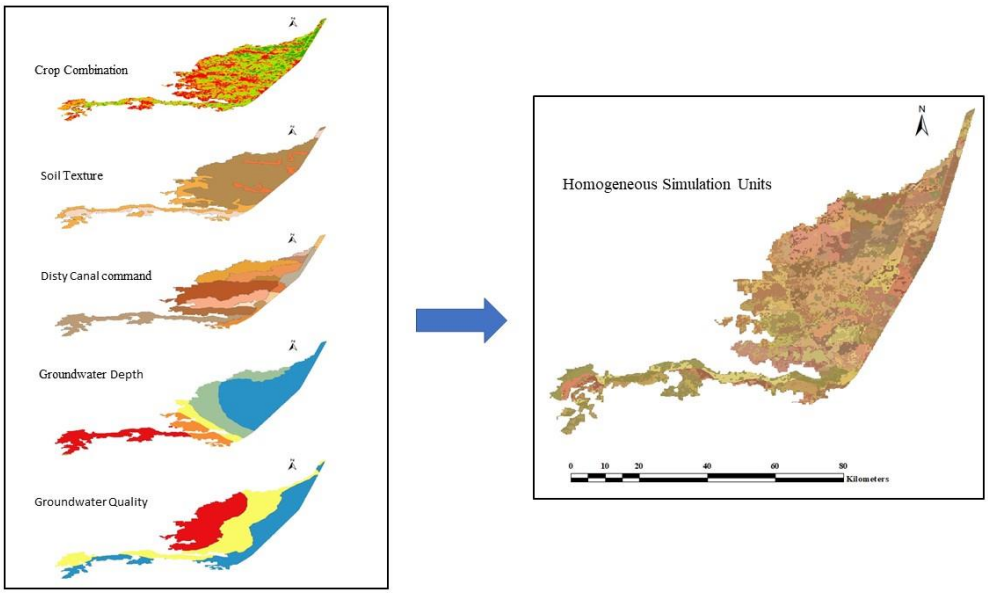

Figure 6.5: Schematic representation of stratification procedure to develop homogeneous simulation units of unique combinations of crop-soil-water in the Hakra Branch Canal command Punjab Pakistan.

6.2.5.1 Climactic data and irrigation inputs

The SWAP model requires its upper boundary conditions specified by the computed daily reference evapotranspiration ET_p (Monteith, 1965; Allen *et al.*, 1998b), records of daily rainfall received, and fluxes of irrigation I application. The required daily metrological data including variables such as solar radiation, maximum and minimum temperature, humidity, wind speed, and rainfall during the study year 2016-2017 (Figure 4.1) were sourced from the IWMI met station at field office Haroonabad, located in the HBC command.

As per Eqs. 6.1 to 6.6 above, the irrigation applications were calculated for different crop combinations in each canal distributary, using the specified average crop and irrigation calendar (Table 6.1). The crop and irrigation calendars of a crop varies from field-to-field due to the farmer's planning and the *Warabandi* system. However, this variation was generally within the range of 10 to 15 days. In absence of accurate records, the crop and

irrigation calendars of different crops were aggregated by specifying the same dates of crops sowing, harvesting and irrigation applications over the entire study area (Table 6.1). The average crop and irrigation calendar for cotton, rice and wheat were derived from the observations at the local farmers' fields in HBC command (Chapter 4). Whereas the existing literature and farmers' interviews are used for the mustard crop (Singh *et al.*, 2006b; Amjad, 2014; Ijaz *et al.*, 2019) (Table 6.1). The specified average crop and irrigation calendars were used to calculate the irrigation applications for different crops in each canal distributary as per Eqs. 6.1 to 6.5 above. Generally, the pre-sown irrigation was heavier than subsequent irrigations during the crop growing season. Therefore, the maximum pre-sown irrigation depth was set equal to 100 mm for cotton, wheat and mustard, and 150 mm for rice (Laghari *et al.*, 2010) .

Table 6.1: Average crop and irrigation calendar for the main crops in Hakra Branch Canal command, Pakistan Punjab.

Crop	**Crop Calendar**			**Irrigation Calendar**		
	Sowing	*Emergence*	*Harvest*	*Number of Irrigations*	*Pre-sowing*	*Irrigation interval (days)*
Cotton	6-May	10-May	31-Oct	9	2-May	17,35,20,20,20,20,30,30
Rice	1-Jun		31-Oct	25	31-May	4,3,3,3,3,4,4,4,5,5,5,5,5,5,5,5,7,7,7,7,7,7,7
Wheat	17-Nov	24-Nov	30-Apr	6	10-Nov	30,35,25,25,20
Mustard	10-Nov	16-Nov	30-Apr	4	5-Nov	52,45,40

The subsequent irrigations during the crop growing period were restricted to a maximum of 80 mm for cotton, wheat and mustard and 50 mm for rice (Singh *et al.*, 2006b; Anwar *et al.*, 2016).

6.2.5.2 Crop growth data

The detailed crop growth module, World Food Studies (*WOFOST*), was applied to simulate crop growth in the HBC. The *WOFOST* module was calibrated and validated for cotton, rice and wheat using soil water and crop yields observed at the local famers'

fields in the HBC (Chapter 4). The crop parameters for mustard are derived from existing literature under similar climatic conditions (Singh *et al.*, 2006b). In addition to the calibrated crop input parameters for cotton, wheat and rice (Table 4.2 from chapter 4), Table 6.2 summarizes the crop input parameters used for mustard growth simulation in the study.

Table 6.2: Main crop parameters for mustard crop specified for SWAP detail crop module.

Temperature sum from emergence to anthesis, *TSUMEA*:	750 ^{o}C
Temperature sum from anthesis to maturity, *TSUMAM*:	1300 ^{o}C
Light use efficiency, ε :	0.40 kg ha^{-1} hr^{-1}/J m^{2} s^{-1}
Maximum CO_2 assimilation rate, *A*:	40 kg ha^{-1}
Light extinction coefficient, K_{gr} :	0.375
Threshold salinity limit. EC_{max}:	7.4 dS m^{-1}
Yield reduction per unit ET, EC_{slope}:	6.6% / dS m^{-1}

6.2.5.3 Soil profile description

The soil profile was divided into two layers, topsoil (0-30 cm) and subsoil (30-160 cm) (Table 6.3). The soil flow domain was further discretized into 30 compartments with a nodal distance of 1 cm for the top 10 compartments followed by 5 cm for next 10 compartments and 10 cm for the remaining compartments (van Dam *et al.*, 1997). The SWAP model requires soil hydraulic functions $\theta(h)$ and $K(\theta)$ to solve Richards' equation for soil water flow (van Dam *et al.*, 1997). The direct measurement of soil hydraulic parameters is difficult. Therefore, pedotransfer functions (PTFs) (Wösten *et al.*, 1998) were generally used to derive the required soil hydraulic properties using easily measured soil texture, bulk density and organic matter content (Droogers *et al.*, 2000; Singh *et al.*,

2006a; Vazifedoust, 2007). In this study, the soil information available in HBC (Figure 6.4) was used to derive the soil hydraulic parameters of different soil types (Table 6.3). The dispersion length L_{dis} for salt transport was set to 5 cm (Nielsen *et al.*, 1986). To limit the soil evaporation, the empirical function of Black *et al.* (1969) was used at a value of 0.35 cm d^{-1} specified for evaporation coefficient (van Dam *et al.*, 1997).

Table 6.3: Soil physical properties and derive soil hydraulic parameters of different soil profiles across Hakra Branch Canal command, Pakistan Punjab. The soil hydraulic parameters were derived from the pedo-transfer function (*PTF*) (Wösten *et al.*, 1998).

Soil ID	Soil Texture	Soil Depth cm	*Silt* %	*Clay* %	*OC* %	*BD* g cm^{-3}	ϑ_{sat} cm^3 cm^{-3}	K_{sat} cm d^{-1}	α cm^{-1}	*n*	λ
1	Loam	0-30	42	13	0.32	1.37	0.38	24	0.027	1.28	-0.58
	Silt Loam	30-160	57	10	0.29	1.45	0.40	22	0.018	1.31	0.91
2	Sandy clay loam	0-30	12	23	0.34	1.52	0.39	87	0.079	1.23	-2.75
	Clay loam	30-160	32	30	0.30	1.52	0.41	14	0.042	1.13	-2.51
3	Sand	0-30	6	5	0.25	1.70	0.32	80	0.07	1.47	0.52
	Loamy sand	30-160	7	5	020	1.70	0.32	32	0.087	1.4	0.21
4	Sandy loam	0-30	34	11	0.24	1.61	0.37	25	0.032	1.29	-0.14
	Silt loam	30-160	56	23	0.20	1.65	0.38	9	0.016	1.15	-1.72

In case of rice simulations, the soil was puddled to reduce the percolation of irrigation to maintain surface water ponding for optimum rice growing conditions. Therefore, in order to capture the surface water ponding and reduce percolation conditions in the SWAP simulation, the K_{sat} of the topsoil layer was reduced by 20% and the empirical function of Black *et al.* (1969) was used to simulate no limit on soil evaporation during the rice simulation period (Singh *et al.*, 2001).

6.2.5.4 Lower boundary and initial conditions

Two bottom boundary conditions were specified for the soil profile based on the depth of the groundwater level, either shallow and deep groundwater. The simulation units were assumed to have a shallow groundwater, when the mean observed groundwater level was < 3 meters below NSL. Whereas all other units were assumed to have a deep groundwater level > 3 m below NSL). In case of shallow groundwater < 3m below NSL, the mean groundwater level of the measured groundwater levels during June 2016 (pre-monsoon) and October 2016 (post-monsoon), was assigned as the lower boundary condition. In case of deep groundwater > 3 m, NSL, a free drainage was assigned as lower boundary condition.

The initial soil water condition under the shallow groundwater condition was set at the pressure head of each discrete soil-profile compartment in hydrostatic equilibrium with initial groundwater level, which was set at a pressure head h = -500 cm for each discrete soil profile compartment under the deep groundwater condition that corresponded to the average soil moisture of 20% (Kroes *et al.*, 2017). The initial soil salinity concentration in the soil profile was specified from 0.5 to 26 dS m^{-1} according to the collected soil information in the HBC command (Muhammad Aamer, 2015). In addition, the SWAP model was run one year in advance with the same inputs to initialise and generate the spatial variation of soil moisture and salinity concentration at the start of the simulation period, 2016-1017.

6.2.6 Remote sensing evapotranspiration

The accuracy and reliability of the distributed SWAP input parameters were evaluated by comparing the evapotranspiration (*ET)* simulated by *SWAP* with the independent satellite remote sensing-based *ET* at different spatial and temporal scales. The satellite

remote sensing *ET* data are derived from the *MOD16A2* product (Running *et al.*, 2017) of the Moderate Resolution Imaging Spectroradiometer (MODIS) multispectral sensor on-board of NASA's TERRA and AQUA satellites. The *MOD16A2* provides global *ET* over accumulated 8-day temporal resolution and at a 500m x 500m spatial resolution. The *MOD16A2* product *ET* values are estimated using the algorithm of Mu *et al.* (2011) which is based on the Penman-Monteith equation (Monteith, 1965). An R-Package *MODIStsp* was used for downloading and post-processing of the *MOD16A2* product *ET* data set (Busetto and Ranghetti, 2016).

A total of 45 *MOD16A2* product *ET* images, including 23 images for the *kharif* (summer) season and 22 images for the *rabi* (winter) season, were downloaded and processed to quantify the remote-sensing based *ET* over the HBC during the study period (2016-2017). The downloaded raster images were corrected for pixels with no data using the ArcMap spatial analyst *IsNull* function. The corrected images were then aggregated to create seasonal images for both the *kharif* and *rabi* seasons. The seasonal *ET* maps were then converted from pixel base to simulation units using ArcMap conversion tool from raster to polygon. Finally, the spatial-analyst zonal statistics tool was implemented to quantify the mean *ET* values for each simulation unit.

The remote sensing-based *ET* and the SWAP simulated *ET* were compared using the key model performance indicators of the mean bias error (*MBE*) (Willmott, 1982) and the index of agreement (*IoA*) (Willmott, 1982) calculated as follows:

$$MBE = \frac{1}{N}\left[\sum_{i=1}^{N}(ET_{sw,i} - ET_{MOD,i}\right] \quad \text{Eq. 6.7}$$

$$IoA = 1 - \left[\frac{\sum_{i=1}^{N}(ET_{sw,i} - ET_{MOD,i})^2}{\sum_{i=1}^{N}(|ET_{sw,i} - \overline{ETMOD}| + |ET_{mod,i} - \overline{ETMOD}|)^2}\right]. \quad \text{Eq. 6.8}$$

Here, $ET_{sw,i}$ is the *SWAP* simulated *ET* for the i_{th} simulation unit, $ET_{MOD,i}$ is the *MODIS* derived *ET* for the i_{th} simulation unit, $\overline{ETMOD}$ is the mean of the ET_{MOD} of all simulation units, and *N* is the number of the paired SWAP simulated and *MODIS* derived *ET* values, which is equivalent to the number of simulation units (142). A positive value of *MBE* indicates that the SWAP simulated *ET* is overestimated, as compared to the remote sensing-based *ET*, and vice versa. The value of *IoA* varies from 0 to 1 with a value of 0 indicating complete disagreement, and value of 1 indicates perfect agreement (Willmott, 1982). In addition to these performance indicators, the accuracy of the distributed SWAP modelling is judged by making graphical and statistical comparisons of the remote sensing-based *ET* and the SWAP simulated *ET* at different spatial and temporal scales.

6.2 Results and discussion

The results of the parametrised distributed SWAP model runs are critically analysed and discussed for all homogeneous simulation units (142) in the HBC command for one year, starting from May 1st, 2016 to 30th April, 2017. The study period is further divided into two crop seasons: the *kharif* (cotton/rice) season from May 1st 2016 to October 31st 2016, and the *rabi* (wheat/mustard) season from November 1st 2016 to April 30th 2017. The simulated soil water and salt balances and crop yields are aggregated and analysed for the *kharif* and *rabi* seasons over the head, middle and tail canal sections with respect to the reduced distance (RD) (Figure 6.6). In IBIS of Pakistan, the RD is used to measure the length of the canal from head to tail reach. In Figure 6.6, the RDs of BS ,1R,1L, 2R, 2L,3R, and 4R are aggregated as head reaches; 3L, 4L, 5R, 6R, 7R, and 8R aggregated

as middle reaches; and 9R, Hakra left and Hakra right distributaries were aggregated as tail reaches of the HBC. The quantified canal inflow, net groundwater recharge, salt build up and crop water productivity are aggregated and analysed across the head, middle and tail reaches of the HBC (Figure 6.6).

In addition, the results of cropping patterns, estimates of irrigation distribution, and a comparison of remote-sensing based *ET* and distributed SWAP simulated *ET* over HBC command are also described in the following sections.

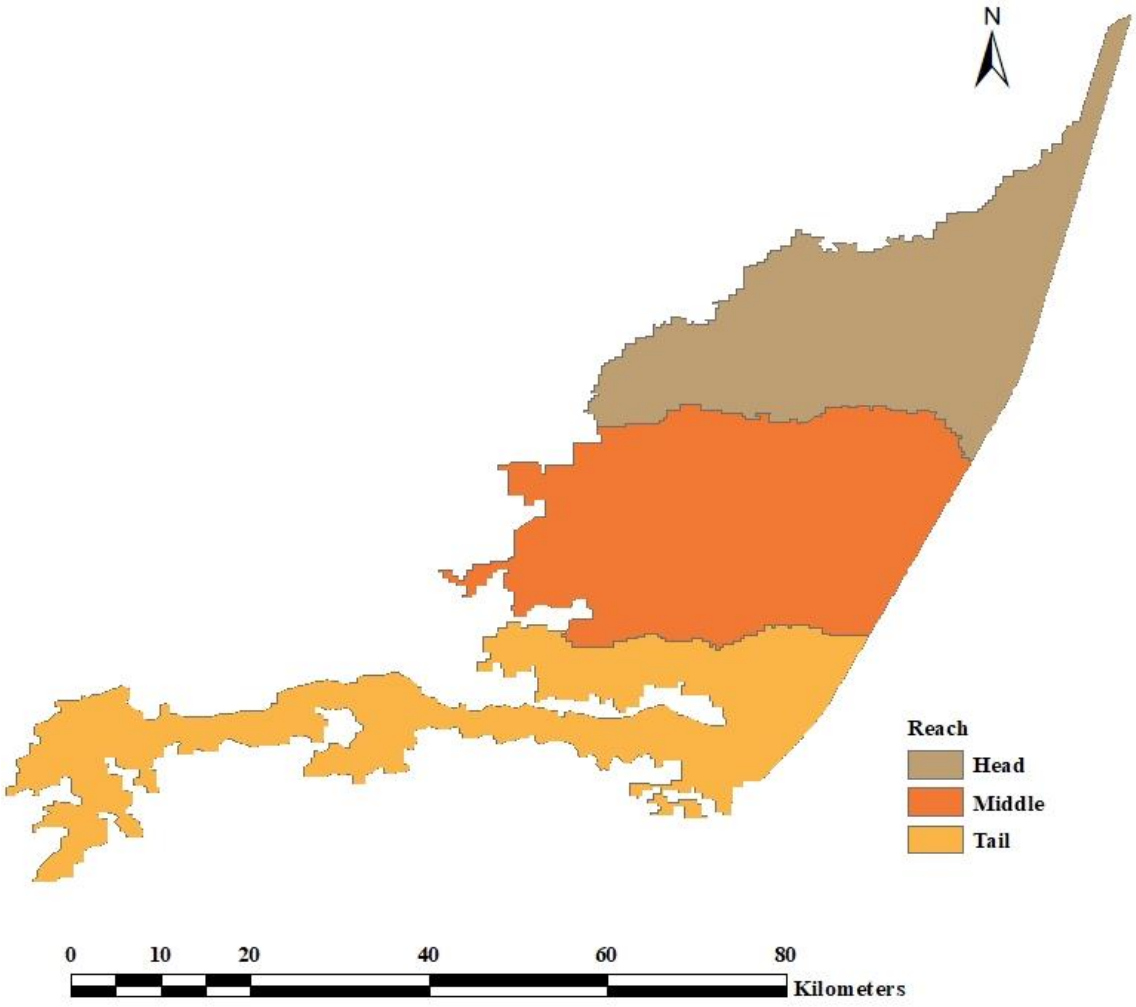

Figure 6.6: Spatial scale distribution of head, middle and tail reaches in the Hakra branch canal command Punjab Pakistan.

6.3.1 Cropping pattern

According to the reclassified crop map (Figure 6.1), approximately 73% of the total culturable command area was under cultivation in HBC during the agricultural year May 2016 to April 2017. Figure 6.7 clearly shows cotton as a dominant crop during the *kharif* (summer) and wheat during the *rabi* (winter) season. The cotton intensity, defined as percentage of the total crop area, varied from 31 to 98% among different canal commands with an average of 82% for the entire HBC command (Figure 6.7a). Wheat intensity ranged from 55 to 90% with an average of 73% for the entire HBC command (Figure 6.7b). Rice is mainly cultivated in the head reaches of the HBC (Figure 6.7a), because of access to canal water, as well as good quality (< 3 dS m^{-1}) groundwater (Figure 6.3). The mustard crop is mainly cultivated in the tail reaches of the HBC, with its intensity varying from 10 to 45% with an average of 25% over the entire HBC command (Figure 6.7b).

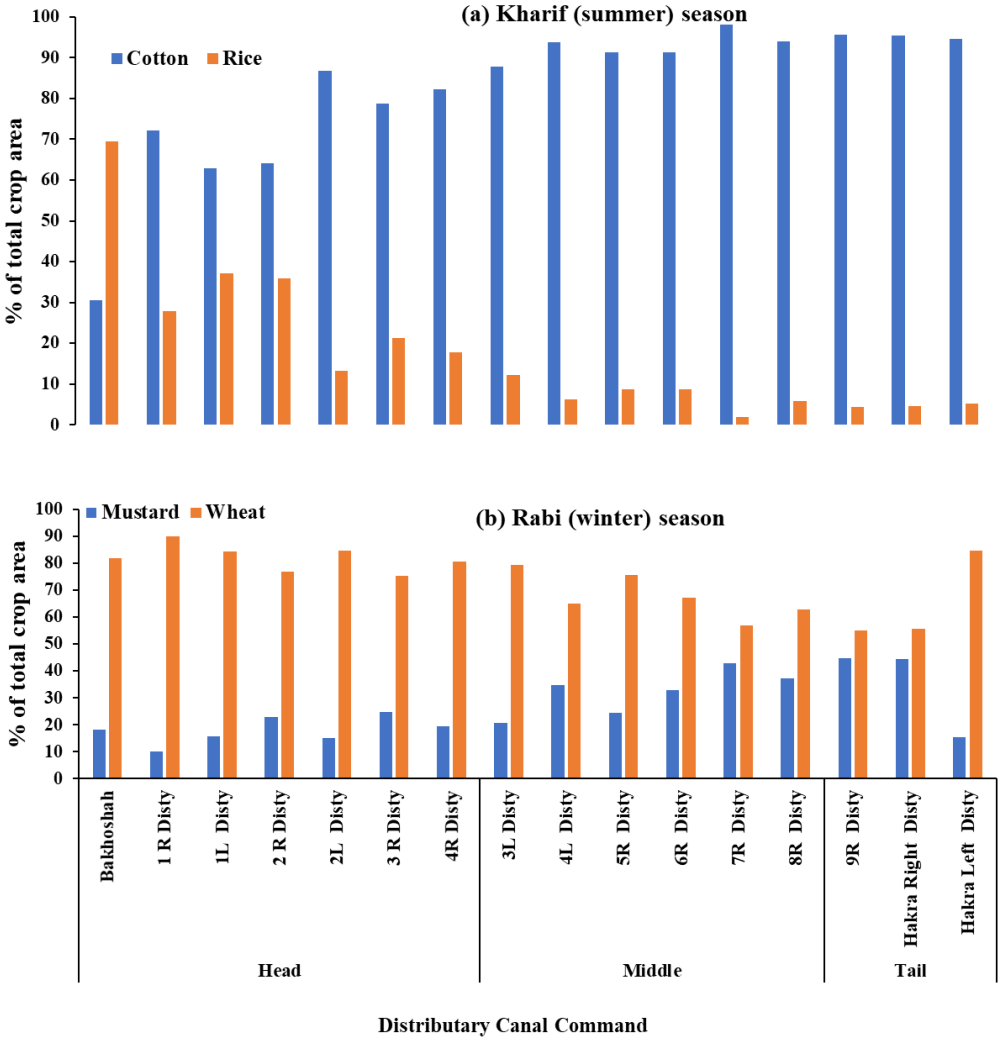

Figure 6.7: Crop intensity (% of the total crop area) in different distributary canal command of the Hakra Branch Command (Punjap Pakistan) during (a) the *kharif* (summer season) and (b) the *rabi* (winter) season of the agricultural year 2016-2017 based on the reclassified crop combination map (Figure 6.1).

6.3.2 Irrigation water distribution

The production of main crops in the HBC command is not possible without supplemental irrigation due to low and scanty rainfall (Figure 4.1). As per Eqs. (6.1) to (6.6), Figure 6.8 shows the estimates of irrigation water distribution including canal water supply and groundwater pumping across the distributary canal commands at the head, middle and tail reaches of the HBC command area during the agricultural year 2016-2017. The net

annual canal inflow was estimated to be about 268 mm yr^{-1} as per canal rostering, with a variation as low as 143 mm yr^{-1} (Hakra left) located at the tail reaches up to 369 mm $year^{-1}$ (2R) at the head reaches (Figure 6.8a). Awan *et al.* (2016) also estimated the net canal-water supply of 253 mm yr^{-1} for the head reaches, 223 mm yr^{-1} for the middle reaches, and 170 mm yr^{-1} for the tail reaches in HBC command area during 2014 – 2015. It is clear from the Figure 6.8b that the average canal inflow received at the head reaches (309 mm yr^{-1}) is estimated 19% higher compared to the middle reaches (i.e. 267 mm yr^{-1}), and 42% higher compared to the tail reaches (i.e. 180 mm yr^{-1}). This highlights the inequality of canal water distribution with the head reach distributaries receiving a relatively higher canal water supply than the middle and tail reaches.

Overall, the average net canal water supply of 268 mm yr^{-1} over the entire HBC equated only 18% of the average ET_p (~1500 mm yr^{-1}) during the agricultural year 2016-2017. Hence, this irrigation deficit is compensated by extensive groundwater pumping over the entire HBC command. As per Eqs. 6.3 to 6.5, the average annual groundwater pumping over the entire HBC command is estimated to be about 279 mm yr^{-1}, with a variation as low as 183 mm yr^{-1} (8R) located at the middle reaches, up to 469 mm/year (1L) at the head reaches (Figure 6.8a). It is clear from Figure 6.8 that groundwater use is estimated to be relatively higher in the head reaches (Bakhoshah, IR, IL, and 2R distributaries) to irrigate mainly high-water demanding crops of the rice-wheat cultivation (Figure 6.7). This is to be expected, due to relatively higher tubewell density, and the availability of good-quality shallow groundwater which is mainly due to seepage from the main canals (Figure 6.3). The low use of groundwater in the middle and tail reaches is attributed to the poor quality of groundwater which is at a greater depth (Figure 6.3). Overall, the middle and tail reach distributaries received 21% and 36% less irrigation (canal + groundwater) water compared to the head reaches distributaries, respectively (Figure

6.8b). Awan *et al.* (2016) also reported similar trend of groundwater use with the head reach distributaries using 42% percent more groundwater than the middle and tail reaches at HBC command during 2014-2015.

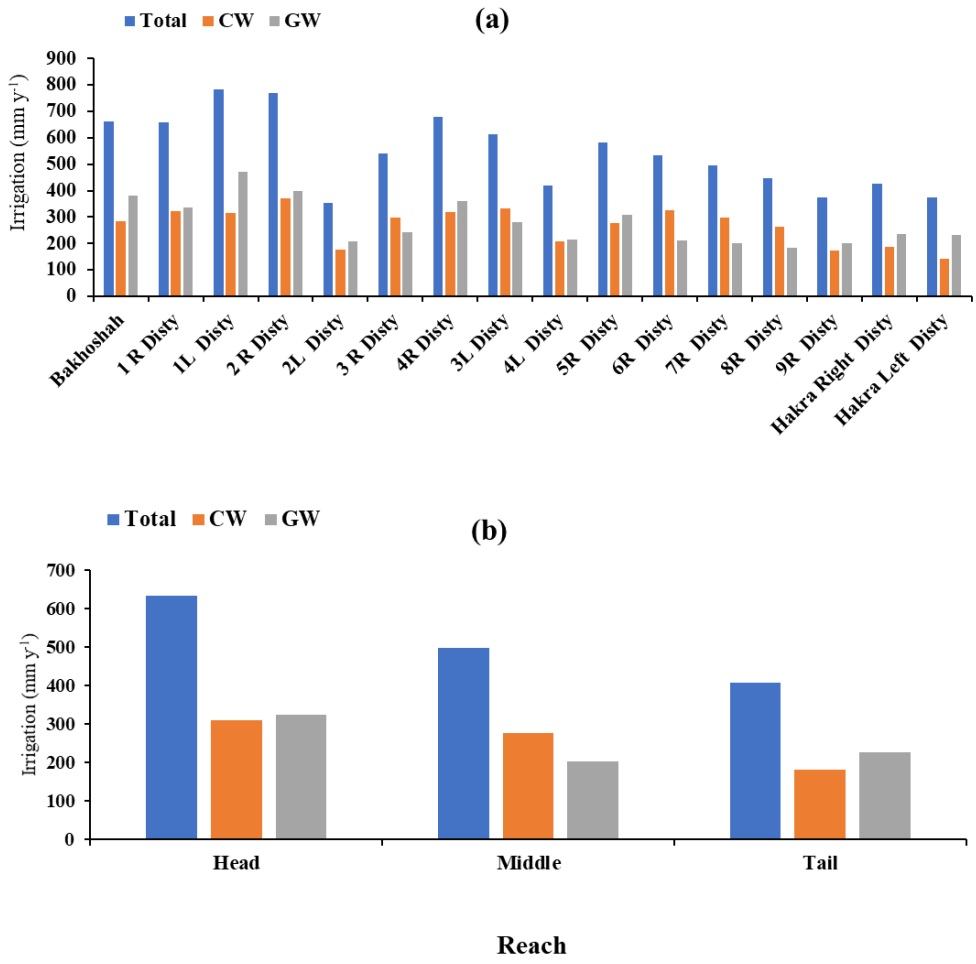

Figure 6.8: Estimated average annual total, canal water (CW) and groundwater (GW) irrigation over the crop areas of different (a) distributaries commands and (b) across the head, middle and tail reaches of HBC during the agricultural 2016-2017. (refer to the appendix C.1 and 2 for estimates of the spatial distribution of canal water and groundwater use across the HBC command).

6.3.3 Comparison of SWAP vs satellite remote sensing-based evapotranspiration

Figure 6.9 shows the actual evapotranspiration *ET* based on the remote sensing and the distributed SWAP modelling during the *kharif* (summer) and the *rabi* (winter) seasons of 2016-2017. The *ET* estimated by *MODIStsp* and distributed SWAP modelling is

referred as ET_{MOD} and ET_{SW}, respectively. Note that SWAP simulated *ET* is based on the stratified homogeneous simulation units (ranging in size from 0.66 to 159 km^2), whereas the *MODIStsp* estimated *ET* is based on 500 x 500 m pixel size. Hence, for the comparison, the ET_{MOD} is aggerated to the scale of ET_{SW} of the simulated homogenous units using Spatial Analyst zonal statistics tool in ArcMap assigning a mean value of ET_{MOD} to each simulation unit (Figure 6.9).

Fig 6.10 shows a scatter plot between the ET_{MOD} and ET_{sw} of individual simulation units on a temporal scale of the *kharif* and *rabi* seasons, and the annual combining of the *kharif* and *rabi* seasons. The plot reveals a positive correlation between the ET_{MOD} and ET_{sw} at both spatial and temporal scales, but also highlights discrepancies of over- or under-estimation for some simulation units, especially desert-barren areas. A statistical analysis (Table 6.4) shows that the ET_{sw} as compared to the ET_{MOD} over the entire HBC command area is slightly overestimated with an *MBE* (Eq. 6.7) of 14 mm during the *kharif* (summer) season. But it is slightly underestimated with an *MBE* (Eq. 6.7) of -5 mm during the *rabi* (winter) season. Overall, the mean annual ET_{sw} is simulated at 715 mm yr^{-1}, about 9 mm higher than the mean annual ET_{MOD} (i.e. 709 mm yr^{-1}) over the entire HBC command area. The index of agreement *IoA* (Eq. 6.8) between the ET_{MOD} and ET_{sw} of individual simulation units is estimated at 0.73, 0.81 and 0.80 during the *kharif*, *rabi* and annual scales, respectively.

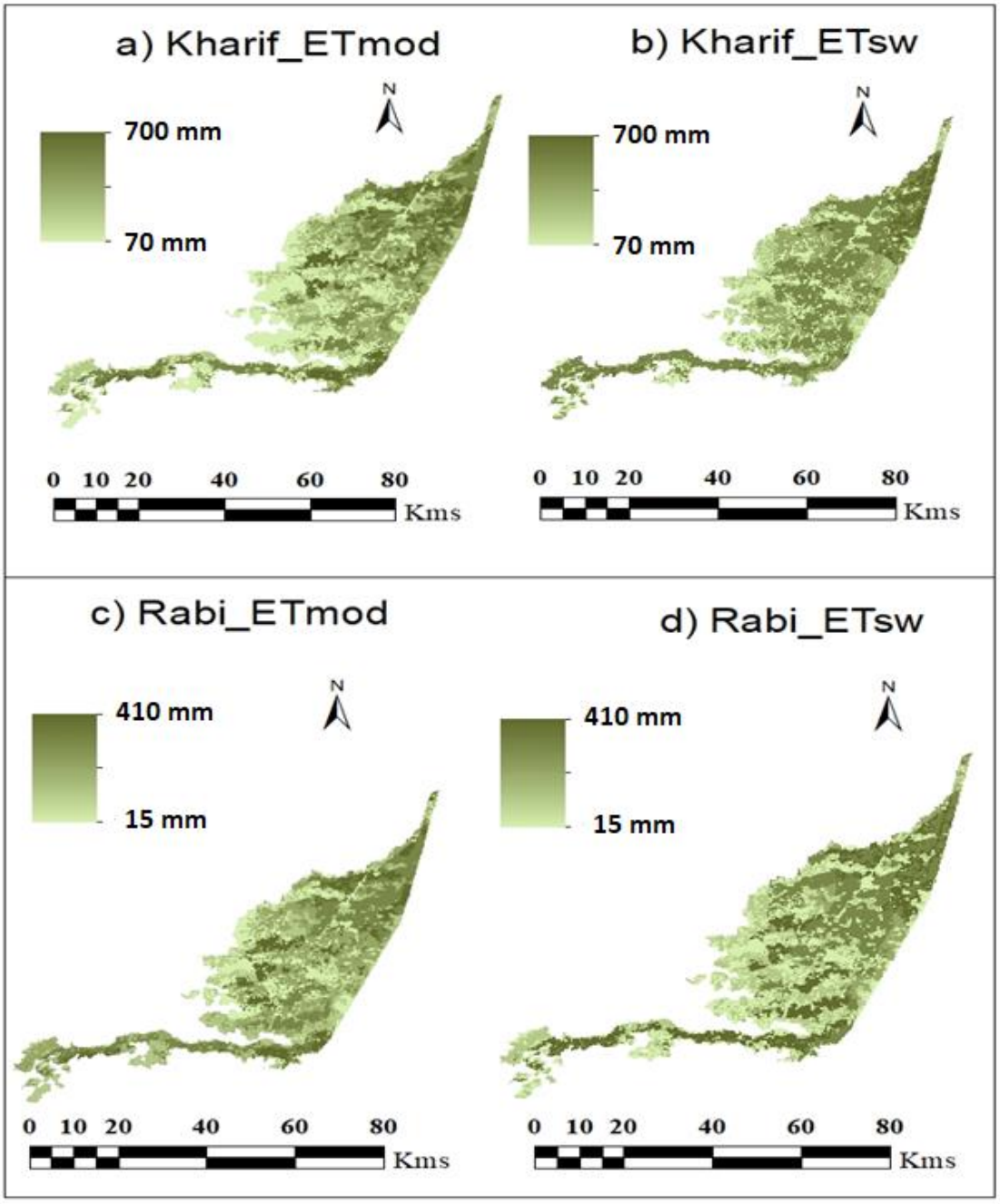

Figure 6.9: Actual evapotranspiration (mm) estimated by the remote sensing based MODIStsp (noted as, ET_{MOD}) and the distributed SWAP modelling (noted as, ET_{SW}) in Hakra Branch Canal command during the *kharif* (summer) and the *rabi* (winter) seasons of 2016-17.

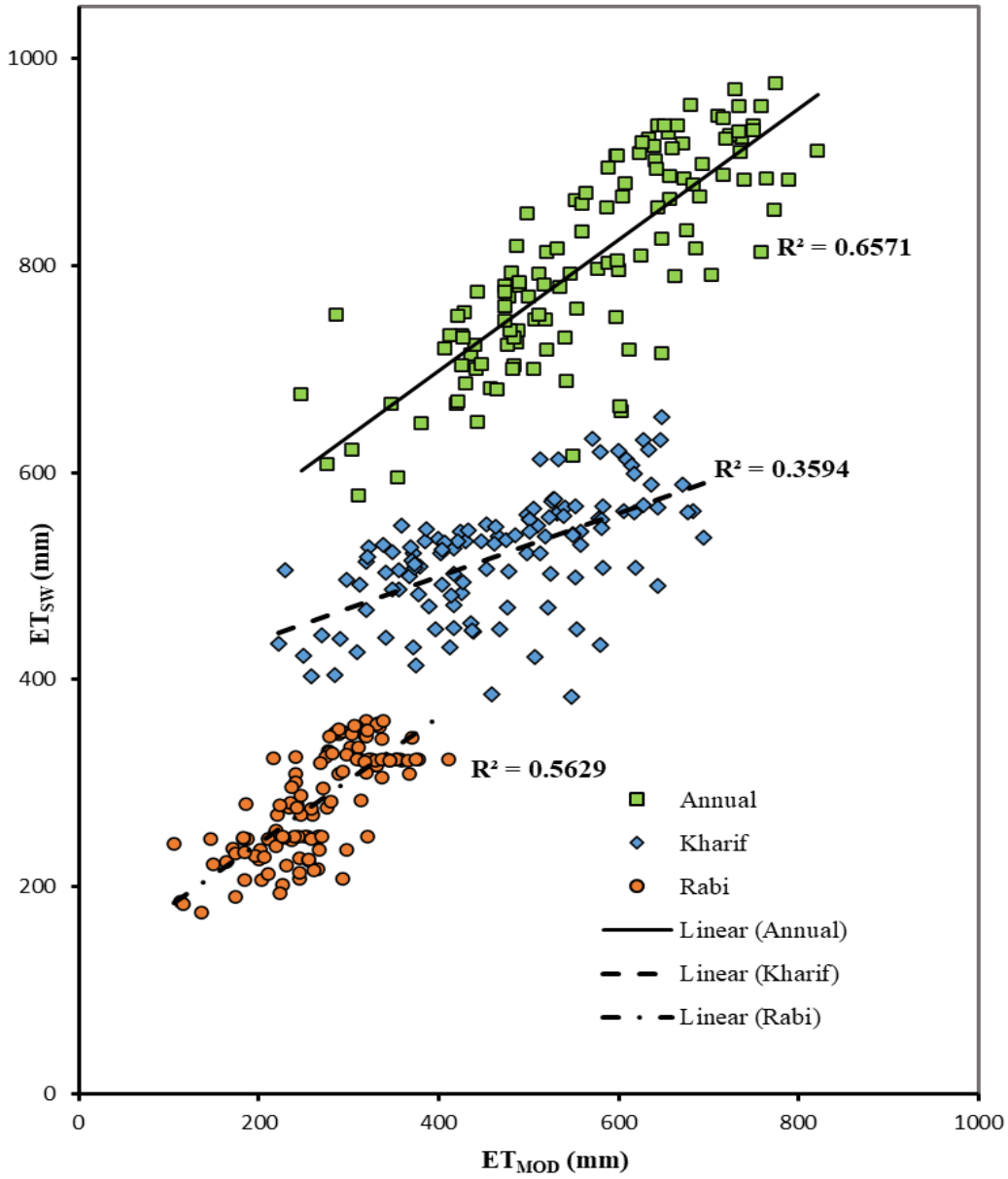

Figure 6.10: Comparison of the remote sensing ET_{MOD} and SWAP simulated ET_{SW} at temporal scale of annual and seasonal in the Hakra Branch Canal command during the agricultural year 2016-2017.

Table 6.4: Seasonal and annual mean evapotranspiration (mm) estimated from remote sensing ET_{MOD} and simulated by SWAP ET_{sw} in the Hakra Branch Canal command during the agricultural year 2016-2017.

Season	Mean		Standard Deviation		Goodness-of-fit measures	
	ET_{MOD} mm	ET_{sw} mm	ET_{MOD} mm	ET_{sw} mm	*MBE* mm	*IoA* ---
Kharif (Summer)	451	465	115	155	14	0.73
Rabi (Winter)	255	249	67	99	-5	0.81
Annual	706	715	131	245	9	0.80

A further comparison between the ET_{MOD} and ET_{sw} is made over the main crops of cotton, rice, wheat, mustard, and the barren soil simulation units over the entire HBC command area (Fig 6.11). Note that the aggregated simulation units are based on the reclassified crop combination map (Figure 6.1). Figure 6.11 shows a close agreement between the ET_{sw} and ET_{MOD} over rice, mustard and wheat crop areas, with simulation of a slightly higher ET_{sw} over cotton crop area. The mean ET_{sw} for cotton areas is simulated at 519 mm, which is 16% higher than the mean ET_{MOD} of 448 mm. Whereas for rice the mean ET_{sw} (580 mm) is slightly underestimated by ~5%. Similarly, for mustard the mean ET_{sw} is 215mm as compared to the mean ET_{MOD} 227mm, and for wheat mean ET_{sw} is 317 mm which is 8% higher than the mean ET_{MOD} 291 mm.

A scatter plot analysis of *ET* of individual simulation units shows a reasonable agreement between the ET_{MOD} and ET_{sw} over the main crops' areas with an R^2 value ranges from 0.27 to 0.47, *IoA* from 0.58 to 0.70, and *MBE* from -38 to 74 (Figure 6.11b). However, Fig 6.11 clearly shows a high discrepancy between the ET_{sw} and ET_{MOD} over the desert-barren simulation units. The size of desert-barren simulation units varied from 0.66 to 158 km^2. The simulated ET_{sw} over the desert-barren units varied from 69 to 106 mm with a mean aggregated value of 73 mm during the *kharif* season and varied from 16 to 27 mm with a mean aggregated value of 16 mm during the *rabi* season. The SWAP simulated ET_{sw} over the desert-barren units accounts for soil evaporation only, which corresponds to the rainfall received by the area. The total rainfall recorded in HBC command area during the study period 2016-2017 is 115 mm out of which 98 mm occurred during the *kharif* season and only 17 mm during the *rabi* season (Figure 4.1). However, the ET_{MOD} over the desert-barren units varied from 172 mm to 548 mm with a mean aggregated value of 296 mm during the *kharif* season, and from 57 mm to 313 mm with a mean aggregated value of 166 mm during the *rabi* season.

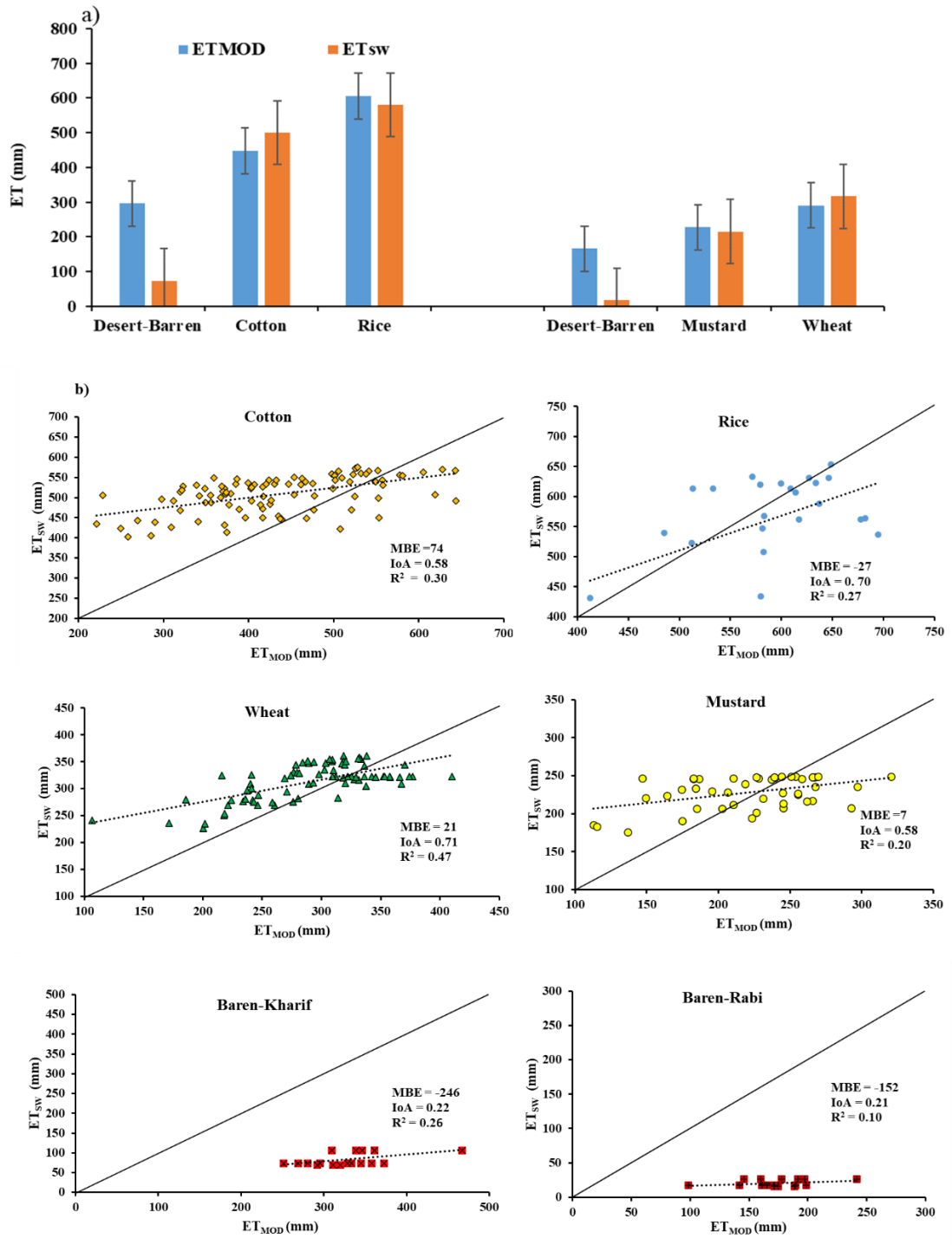

Figure 6.11: Comparison of actual evapotranspiration estimated by the remote sensing ET_{MOD} and simulated by the *SWAP* ET_{sw} over different crop areas and barren lands in the Hakra Branck Canal command during the agriculture year 2016-2017.

Furthermore, the ET_{MOD} of an individual bare-soil pixel was estimated as high as 658 mm during the *kharif* season, and 397 mm during the *rabi* season. This indicates that small-size crops fields lying in the desert-barren areas might be identified as desert-barren simulations units based on the reclassification map (Figure 6.1). Singh *et al.* (2006b) also highlighted such a discrepancy between the SWAP simulated *ET* and remote sensing-based *ET* over the barren soils in Sirsa district, India.

Figures 6.9 to 6.11 show a close agreement between the ET_{sw} and ET_{MOD} especially over the main crops of wheat, rice, cotton, and mustard across entire area of the HBC during 2016-17. This provides confidence in the use of distributed SWAP modelling for quantification of soil water and salt balances, and crop water productivity in HBC command area.

6.3.4 Soil water and salt balances

Table 6.5 presents soil water and salt balances simulated and aggregated over the main crop combinations in HBC command during the agriculture year 2016-17. The annual rainfall was 115 mm, which is 59% less than the long-term average annual rainfall of 280 mm in HBC during 1979-2017. This low amount of rainfall compared only 7 to 10% of the average annual reference evaporation ET_P of about 1500 mm. Canal irrigation contributes, 34% (cotton-wheat), 33% (cotton-mustard) and 32% (rice-wheat) to the annual actual evapotranspiration ET_a during the year 2016-17 (Table 6.5). The total irrigation (canal plus groundwater) varied from 488 mm yr^{-1} for cotton-mustard combination to 870 mm yr^{-1} for rice-wheat combination. Over the entire HBC, the average irrigation is estimated to be highest at 552 mm for rice, followed by 366 mm for cotton, 285 mm for wheat and 162 mm for mustard crops (Table 6.5). The average estimated irrigation (canal plus groundwater) was 459 mm during the *kharif* season, and

224 mm during the *rabi* season of 2016-2017 (Table 6.5). Liaqat *et al.* (2016) estimated the average seasonal irrigation (canal + groundwater) applied from 413 mm during the *kharif* (cotton and rice) season, and 281 mm during the *rabi* (wheat and mustard) season in HBC from 2008 to 2014. A significant amount of total irrigation was supplied by groundwater I_{gw} (Table 6.5), with the average groundwater irrigation over the entire HBC estimated at 260 mm during the *kharif* season (cotton-rice), and 140 mm during the *rabi* season (wheat- mustard) (Table 6.5). These simulated values were in line with findings of Liaqat *et al.* (2016), as they reported average groundwater abstractions of 281 mm during the *kharif* season (cotton and rice), and 182 mm during the *rabi* season (wheat and mustard) in the HBC from 2008 to 2014. As expected, the annual groundwater abstraction over the rice-wheat fields is estimated to be 37% to 57% higher, as compared to the cotton-wheat and cotton-mustard fields (Table 6.5), respectively. This is mainly due to the need to maintain water ponding for rice cultivation.

The mean actual evapotranspiration ET_a is simulated to be 905 mm for the rice-wheat, 854 mm for the cotton-wheat, and 729 mm for the cotton-mustard fields (Table 6.5). Over the entire HBC, the average ET_a is estimated to be highest at 586 mm for rice, followed by 516 mm for cotton, 323 mm for wheat and 226 mm for mustard crops (Table 6.5). These values correspond with Liaqat *et al.* (2015), they estimated the average ET_a from 578 to 786 mm during the *kharif* (cotton and rice) season, and from 285 and 338 mm during the *rabi* (wheat and mustard) season across all the distributary canal commands of the HBC during 2008 – 2014. However, the simulated lower ET_a of the cotton-mustard fields was due to these fields being mainly located in the tail reaches of the canal network, The tail reaches received lower amounts of canal water supply (Figure. 6.1) and there was somewhat limited groundwater irrigation due to poor quality groundwater (Figure. 6.3).

The mean annual percolation Q_{bot} is simulated significantly higher at -116 mm yr^{-1} in the rice-wheat fields, followed by -44 mm/yr in the cotton-wheat fields and -21 mm yr^{-1} in the cotton-mustard fields (Table 6.5). The rice-wheat Q_{bot} was simulated higher due to high depth of irrigation applied for maintaining surface ponding for optimal rice cultivation conditions. Despite this, the Q_{bot} was simulated relatively higher (at -81 mm) during the *rabi* (wheat) season than the *kharif* (rice) season (at -35 mm) (Table 6.5). This was mainly due to topsoil layer puddling to maintain surface ponding by restricting the percolation in the rice fields results in higher evapotranspiration during the *kharif* (rice) season.

Table 6.5: SWAP simulated soil water and salt balances* of the main crop combinations in Hakra branch canal command during the *kharif* (May 1st to Oct 31st, 2016) and the *rabi* (Nov 1st, 2016 to Apr 30th, 2017) seasons. The mean values are aggregated over the entire crop area.

Crop season /Components	Cotton	Wheat	Cotton	Mustard	Rice	Wheat	Baren	Baren
	Kharif	*Rabi*	*Kharif*	*Rabi*	*Kharif*	*Rabi*	*Kharif*	*Rabi*
P	98	17	98	17	98	17	98	17
I	407	251	326	162	552	318	0	0
I_{cw}	183	110	152	87	171	116	0	0
I_{gw}	224	141	174	75	381	202	0	0
T_p	535	290	535	170	336	296	0	0
ET_p	953	530	953	585	974	530	905	497
T_a	447	239	424	156	264	232	0	0
ET_a	529	325	503	226	586	319	77	19
Q_{bot}	-27	-17	-12	-9	-35	-81	-1	-1
ΔW	-51	-74	-91	-57	29	-65	20	-3
Salt balance mg cm^{-2}								
IC_i	50	33	32	14	52	29	0	0
$Q_{bot}C_{bot}$	-9	-11	-6	-2	-18	-35	-0.07	-0.01
ΔC	41	21	26	12	35	-6	-0.07	-0.01

*Height of soil column considered is 160 cm.

The saturated soil profile left after the rice cultivation (29 mm) and the application of heavy irrigation in the early stages of wheat crop resulted into relatively higher Q_{bot} during the *rabi* (wheat) season. However, the mean change in soil water storage ΔW of

the soil profile indicates a loss of soil water storage in all simulation units, ranging from -36 mm in rice-wheat fields to -148 mm cotton-mustard fields (Table 6.5).

6.3.5 Net Groundwater recharge

The net groundwater recharge is an important hydrological component in the soil-water-plant-continuum. This quantifies the effects of the soil-water balance on groundwater system. The *SWAP* model simulated soil-water balance components of the simulation units were aggregated to quantify the net groundwater recharge, as follows:

$$Q_R = P + I_{gcw} - ET - \Delta W. \qquad \text{Eq 6.9}$$

Here, Q_R is the net groundwater recharge [L], P is precipitation [L], I_{gcw} is the gross canal water supply (i.e., canal irrigation + seepage losses from the canal network) [L], ET is actual evapotranspiration [L], and ΔW is change in the soil water storage in the soil profile [L]. The positive value of Q_R indicates a rise in the groundwater level and the negative value indicates a decline in the groundwater level.

Using the soil-water balance components (Table 6.5), Eq. 6.9 was applied to quantify the net groundwater recharge across all the distributaries command and at the spatial scale of the head, middle and tail reaches in the HBC command for 2016-2017 (Figure 6.12). It can be observed that the current cropping and irrigation system is contributing to declining groundwater levels across all distributaries in the HBC command area. The estimated annual Q_R varied from -36 mm yr^{-1} in the 2R distributary, to -107 mm yr^{-1} in the 5R distributary. The estimated annual Q_R ranged from -36 to -104 mm $yr^{-1}$with a mean annual recharge of -91 mm yr^{-1} in the head reaches, from -39 to -107 mm y^{-1} with a mean annual recharge of -68 mm yr^{-1} in the middle reaches, and from -44 to -100 mm yr^{-1} with a mean annual recharge of -53 mm yr^{-1} in the tail reaches of the HBC command.

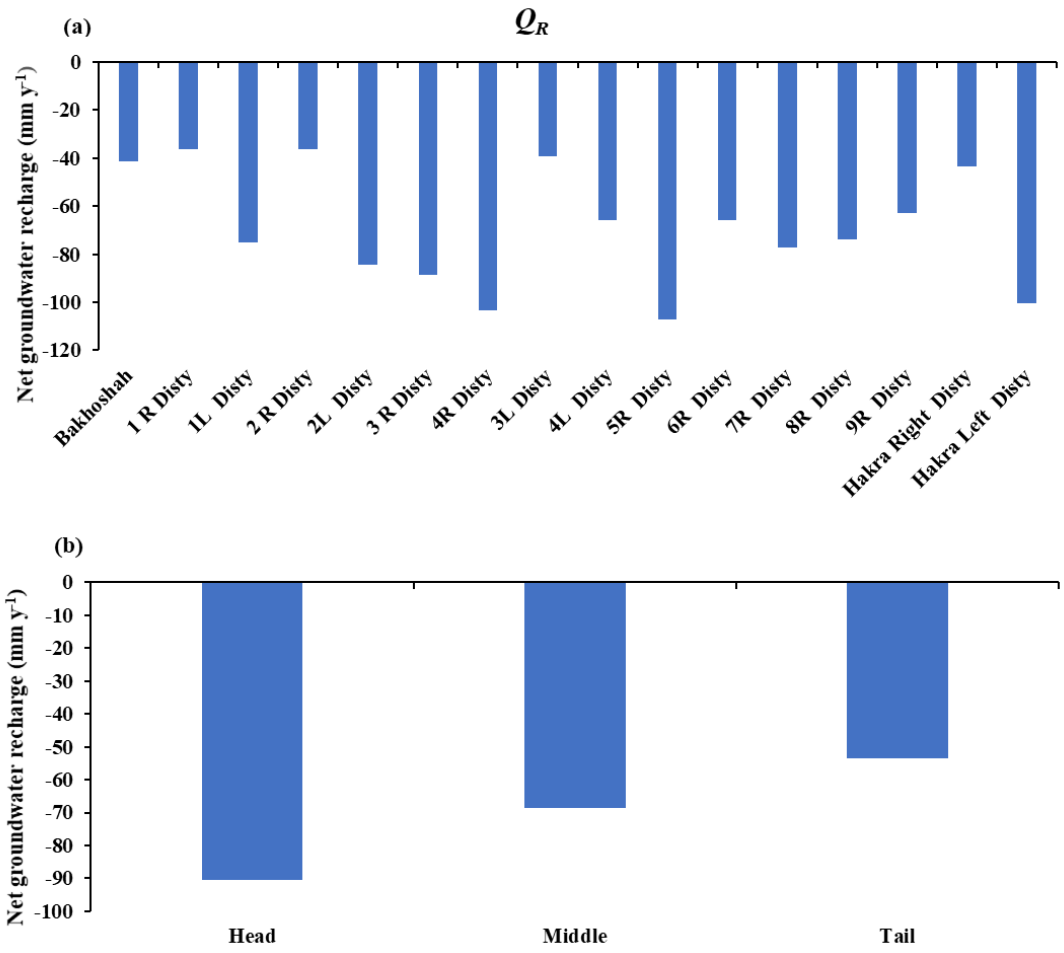

Figure 6.12: SWAP simulated annual net groundwater recharge (mm yr^{-1}) over (a) different distributary canal commands and (b) head, middle and tail reaches of Hakra branch canal command during the agricultural year 2016-2017. The mean value apply to the entire command area. (refer to the appendix C.3 for estimation of the spatial distribution of groundwater recharge across the Hakra branch canal command)

This suggests a net abstraction of groundwater, namely a negative Q_R, across all the distributaries of the HBC during the year 2016-17. However, the net groundwater abstraction was estimated about 25% and 41% less in the middle and tail reaches, respectively as compared to the head reaches of the HBC. The high abstraction in the head reaches was due to availability of relatively good quality of groundwater used for irrigation of water-intensive wheat-rice cultivation. Awan *et al.* (2016) reported that 42% of the total irrigation comes from groundwater in the head reaches of the HBC. The seepage losses from the canal network compensate the groundwater abstraction, though

the highly negative values of Q_R indicates a decline of groundwater levels across the entire HBC area. The mean annual Q_R over the entire HBC is estimated at -71 mm yr^{-1} which represents a decline of groundwater during 2016-2017. This agrees with (Shafeeque *et al.*, 2016) who estimated a mean value of -91 mm yr^{-1} of net groundwater recharge in the HBC using Soil and Water Assessment Tool (SWAT) model over a period from 2006 – 2011. Liaqat *et al.* (2016) also estimated net groundwater recharge of -115 mm yr^{-1} in the HBC using a geo-informatic approach over a period from 2008-2014.

6.3.6 Salinity build-up

The quantification of the soil salinity provides useful information about the potential impact of current irrigation practices on the sustainability of irrigated agriculture. The soil salinity level in the root zone must be kept below the crop specific threshold levels for successful crop production. In this study, the SWAP model simulated salt balance components of the simulation units were aggregated to quantify change in soil salinity as follows:

$$\Delta C = PC_p + IC_i + Q_{bot}C_{bot} \qquad \text{Eq. 6.10}$$

where, ΔC is the change in soil salt storage [M L^{-2}], C is the solute concentration [M L^{-3}], and subscript p refers to rainfall (P), i refers to irrigation (I), and *bot* refers to percolation (Q_{bot}) (positive upward, negative downward) from soil profile. The use of poor-quality groundwater results into salt build up in the soil profile. The mean annual salt storage was simulated at 62 mg cm^{-2} for the cotton-wheat fields, 38 mg cm^{-2} for the cotton-mustard fields, and 29 mg cm^{-2} for the rice-wheat fields (Table 6.5). The relatively lower salt storage in the rice-wheat fields, despite a higher use of groundwater was because this crop combination is cultivated in the head reaches of the HBC where the

groundwater quality is relatively good (< 3dS/m). Figure 6.14 shows the salt build up across all distributary commands and the head, middle and tail reaches of HBC. The change in salt storage ΔC was simulated from 1.7 ton ha^{-1} yr^{-1} in the 1L distributary command, to 4.6 ton ha^{-1} yr^{-1} in the Hakra left (HL) distributary command (Figure 6.14a). The mean ΔC in the head reaches is simulated at 3.2 ton^{-1} ha^{-1} yr^{-1}, followed by 4.3 and 4.1 ton ha^{-1} yr^{-1}, respectively in the middle and tail reaches. A relatively higher salt build up in the middle and tail reaches can be attributed to the relatively poor groundwater quality in the middle and tail reaches of the HBC (Figure 6.13).

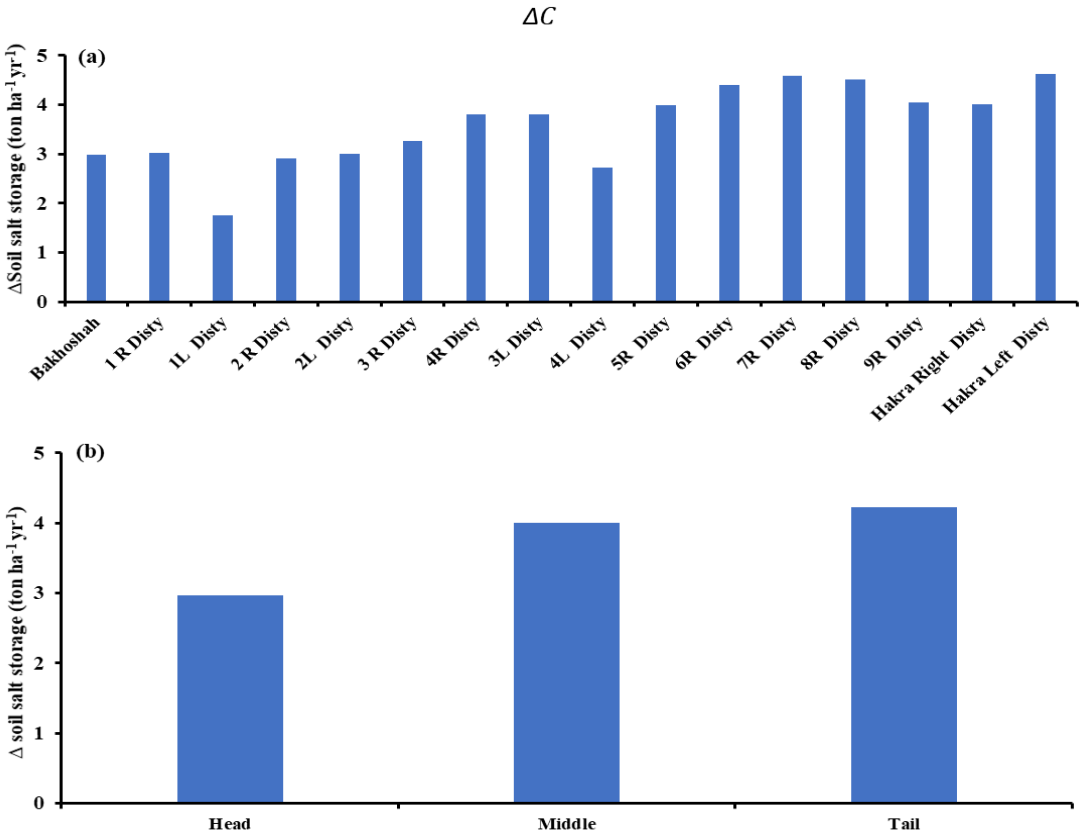

Figure 6.13: SWAP simulated mean annual salt build up (ton ha^{-1} yr^{-1}) at (a) different distributary canal commands and at (b) spatial scale of head, middle and tail reaches of Hakra branch canal command during the agricultural year 2016-2017. The mean value apply to the entire command area. (refer to the appendix C.4 for estimates of the spatial distribution of salt build up across the Hakra branch canal command).

According to Maas and Hoffman (1977), the soil salinity concentration has to be kept below the crop threshold salinity level for optimum crop growth. The simulated salt balance components of homogenous simulation units indicate the soil *EC* ranged from 2.10 to 5.86 dS m^{-1} in the head reaches, and from 2.93 to 8.26 dS m^{-1} in the middle reaches, and from 3.2 to 11.7 dS m^{-1} in the tail reaches of the HBC. The simulated soil *EC* values, particularly in the middle and tail reaches, ranged higher than the soil salinity threshold values for the selected crop combinations of cotton 7.7 dS m^{-1}, rice 5.0 dS m^{-1}, wheat 6.0 dS m^{-1} and mustard 7.4 dS m^{-1} (Tables 4.2 and 6.2). This was mainly due to low canal inflow and the higher use of poor-quality groundwater in the middle and tail reaches.

6.3.7 Crop Water productivity

The simulated water- and salt-limited crop yields and soil water balance components of the individual simulation units are aggregated to analyse the spatial and temporal variations in the crop's relative transpiration ratio (T_a/T_p) as the indicator of water and salt stress on crop growth, plus the crop water productivity in terms of actual evapotranspiration (WP_{ET}) (Eq. 5.3) and depth of irrigation applied (WP_{Irr}) (Eq. 5.4). Table 6.6 presents the mean values of T_a/T_p, WP_{ET} and WP_{Irr} simulated for the main crops of cotton, rice, mustard and wheat over the entire HBC command during 2016-2017. It should be noted that these values are based on the simulated water- and salt-limited crop yields, which could be simulated higher than the actual crop yields, as the SWAP model used here did not account for other agronomic stresses such as pests, disease, and inadequate nutrition. Figure 6.14 reports the spatial variation of water- and salt-limited crop yields across all the simulation units of the HBC command during 2016-2017. The variation is high for rice followed by wheat, whereas the cotton and mustard crops performed more equal in their respective simulation units. This variation in crop yields

is attributed to the different sensitivity of crops to water and salt stress. The simulated water-and salt-limited cotton yield varied from 1.14 ton ha^{-1} to 2.73 ton ha^{-1}, with average yield of 1.94 ton ha^{-1}. The rice yield varied from 1.40 ton ha^{-1} to 7.51 ton ha^{-1} with average yield of 4.37 ton ha^{-1}. The wheat yield varied from 1.22 ton ha^{-1} to 6.56 ton ha^{-1} with average yield of 4.49 ton ha^{-1}. The mustard yield varied from 0.7 ton ha^{-1} to 2.21 ton ha^{-1} with average yield of 1.46 ton ha^{-1}. According to the crop reporting services of the Punjab agricultural department (CRS, 2017), during the agricultural year of 2016-2017 the recorded crop yield of Bahawalnagar district (HBC Command) was 1.76 ton ha^{-1} for cotton, 2.02 ton ha^{-1} for rice, 3.27 ton ha^{-1} for wheat and 1.19 ton ha^{-1} for mustard. As expected, the SWAP simulated water- and salt-limited crop yield is 10 to 50% higher than the recorded crop yield values.

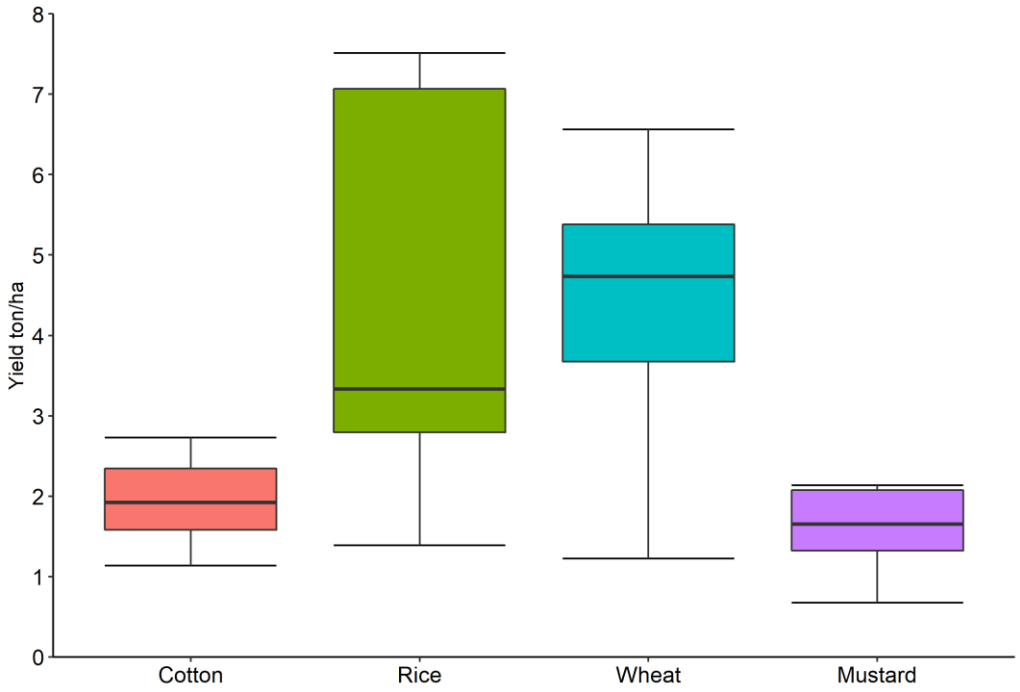

Figure 6.14: SWAP simulated water- and salt-limited crop yield across all the homogeneous simulation units at Hakra branch canal command during 2016-2017. Whisker represents the extreme values and the middle line represents the median of the aggregated data.

This is because SWAP model does not consider nutritional, pest and disease stresses in crop growth simulations. However, under actual condition such stresses could significantly affect the crop yield. Therefore, improved crop management in terms of optimal fertilizer application, better pest and disease control is expected to achieve this potential crop yield in HBC command. The mean values of water- and salt-limited WP_{ET} (kg m^{-3}) are simulated at 1.19 for wheat, followed by 0.96 for rice, 0.73 for mustard, and 0.40 for cotton crops. (Zwart and Bastiaanssen, 2004) reviewed global crop water productivity and according to their analyses, the WP_{ET} (kg/m^3) was estimated 0.63 for cotton, 1.09 for rice and 1.08 for wheat. Singh *et al.* (2006b) estimated the mean values of water- and salt-limited WP_{ET} (kg/m^3) of 0.36 for cotton, 0.47 for rice, 1.37 for wheat and 0.47 for mustard in the Sirsa Irrigation Circle of Haryana, India. The coefficient of variation (*CV*), calculated as the mean value divided by the standard deviation, varied from 9% to 34% for the WP_{ET}, and from 21% to 39% for the WP_{Irr} values (Table 6.6). This shows a scope of improvement in the crop water productivity in the HBC command. The spatial variability of cropping practices, and environmental and physical conditions such as soil type, water quality and availability in root zone, affects water and salt stress and the water productivity of crops. This is evident from Figure. 6.15 that the relative transpiration is simulated to be relatively higher in the head reaches, compared to the middle and tail reaches of the HBC. The high T_a/T_p (> 0.80) shows relatively less water and salt stress on the main crops of cotton, rice, mustard, and wheat in the head reaches. This could be attributed mainly due to availability of sufficient canal water and good quality of groundwater across the head reaches of the HBC (Fig 6.3).

Table 6.6: SWAP simulated mean relative transpiration, water- and salt-limited crop yields, and crop water productivity for the main crops in all the Hakra branch canal command during the agricultural year 2016-2017. The mean values apply to the entire area under the specific crop, *SD* is the standard deviation.

	Cotton*		Rice		Mustard		Wheat	
Variable	*Mean*	*SD*	*Mean*	*SD*	*Mean*	*SD*	*Mean*	*SD*
T_a/T_p (-)	0.71	0.12	0.72	0.12	0.72	0.22	0.77	0.12
Y (kg/ha)	1942	428	4366	2211	1458	632	4493	1372
WP_{ET} (kg/m^3)	0.40	0.04	0.96	0.31	0.73	0.25	1.19	0.35
WP_{Irr} (kg/m^3)	0.69	0.15	1.05	0.32	1.12	0.44	2.00	0.43

*cotton seed yield

Similarly, the water- and salt-limited WP_{ET} values were simulated relatively higher, especially for wheat and rice, in the head reaches of the HBC (Figure. 6.16). This is attributed to the optimum conditions in terms of higher canal inflow and good quality of groundwater due to seepage from canal network at the head reach of HBC (Figure. 6.3). However, the cultivation of high water consuming crops like rice in the head reaches could pose a threat of water logging and secondary salinization due to the high amounts of irrigation, high seepage losses from the canal network, and the shallow groundwater levels in the head reaches. Therefore, efforts to replace rice with less water intensive crops such as cotton in the head reaches will help to increase the canal flow and reduce abstraction of poor-quality groundwater in the tail reaches.

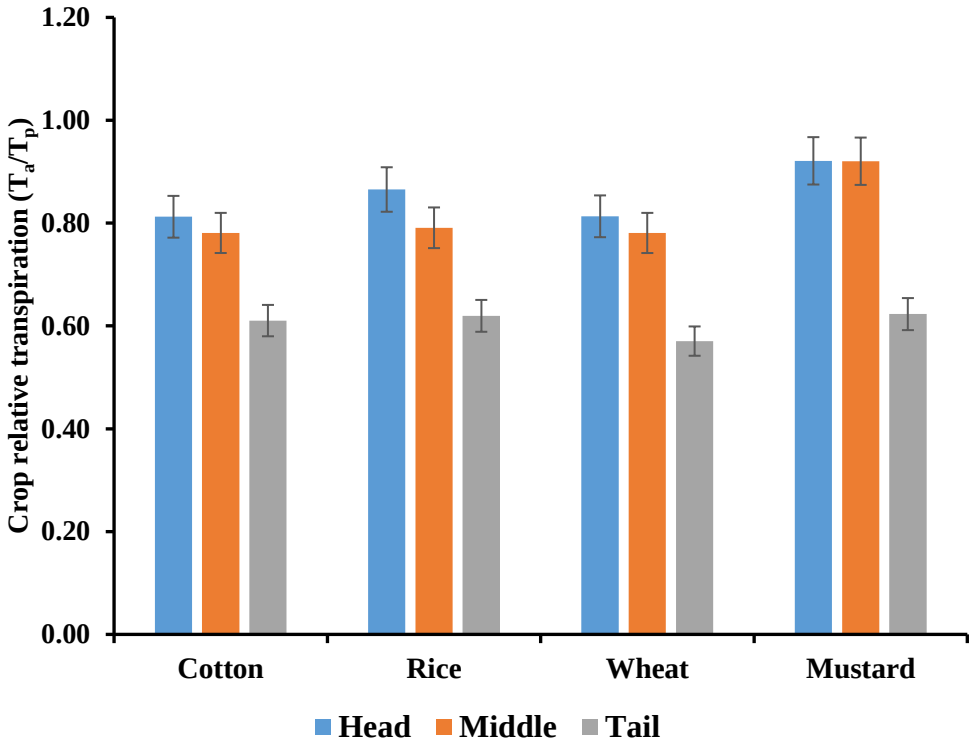

Figure 6.15: Comparison of SWAP simulated relative transpiration of the main crops in the head, middle and tail reaches of Hakra branch canal command during the agricultural year 2016-2017. The mean values apply to the area under the specific crop.

The variation in the WP_{ET} and WP_{Irr} for cotton is almost negligible while other crops showed a higher spatial variation across the head, middle and tail reaches. This indicates that cotton was an efficient crop in terms of water and salt stresses at a spatial scale of head, middle and tail reaches in the HBC. Whereas other crops such as rice, wheat, and mustard have a variation from 7% to 28% in the middle reaches, and from 23% to 59% for the tail reaches, compared to the head reaches of the HBC. This shows a substantial potential for water productivity improvement in HBC command.

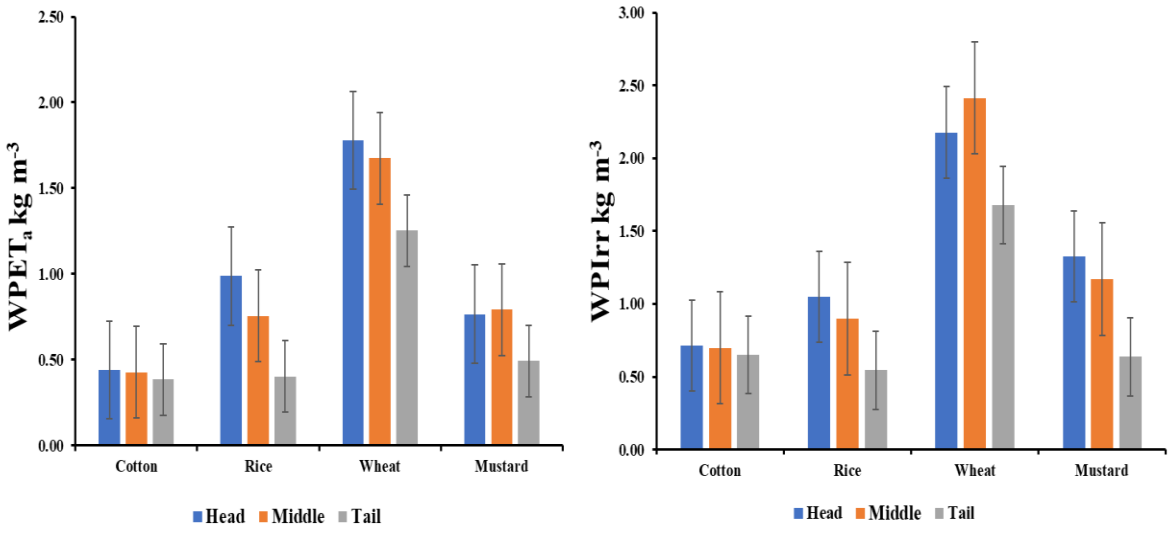

Figure 6.16: Comparison of SWAP simulated water- and salt-limited water productivity for the main crops in head, middle and tail reaches of the Hakra branch canal command during the agricultural year 2016-2017. The mean values apply to the entire area under a specific crop at the head, middle and tail reach of HBC.

The spatial variation of water productivity of the main crops is also compared with the water- and salt-limited yields (Figure 6.17). The positive linear relationship (R^2 from 0.92 to 0.96) between the simulated water- and salt-limited crop yields (Y) and WP_{ET} shows that the response of crop yield to actual evapotranspiration is not constant, and the WP_{ET} increased with higher crop yields for all the mains crops in the HBC during 2016-2017. This suggests that efforts to increase crop yields by improving agronomic practices and reducing water and salt stress could help increase water productivity of crops.

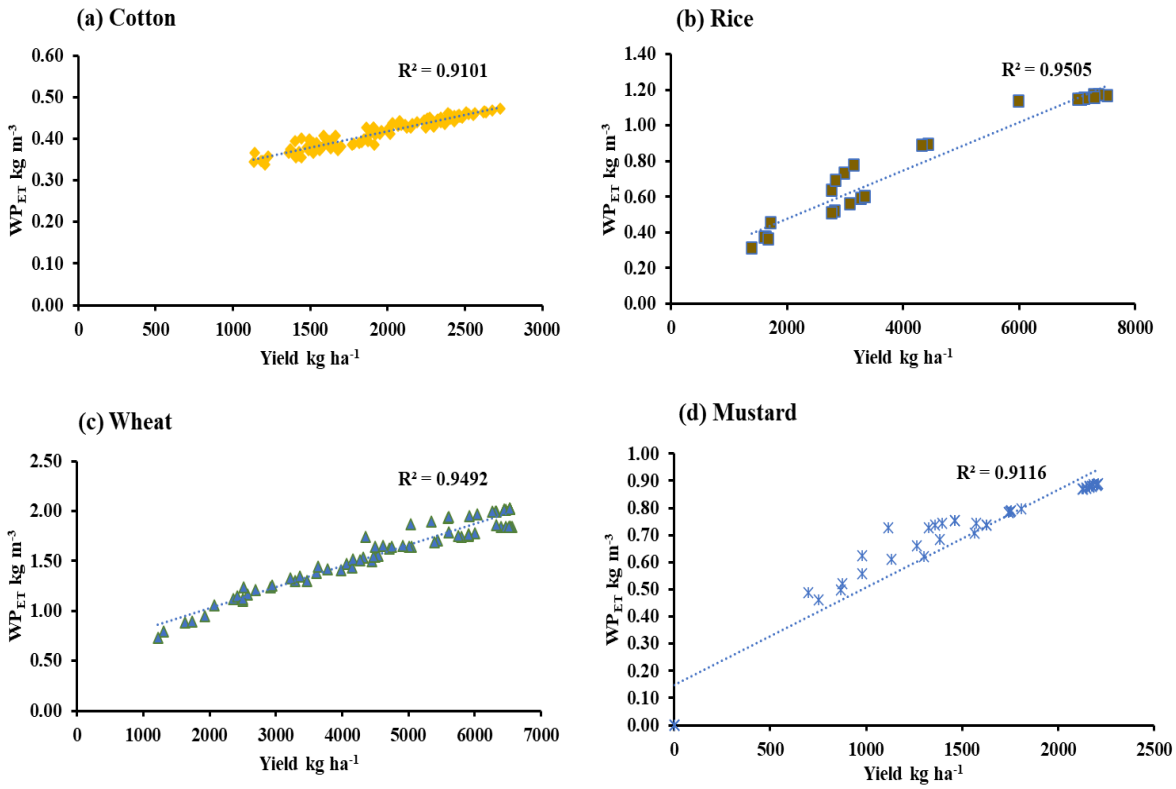

Figure 6.17: Relationship between SWAP simulated water- and salt-limited crop yields and water productivity WP_{ET} (Y/ET_a) of the main crops (a) cotton (b) rice (c) wheat (d) mustard in Hakra branch canal command during the agricultural year 2016-2017. The value represents the mean value at distributary command.

6.3 Conclusions

This chapter demonstrates the potential for integrating valuable information acquired from field experiments, secondary data and remote sensing for calibration and validation of the distributed simulation of soil water and salt balances, and crop growth of main crops for cotton, rice, wheat, and mustard at the canal command level. The SWAP model was implemented in a distributed way, aggregating spatially distributed information of land use, canal irrigation, groundwater, and soil types, to quantify the impacts of current irrigation practices on soil-water and salt balances, and crop-water productivity across the HBC command area. The HBC command was divided into 142 homogeneous simulation units, representing unique combinations of crops, soils, and irrigation practices in the study area.

To validate the accuracy of the spatial aggregation of the input parameters, the actual evapotranspiration ET_a simulated by *SWAP* model was compared with the ET_a from independent satellite remote-sensing based ET_a *MOD16A2* obtained from *MODIS* at 500 m resolution. The goodness-of-fit (*IoA*=0.8) between the *SWAP* simulated ET_a and *MODIS* ET_a suggested an acceptable parametrization of the distributed *SWAP* modelling over the main crop areas. However, the discrepancy in *SWAP* simulated ET_a and *MODIS* ET_a for barren soils simulation units highlighted the need for improvement of the reclassification of land use in the distributed modelling. The low accuracy in the reclassification of land use could result in unrealistic values of soil water and salt-balance components. Though the acceptable agreement between independent satellite remote-sensing *ET* and *SWAP*-simulated *ET* of the main crops gave confidence of using the distributed SWAP modelling for further analysis.

The simulation results suggest that current crop cultivation practices in HBC command are contributing to significant variation in irrigation water supplies, soil salinity build-up and over-exploitation of groundwater resources. The mean annual net groundwater recharge Q_R for the entire HBC command is simulated to be -70 mm yr^{-1}. Here, the negative sign shows a groundwater decline. This ranged from as high as -90 mm yr^{-1} in the head reaches to -53 mm y^{-1} in the tail reaches. This was mainly due to the good quality of groundwater (EC < 3 dS m^{-1}) and cultivation of high water consuming crops such as rice in the head reaches. The canal-water inflow is relatively higher in the head reaches, but the farmers also use the groundwater to fulfill the crop water requirement. Whereas across the middle and tail reaches, the canal flow was relatively low, which means the farmers of the middle and tail reaches use poor quality groundwater (EC > 3dS m^{-1}) for irrigation of crops. The use of poor-quality groundwater leads to salt build up in the soil profile which increase the soil salinity. The change in the soil salt balance was simulated

from 3.22, 4.33 and 4.06 ton ha^{-1} yr^{-1} in the head, middle and tail reaches, respectively of the HBC during 2016-17. This high amount of salt build-up significantly affected crop growth and ultimately the crop water productivity.

The spatial variability in environmental and physical conditions such as soil type, water quality and availability affect water and salt stress and the water productivity of crops. The water- and salt-limited WP_{ET} (kg m^{-3}) was simulated to be 0.4 for cotton, 0.96 for rice, 0.73 for mustard, and 1.19 for wheat in the HBC command during 2016-2017. The co-efficient of variation *CV* in the WP_{ET} values are simulated to be as high as 29% for wheat, 33% for rice and 34% for mustard crops. The variation in the cotton WP_{ET}, is simulated relatively low at 9%, which represents the only crop that performs well in the HBC command.

It is evident from the simulation results that the current irrigation and water management practices are leading to unfavorable ecohydrological conditions that affect the sustainability of agriculture in the HBC command. The cultivation of high water consuming crops like rice in the head reaches consumes relatively more water than the middle and tail reaches. Whereas in the middle and tail reaches, low canal inflow and the use of poor-quality groundwater is resulting in secondary salinization. The low mean annual rainfall in the HBC command is not sufficient to leach out the huge amount of salt that build up, namely 4.0 ton ha^{-1} yr^{-1}. Therefore, efforts to improve the irrigation efficiency by adopting the modern irrigation must be carefully evaluated in terms of their long-term potential effects on the soil water and salt balances and crop water productivity in the study area.

Chapter 7 : Modelling potential impacts of modernized irrigation systems on soil water and salt balances, and crop-water productivity under current and future climate scenarios at the canal command scale

7.1 Introduction

Current irrigation practices in the Indus basin irrigation system are putting tremendous pressure on limited water resources, and as a response to this water managers are encouraging modernization of the traditional flood-irrigation to high-efficiency irrigation systems like drip and sprinkler irrigation system (DGA, 2011). These modern irrigation systems aim to improve water application efficiency, crop water productivity, and potentially save water (Narayanamoorthy, 2009).

Research over recent decades has highlighted the benefits of modernization of irrigation in terms of water saving, reduced labour cost, increased crop yield, and reducing overall water use (Jones, 2004; Smith, 2010; Almarshadi and Ismail, 2011; Işık *et al.,* 2017). However, in a water-scarce region such as the Indus basin where surface water is limited, and aquifers are over drawn, the reduction in irrigation water applications must be carefully evaluated in terms of its long-term potential impacts on soil water balances, soil salinity, and crop water productivity under current and projected climatic-change conditions. For instance the Food and Agriculture Organization (FAO) has done a comprehensive review on the implications of use of modernized irrigation technologies on the sustainability of irrigated agriculture (Perry *et al.,* 2017). The report concludes that potential improvement in irrigation efficiency could lead to increased water consumption (evapotranspiration) and the balance between sustainable water supply and water consumption requires physical control of the water resources by government agencies for the sustainability of the system. These findings were only limited to the saving of water and increased in crop yield by adopting modernize irrigation systems. However, potential improvement in irrigation efficiency by adopting modernized irrigation systems poses a risk of salt build-up in soil profile (Raine *et al.,* 2007; Kooij *et*

al., 2013) (chapter 5). Moreover, projected changes in climatic conditions may impose significant impacts on the irrigation hydrology and the pace of salt build-up in the soil profile in semi-arid regions (Stocker *et al.*, 2014; Haj-Amor and Bouri, 2019). In arid and semi-arid regions, the soil salinity and irrigation management go side by side because soil salinity is controlled by the irrigation hydrology which affects a balance of salt inputs through irrigation applications and leaching through soil drainage (Connor *et al.*, 2012; Corwin, 2021). There are many studies that quantify the impact of climate change linked with agronomic, hydrologic, and economic aspect of irrigated agriculture (Yeo, 1998; Hurd *et al.*, 2004; Quiggin *et al.*, 2010). However, there are limited studies that have focused on assessment of the impact of projected climate change on the soil water and salt balances, soil salt build-up, and crop water productivity, using modernized irrigation systems such as sprinkler in arid and semi-arid regions, such as the Indus basin. As for the quantification of the impact of modernized irrigation systems on soil water and salt balance, it is practically difficult to conduct long-term experiments of irrigation practices, especially for the range of spatial heterogeneity in soil-water-plant-atmosphere combinations. This is even more challenging to do under projected climate-change conditions. However, a well calibrated and validated agrohydrological model like SWAP, offers a robust tool to do this job, and to quantify the practically difficult to measure soil water and salt balance components. Agrohydrological models are also vital tool for evaluating impact of climate change on soil water and salt balance, crop yield and water productivity as they efficiently consider various environmental factors that are difficult to control in actual field conditions (Webber *et al.*, 2017; Shelia *et al.*, 2019).

The objective of this chapter is to integrate global climate change model (GCM) projections with the distributed SWAP model to quantify potential impacts of modernized irrigation systems on soil water and salt balances, and crop water

productivity under current and future climate scenarios at canal command scale. This modelling framework is applied on two modernized irrigation scenarios, namely precision surface irrigation and sprinkler irrigation, in the Hakra Branch Canal (HBC) in Punjab Pakistan. The study aims to provide insights to potential impacts of modernized irrigation systems on soil water and salt balances and crop water productivity of cotton and wheat crops cultivation under current and projected climate change conditions in the HBC, and which would be applicable to other similar semi-arid regions worldwide.

7.2 Study area

Chapter 3 described in detail the HBC command used as the case study. Water management in the HBC command is a complex system due to erratic and low rainfall, fluctuating canal water supply, marginal to poor groundwater quality, rising and declining groundwater levels, high evaporative demands and sandy soils with low water holding capacity.

7.3 Distributed SWAP model

The agro-hydrological model SWAP, with a detailed crop growth module was implemented in a distributed mode for simulation of biophysical and hydrological variables at canal command scale. The implementation of distributed SWAP model at canal command scale requires derivation of temporal and spatial data for all combination of weather-water-soil-crop in the study area. Therefore, the HBC command was distributed into homogeneous simulation units by pre-processing in geographic information system (GIS). The detail of this distributed SWAP modelling approach and the data used are described in Chapter 6.

In this chapter, the distributed SWAP modelling focused only on the cotton-wheat combination, being the dominant crop rotation in HBC command. A coupling program

was written in *VB.NET* that pre-processed the input data and ran SWAP for each homogeneous simulation unit for long-term duration of 30 years under current (1987-2017) and projected (2070-2099) climate conditions for different irrigation scenarios.

The simulated soil-water and salt balances, and water- and salt-limited crop yields were post-processed to quantify changes in soil percolation (indicative of groundwater recharge), changes in soil salinity, and crop water productivity. Chapter 5 provides the definitions of these irrigation performance measures.

7.4 Climate Change Scenarios

7.4.1 Current 'baseline' climatic conditions

The current 'baseline' climatic conditions were represented by the long-term (39 years, from 1979 to 2017) historical daily climate data of the maximum and minimum temperature, precipitation, relative humidity, and wind speed. These were sourced from the Pakistan Metrological Department (PMD) weather station in the district of Bahawalnagar in the study area. The data on solar radiation from the PMD have significant inconsistencies which could give unrealistic model outputs. Therefore, the solar radiation data was downloaded from NASA website using R package *nasapower* (Sparks, 2018). Figure 7.1 shows the long-term monthly statistics of the climate variables of the maximum and minimum temperature, rainfall, solar radiation, relative humidity, and wind speed in HBC over a period of 39 years (1979-2017).

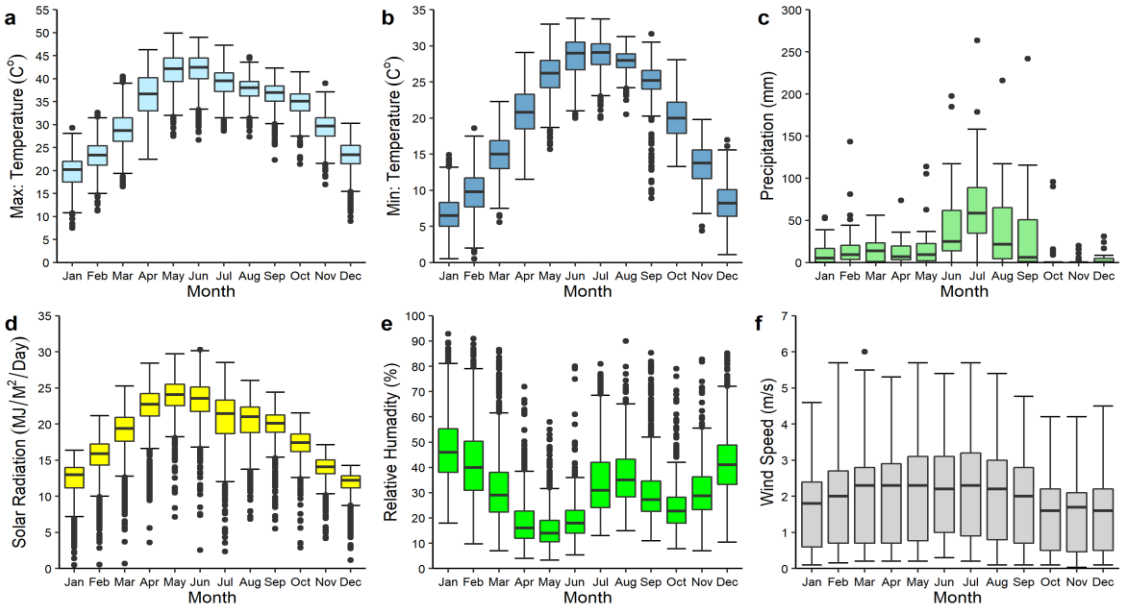

Figure 7.1: Monthly statistics of climate variables measured in the Hakra branch canal command over a period of 39 years (1979-2017). The centre lines represent median of the data, lower line the first quartile and upper line the third quartile. The dots represent the extreme values.

7.4.2 Projected climate change conditions

The trends of projected climate have been derived from the General Circulation Models (GCMs) that simulate the future global climate scenarios based on different greenhouse gases (GHGs) emission scenarios (Bjørnæs, 2013). The Intergovernmental Panel on Climate Change (IPCC) has published Assessment Reports (AR) of various GHG emissions scenarios over the time (Vasileiadou *et al.*, 2011). According to the fifth assessment report of the IPCC, the new GHG emission scenarios called Representative Concentration Pathways (RCPs) were developed by researchers from different disciplines involved in climate-change research (van Vuure Edmonds, et al. 2011, Wayne, 2013). These are RCP 2.6 (Van Vuuren *et al.*, 2011c), RCP 4.5 (Thomson *et al.*, 2011), RCP 6 (Van Vuuren *et al.*, 2011c) and RCP 8.5 (Riahi *et al.*, 2011). These RCPs were named according to the change in the radiative power of 2.6, 4.5, 6.0 and 8.5 watts per square meter (W/m^2), respectively. These RCPs scenarios represents different global

projected climatic conditions, considering the ways in which global population, economy and climate policies may evolve over the future decades (Van Vuuren *et al.*, 2011b).

In this study, we used the RCP 2.6 (a low-emission scenario) and RCP 8.5 (a high-emission scenario) described as follows:

RCP 2.6

The RCP 2.6 was developed by the Integrated Model to Assess the Global Environment (IMAGE) of Netherlands Environmental Assessment Agency for IPCC fifth assessment report (Van Vuuren *et al.*, 2011a). This concentration pathway aims to limit the global mean temperature by 2^{o} C and termed as low-end scenario in terms of low GHGs emissions and radiative forcing. This pathway indicates that by assuming full participation from all countries, the cumulative emission of all the GHGs needs to be reduced by 70% compared to the baseline, or business as usual scenario, by the end 2100 (Van Vuuren *et al.*, 2011c). This requires a substantial change in energy usage and emission of GHGs by adopting bioenergy, renewable energy resources, reforestation, developing of carbon capture devices, and reduction in usage of coal and fossil fuels for energy (Van Vuuren *et al.*, 2007; Van Vuuren *et al.*, 2011c).

RCP 8.5

The RCP 8.5 was developed by the International Institute for Applied System Analysis (IIASA) as part the Integrated Assessment Framework using MESSAGE model (Model for Energy Supply Strategy and their general Environmental Impact) (Riahi *et al.*, 2007; Riahi *et al.*, 2011). This pathway is representative of a high-emission scenario and is consistent with projected climate change with no change in climate policies to reduce GHGs emission (Bjørnæs, 2013). This pathway is also known as *business-as-usual* scenario that includes no mitigation target, or no explicit climate policies. The important

assumptions of RCP 8.5 are continuous increase in population leading towards 12 billion by 2100, low economic growth with slow rates of technological progress, high energy demands, high use of coal intensive technologies due to modest improvement in energy intensity (Riahi *et al.*, 2011).

General Circulation Model (GCM) and downscaling of its projection data

The GCM used in this study is the second generation Canadian Earth System Model (CanESM2) (Chylek *et al.*, 2011) developed by Canadian Centre for Climate Modelling and Analysis (CCCma). The CanESM2 is the fourth generation of the coupled global climate model (CGCM4) prepared for Coupled Model Intercomparison Project Phase 5 (CMIP5) (Taylor *et al.*, 2012) and was presented in the IPCC fifth Assessment Report (Arora *et al.*, 2011). The CanESM2 provides daily climatic data predictions that are directly fed to the statistical downscaling model. In addition to the raw atmospheric variables from the CanESM2 output, large scale atmospheric variables from the National Centre for Environmental Prediction (NCEP), and the National Centre for Atmospheric Research (NCAR) reanalysis project 1 (Kalnay *et al.*, 1996), were also used to establish statistical relationship with the observed climate data of the study area. A total of 26 predictor variables of CanESM2 and NCEP/NCAR were downloaded from the Canadian Climate Data and Scenario website *https://climate-scenarios.canada.ca/* and are used in this study. The NCEP/NCAR provides the past-climate conditions over the period from 1961 to 2005 (Kalnay *et al.*, 1996) and the CanESM2 provides projected climate change based on the period from 2006 to 2100 (Arora *et al.*, 2011).

Like other GCMs the CanESM2 also provides climate information on a scale usually larger than hundreds of kilometres (Mearns, 2009). The CanESM2 also simulates weather typically in the order of 2 to 3 degrees, resulting into a very coarse output

(Ghazavi and Moosavian, 2017). Researchers have developed different approaches and tools to link 'downscaled' to the spatial disparity between GCM outputs such as the CanESM2 and the local scale climate variables for local climate change impact analysis (Abdo *et al.*, 2009). There are two approaches of downscaling GCMs data, namely dynamical and statistical downscaling (Zhang *et al.*, 2020). The dynamical downscaling is based on a regional climate model (RCM) and has a finer horizontal resolution such as through surface terrain (Pielke Sr and Wilby, 2012). The high computation demand of dynamic downscaling limits its use, whereas the statistical downscaling uses transfer functions of the regression relationships between large scale GCM outputs (predictors) and local scale observed climate variables (predictands) (Pielke Sr and Wilby, 2012). (Wilby *et al.*, 2002) developed a Statistical Downscaling Model (SDSM) which is based on multi-linear regression and stochastic weather generator.

In this study, the SDSM is used to downscale the CanESM2 RCP 2.6 and RCP 8.5 scenarios to generate daily climatic variables as inputs into the distributed SWAP modelling for the study area. The SDSM have been extensively employed in many climate-change impact studies (Gagnon *et al.*, 2005; Hashmi *et al.*, 2011; Zhou *et al.*, 2017; Kristvik *et al.*, 2018). The SDSM technique is quicker and has a low computation cost. The SDSM version 4.2.9 can be downloaded free of cost from the *https://sdsm.org.uk/software.html* website. The model is composed of four main steps such as identification of predictors, model calibration, weather generator, and scenario generation of future climate variables. The detail description of the procedure used for each step are available at (Wilby *et al.*, 2002; Wilby and Dawson, 2007).

7.5 Calibration and Validation of Statistical Downscaling Model (SDSM)

The calibration process of SDSM is based on multiple regression analysis of daily observed data (predictand) of the case study and the large scale GCM atmospheric variables (predictors) (Wilby *et al.*, 2002). According to the methodology of Wilby and Dawson (2007), the observed data period must lie between the data period of the NCP/NCER, that is 1961–2005. In this study, the observed climatic data from 1979-2005 was used and was split in to two groups, the period from 1979 to 1995 which was used for calibration of the SDSM, and from 1996 to 2005 for validation of the model. During the calibration process manual adjustment of the variance inflation and bias correction was performed to control the magnitude of variance and to compensate the tendency of over- and under-estimation in the downscaled daily weather variables. The adjustment was performed several times until the best agreement between the observed and simulated outputs was achieved.

7.6 Statistical Evaluation of the SDSM

To test the statistical significance between the observed and SDSM simulated climate-variables, the well-defined quantitative statistical indicators, of the Root Mean Square Error (*RMSE*), Index of Agreement (*IoA*), Coefficient of determination (R^2), and Mean Bias Error (*MBE*) are used (Moriasi *et al.*, 2007). The *RMSE* quantifies the average percentage error in the units of the observed and simulated variables (Willmott, 1982). The *IoA* indicates the agreement between the observed and simulated variables (Willmott, 1982), whereas the R^2 compares the explained variance of the simulated data with the total variance of observed data (Moriasi *et al.*, 2007). The *MBE* measures the overall bias estimate whether the model is overestimating or under estimating (Moriasi

et al., 2007). The positive value of *MBE* represents overestimation by model, and vice versa. These statistical indicators can be mathematically expressed as:

$$RMSE = \frac{1}{N}\sum_{i=1}^{N}(S_i - O_i) \quad \text{Eq. 7.1}$$

$$IoA = 1 - \frac{\sum_{i=1}^{N}(S_i - O_i)}{\sum_{i=1}^{N}(|O_i - \bar{O}| + |S_i - \bar{O}|)} \quad \text{Eq. 7.2}$$

$$R^2 = \frac{\sum_{i=}^{N}(O_i - \bar{O})^2}{\sum_{i=}^{N}(S_i - \bar{O})^2} \quad \text{Eq. 7.3}$$

$$MBE = \frac{1}{N}\left[\sum_{i=1}^{N}(S_i - O_i)\right] \quad \text{Eq. 7.4}$$

where, S_i is the i_{th} SDSM simulated value, O_i is the i_{th} observed value, $\bar{O}$ is the mean of the observed values, and N is the number of paired observed and simulated values. The estimated values closer to 1 by *RMSE*, *IoA* and R^2 indicates better model performance, and for *MBE* a value close to zero represents good model performance.

7.7 Irrigation scenarios

Three irrigation scenarios of precision surface irrigation system (*PSIS*), and high-efficiency irrigation system (*HEIS*), with and without leaching fraction (*LF*), (defined in Chapter 5) are implemented here, and their potential impacts on soil water and salt balances, and crop water productivity are quantified for wheat-cotton cultivation across the HBC command under current 'baseline' and projected future climatic conditions. This was achieved by simulations using the calibrated and validated distributed-SWAP model for the HBC command (Chapter 6). The distributed SWAP was set-up for different combinations of scenarios of three irrigation systems (*PSIS*, *HEIS_LF*, *HEIS_noLF*) and current and projected climatic change conditions. The current 'baseline' climatic period was simulated using the observed weather variables over 30 years (1987–2017), and the

projected future climate period was simulated using the SDSM downscaled weather variables for 30 years (2070 – 2099) for the RCP 2.6 and RCP 8.5 emission scenarios.

The *PSIS* irrigation scenario simulates a modernized surface irrigation that schedules irrigation according to water stress criteria. In the distributed SWAP model this is defined as fixed-depth irrigation criterion, in which the timing of irrigation is based on the crop daily water stress criterion, defined by relative transpiration being the ratio of actual to potential transpiration. A fixed depth of 80 mm is applied at each irrigation interval, when the crop water stress (i.e., the relative transpiration, T_a/T_p) reached a predefined level of 0.95. In this scenario, the irrigated fields are assumed properly levelled, and the water is distributed uniformly over the entire field area.

The *HEIS* irrigation scenario characterizes a highly efficient sprinkler irrigation system that applies a flexible depth of irrigation to bring the soil moisture back to field capacity. The built-in option of sprinkler irrigation in SWAP model was implemented to schedule irrigation when the crop water stress (T_a/T_p) reached 0.95. To explore the effects of salinity in the soil profile, *HEIS* scenario was first implemented without leaching friction (*HEIS_noLF*) and then with a leaching friction (*HEIS_LF*) of additional pre-sown irrigation depth of 60 mm followed by additional 10 mm depth with each subsequent irrigation.

The irrigation scenarios *PSIS* and *HEIS* assumed a conjunctive use of canal and groundwaters. Based on the groundwater quality information (Figure 6.3a) the HBC command was divided into three groundwater quality zone Good (EC<3dS m^{-1}), Marginal (EC=3 to 6 dS m^{-1}) and Poor (EC > 6 dS m^{-1}). The mean conjunctive canal water and groundwater quality of EC 2.25 dS m^{-1} (1.44 mg cm^{-3}) is assigned to simulation units in good water quality zone, 3.9 dS m^{-1} (2.5 mg cm^{-3}) in marginal zone and 5.5 dS

m-1 (3.5 mg cm^{-3}) in poor water quality zone. The EC of canal water is assumed 0.3 dS m^{-1} (0.45 mg cm^{-3}). The long-term impact of *PSIS* and *HEIS* irrigation scenarios under the baseline period, and projected future climate, are simulated and analysed in terms of soil water and salt balances and crop water productivity performance indicators. Chapter 5 provides detailed descriptions of these performance indicators to quantify percolation, changes in soil salinity, and crop water productivity values.

7.8 Results and discussion

7.8.1 Comparison of current and projected climate conditions

Table 7.1 summarizes the performance evaluation of SDSM for downscaling the climate variables of the maximum temperature, minimum temperature, solar radiation, relative humidity, wind speed and precipitation for the HBC. The quantified *RMSE*, *IoA*, R^2 and *MBE* suggest good agreement between the daily mean observed and simulated climatic variables during the calibration and validation periods. However, the performance of daily precipitation is not satisfactory when compared to all other variables. This low performance for precipitation is due to the variation in daily wet spells which is underestimated by the SDSM simulation. This discrepancy in the calibration and validation of daily precipitation has been pointed out by several studies (Hu *et al.*, 2013; Ghazavi and Moosavian, 2017; Nury *et al.*, 2019). The results of SDSM can be considered satisfactory given the fact that downscaling of daily precipitation is difficult, compared to other climate variables. However, the monthly precipitation shows a good agreement between the observed and simulated precipitation (Table 7.1).

Table 7.1: Calibration (1979-1995) and validation (1996-2005) of the Statistical Downscaling Model (SDSM) for daily climatic variables in Hakra Branch Canal command, Punjab Pakistan. (refer to appendix D.1 for monthly comparison of the observed and simulated climate variables)

Climate variables	*IoA*		*RMSE*		R^2		*MBE*	
	Calibration	Validation	Calibration	Validation	Calibration	Validation	Calibration	Validation
T_{max} (C°)	0.97	0.96	2.43	3.07	0.91	0.89	-0.03	-0.92
T_{min} (C°)	0.98	0.99	2.08	1.95	0.95	0.92	0.00	-0.59
Slr Rad ($kJ/M^2/Day$)	0.89	0.90	2.81	2.72	0.67	0.69	-0.03	-0.02
RH (kPa)	0.86	0.82	1.88	2.01	0.83	0.82	0.05	0.07
WS (m/s)	0.73	0.70	0.65	0.69	0.40	0.38	0.00	-0.06
PCP (mm)	0.15	0.18	4.94	4.19	0.16	0.12	0.01	-0.03
**PCP (mm)*	0.89	0.85	2.33	10.34	0.99	0.70	1.13	1.35

**PCP* is the mean monthly statistical comparison between the observed and downscaled precipitation

Figure 7.2 compares the analysis of projected climate variables under RCP 2.6 scenario and RCP 8.5 scenario (2070–2099) with the current 'baseline' period (1987–2017) on mean monthly basis. The projection of future maximum and minimum temperatures clearly show an increasing trend with relatively high increase for the RCP 8.5 scenario. The mean annual maximum temperature is projected to increase by 1.6 ^{o}C and 4 ^{o}C under the RCP 2.6 and RCP 8.5 scenarios, respectively, as compared to the 32 ^{o}C of the baseline scenario (Figure 7.2a). The highest increase in maximum temperature is projected to be in the summer months (Apr – July), by 3^{o}C and 6^{o}C under the RCP 2.6 and RCP 8.5 scenarios, respectively, compared to 38 ^{o}C in the baseline scenario. However, under the RCP 2.6 scenario, a decrease (3 ^{o}C) in maximum temperature is projected during the winter months (October– December) (Figure 7.2a).

Similarly, the minimum temperature also showed an increasing trend in the projected climate change scenarios. The mean annual increase is projected to be 2 ^{o}C and 4.5 ^{o}C under RCP 2.6 and RCP 8.5 scenarios, respectively, compared to the baseline temperature of 18 ^{o}C (Figure 7.2b). However, there is a significant change in the summer

months (April – July), where the increase is 2.8 ^{o}C and 5.6 ^{o}C under RCP 2.6 and RCP 8.5 scenarios, respectively, as compared to the 26 ^{o}C of the baseline period. A decrease of 3 ^{o}C in minimum temperature is predicted in the winter months (October- December) under RCP 2.6 scenario, compared to the 14 ^{o}C of baseline scenario. Overall, there will be significant change in both maximum and minimum temperatures in the summer months, and the change is not surprisingly more pronounced under the RCP 8.5 scenario (Figure 7.2b).

Unlike temperature, the precipitation projection shows a decreasing trend in annual precipitation in both projected climatic change scenarios. The model projected the possibility of a 73 mm and 106 mm decrease in the mean annual precipitation under the RCP 2.6 and RCP 8.5 scenarios, respectively, compared to 283 mm of mean annual precipitation in the baseline scenario. Though the mean monthly precipitation under projected climatic change indicates slightly increase by 4 to 10 mm during the winter months (November – February), it is projected to significantly decrease by 81 mm and 97 mm during the summer months (May to September) (Figure 7.2c) under RCP 2.6 and RCP 8.5 scenarios, respectively. There is an exception of a slight increase in mean monthly precipitation in the month of June under the RCP 2.6 and RCP 8.5 scenarios (Figure 7.2c). Overall, the same peak for precipitation from June to August is observed for all the scenarios (Figure 7.2c).

The analysis of solar radiation shows an increasing trend under both the RCP 2.6 and RCP 8.5 climatic scenarios compared to the baseline scenario (Figure 7.2d). An annual increase of 7% and 10% is projected under the RCP 2.6 and RCP 8.5 scenarios, respectively. This increase in solar radiation is projected to be relatively higher from December to April, the months of *rabi* (wheat) cultivation season in the study area. The annual mean relative humidity is also projected to increase by 10% and 19% under the

RCP 2.6 and RCP 8.5 scenarios, respectively, compared to the baseline scenario. This increase in relatively humidity is projected relatively higher in the months of June to September (Figure 7.2e), while a slight decrease in relatively humidity is projected in the months of February to April (Figure 7.2e).

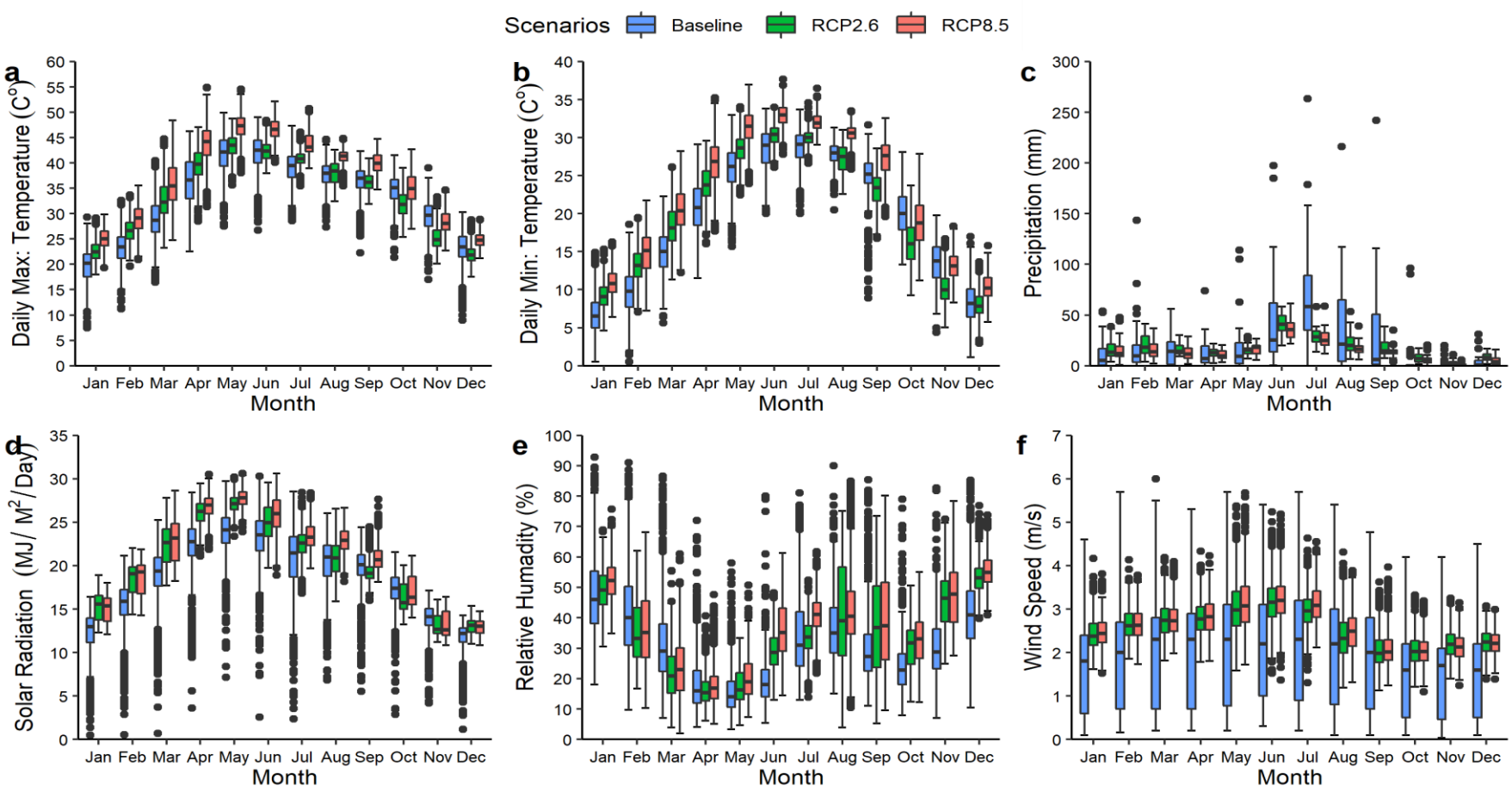

Figure 7.2: A comparison of current 'baseline' observed (1987 – 2017) and projected (2070 – 2099) climate variables at the Hakra Branch Canal command in Punjab Pakistan. The centre lines represent median of the data, lower line the first quartile, upper line the third quartile. The dots represent the extreme values.

Similarly, the mean wind speed is projected to increase by 31% and 37% under the RCP 2.6 and RCP 8.5 scenarios, respectively (Figure 7.2f). It is clear from the analysis that projected climate conditions are leading towards more severe aridity, particularly under the high emission scenario of RCP 8.5. There is predicted to relatively increased temperature and solar radiation and reduced annual precipitation in the study area. This corresponds with results of Alvar-Beltrán *et al.* (2021), Habib (2021) and Shrestha *et al.* (2019) indicating an increasing trend in projected temperatures and a decreasing trend in precipitation by the end of the century.

7.8.2 Performance of modernized irrigation scenarios under current 'baseline' climatic conditions

Table 7.2 summarizes potential effects of modernized irrigation scenarios on simulated soil water and salts balances, crop yields and crop water productivity values for cotton-wheat crop rotation under the current 'baseline' climatic conditions (1987–2017). The average gross irrigation under *PSIS* scenario is simulated at 646 mm for cotton during the *kharif* season, and at 293 mm for wheat during the *rabi* season. Similarly, under the *HEIS_LF* scenario, the average gross irrigation is simulated at 716 mm for cotton, and at 268 mm for wheat. Whereas the average gross irrigation under *HEIS_noLF* scenario is simulated t about 18 to 20% less for the wheat and cotton irrigations, respectively, as compared to the *HEIS_LF* scenario. However, the average percolation under *HEIS_noLF* scenario is simulated 46 to 71% less for the wheat and cotton seasons, respectively, compared to the *HEIS_LF* scenario (Table 7.2). The average annual change in salt storage is simulated from 7 to 9 mg cm^{-2} (0.7 to 0.9 ton ha^{-1}) under *PSIS* and *HEIS_LF*, whereas it is simulated at 17 mg cm^{-2} (1.7 ton ha^{-1}) under *HEIS_noLF* (Table 7.2). The impact of a higher salt build-up under *HEIS_noLF* affected crop yields and crop water productivity for both the cotton and wheat crops. The average water- and salt-limited crop yields are

simulated about 38% less for cotton and about 48% less for wheat under the *HEIS_noLF* as compared to *HEIS_LF* and *PSIS*. Similarly, the average WP_{ET} and WP_{Irr} values are simulated 22 to 33% less for cotton and 35 to 44% less for wheat under the *HEIS_noLF* compared to *HEIS_LF*. Clearly, the crops experienced higher water and salt stress under *HEIS_noLF* irrigations. This is reflected in the average actual evapotranspiration (ET_a) under the *HEIS_noLF* scenario is simulated to be only 7% and 8% less for wheat and cotton, respectively compared to the *HEIS_LF* scenario.

Table 7.2: Distributed SWAP simulated long-term soil water and salt balance components, water- and salt-limited crop yields and crop water productivity values for cotton-wheat cultivation under current 'baseline' climactic conditions (1987-2017) in Hakra Branch Canal command area in Punjab Pakistan. The values are presented as the average ± standard deviation.

Soil water and salt balance/ Crop water productivity	*PSIS*		*HEIS_LF*		*HEIS_noLF*	
	Kharif (Cotton)	*Rabi (Wheat)*	*Kharif (Cotton)*	*Rabi (Wheat)*	*Kharif (Cotton)*	*Rabi (Wheat)*
Rain(mm)	217±0.03	65±0.13	217±0.00	65±0.03	217±0.00	65±0.00
Irrigation (mm)	646± 3.03	293±1.29	716±3.63	268±1.52	571±4.09	219±1.27
E_p (mm)	315±0.16	276±0.31	316±0.63	276±0.41	319±0.78	293±1.34
T_p (mm)	706±0.16	217±0.43	696±0.22	213±0.21	676±0.82	193±1.24
T_a (mm)	679±0.39	206±0.44	674±0.14	203±0.16	602±2.90	164±1.92
T_a/T_p (mm)	0.96±0.00	0.95±0.01	0.97±0.01	0.95±0.01	0.88±0.07	0.84±0.05
ET_a (mm)	751±3.76	275±4.76	746±6.06	273±1.68	684±23.62	255±7.36
Q_{bot} (mm)	-101±2.42	-74±1.98	-164±2.84	-46±1.95	-47±1.33	-25±1.40
ΔW (mm)	11±0.91	9±0.91	23±0.85	14±0.78	56±0.84	3±0.85
IC_i (mg/cm^2)	116±26.24	53±11.82	126±26.79	47±11.28	97±22.17	37±8.50
C_{bot} (mg/cm^2)	-96±20.82	-65±18.98	-128±23.40	-38±15.10	-79±14.73	-38±17.55
ΔC (mg/cm^2)	20±8.97	-13±7.60	-1±6.70	10±4.76	18±8.84	-1±10.18
Crop yield kg/ha	3573±36	7681±73	3663±62	7655±141	2286±361	4029±572
WP_{ET} (kg/m^3)	0.48±0.00	2.79±0.06	0.49±0.00	2.80±0.04	0.33±0.04	1.58±0.18
WP_{Irr} (kg/m^3)	0.55±0.03	2.62±0.13	0.51±0.02	2.85±0.19	0.40±0.04	1.84±0.21

Height of soil column considered is 160 cm

The average relative transpiration under the *HEIS_noLF* scenario is simulated at 0.84 and 0.88 for wheat and cotton, respectively, while it is simulated >0.95 for both cotton and wheat under *HEIS_LF* and *PSIS* scenarios. Interestingly, the *PSIS* and *HEIS_LF* resulted into similar crop yields, crop water productivity values, and soil water and salt balances, except for relatively less percolation under the *PSIS* scenario (Table 7.2).

7.8.3 Performance of modernized irrigation scenarios under projected future climate conditions

Tables 7.3 and 7.4 summarizes the simulated soil water and salts balances, crop yields and crop water productivity values for cotton-wheat crop rotation under the projected climatic conditions (2070 – 2099) under RCP 2.6 and RCP 8.5, respectively. According to RCP 2.6, the average annual irrigation for both *kharif* (cotton) and *rabi* (wheat) seasons is simulated to be 1352 mm under *PSIS*, 1349 mm under *HEIS_LF*, and 902 mm under *HEIS_noLF* (Table 7.3). The average annual actual evapotranspiration is 1290 mm with *PSIS*, and 1280 mm with *HEIS_LF*. Whereas the average annual actual evapotranspiration with *HEIS_noLF* is 23% and 24% less as compared to *HEIS_LF* and *PSIS*, respectively. (Table 7.3). The average annual percolation is -215 mm under *PSIS*, and -196 mm under *HEIS_LF*. Whereas the percolation is 71% and 74% less under *HEIS_noLF*, as compared to *PSIS* and *HEIS_LF* respectively. As a result, the average annual salt build is 59% and 69% higher for *HEIS_noLF*, as compared to *PSIS* and *HEIS_LF* respectively (Table 7.3).

Table 7.3: Distributed SWAP simulated long-term soil water and salt balance components, water- and salt-limited crop yields and crop water productivity values for cotton-wheat cultivation under projected 'RCP2.6' climactic conditions (2070-2099) in Hakra Branch Canal command area in Punjab Pakistan. The values are presented as the average ± standard deviation.

Soil water and salt balances/crop water productivity	*PSIS*		*HEIS_LF*		*HEIS_noLF*	
	Kharif (Cotton)	*Rabi (Wheat)*	*Kharif (Cotton)*	*Rabi (Wheat)*	*Kharif (Cotton)*	*Rabi (Wheat)*
Rain(mm)	134±0.00	77±0.04	134±0.01	77±0.04	134±0.00	77±0.00
Irrigation (mm)	997±3.75	355±1.50	1025±4.21	323±1.63	682±10.53	220±4.13
E_p ***(mm)***	340±0.11	327±0.23	341±0.10	327±0.22	385±4.07	415±4.81
T_p ***(mm)***	962±0.14	286±0.18	945±0.41	281±0.22	896±3.34	202±4.43
T_a ***(mm)***	898±0.87	267±0.33	890±1.78	259±0.43	602±10.66	126±5.41
T_a/T_p ***(mm)***	0.93±0.01	0.93±0.01	0.94±0.01	0.92±0.01	0.67±0.10	0.60±0.13
ET_a ***(mm)***	964±8.26	326±1.88	956±17.03	325±2.27	720±76.79	261±34.82
Q_{bot} ***(mm)***	-118±3.57	-97±2.03	-133±2.77	-63±2.04	-18±1.32	-38±1.17
ΔW ***(mm)***	49±1.04	8±0.98	70±1.22	13±0.97	77±1.91	-1±0.51
IC_i ***(mg/cm²)***	179±39.46	64±14.17	180±36.88	57±12.89	116±31.95	38±10.36
C_{bot} ***(mg/cm²)***	-130±35.89	-105±19.67	-158±27.42	-67±26.95	-49±22.40	-78±23.56
ΔC ***(mg/cm²)***	50±8.16	-41±7.36	22±16.26	-11±14.91	67±10.58	-40±13.79
Yield kg/ha	4319±42	6250±71	4341±165	6118±83	2003±675	1997±1538
WP_{ET} ***(kg/m³)***	0.45±0.00	1.92±0.02	0.45±0.01	1.89±0.02	0.28±0.06	0.77±0.49
WP_{Irr} ***(kg/m³)***	0.43±0.02	1.76±0.09	0.42±0.02	1.89±0.10	0.29±0.05	0.91±0.53

Height of soil column considered is 160 cm

Similarly, according to RCP 8.5, the average annual simulated irrigation is 33% and 34% higher under *HEIS_LF* and *PSIS* respectively as compared with *HEIS_noLF* (Table. 7.4). This results in to 22% higher actual evapotranspiration under *PSIS* and similarly with HEIS_LF than *HEIS_noLF*. The average annual percolation is 74% higher under *PSIS*, and 68% higher under *HEIS_LF* than *HEIS_noLF* (Table. 7.4). The low percolation under *HEIS_noLF* added 3 times more salts to the soil profile, as compared to *PSIS* and 2 times more salts as compared to *HEIS_LF* (Table 7.4).

Table 7.4: Distributed SWAP simulated long-term soil water and salt balance components, water- and salt-limited crop yields and crop water productivity values for cotton-wheat cultivation under projected 'RCP 8.5' climactic conditions (2070-2099) in Hakra Branch Canal command area in Punjab Pakistan. The values are presented as the average ± standard deviation.

Soil water and salt balance/ Crop water productivity	*PSIS*		*HEIS_LF*		*HEIS_noLF*	
	Kharif (Cotton)	*Rabi (Wheat)*	*Kharif (Cotton)*	*Rabi (Wheat)*	*Kharif (Cotton)*	*Rabi (Wheat)*
Rain(mm)	117±0.00	58±0.00	117±0.00	58±0.00	117±0.00	58±0.00
Irrigation (mm)	910±3.18	330±2.24	911±3.86	301±1.88	618±10.83	199±4.13
E_p ***(mm)***	637±0.21	400±0.24	640±0.36	400±0.30	804±7.06	493±3.81
T_p ***(mm)***	819±0.20	239±0.21	807±0.45	235±0.26	651±6.61	148±3.82
T_a ***(mm)***	769±0.79	224±0.36	759±1.68	217±0.45	442±10.86	88±4.60
T_a/T_p ***(mm)***	0.94±0.01	0.94±0.01	0.94±0.02	0.92±0.01	0.67±0.09	0.56±0.14
ET_a ***(mm)***	885±7.18	295±1.62	877±1.33	297±0.21	686±83.09	232±36.63
Q_{bot} ***(mm)***	-109±2.86	-99±2.84	-107±2.33	-63±2.17	-17±1.16	-36±1.32
ΔW ***(mm)***	33±1.03	-6±0.95	45±1.06	-1±1.01	33±1.80	-11±0.70
IC_i ***(mg/cm²)***	164±35.50	60±14.78	161±32.92	53±12.83	109±30.63	35±10.56
C_{bot} ***(mg/cm²)***	-113±27.81	-102±25.20	-132±22.32	-69±27.72	-45±18.93	-72±25.98
ΔC ***(mg/cm²)***	51±12.0	-42±11.48	29±16.79	-16±15.40	64±12.40	-37±15.79
Yield kg/ha	4840±70	5635±94	4793±210	5461±123	1473±1163	1253±1362
WP_{ET} ***(kg/m³)***	0.55±0.00	1.91±0.03	0.55±0.02	1.84±0.04	0.21±0.13	0.54±0.45
WP_{Irr} ***(kg/m³)***	0.53±0.02	1.71±0.14	0.53±0.02	1.82±0.14	0.24±0.13	0.63±0.49

Height of soil column considered is 160 cm

This high amount of salt build up in the soil profile significantly reduced the crop yields under *HEIS_noLF*. The cotton yield is decreased by 70% and wheat yield is decreased by 78% under *HEIS_noLF* as compared to *PSIS* and similarly with *HEIS_LF* (Table. 7.4). This significant reduction in the crop yields for both cotton and wheat is attributed to the combined impact of climate change and high salt build up under *HEIS_noLF*.

7.8.4 Impact of climate change on soil water and salt balances

Figure 7.3 compares the annual soil water and salt balance components, of irrigation, percolation, and salt storage, of the simulated irrigation scenarios of *PSIS*, HEIS_LF and *HEIS_noLF* under the current 'baseline' (1987-2017) and the projected future climate change (RCP 2.6 and RCP 8.5) period (2070-2099) conditions. The average annual irrigation under *PSIS* is simulated to be 30% and 24% higher under RCP 2.6 and RCP 8.5, respectively, compared to the baseline period. Similarly, the average annual

irrigation under *HEIS_LF* is simulated as 27% and 19% higher under *RCP 2.6* and *RCP 8.5*, respectively.

Interestingly, the irrigation demands for all scenarios are simulated relatively less under *RCP 8.5* compared to *RCP 2.6* (Figure 7.3), despite the simulated higher potential evapotranspiration (E_p plus T_p) under the *RCP 8.5* (Table 7.3 and 7.4). This is attributed to the early maturity of the crops and the shortened crop period simulated due to the projected higher increase in temperature under the *RCP 8.5* (Figure 7.2 a&b). Higher temperature accelerates the crop development leading to shorter crop period (van Dam *et al.*, 1997). The average crop duration is simulated as 38 days less for wheat and 15 days less for cotton under *RCP 8.5*, respectively as compared to *RCP* 2.6 scenario.

The *HEIS_noLF* required about 16% to 34% less annual irrigation amounts compared to the *PSIS* and *HEIS_LF* in all three climate scenarios (Figure. 7.3). However, this saving of irrigation water resulted in relatively low percolation in the *HEIS_noLF*, compared to the *PSIS* and *HEIS_LF*. This is evident from the positive linear relationship between irrigation and percolation (Figure. 7.3), in which the percolation is simulated to be higher under the *PSIS* and *HEIS_LF* as compared to *HEIS_noLF*. The soil percolation is an important soil hydrological phenomenon that serves two main purposes. Firstly, it is the major source of groundwater recharge in a semi-arid region like HBC (Dagès *et al.*, 2008). Secondly, an appropriate level of soil percolation leaches out the accumulated salts to deeper soil profiles and avoids soil salinization of the soil profile (Rawlins, 1973; Caballero *et al.*, 2001). However, higher percolation rate can also pose a threat of rising of water level in shallow groundwater areas and cause waterlogging and secondary soil salinization (Qureshi *et al.*, 2008).

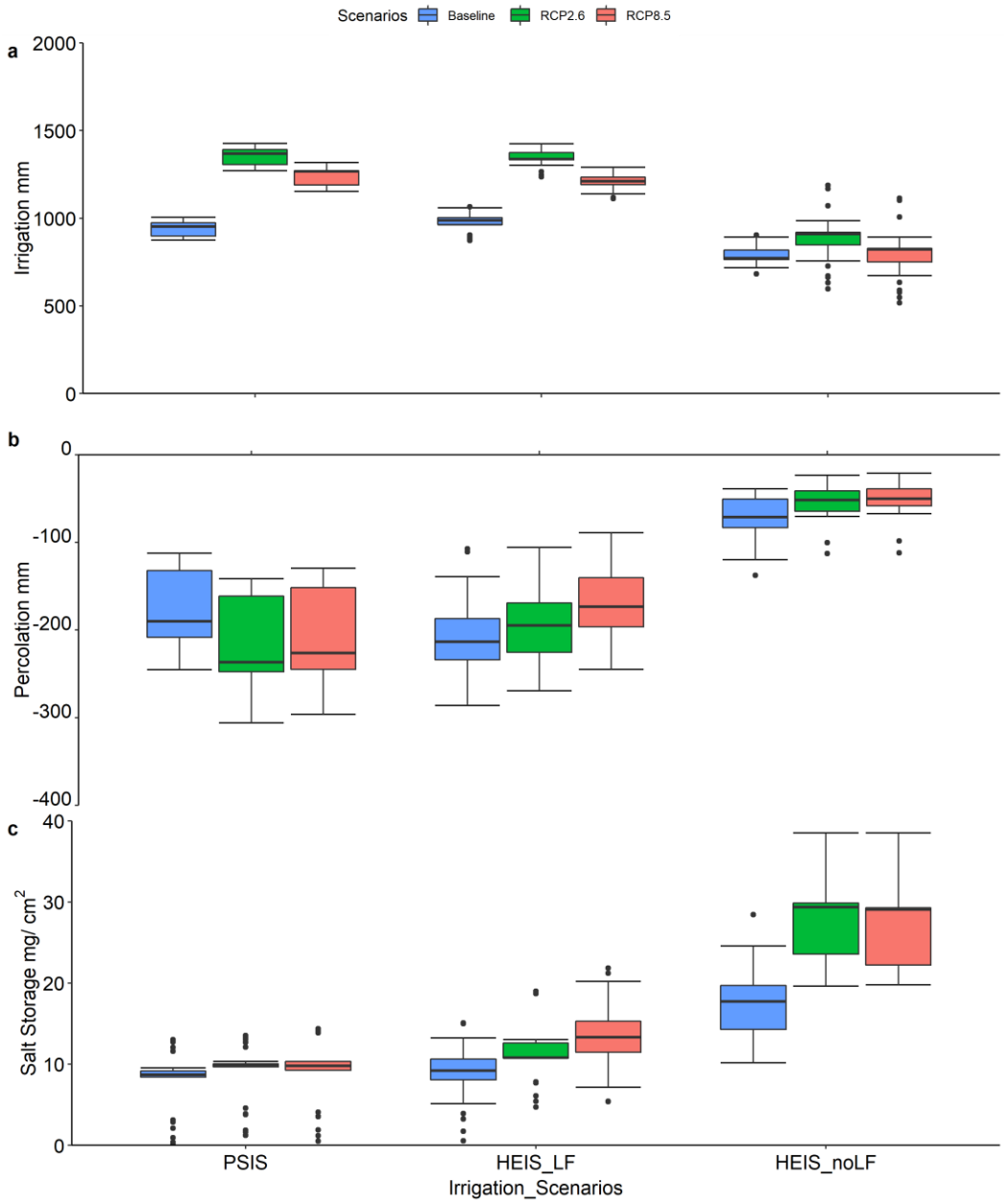

Figure 7.3: SWAP simulated irrigation, soil water percolation, and soil salt storage for cotton-wheat cultivation with modernized irrigation systems under the current 'baseline' (1987 to 2017) and the projected climate change scenarios (RCP 2.6 as low emission, and RCP 8.5 as high emission, 2070- 2099) in Hakra Branch Canal command in Pakistan Punjab. The centre line represents the mean value, the lower line the first quartile and the upper line third quartile. The dots representthe extreme values.

In case of the HBC command, the shallow groundwater areas are limited to the head reaches of the canal network, where seepage from large canals contributes to a rise of good quality groundwater. Due to low rainfall and limited canal water availability, the use of groundwater is an integral part of irrigated agriculture in HBC command (Qureshi,

2014). According to Awan *et al.* (2016) the dependence on groundwater in the HBC varies from 30% to 50% due to variable and limited supply of the canal water and low average annual precipitation. Farmers use the practices of conjunctive water application of canal water and groundwater to fulfil crop water requirements in areas where the canal water supply is limited. In this situation, soil percolation is considered a useful source of groundwater recharge, which is reused as groundwater irrigation. So any reductions in soil percolation is not translated into actual 'real' water savings, but only 'dry' water savings reducing the groundwater recharge (Kendy *et al.*, 2004).

The other positive effect of soil percolation rate is the leaching of the salts from the root zone. This is also evident from Figure 7.3, which shows the higher percolation rate simulated under the *PSIS* and *HEIS_LF* scenario restricted the salt build-up to a mean annual value of 7 to 13 mg cm^{-2} (0.7 to 1.3 ton ha^{-1}) under all the climate scenarios (Tables 7.2 – 7.4). Whereas there is simulated higher increase in the salt build-up with the *HEIS_noLF*, especially under the projected future climate scenarios (Figure 7.3). The mean annual salt build-up under the *HEIS_noLF* is simulated from 17 to 27 mg cm^{-2} (1.7 to 2.7 ton ha^{-1}), which is about 89 to 145% higher than the *HEIS_LF*, and about 143 to 200% higher than the *PSIS* scenario (Figure 7.3, Tables 7.2-7.4). Also, the *HEIS_noLF* resulted into the highest increase in the mean annual salt build-up of 27 mg cm^{-2} under the future projected climate scenarios of RCP2.6 and RCP 8.5, compared to 17 mg cm^{-2} under the current 'baseline' climactic conditions (Figure 7.3). This suggests that soil salinity build-up under high-efficiency irrigation systems with no leaching fraction (as represented by the *HEIS_noLF*) could be further exacerbated by the projected changes in future climatic conditions in the HBC command area. Corwin (2021) provided a comprehensive review of the impact of climate change on soil salinity in agricultural lands. He concluded that the impact of climate change on soil salinization has been

overlooked and needs to be monitored. He further argued that the change in the climate patterns would high likely increase the risk of the accumulation of salts in irrigated agricultural areas of the world. This will require addition water for leaching the accumulated salts in the soil profile.

7.8.5 Impact on crop yield and water productivity

Figure 7.4 presents the simulated impacts of the projected climate change conditions on water- and salt-limited crop yields and crop water productivity (WP_{ET} and WP_{Irr}) for cotton-wheat cultivation under the proposed irrigation scenarios in the HBC. Interestingly, the water- and salt-limited cotton yields for the *PSIS* and *HEIS_LF* scenarios are simulated to be higher under *RCP 2.6* and *RCP 8.5*, compared to the baseline conditions. Under *PSIS*, the water- and salt-limited cotton yield is simulated 21% and 29% higher in *RCP 2.6* and *RCP 8.5*, respectively. Similarity, under *HEIS_LF*, the water- and salt-limited cotton yield is simulated 16% and 24% higher in *RCP 2.6* and *RCP 8.5*, respectively. According to Adhikari *et al.* (2016), the simulated increase in cotton yields under the projected future climate scenarios could be due to the effects of increased temperature and elevated CO_2 concentrations. The cotton yield is very sensitive to temperature (Gérardeaux *et al.*, 2013). Reddy *et al.* (1998) quantified the effects of temperature on cotton leaf development and observed a significant expansion in the main- stem leaves due to increased temperature under a controlled temperature in naturally-lit plant growth chambers. Chen *et al.* (2015) quantified the impact of climate change on cotton yield in three major cotton producing regions of China. They found that average increase of 1^{o}C in temperature increases cotton yield by 0 -14%. Several studies have also reported a simulated increase in cotton yield under future climate conditions (McRae *et al.*, 2007; Gérardeaux *et al.*, 2013; Williams *et al.*, 2015; Williams *et al.*, 2019). Their results indicate that the increase in cotton yield could be attributed to future

increase in temperature, provided optimum nutrient availability and disease and pest control, and no water and salt stress on the crop growth. Thus according to Adhikari *et al.* (2016) well-irrigated cotton is able to benefit from increased future temperatures.

However, under the high-efficiency irrigation system with no leaching fraction (*HEIS_noLF*) scenario, the water- and salt-limited cotton yield is reduced by 12% under *RCP 2.6*, and reduced by 36% under *RCP 8.5*, compared to the baseline conditions (Figure 7.4). This suggests that despite of favourable climate conditions, a potential salt-build up under high efficiency irrigation with no leaching fraction (represented by *HEIS_noLF*) could significantly reduce the cotton yield due to soil salinity stress. Figure 7.5 shows the water-limited cotton and wheat crop yields simulated by accounting for only water stress under all irrigation scenarios. The SWAP model offers options to simulate crop growth and its yield with, or without, soil salinity stress by setting on, or off, the solute transport module for the soil profile (Kroes *et al.*, 2008). Switching off solute transport allows SWAP to bypass the Maas and Hoffman (1977) linear-reduction function for root water uptake due to salinity stress (see Chapter 3). Under no salinity stress, it can be observed (Figure 7.5) that the water-limited only crop yields of cotton and wheat is improved only by 5 to 10% under the *PSIS* and *HEIS_LF* irrigation scenarios under all climate scenarios. This suggests a relatively low salinity stress due to low salt-build up in *PSIS* and *HEIS_LF* scenarios due to appropriate level of percolation leaching salts from the soil profile (Figure 7.2). However, Figure 7.5 suggests a drastic improvement by 40 to 80% in the water-limited only cotton and wheat yields with *HEIS_noLF* under all the climate scenarios. In the simulations, without the soil salinity stress, *HEIS_noLF* produced the water-limited only crop yields equivalent to the *PSIS* and *HEIS_LF* (Figure 7.5). This suggests a relatively high salinity stress due to high salt-

build up in the *HEIS_noLF* scenario caused by lack of appropriate leaching of salts due to low percolation from the soil profile (Figure 7.2)

The salt build-up during the cotton crop with *HEIS_noLF* is simulated at 67 mg cm^{-2} (~18 dS m^{-1}) and 64 mg cm^{-2} (~ 16 dS m^{-1}) under *RCP 2.6* and *RCP 8.5*, respectively (Tables 7.3 and 7.4). This soil salinity level is simulated to be significantly high relative to the soil *EC* threshold values of 7.7 dS m^{-1} for cotton and would cause a high salt stress on the crop growth. This is reflected by a lower relative transpiration (T_a/T_p <0.67) simulated for the cotton crop with *HEIS_noLF* under *RCP 2.6* and *RCP 8.5* scenarios (Tables 7.3 and 7.4). Cotton is considered a salt-tolerant crop with high soil electrical conductivity (*EC*) threshold value of 7.7 dS m^{-1} (Maas and Hoffman, 1977). Beyond this threshold value, the root-water uptake declines at the rate of 5.2% per dS m^{-1} increase (Maas, 1990). However, crop growth and yield are negatively affected by excessive salts in the soil profile. The high salinity in the soil delays and reduces germination and emergence, decreases cotton shoot growth and finally reduces cotton seed yield and total biomass (Abd Ella and Shalaby, 1993; Khorsandi and Anagholi, 2009).

The average water- and salt-limited WP_{ET} of cotton crop showed no significant variation with *PSIS* and *HEIS_LF* under the baseline and RCP 2.6 scenarios. However, an increase of 13% and 10% in the water- and salt-limited WP_{ET} for cotton crop is predicted under RCP 8.5 scenario with *PSIS* and *HEIS_LF*, respectively (Figure 7.4 c&e). This is mainly attributed to the increase in cotton yield due to elevated temperatures. The predicted water- and salt-limited WP_{ET} and WP_{Irr} with *HEIS_noLF* is significantly lower under the projected future climate scenarios. This is attributed to extremely low cotton yield due to high salinity stress.

In contrast to cotton, the wheat yield is significantly reduced for all three irrigation systems under the projected climate change scenarios as compared to the baseline climatic conditions. Using *PSIS* and *HEIS_LF* irrigations, the mean water- and salt-limited wheat yield is about 20% less under *RCP 2.6* and about 30% less under *RCP 8.5*. Using the APSIM and STICS crop growth models (Brisson *et al.*, 2003a; Keating *et al.*, 2003), and Azmat *et al.* (2021) quantified the impact of climate change (RCP 4.5 and RCP 8.5) on wheat phenology and yield in the Indus basin of Pakistan. According to their findings, the projected increase in temperature significantly reduced anthesis to maturity length (days), which ultimately reduced the wheat crop-growth period. In this study, SWAP simulated the average wheat crop-growth period from 110 to 92 days under the RCP2.6 and RCP8.5, respectively, as compared to 124 days under the baseline climatic conditions.

The high temperatures during critical crop-growth stages of the wheat crop could also reduce grain number and grain weight affecting the grain yield (Stone and Nicolas, 1994; Wollenweber *et al.*, 2003). Heat stress can substantially reduce the grain mass even if exposed to high temperature for short time during flowering period (Talukder *et al.*, 2010). For instance, Nuttall *et al.* (2012) indicated that an exposure to temperatures of 36-38 ^{o}C for just six days during flowering could result in a 12% reduction in the number of grains per tiller and therefore reduced wheat grain yield up to 13%. In a modelling study for a wheat growing region in Australia, Asseng *et al.* (2011) demonstrated that a variation of 2 ^{o}C in the average growing-season temperature caused a reduction of up to 50% in wheat yield.

Another influencing factor that significantly affects wheat yield is the effect of soil salinity that is caused by limited available soil water and a high evaporation rate. According to Maas and Grattan (1999) the combined effects of high evaporative demand

due to elevated temperature and soil salinity are more stressful than the soil salinity effects alone. In this study, a substantial reduction of 50 to 139% in the average wheat yield is simulated with *HEIS_noLF* under the projected climate scenarios (Figure 7.4, Tables 7.2 to 7.4; refer to appendix D for trend of the water- and salt-limited crop yields simulated under the current and the projected climate change scenarios and with different irrigations systems)

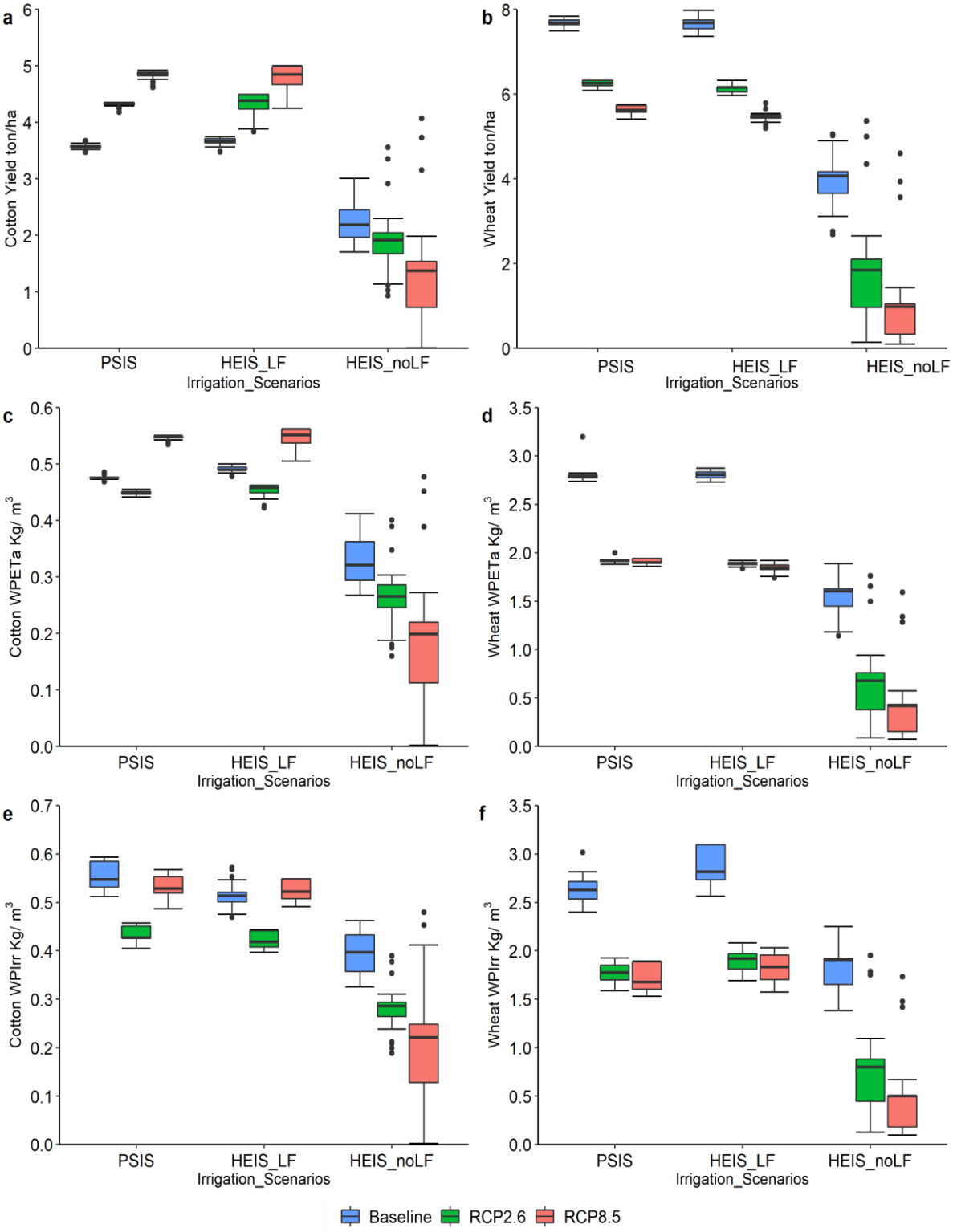

Figure 7.4: SWAP simulated water- and salt limited crop yields and crop water productivity (WP_{ET} and WP_{Irr}) for cotton and wheat crops with modernized irrigation systems under the current 'baseline' (1987 to 2017) and the project climate change scenarios (RCP 2.6 as low emission, and RCP 8.5 as high emission, 2070-2099) in Hakra Branch Canal command in Pakistan Punjab. The centre line represents the median value, the lower line the first

quartile and the upper line third quartile. The dots represent the extreme values.

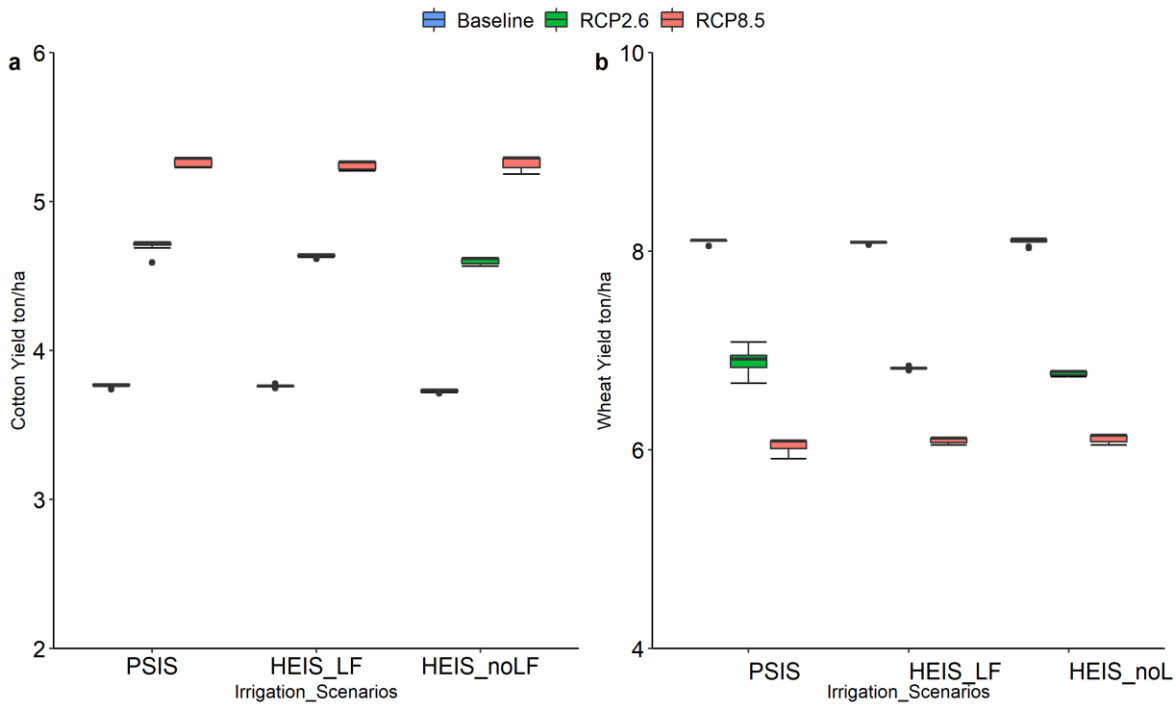

Figure 7.5: SWAP simulated crop yields with only water stress accounted for cotton (a) and wheat (b) with modernized irrigation systems under the current 'baseline' (1987 to 2017) and the projected climate change scenarios (RCP 2.6 as low emission, and RCP 8.5 as high emission, 2070-2099) in Hakra Branch Canal Command, Pakistan Punjab.

One of the main reasons for this substantial reduction in the simulated water- and salt-limited wheat yield with *HEIS_noLF* is the significant salt build-up of 67 mg cm^{-2} under RCP 2.6 (Table 7.3) and 64 mg cm^{-2} under RCP 8.5 (Table 7.4). This high amount salt build-up in the soil profile is beyond the threshold soil salinity limit (6 dS m^{-1}) for a wheat crop (Maas and Hoffman, 1977). As the crop yield and crop water productivity are linearly related, when all other factors are optimum (Singh *et al.*, 2006b). The reduction in water- and salt-limited wheat yields reduced the water- and salt-limited wheat WP_{ET} and WP_{Irr} values by 31 to 36% with *PSIS* and *HEIS_LF* irrigations under both the projected *RCP 2.6* and *RCP 8.5* scenarios (Figure 7.4 c & e), compared to the baseline scenario. The water- and salt-limited wheat WP_{ET} and WP_{Irr} values are simulated to be

50% to 66% less with *HEIS_noLF* irrigation under *RCP 2.6* and *RCP 8.5*, respectively, compared with the baseline scenario (Figure 7.4 d & f). This lower water productivity is mainly due to substantially low wheat yield as result of higher salt stress (Figure 7.4 a & b). Wheat is considered a moderately salt-tolerant crop (Maas and Hoffman, 1977). According to Abbas *et al.* (2013), high soil salinity results in a significant reduction in the grain protein, fat and fibre content and ultimately a reduction in crop yield. High salinity reduces number of tillers per plant followed by grain weight per plant (Mostafazadeh-Fard *et al.*, 2009; Abbas *et al.*, 2013)

7.9 Conclusions

This study assessed the long-term effects of modernized irrigation systems on canal command scale soil water and salt balances, and crop water productivity values for cotton and wheat crops in Hakra Branch Command under the baseline (1987 – 2017) and the projected future climate scenarios (2070 – 2099). The well-known SDSM is used for statistically downscaling the future climate from CanESM2 GCM data for RCP 2.6 and RCP 8.5 scenarios. The model projections show a significantly increasing trend in all the climate variables except precipitation which shows decreasing trend. The mean annual temperature is predicted to increase by 2 ^{o}C under RCP 2.6, and 5 ^{o}C under RCP 8.5 scenario, whereas the precipitation is predicted to be reduced by 25% under RCP 2.6, and 38 % under RCP 8.5 as compared to the baseline period.

The modelling results under the baseline period (1987-2017) indicated that modernised irrigation scenarios of precision surface irrigation system (*PSIS*) and a high efficiency irrigation (sprinkler) system with appropriate leaching fraction (*HEIS_LF*) performed similarly in terms of the irrigation supplied, salt build-up, crop yields and crop water productivity. Whereas the high efficiency irrigation (sprinkler) system with no leaching

fraction (*HEIS_noLF*) potentially saved up to 40% more water than the *PSIS* and *HEIS_LF*. However, the water saving with the *HEIS_noLF* irrigation would impose a high risk of increase in the soil salinity due to low percolation and a high amount of salt build-up. The *HEIS_noLF* added 2 times more salts into the root zone than the *PSIS* and *HEIS_LF*. This reduced the water- and salt-limited average cotton yield by 40% and wheat yield by 60% under the baseline period.

Due to the expected high evaporative demand under the projected climate (2070-2099) scenarios the mean annual irrigation requirements with *PSIS* is increased by 31% and with *HEIS_LF* increased by 27% under RCP 2.6 compared to the baseline period. Similarly, under RCP 8.5 the annual irrigation is increased by 24% with *PSIS* and 19% with *HEIS_LF*, compared to baseline period. However, the irrigation requirement is low under RCP 8.5 compared to RCP 2.6. The lower annual mean irrigation requirement under RCP 8.5 scenario could be due to a reduction in the crop-growth period due to earlier crop maturity caused by elevated temperature. The lower irrigation requirement also reduced the percolation rate which contributed to a higher salt build in the projected climate scenarios specifically with *HEIS_LF*, which added around 26% more salts under RCP 2.6 and 37% under RCP 8.5 as compared to the baseline period. However, *PSIS* showed no significant increase in the mean annual salt build-up under RCP 2.6 and just 12% increase under RCP 8.5. This is mainly due to surface flooding during each irrigation interval that causes a 25 to 30% higher percolation rate than the *HEIS_LF*. The high percolation rate contributes to leaching of salts from the soil profile and helps the groundwater recharge.

The projected climate resulted in a negative impact on *HEIS_noLF* in terms of a high amount of salt build-up in the soil profile. The average soil salt-build up under *HEIS_noLF* is simulated about 52% and 68% greater than *HEIS_LF* and *PSIS*,

respectively. This high soil salinity build-up under *HEIS_noLF* is simulated to significantly reduce the water- and salt-limited crop yields and the water productivity for cotton and wheat crops in HBC, especially under the projected climate change conditions. This indicates the importance of additional flow, more than the crop water requirements, to leach out salts from the root zone. Climate change may complicate the soil salinity challenges in semi-arid regions where high evaporative demand and reduced inflows provide less dilution and result in higher salt concentrations. The long-term modelling results suggest that benefits associated with *HEIS* through a sprinkler irrigation system, in terms of saving water, is limited due to potential risk of a high rate of salt build-up in the root zone. To avoid salt build-up a significant leaching fraction is needed to minimize the adverse effects of soil salinity on crop yield and water productivity.

The modelling analysis in this study illustrates how the impact of climate change on adoption of modernized irrigation system could affect the soil water and salt balances of irrigated agriculture in arid and semi-arid regions. This demonstrates that as the climate change intensifies the conception related to the *HEIS* in terms water saving is constraint by potential risk of increase in soil salinity that could adversely affect the crop yield and water productivity. By performing our analysis across the HBC command, it is concluded that under the projected future climates the traditional gravity surface irrigation, with flexible irrigation supply and precise irrigation schedules, such as the *PSIS* scenario, could deliver better results in terms of soil water and salt balances, crop yields and water productivity than the high efficiency irrigation systems even with appropriate leaching fractions (*HEIS_LF*) to control or reduce salt build-up in the soil profiles. However, the study results were based on the modelling simulations and used only CanESM2 climate change projections. Further studies are suggested to use multiple GCMs for studying climate-change impacts on irrigation hydrology and crop growth in semi-arid regions.

Also, long-term experiments are suggested to evaluate potential impacts of high efficiency irrigation systems (such as sprinkler) on soil water and salt balances, crop yields and crop water productivity, before a widespread adoptions of high efficiency irrigation systems (such as sprinkler) in semi-arid regions like HBC in Punjab Pakistan.

Chapter 8 : Synthesis, Conclusions and Recommendations

8.1 Problem Statement and Knowledge Gap

Irrigated agriculture is a major contributor to the food security and economy of Pakistan. However, the sustainability of irrigated agriculture in the Indus basin irrigation system of Pakistan is threatened by water scarcity, low irrigation efficiency, declining groundwater, waterlogging, soil salinization and low crop water productivity. These issues are the result of multiple factors, including seepage losses from unlined canal systems, poor water management practices, low surface water availability and injudicious use of poor-quality groundwater for irrigation. These problems are becoming more challenging as the demand for food is rising due to the rapid increase in population and declining quantity and quality of the water resources. This requires enhancing crop water productivity and focusing on "*more crop per drop, by producing more food with the same water resources or producing the same amount of food with less water resources"*. To achieve high crop-water productivity, both efficient planning and good management are required keeping in view the potential impact of climate change.

In response to the declining groundwater resources, limited canal-water supply, low crop water productivity, and rising concerns about water scarcity due to climate change, the policymakers in Pakistan have suggested modernization of the irrigation system by adopting sprinkler and drip irrigation to improve irrigation efficiency and save water. For these policies and management programmes to be effective, a sound understanding of their effects on soil water and salt balances, and crop water productivity under current and potential climate change conditions are required for the sustainability of irrigated agriculture. Effective implementation and sustainability of the proposed modernized irrigation system require not only a focus on water saving and improved irrigation efficiency, but also on the long-term effect on soil water and salt balances at the field- to regional-scale, and adaptation to climate change.

In the literature review (chapter 2), the modernised/advanced irrigation system (sprinkler and drip) features prominently in water policy debates as a possible solution to low irrigation efficiency and water scarcity (Perry *et al.*, 2017), with the assertion that it will improve crop water productivity. Most studies claim that with the modernised/advanced irrigation system the water use is more precise and efficient, and the crop yield will be enhanced. The majority of studies derive their conclusion from the experiments mostly done at a small field scale and short temporal scale (Anwar *et al.*, 2016; Latif *et al.*, 2016). It has also been reported in the literature that with the increase in irrigation efficiency the water will be "saved" and can be reallocated to other sectors such as domestic and industries. However, there is a paradox that increasing irrigation efficiency will save water and can be used for other purposes. Evidence has shown that advanced efficient irrigation technologies save water by reducing water losses in terms of percolation at the field scale. However, soil percolation recharges groundwaters and is potentially used elsewhere downstream in the basin. Moreover, reducing percolation increases the risk of salt build-up in the soil profile and seriously affects soil water and salt balances at a larger scale, particularly in semi-arid and arid regions. Hence more water is needed for the leaching of salts from the soil profile. Furthermore, improved irrigation efficiency generally increases crop evapotranspiration, and does not necessarily contribute to 'real' water savings (Perry *et al.*, 2017). This indicates that water saved at the farm scale does not reduce water use at the canal command scale, or at the basin scale. Therefore, the increase in irrigation efficiency must be combined with robust water accounting and a good understanding of the long-term impact on soil water and salt balances, and crop water productivity at the canal command scale, particularly under potential climate change. However, no study in semi-arid regions of Indus Basin Pakistan has evaluated the uncertainties associated with the long-term impact of a modernised irrigation system

on soil water and salt balances, and crop water productivity at the field as well as canal command scale, particularly under projected climate change scenarios.

Field studies to quantify accurately soil water and salt balance components and crop biophysical variables are difficult, due to expensive instrumentations and time-consuming experiments such as measurement of evapotranspiration, and its partitioning into evaporation and transpiration under partial soil cover, percolation of water under different irrigation and salt movement in the soil profile. However, in recent decades, researchers have devoted significant efforts in developing simulation models to quantify these difficult-to-measure hydrological and biophysical variables. The simulation model such as Soil-Water-Atmosphere-Plant (SWAP) efficiently estimates soil-water balance components such as evaporation, transpiration and percolation, salt transport process and evaluates alternative irrigation scenarios under specified climatic conditions (Singh, 2005; Vazifedoust, 2007; van Dam *et al.*, 2008; Vazifedoust *et al.*, 2008; Woldegebriel, 2011; Yuan *et al.*, 2019).

Therefore, *the main aim of this study was to utilize simulation agrohydrological models to integrate available operational knowledge of soil water flow, salt transport and crop growth with field experiments, remote sensing, and global climate models to evaluate long-term soil water and salt balances, plus crop water productivity with modernized irrigation systems under potential climate change scenarios at the field as well as canal command scale.*

8.2 Case Study and Field Experiments

The case study was the Hakra Branch Canal (HBC) command (chapter 3), located in the Punjab Province of Pakistan. Geographically the HBC command is located in the middle of the Indus basin. It covers an area of 2031 km^2, of which 73% is under crop cultivation.

The HBC command comes under the *cotton-wheat* agro-climate zone of the Indus basin irrigation system of Pakistan. However, rice, oilseed and fodder are also grown in the command area. Cotton and rice are the main crops in the *kharif* (summer) season, which are followed by wheat and oilseed (mustard) in the *rabi* (winter) season. The climate is characterized as dry, with extreme temperatures up to 48 ^{o}C in summer, and scant rainfall from 100 to 250 mm per year. Agricultural production is very limited without irrigation, even in the rainy (monsoon) season.

The HBC command area is irrigated through 16 perennial distributaries and one seasonal distributary which only gets water in summer. These distributary canals are off-takes from the HBC. Due to limited canal water availability, the distributary canals are operated on a canal rostering system with the objective to divert water to each distributary with full design supply for one week at least once a month. The limited canal-water supply is supplemented by freely accessible groundwater pumping in the HBC command. The major water management problems in HBC command are canal water scarcity, poor quality groundwater, low crop yields, waterlogging, and soil salinity. The extent of waterlogging is higher at the head reaches of the canal system, whereas the soil salinity is higher at the tail reaches of the canal system.

The complex interaction between irrigation, percolation, crop yield, waterlogging and soil salinity can be described using simulation models. The field-scale agrohydrological model, Soil-Water-Atmosphere-Plant (SWAP) is used due to its capability to efficiently assess soil water flow, and solute transport in close interaction with crop growth (van Dam *et al.*, 1997). The SWAP model is a one-dimensional hydrological model, which uses the well-known Richards' equation to compute water flow and the convection-dispersion equation to compute solute transport (Chapter 3). The SWAP model requires local soil, water and plant information for its calibration and validation. This information

was derived from two different sources, namely specific field experiments and secondary information from existing sources. The existing agrohydrological conditions and their variation under actual field conditions at HBC command were acquired from four selected farmers' fields two each of *cotton-wheat* and *rice-wheat* crop rotation. To accurately represent the hydrological condition at the HBC command the selection of farmers' fields was based on various combinations of soil, crop and irrigation amount and quality. One of the cotton-wheat fields has a good supply of canal water and has access to good quality groundwater, whereas the other cotton-wheat field has no access to canal water in the *kharif* season and has poor quality groundwater (3.28 dS m^{-1}). Similarly, for rice-wheat fields, one field has optimum soil and water conditions, and the other field has saline and waterlogged conditions. These fields were extensively monitored for irrigation applied, soil condition, crop phenology, and crop yields during the agricultural year 2016-2017. The spatial information on weather, soil, irrigation, groundwater level and quality at the HBC command scale were collected from allied government agencies. The spatial land use and actual evapotranspiration at the HBC command scale were derived through satellite remote-sensing techniques. The acquisition of this substantial amount of data made it possible to conduct a detailed agrohydrological assessment from field- to canal command-scale at the HBC command.

8.3 Calibration and Validation of SWAP model

The SWAP model is a well-defined and widely used for simulation of soil water and solute flows, in interaction with crop growth in irrigated fields. However, for the successful application of simulation models such as SWAP, more attention should be given to accurate measurements of input parameters and the calibration and validation of their sensitive input parameters such as soil hydraulic parameters. In Chapter 4, the information obtained from the field experiment at the four farmers' field was utilised to

parametrise, calibrate and validate the SWAP model in the case study. Most of the input parameters were derived from the experiments at the farmers' fields. However, some difficult-to-measure soil hydraulic parameters remained uncertain and were estimated through the inverse modelling technique. A non-linear parameter estimation program PEST was linked with SWAP to perform automatic calibration, using the observed soil moisture (ϑ) and salinity (*EC*) of the soil profile at all the selected fields. The inverse modelling was found to be efficient in estimating soil hydraulic parameters using the observed and simulated ϑ and *EC*. A good agreement between the observed and simulated ϑ and *EC* shows the capability of the SWAP model to successfully simulate the soil water dynamics and its effect on crop growth simulation. Using the calibrated and validated SWAP model with a detailed crop module, the simulated soil water and salt balance components and crop yields were used to explore the current irrigation practices at the field scale through quantification and analysis of a range of water management response indicators and crop water productivity values.

8.4 Analysis of current irrigation practices, soil water and salt balances, and crop water productivity at field-scale

The SWAP-simulated water and salt balance components were used to quantify the water and salt stress, percolation and salt build-up using water management response indicators. The simulation results suggested a significant variation in the relative transpiration ranging from 0.61 to 0.74 for cotton and 0.57 to 0.97 for wheat across the cotton-wheat fields. Similarly, in the rice-wheat fields, the relative transpiration varied from 0.63 to 0.86 for rice and 0.54 to 0.81 for wheat. This shows significant water and salt stress due to poor irrigation scheduling, limited canal water supply and use of poor-quality groundwater.

The contribution of rainfall to crop water requirement was very low (0.05 to 0.18) during the agricultural year 2016-2017, and could be characterised as a *dry* year with low rainfall of 115 mm. The amount of water supply (rainfall and irrigation) was relatively high (1043 mm) during the *kharif* season (cotton and rice) than in the *rabi* season (wheat). The water use was low for wheat in the rice-wheat fields (130 mm) compared to the cotton-wheat fields (244 mm) during the *rabi* season. This was because a significant amount of moisture was left after the rice crop and shallow water table in these fields. The average annual percolation was simulated significantly high in the cotton-wheat fields (-619 mm). This was due to the high amount of irrigation during the *kharif* season and sandy soil texture at the cotton-wheat fields. The high percolation could be beneficial in terms of groundwater recharge and contributed to the leaching of salts from the soil profile in these fields. The salt storage at the cotton-wheat fields was simulated at -10 to -39 mg cm^{-2}, this indicates no salt build-up in these fields.

However, in the rice-wheat fields the percolation was simulated significantly low (-145 mm) during the *kharif* (rice) season. This was because of creating water ponding by puddling the soil surface, which reduces hydraulic conductivity of the soil profile below the root zone during rice cultivation. In the following *rabi* season, the percolation index was simulated positive indicating high capillary rises due to shallow groundwater table and showed salt build up in the soil profile. This contributed to the water table rise and could potentially cause the problem of waterlogging and secondary salinization.

The field-scale modelling analysis showed the current irrigation management in the selected cotton-wheat farmer's fields is causing salt build-up in the *kharif* season but leaching in the *rabi* season with overall no salt build-up due to high depth of percolation. Despite the low salt build-up, the crops are experiencing stress as can be observed from the low relative transpiration. This could be due to infrequent irrigation applied with

heavy irrigation depths when the water becomes available to the farmers. However, in the rice-wheat fields, simulation of low percolation and high salt build-up indicate the sign of water logging and salinization.

The SWAP model could simulate potential crop yield and water- and salt-limited crop yield, accounting for water- and salt-stress only on crop growth. However, factors such as seed quality, nutrient deficiency, and the effect of pests and weeds are not considered in SWAP model as it assumes optimum agronomic conditions. The potential yields for cotton, rice and wheat were simulated 30%, 15% and 25% higher respectively than the corresponding water- and salt-limited crop yields, and 30% to 50% higher than the observed yield.

The crop water productivity values were analysed using the SWAP simulated soil water balance components transpiration *T*, evapotranspiration *ET*, percolation Q_{bot}, the applied irrigation *I* and the simulated (Y_{sim}) and observed (Y_{obs}) grain (or seed) yield. This flexibility in defining the crop water productivity in different forms (WP_T, WP_{ET}, WP_{ETQ} *and* WP_I) provides insights to assess irrigation systems, and to identify where and when water can be saved. The WP_T refers to *Y* (grain or seed yield)/*T* (transpiration) and sets the lowest limit of water used by the crop through only crop transpiration. The average WP_T (kg/m^3) based on the observed yield was quantified at 0.34 for cotton, 1.25 for rice and 1.91 for wheat at the study farmer's fields during the agriculture year 2016-2017. This represents wheat as a single efficient crop in terms of crop production. The WP_T based on the water- and salt-limited crop yields was simulated 30% higher than the WP_T based on the observed crop yields. This indicates further improvement can be possible by providing optimum agronomic conditions such as the use of good quality seeds and controlling pests and diseases.

The average WP_{ET} (kg/m^3), expressed as Y (grain or seed yield)/ET (evapotranspiration), based on the observed yield was quantified at 0.29 for cotton, 0.66 for rice and 1.52 for wheat at the study farmer's fields. The ET is considered as the total amount of water used in crop production. The average WP_{ET} is significantly lower than the average WP_T, namely 47% for rice, 20% for wheat and 15% for cotton. The WP_{ET} can be improved by efficient agronomic practices such as reducing non-beneficial water loss through soil evaporation by soil mulching and especially dry rice cultivation. Percolation further reduces the WP_{ET} to WP_{ETQ} (kg/m^3). The reduction in WP_{ET} due to percolation was simulated at 18% for rice, 41% for wheat, and 42% for cotton at the study farmer's fields. However, the percolation is a source of groundwater recharge in areas of deep water table and contributes to the leaching of salts from the root zone. However, in the shallow water table, the percolation can cause waterlogging and secondary salinization.

The average WP_I (kg/m^3) refers to the crop yield and total depth of irrigation applied. The WP_I based on the water- and salt-limited crop yields was quantified, as compared to the WP_{ET}, about 27% less for rice, and 30% and 37% less for wheat and cotton, respectively at the cotton-wheat fields. This reduction in WP_I was due to the high depth of percolation in these cotton-wheat fields. However, the WP_I was simulated 2 times higher than WP_{ET} for wheat in the rice-wheat fields. This was because of less depth of irrigation applied due to sufficient moisture left after the rice crop. This substantial difference in WP_{ET} and WP_I indicates the need for improving on-farm irrigation management such as controlling percolation, improving application efficiency by laser land levelling and irrigation scheduling according to crop water requirements.

The results of the modelling exercise in this study (Chapter 4) suggest the capability of the SWAP model to efficiently quantify the soil water flow and salt transport dynamics

and crop growth at the field scale. The analysis also highlights the scope of improvement in crop water productivity.

8.5 Long-term impact of modernised irrigation systems on soil water and salt balance and crop water productivity at field scale

The calibrated and validated SWAP model (Chapter 4) has the capability to schedule irrigation according to pre-defined criteria such as type of irrigation (surface or sprinkler), time of irrigation (when to irrigate) and depth of irrigation (how much to irrigate).

In Chapter 5 the effects of adopting modernised irrigation systems on soil water and salt balances, and water- and salt-limited crop yields and crop water productivity for cotton-wheat cultivation at the field scale have been evaluated over a period of 10 years (2007-2017) through the following irrigation scenarios:

Scenario 1: *'Business as usual'* or *'Reference irrigation scenario'*

Scenario 2: Precision Surface Irrigation System (*PSIS*)

Scenario 3: High-Efficiency Irrigation System (*HEIS*)

Scenario 1 (*Reference irrigation-scenario*) quantified the current irrigation management practices performed by the farmer at the study cotton-wheat experimental field. The irrigation was scheduled as per the fixed rotation (*Warabandi*) system of the HBC. In the reference irrigation scenario, the simulation was performed over a period of 10 years from May 1st 2007 to April 30th, 2017, keeping all the input parameters constant except the metrological data. This scenario served as a base for further analysis and comparison with modern irrigation systems.

The Scenario 2 (*PSIS*) represented a modernized gravity-fed surface irrigation system using allowable daily crop-stress define by relative transpiration (ratio of actual

transpiration to potential transpiration, T_a/T_p) to schedule the irrigation application (when to irrigate). Six scheduling criteria corresponding to crop T_a/T_p of 0.5, 0.6, 0.7, 0.8, 0.9 and 0.95 were set to apply a fixed irrigation depth when the crop reached a predefine level of T_a/T_p due to water and salt stress. In the *PSIS* scenario, two fixed irrigation depths 60 mm and 80 mm for each irrigation event were simulated. The simulation was performed for 10 years (2007-2017) with the same inputs apart from climate data and irrigation scheduling which was calculated by the SWAP.

The Scenario 3 (*HEIS*) represented a modern sprinkler irrigation that can apply a specific amount of irrigation as per crop-water requirements. The same irrigation scheduling criteria of *PSIS* were used for the *HEIS* scenario. However, instead of defining a fixed depth, the irrigation amount was calculated by SWAP and applied to bring the soil "back to field capacity" corresponding to the defined scheduling criteria (T_a/T_p). To investigate salinity dynamics in the soil profile due to changes in the irrigation system, the *HEIS* scenario simulation was first performed without leaching fraction (*HEIS_noLF*) and then with a leaching fraction (*HEIS_LF*). In *HEIS_LF* an additional depth of 60 mm was applied before the crop sowing, followed by an additional 10 mm with subsequent irrigation interval. The simulation period and the input parameters were the same as *PSIS* whereas the irrigation amount and scheduling were calculated by SWAP.

In the comparison of the *Reference* scenario with the advanced irrigation scenarios (*PSIS* and *HEIS*), the simulation results suggested the scope of water-saving as high as > 40% particularly under the *PSIS_80mm* and *HEIS_LF*, compared to the *reference* irrigation scenario. The results also suggested an increase of 30% in average water- and salt-limited crop yields and a 60% increase in average water- and salt-limited crop water productivity values under the *PSIS_80mm* and *HEIS_LF*. This could be attributed to flexible irrigations allowed in the *PSIS_80mm* and *HEIS_LF* scenarios, as compared to the fixed

depths and fixed schedule irrigations simulated in the *reference* irrigation scenario. However, the *HEIS_noLF* could adversely affect the soil water and salt balances by reducing the percolation and increasing the salt build in the soil profile. The detrimental effects of a significant amount of salt build-up under *HEIS_noLF* resulted in the reduction of water- and salt-limited crop yields and water productivity values for both wheat and cotton crops in the study fields.

The findings of this study clearly suggests that both *PSIS_80mm* and *HEIS_LF* irrigation systems under 0.95 irrigation scheduling criteria resulted into improved long-term soil water and salt balances, and similar water- and salt-limited crop yields and crop water productivity values for cotton-wheat cultivation in the study area. This indicates that there is potential for the current fixed schedule high irrigation depths surface irrigation system to improve irrigation efficiency provided the irrigation is scheduled flexibility according to the crop water requirements with control over field application losses. The implementation of high-efficiency irrigation systems such as sprinkler irrigation requires high installation costs, intensive supervision, skilled operators, and proper maintenance and operation. However, a gravity-fed precision surface irrigation system such as *PSIS_80mm* requires no major infrastructure changes, less operation cost and could deliver similar water-saving, crop yield and crop water productivity values as by the high-efficiency irrigation system such as *HEIS_LF* for cotton-wheat irrigation in the study fields.

8.6 Analysis of current irrigation practices, soil water and salt balances, and crop water productivity at canal-command scale.

The results of Chapters 4 and 5 provided confidence to assess the current water management and crop productivity of the Hakra Branch Canal command. Chapter 6 described the development of distributed SWAP model at the HBC command scale by

applying the calibrated and validated detailed SWAP model in a distributed mode to quantify the water and salt balances and crop water productivity of current irrigation practices. The simulation of all combinations of *soil-water-weather-crop* was performed at the spatial scale of the *head, middle* and *tail* reaches of the canal and at a temporal scale of the *kharif* season and the *rabi* season in the HBC command during the agriculture 2016-2017. The HBC command was divided into homogeneous simulation units by overlaying thematic maps of land use, soil type, water distribution, groundwater level and groundwater quality of the HBC command in a GIS environment. The soil hydraulic parameters were estimated for the different simulation units by pedotransfer functions, which relate hydraulic functions $\vartheta(h)$ and $K(\vartheta)$ to the measured soil information in the study area. The information from field experiments, secondary data sources, satellite remote sensing and existing geographical data were used to derive and aggregate the input parameters attached to all the simulation units. To link this information with SWAP, a coupling program was written in *VB.Net* to write input and output data from one system to another and to execute the SWAP model in *Batch* for all the simulation units.

To validate the accuracy and reliability of the spatial aggregation of the input parameters, the actual evapotranspiration simulated by SWAP denoted at ET_{sw} was compared with independent satellite remote sensing actual evapotranspiration obtained from *MOD16A2* product of *MODIS* and denoted as ET_{MOD} at different spatial and temporal scales. The close agreement between the ET_{SW} and ET_{MOD} suggested an acceptable parameterization of SWAP modelling over the main crops (cotton, rice, wheat and mustard). However, a high discrepancy between the ET_{SW} and ET_{MOD} over the baren soils indicated the importance of accurate land use classification in distributed modelling. Though the good agreement between SWAP simulated ET_{SW} and independent remote sensing ET_{MOD} over

the main crops provided confidence in using distributed SWAP modelling for further analysis of current irrigation practices in the study area.

The distributed SWAP modelling results quantified that the net annual canal water supply was only 273 mm against the potential demand (ET_p) of 1520 mm, and the actual water consumed (ET_a) of 837 mm during the agriculture year 2016-2017. This means that the canal irrigation system contributed only 18% to the ET_p and 33% to the ET_a. This significant deficit in the crop water requirement was fulfilled to some extent by unrestricted groundwater use. Access to groundwater in Pakistan by tubewells has assisted farmers to reduce their vulnerability to the canal water shortages, fulfil their crop water requirements, and improve their livelihoods. The simulated groundwater abstraction contributed 48% to the ET_a. The mean annual net groundwater recharge Q_R for the entire HBC command ranged from -90 mm yr^{-1} at the head reaches to -53 mm yr^{-1} at the tail reaches. The negative sign indicates a decline in the groundwater level during the study period (2016-2017). This could be mainly due to significantly low rainfall (115 mm) and insufficient canal water supply, plus the overexploitation of the groundwater. The abstraction of groundwater was estimated higher at the head reaches due to the availability of good quality groundwater and the cultivation of high water-consuming crops such as rice. This supports that current water management is contributing to the decline of groundwater in the HBC command. Moreover, the quality of groundwater has also deteriorated spatially downstream along the canal network. The quality is better at the head reaches and poor at the tail reaches of the HBC command. The use of poor-quality groundwater results into salt build-up in the soil profile. The distributed SWAP simulation results quantified the mean annual salt build-up varied from 1.7 mg cm^{-2} (i.e., 0.17 ton ha^{-1}) at the head reaches to > 4 mg cm^{-2} (i.e., 0.4 ton ha^{-1}) in the tail reaches of the HBC command during the agriculture year 2016-2017. The low salt build-up at the

head reaches was due to the use of relatively good quality groundwater and sufficient access to the canal water. With the low canal water availability and use of poor-quality groundwater the soil salinity (*EC*) values varied from 2.93 to 8.26 dS m^{-1} at the middle reaches and from 3.2 to 12 dS m^{-1} at the tail reaches of the HBC command. These simulated soil salinity values for some simulation units were higher than the soil salinity threshold values of 7.7 dS m^{-1} for cotton, 5.0 dS m^{-1} for rice, 6.0 dS m^{-1} for wheat and 7.4 dS m^{-1} for mustard.

The simulated crop yield and water productivity in terms of actual evapotranspiration (WP_{ET}) and depth of irrigation applied (WP_{Irr}) were based on the water- and salt-limited crop yields, which were higher than the actual yields. This is because the SWAP simulated crop yield does not account for the other agronomic stress such as pests, weeds, diseases and nutrition deficiency. The mean water- and salt-limited WP_{ET} (kg m^{-3}) were simulated at 0.40 for cotton, 0.96 for rice, 0.73 for mustard and 1.19 for wheat. Similarly, the mean water- and salt-limited WP_{Irr} (kg m^{-3}) were simulated at 0.69 for cotton, 105 for rice, 1.12 for mustard and 2.00 for wheat. Considerable variation was observed in the water productivity with a coefficient of variation of 9 to 34% for WP_{ET} and from 21 to 39% for WP_{Irr}. The water productivity was quantified relatively higher at the head and middle reaches of the HBC command than the tail reaches. The low crop water productivity is related to the low canal water supply and use of poor-quality groundwater in the tail reaches of HBC command.

The results of the distributed SWAP modelling highlighted that the current irrigation practices in the HBC command are leading to unfavourable ecohydrological conditions. For instance, the high water-consuming crop such as rice and relative high irrigation application, combined with significant seepage losses from the canal network, is contributing to the rising of the groundwater level at the head reaches. Whereas low canal

inflow and use of poor-quality groundwater are increasing soil salinity at the tail reaches of the HBC command. This could affect the sustainability of irrigated agriculture in HBC command. Moreover, there are very limited evaluation of current and proposed modernised irrigation practices on soil water and salt balances and crop water productivity, especially under the project climate change conditions in semi-arid irrigation systems such as HBC in the Indus basin Pakistan.

8.7 Long-term impact of modernised irrigation systems and projected climate changes on soil water and salt balances and crop water productivity at the canal command scale

The impact of projected climate change needs to be considered carefully within current and proposed modernised irrigation practices for improving productivity and sustainability of irrigated agriculture in the study area. The rapidly increasing trends in the global mean temperature and changes in precipitation have become more irregular and unpredictable. These changes in climatic conditions are affecting natural resources such as energy, land and water. The climate change and its resulting impacts could be more intense in the water short semi-arid and arid regions such as HBC command. The simulation results of distributed SWAP modelling (Chapter 6) enumerate that the current water management practices at the HBC command cause rise and decline of groundwater level, increasing secondary salinization and low crop yield and water productivity. Productive and sustainable irrigation management can be achieved through the implementation of an efficient irrigation system.

In Chapter 5, a field-scale simulation was performed over a period of ten years to quantify the impact of modernized irrigation systems on soil water and salt balances and crop water productivity of cotton-wheat cultivation in the study fields. However, simulation results belong to the isolated fields and could not be represented at a larger scale due to

heterogeneity of various parameters such as crops grown, soil texture, canal water supply, groundwater levels and groundwater quality. Therefore, in Chapter 7, the long-term (30 years) assessment of modernized irrigation systems (*PSIS, HEIS_LF and HEIS_noLF*) under contemporary climate and potential climate change scenarios were performed using distributed SWAP modelling for *cotton-wheat* crop combination across the HBC command. The irrigation scheduling criteria (T_a/T_p) was set to 0.95. A fixed depth of *80 mm* was applied under *PSIS* and *back-to-field capacity* depth criteria is defined for *HEIS*. Three long-term climate scenarios were defined to quantify the impact of projected climate change on soil water and salt balances and crop water productivity under modernized irrigation systems, as follows:

Scenario 1: Current climate '*baseline*' (1987-2017)

Scenario 2: RCP 2.6 '*Low emission*' (2070-2099)

Scenario 3: RCP 8.5 '*High emission*' (2070-2099)

In case of the current climate (Scenario 1), the simulation results suggested that *HEIS_noLF* could save 20% on the average annual irrigation as compared to the *PSIS* and *HEIS_LF*. However, the less irrigation under *HEIS_noLF* also reduced the percolation, which resulted into a significant amount of salt build-up in the soil profile. This affected the crop yield and water productivity. The average water- and salt-limited crop yields under *HEIS_noLF* were simulated at 38% less for cotton and 48% less for wheat, as compared to *PSIS* and *HEIS_LF*. Similarly, the average water- and salt-limited WP_{ET} under *HEIS_noLF* were simulated 50% less for cotton and 66% less for wheat, as compared to *PSIS* and *HEIS_LF*. This suggests that the soil water and salt balances and crop yields, and crop water productivity obtained under *PSIS* and *HEIS_LF* irrigations are suitable for productive and sustainable irrigated agriculture at HBC command.

The climate projections for Scenario 2 and Scenario 3 were downscaled from CanESM2 GCM model using the statistical downscaling model (SDSM). The downscaling results suggested that the mean maximum temperature will be increased by 1.6 ^{o}C under RCP 2.6 (scenario 2) and 4 ^{o}C under RCP 8.5 (scenario 3) during the time slice from 2070 to 2099 at HBC command. The projected increase by 3 ^{o}C and 6 ^{o}C are expected during the summer months (Apr-July) under RCP 2.6 and RCP 8.5, respectively. Similarly, all other climate parameters (minimum temperature, solar radiation, relative humidity, wind speed) showed increasing trends except precipitation which is predicted to have a decreasing trend under potential climate scenarios. These climate projections indicate an unfavourable hydrological condition for the agricultural production system at the HBC command.

The average annual irrigation under *PSIS* and *HEIS_LF* was simulated 30% higher under Scenario 2 (RCP 2.6) and 20% higher under Scenario 3 (RCP 8.5) compared to Scenario 1 (baseline). Despite of high evaporative demand, the irrigation demand under Scenario 3 was simulated less compared to Scenario 2. The higher temperature under Scenario 3 simulated the accelerated crop growth leading to a shorter crop period and early maturity of the crop. The average crop growth period was simulated 15 to 38 days less under Scenario 3 compared to Scenario 2. However, the simulation results suggested that the cotton yield under potential climate change scenarios was increased by 21 to 29% as compared to Scenario 1. This indicates that, provided optimum agronomic conditions, the cotton crop can efficiently adapt to climate change. However, the wheat yield was simulated significantly reduced under the potential climate scenarios as compared to Scenario 1. This could be because the high heat stress during the critical growth period reduces grain number per tiller and grain mass affecting overall crop yield.

Interestingly, the *HEIS_noLF* saved up to 40% of irrigation water under the potential climate scenario by significantly reducing the percolation rate as compared to *PSIS* and *HEIS_LF*. However, the low percolation under *HEIS_noLF* significantly increased the salt build-up by up to 200% as compared to *PSIS* and *HEIS_LF*. The high amount of salt build-up resulted in significant reductions in the simulated water- and salt-limited cotton and wheat crop yields and their lower crop water productivity values. This highlights that the modernized irrigation without leaching fraction could intensify the risk of salt accumulation in irrigated agriculture, particularly under potential climate change conditions.

The simulation results also suggested relatively much less increase in the soil salt build with *PSIS* under the potential climate change scenarios compared to the *baseline* scenario. However, *HEIS_LF* simulated a 25 to 38% increase in in the soil salt build-up under the potential climate scenarios compared to the corresponding baseline scenario despite almost a similar amount of irrigation applied as *PSIS*. The low salt build-up with *PSIS* could be attributed to surface flooding during each irrigation interval that produces up to 30% more percolation as compared to *HEIS_LF*. The high percolation helps in leaching salts from the soil profile and also helps in groundwater recharge. From the findings of the long-term simulation under current and potential climate change scenarios it can be concluded that the traditional gravity surface irrigation with a precise irrigation schedule (*PSIS*) and flexible irrigation supply could maintain better soil water and salt balances, better crop yield and crop water productivity than modernize high-efficiency irrigation system (*HEIS_LF*) for cotton-wheat cultivation in the HBC command under the potential climate change scenarios.

8.8 Key findings

The following key findings are made for sustainable and efficient irrigation management and improved crop water productivity in the HBC command.

- The integration of field scale observations and canal command scale information with agrohydrological model SWAP and global climate modelling offers a comprehensive tool to analyse the long-term effects of different irrigation practices from field- to canal command-scales.
- The assessment of current irrigation practices suggests a significant spatial variation in the soil water and salt balances, crop yields and water productivity in the study area. The canal water supply is relatively higher at the head reaches as compared to the middle and tail reaches of the canal command. Similarly, the use of groundwater is also high at the head reaches due to the availability of relatively good quality groundwater than in the middle and tail reaches.
- The issue of waterlogging is higher at the head reaches of the canal due to high water-consuming crops such as rice and seepage from the canal network. Whereas the soil salinity is high at the middle and tail reaches due to a limited supply of good quality canal water and the use of poor-quality groundwater.
- The detrimental effects of insufficient good quality canal water supply and use of poor-quality groundwater cause a significant reduction in crop yields and water productivity specifically in the tail reaches of the canal command.
- The long-term simulation of proposed modernized high-efficiency irrigation without leaching fraction (*HEIS_noLF*) suggests saving of water by 40% compared to the current irrigation practices. However, it would potentially increase soil salinity (e.g., from 2.6 to 8.0 dS m^{-1}) at the field scale, and adversely

affect the crop yields due to high salt stress. The long-term simulation of *HEIS_noLF* under the current climate (1987-2017) at the HBC command scale quantified a potential saving of 20% irrigation water by reducing the percolation. However, this resulted in low percolation rate. The low percolation rate encouraged the salt build-up which increased the soil salinity from < 2 to > 12 dS m^{-1} at the canal command scale. The high salt build-up significantly reduced the water- and salt-limited crop yield by 34% for cotton (from 3.45 to 2.28 ton/ha) and 40% for wheat (from 6.28 to 3.73 ton/ha) at the canal command scale under the current climate (1987-2017). The soil salinity is simulated even worse in the poor groundwater areas.

- High-efficiency irrigation systems without appropriate salt leaching from the soil profile under potential climate change could potentially pose a very negative impact on crop production and soil water and salt balance. The simulation results suggested more than 80% increase in the salt build-up under potential climate change as compared to the current climate. The high salinity build-up simulated a crop failure specifically in poor-quality groundwater areas under business as usual (RCP 8.5) potential climate change scenario (2070-2099).
- Clearly, the research suggests that a leaching fraction of a certain amount will be needed more than the crop water requirement to leach out the salts and maintain proper salinity level. This leaching fraction can be achieved either with additional water with a high-efficiency irrigation system simulated as *HEIS_LF* or with a precise surface irrigation system (*PSIS*).
- The modelling analysis suggested that the performance *HEIS_LF* and *PSIS* resulted in similar soil water and salt balances under the current climate (1987-2017). The simulation results obtained a 50 to 70% increase in the water- and

salt-limited crop water productivity (WP_{ET}) under *HEIS_LF* and *PSIS*, as compared to *HEIS_noLF* in the current climate (1987-2017). However, under potential climate change scenarios (2070-2099), the *PSIS* was simulated to perform even better in maintaining soil water and salt balances, crop yields and crop water productivity. The percolation rate with *PSIS* was simulated 20 to 30% higher, resulting in 20 to 30 % more leaching of salts than the *HEIS_LF*.

- The modelling assessment clearly suggests that the implementation of *HEIS* without appropriate leaching would compromise the salt build-up. This would potentially reduce crop yields and crop water productivity in the long term, especially under potential climate change (2070 -2099) conditions. There appears very limited scope for real irrigation water savings using a *HEIS* for long-term sustainable crop production in semi-arid and arid areas making conjunctive use of limited canal water supplies and marginal- to poor-quality groundwaters.

8.9 Recommendations

The following recommendations are drawn from the modelling assessment in this study:

- Real water saving in terms of high-efficiency irrigation system need to be assessed carefully on long-term basis. The short-term field experiments, considering only the irrigation application depth over an agricultural year, are somewhat limited in their evaluation of soil water and salt balances, especially considering potential impacts of projected climate change conditions in semi-arid regions.
- The sustainability of irrigated agriculture under potential climate change particularly in semi-arid regions requires sufficient leaching to keep the salinity under control. This could be achieved through a precision surface irrigation system which potentially requires less energy and investment cost. Hence, the

proposal for adopting high-efficiency irrigation systems such as sprinkler and drip irrigation must be further evaluated in terms of their potential effects on soil salt build-up, leaching fraction requirement and crop water productivity on a long-term basis under the projected future climate change conditions.

- There is further scope to improve the distributed agro-hydrological modelling applications and their performance and uncertainties. Long-term field experiments on precise surface irrigation systems are recommended to further evaluate their potential impacts on the leaching fraction, soil water and salt balances and crop yields; and inform improved distributed agro-hydrological modelling applications from field- to canal-command scale.

8.10 Future research

The key findings of this study suggest several actions that are required in future studies for achieving greater insights and effectiveness of the long-term modelling assessment at the command scale. These aspects are listed below:

- The number of field scale analyses should be increased to get better insights into the soil hydraulic parameters that will help in the accurate calibration of the model. Increasing field-scale modelling assessment at a spatial scale of the head, middle and tail reaches of the irrigation conveyance system would be expected to result in a better understanding of the soil water and salt balance components and help to capture the spatial heterogeneity of soil hydraulic parameters.
- In this study the SWAP model was calibrated and validated only under a surface irrigation system. However, for future studies it is recommended to calibrate and validate the model under high-efficiency irrigation system (sprinkler or drip), to

evaluate soil water and salt balances, and crop growth. This will improve the plausibility of the modelling simulation results.

- In this study, the land use information acquired from the remote sensing technique for the agriculture year 2014-2015 was used in the analysis, assuming no change in the land use in the study period (2016-2017). However, the parameterization of distributed SWAP model depends on the accuracy of land use classification. Future studies are recommended to investigate high-resolution land use maps and actual temporal changes in land use for accurate assessment and influence of changes in land use on soil water and salt balances and crop yields over the command scale.
- In this study, the climate change impact assessment was based on only CanESM2 general circulation model. However, it is recommended to use multiple GSMs for studying hydrological impacts of climate change to improve the accuracy of the results. Moreover, it is also recommended to use multiple downscaling techniques to enhance the plausibility of the downscaling projected climate change projects and their potential effects of soil water and salt balances and crop yields.
- The SWAP model did not consider potential effects of changes in atmospheric CO_2 levels (due to climate change) and any nutritional/pest/disease stresses on crop growth simulations. These factors may influence the crop growth dynamics and its potential effects of soil water and salt balances in the soil profile. These factors should be considered in simulations of long-term effects of different irrigation scenarios and project climate change conditions on long-term soil water and salt balances and crop yields in semi-arid regions

- The distributed SWAP model used in this study is based on the climate, irrigation, soil texture and hydrological conditions of HBC command. It is highly recommended to apply the developed approach for the assessment of soil water and salt balances, crop yields and crop water productivity in other canal commands of similar agrohydrological conditions for efficient management and decision making in semi-arid irrigation systems.

References

Aamer, M., Javed, Q., Mustafa, G., Mahmood, S., 2015. Soil Fertility Management for Sustainable Agriculture: A Case Studyof District Bahawalnagar, Pakistan. Journal of Natural Sciences Research Vol.5, No.19.

Abbas, G., Saqib, M., Rafique, Q., Rahman, A., Akhtar, J., Haq, M., Nasim, M., 2013. Effect of salinity on grain yield and grain quality of wheat (Triticum aestivum L.). Pak J Bot 50, 185-189.

Abd Ella, M., Shalaby, E.E., 1993. Cotton Response to Salinity and Different Potassium-Sodium Ratio in Irrigation Water. Journal of Agronomy and Crop Science 170, 25-31.

Abdo, K., Fiseha, B., Rientjes, T., Gieske, A., Haile, A., 2009. Assessment of climate change impacts on the hydrology of Gilgel Abay catchment in Lake Tana basin, Ethiopia. Hydrological Processes: An International Journal 23, 3661-3669.

Abishek, B., Priyatharshini, R., Eswar, M.A., Deepika, P., 2017. Prediction of effective rainfall and crop water needs using data mining techniques. 2017 IEEE Technological Innovations in ICT for Agriculture and Rural Development (TIAR). IEEE, pp. 231-235.

Adhikari, P., Ale, S., Bordovsky, J.P., Thorp, K.R., Modala, N.R., Rajan, N., Barnes, E.M., 2016. Simulating future climate change impacts on seed cotton yield in the Texas High Plains using the CSM-CROPGRO-Cotton model. Agricultural Water Management 164, 317-330.

Adnan, S., Khan, A.H., 2009. Effective rainfall for irrigated agriculture plains of Pakistan. Pakistan Journal of Meteorology 6, 61-72.

Agarwal, A.S., Singh, B.R., Kanehiro, Y., 1971. Ionic effect of salts on mineral nitrogen release in an allophanic soil. Soil Science Society of America Journal 35, 454-457.

Ageta, Y., Kadota, T., 1992. Predictions of changes of glacier mass balance in the Nepal Himalaya and Tibetan Plateau: a case study of air temperature increase for three glaciers. Annals of Glaciology 16, 89-94.

Aghdam, E.N., Babazadeh, H., Vazifedoust, M., Kaveh, F., 2013. Regional modeling of wheat yield production using the distributed agro-hydrological SWAP. Advances in Environmental Biology, 86-94.

Ahmad, M.-u.-D., 2002. Estimation of net groundwater use in irrigated river basins using geo-information techniques: A case study in Rechna Doab, Pakistan. [Sl: sn].

Ahmad, M.-u.-D., Masih, I., Turral, H., 2004. Diagnostic analysis of spatial and temporal variations in crop water productivity: A field scale analysis of the rice-wheat cropping system of Punjab. Journal of Applied Irrigation Science 39, 43-63.

Ahmad, M.-u.-D., Turral, H., Masih, I., Giordano, M., Masood, Z., 2007. Water saving technologies: Myths and realities revealed in Pakistan's rice-wheat systems. International Water Management Institute. 44p (IWMI Research Report 108), Colombo, Sri Lanka.

Ahmad, S., Majeed, R., 2001. Indus basin irrigation system water budget and associated problems. J. Engineering and Applied Sciences 20, 69-77.

Ahmad, Z., Asad, E.U., Muhammad, A., Ahmad, W., Anwar, A., 2013. Development of a low-power smart water meter for discharges in indus basin irrigation networks. Wireless Sensor Networks for Developing Countries. Springer, pp. 1-13.

Ahmed, N., Lü, H., Ahmed, S., Nabi, G., Wajid, M.A., Shakoor, A., Farid, H.U., 2021. Irrigation Supply and Demand, Land Use/Cover Change and Future Projections of Climate, in Indus Basin Irrigation System, Pakistan. Sustainability 13, 8695.

Alam, A., 2015. Analysis of Salinity Control and Reclamation Projects.

Alam, M., Bhutta, M., 2004. Comparative evaluation of canal seepage investigation techniques. Agricultural Water Management 66, 65-76.

Ali, M., Mubarak, S., 2017. Effective rainfall calculation methods for field crops: an overview, analysis and new formulation. Asian Research Journal of Agriculture, 1-12.

Allen, R.G., Pereira, L.S., Raes, D., Smith, M., 1998a. Crop evapotranspiration-Guidelines for computing crop water requirements-FAO Irrigation and drainage paper 56. FAO, Rome 300, D05109.

Allen, R.G., Pereira, L.S., Raes, D., Smith, M., 1998b. Crop evapotranspiration-Guidelines for computing crop water requirements-FAO Irrigation and drainage paper 56. FAO, Rome, Italy. 300, D05109.

Almarshadi, M.H., Ismail, S.M., 2011. Effects of precision irrigation on productivity and water use efficiency of alfalfa under different irrigation methods in arid climates. Journal of Applied Sciences Research 7(3), 299-308.

Alvar-Beltrán, J., Heureux, A., Soldan, R., Manzanas, R., Khan, B., Dalla Marta, A., 2021. Assessing the impact of climate change on wheat and sugarcane with the AquaCrop model along the Indus River Basin, Pakistan. Agricultural Water Management 253, 106909.

Amarasinghe, U.A., Shah, T., Malik, R., 2009. India's water futures: drivers of change, scenarios and issues.

Amjad, M., 2014. Oilseed crops of Pakistan. Pakistan Agricultural Research Council Islamabad,(PARC), 1-59.

Anwar, A.A., Ahmad, W., Bhatti, M.T., Haq, Z.U., 2016. The potential of precision surface irrigation in the Indus Basin Irrigation System. Irrigation science 34(5), 379-396.

Anwar, A.A., Ul Haq, Z., 2013. An old–new measure of canal water inequity. Water international 38(4), pp. 536-551.

Archer, D., 2003. Contrasting hydrological regimes in the upper Indus Basin. Journal of Hydrology 274, 198-210.

Archer, D.R., Forsythe, N., Fowler, H.J., Shah, S.M., 2010. Sustainability of water resources management in the Indus Basin under changing climatic and socio economic conditions. Hydrology and Earth System Sciences 14, 1669-1680.

Arora, V., Scinocca, J., Boer, G., Christian, J., Denman, K., Flato, G., Kharin, V., Lee, W., Merryfield, W., 2011. Carbon emission limits required to satisfy future representative concentration pathways of greenhouse gases. Geophysical Research Letters 38.

Ashraf, M., Ejaz, K., Arshad, M.D., 2017. Water use efficiency and economic feasibility of laser land leveling in the fields in the irrigated areas of Pakistan. Science, Technology and Development 36(2), 115-127.

Ashraf, M., Yasin, Q., 2012. Drip Irrigation for Sustaining Irrigated Agriculture in Punjab, Pakistan: Issues and Strategy. Proceedings of Irrigation Show and Education Conference.

Asif, M., Akram, M., Ali, A., 2016. Multi-locational trials to compare the relative water use and vegetable crops productivity by drip irrigation and conventional furrow irrigation systems in district Toba Tek Singh, Pakistan. Science Letters 4, 60-65.

Aslam, M., Prathapar, S., Aslam, M., Prathapar, S., 2006. Strategies to mitigate secondary salinization in the Indus Basin of Pakistan: A selective review. IWMI.

Asseng, S., Foster, I., Turner, N.C., 2011. The impact of temperature variability on wheat yields. Global Change Biology 17, 997-1012.

Awan, N., Latif, M., 1982. Socio-economic aspects of water management of salinity control and reclamation project no. 1 in Pakistan: A case study. Polders of the World, 571-585.

Awan, U.K., Anwar, A., Ahmad, W., Hafeez, M., 2016. A methodology to estimate equity of canal water and groundwater use at different spatial and temporal scales: a geo-informatics approach. Environmental Earth Sciences 75(5), 409.

Azmat, M., Ilyas, F., Sarwar, A., Huggel, C., Vaghefi, S.A., Hui, T., Qamar, M.U., Bilal, M., Ahmed, Z., 2021. Impacts of Climate Change on Wheat Phenology and Yield in Indus Basin, Pakistan. Science of The Total Environment, 148221.

Babiker, A.E., Maria, H.E., Abd Elbasit, M.A., Abuali, A.I., Abu-Zerig, M.M., Liu, G., 2021. Potential of low-cost subsurface irrigation system in boosting food production in high water scarcity regions. Agricultural Engineering International: CIGR Journal 23.

Bakhsh, A., Ashfaq, M., Ali, A., Hussain, M., Rasool, G., Haider, Z., Faraz, R., 2015. Economic evaluation of different irrigation systems for wheat production in Rechna Doab, Pakistan. Pak. J. Agri. Sci 52, 821-828.

Bakhsh, A., Chauhdary, J.N., Ahmad, N., 2018. Improving crop water productivity of major crops by adopting bed planting in Rechna Doab Pakistan. Pak. J. Agric. Sci 55, 963-970.

Bandaragoda, D., 1998. Design and practice of water allocation rules: lessons from warabandi in Pakistan's Punjab. IWMI.

Bandaragoda, D., Rehman, S.u., 1995. Warabandi in Pakistan's canal irrigation systems: Widening gap between theory and practice. IWMI.

Bank, W., 2006. Reengaging in agricultural water management: Challenges and options. The World Bank.

Bar-Tal, A., Feigenbaum, S., Sparks, D., 1991. Potassium-salinity interactions in irrigated corn. Irrigation Science 12, 27-35.

Bastiaanssen, W.G., Allen, R.G., Droogers, P., D'Urso, G., Steduto, P., 2007. Twenty-five years modeling irrigated and drained soils: State of the art. Agricultural Water Management 92, 111-125.

Bastiaanssen, W.G., Singh, R., Kumar, S., Schakel, J., Jhorar, R., 1997. Analysis and recommendations for integrated on-farm water management in Haryana, India: a model approach. SC-DLO.

Batchelor, C., Lovell, C., Murata, M., 1996. Simple microirrigation techniques for improving irrigation efficiency on vegetable gardens. Agricultural Water Management 32, 37-48.

Bell, A.R., Shah, M., Ward, P.S., 2014. Reimagining cost recovery in Pakistan's irrigation system through willingness-to-pay estimates for irrigation water from a discrete choice experiment. Water resources research 50, 6679-6695.

Bellot, J., Chirino, E., 2013. Hydrobal: An eco-hydrological modelling approach for assessing water balances in different vegetation types in semi-arid areas. Ecological modelling 266, 30-41.

Berbel, J., Expósito, A., Gutiérrez-Martín, C., Mateos, L., 2019. Effects of the irrigation modernization in Spain 2002–2015. Water Resources Management 33, 1835-1849.

Bernstein, L., 1961. Osmotic adjustment of plants to saline media. I. Steady state. American Journal of Botany 48, 909-918.

Bernstein, L., Francois, L., 1973. Leaching requirement studies: sensitivity of alfalfa to salinity of irrigation and drainage waters. Soil Science Society of America Journal 37, 931-943.

Bessembinder, J., Dhindwal, A., Leffelaar, P., Ponsioen, T., Singh, S., 2003. Analysis of crop growth. Water productivity of irrigated crops in Sirsa District, India. Wageningen UR, pp. 59-83.

Bhardwaj, A.K., Mishra, V.K., Singh, A.K., Arora, S., Srivastava, S., Singh, Y.P., Sharma, D.K., 2019. Soil salinity and land use-land cover interactions with soil carbon in a salt-affected irrigation canal command of Indo-Gangetic plain. Catena 180, 392-400.

Bhatti, A., 1987. A review of planning strategies of salinity control and reclamation projects in Pakistan. Proceedings, Symposium 25th International Course on Land Drainage. ILRI publ.

Bhatti, A.M., Suttinon, P., Nasu, S., 2009. Agriculture water demand management in Pakistan: a review and perspective. Society for Social Management Systems 9, 1-7.

Bhatti, M.A., Kijne, J.W., 1990. Irrigation allocation problems at tertiary level in Pakistan. Overseas Development Institute.

Bhatti, M.T., Anwar, A.A., Aslam, M., 2017. Groundwater monitoring and management: Status and options in Pakistan. Computers and Electronics in Agriculture 135, 143-153.

Bhutta, M.N., Smedema, L.K., 2007. One hundred years of waterlogging and salinity control in the Indus valley, Pakistan: a historical review. Irrigation and Drainage: The journal of the International Commission on Irrigation and Drainage 56, S81-S90.

Bhutto, A.W., Bazmi, A.A., 2007. Sustainable agriculture and eradication of rural poverty in Pakistan. Natural Resources Forum. Blackwell Publishing Ltd,Oxford., pp. 253-262.

Bingham, F., 1973. Salt Tolerance of Mexican Wheat: I. Effect of NO3 and NaCl on Mineral Nutrition, Growth, and Grain Production of Four Wheats 1. Soil Science Society of America Journal 37, 711-715.

Bjørnæs, C., 2013. A guide to representative concentration pathways. CICERO. Center for International Climate and Environmental Research, 351-357.

Black, T., Gardner, W., Thurtell, G., 1969. The Prediction of Evaporation, Drainage, and Soil Water Storage for a Bare Soil 1. Soil Science Society of America Journal 33(5), 655-660.

Boesten, J., Van der Linden, A., 1991. Modeling the influence of sorption and transformation on pesticide leaching and persistence. Wiley Online Library.

Bookhagen, B., Burbank, D.W., 2010. Toward a complete Himalayan hydrological budget: Spatiotemporal distribution of snowmelt and rainfall and their impact on river discharge. Journal of Geophysical Research: Earth Surface (2003–2012) 115.

Boretti, A., Rosa, L., 2019. Reassessing the projections of the world water development report. NPJ Clean Water 2, 1-6.

Bos, M.G., 1979. Standards for irrigation efficiencies of ICID. Journal of the Irrigation and Drainage Division 105, 37-43.

Bresler, E., Hoffman, G.J., 1986. Irrigation management for soil salinity control: theories and tests. Soil Science Society of America Journal 50, 1552-1560.

Briscoe, J., Qamar, U., 2008. Pakistan's Water Economy: Running Dry.

Brisson, N., Gary, C., Justes, E., Roche, R., Mary, B., Ripoche, D., Zimmer, D., Sierra, J., Bertuzzi, P., Burger, P., 2003a. An overview of the crop model STICS. European Journal of agronomy 18, 309-332.

Brisson, N., Gary, C., Justes, E., Roche, R., Mary, B., Ripoche, D., Zimmer, D., Sierra, J., Bertuzzi, P., Burger, P., 2003b. An overview of the crop model STICS. European Journal of agronomy 18, 309-332.

Brooks, D.B., 2006. An operational definition of water demand management. International Journal of Water Resources Development 22, 521-528.

Burt, C.M., 1995. The Surface Irrigation Manual. Waterman Industries. Inc. Exeter, CA.

Burt, C.M., Clemmens, A.J., Strelkoff, T.S., Solomon, K.H., Bliesner, R.D., Hardy, L.A., Howell, T.A., Eisenhauer, D.E., 1997. Irrigation performance measures: efficiency and uniformity. Journal of irrigation and drainage engineering 123, 423-442.

Busetto, L., Ranghetti, L., 2016. MODIStsp: An R package for automatic preprocessing of MODIS Land Products time series. Computers & geosciences 97, 40-48.

Byrnes, K.J., 1992. Water users associations in World Bank-assisted irrigation projects in Pakistan.

Caballero, R., Bustos, A., Roman, R., 2001. Soil salinity under traditional and improved irrigation schedules in central Spain. Soil Science Society of America Journal 65, 1210-1218.

Cai, X., Sharma, B.R., Matin, M.A., Sharma, D., Gunasinghe, S., 2010. An assessment of crop water productivity in the Indus and Ganges river basins: Current status and scope for improvement. IWMI.

Cardon, G., Letey, J., 1992. Plant water uptake terms evaluated for soil water and solute movement models. Soil Science Society of America Journal 56, 1876-1880.

Cheema, M., Immerzeel, W., Bastiaanssen, W., 2014. Spatial quantification of groundwater abstraction in the irrigated Indus basin. Groundwater 52, 25-36.

Chen, B., Ouyang, Z., Sun, Z., Wu, L., Li, F., 2013. Evaluation on the potential of improving border irrigation performance through border dimensions optimization: a case study on the irrigation districts along the lower Yellow River. Irrigation science 31(4), 715-728.

Chen, C., Pang, Y., Pan, X., Zhang, L., 2015. Impacts of climate change on cotton yield in China from 1961 to 2010 based on provincial data. Journal of Meteorological Research 29, 515-524.

Chhabra, R., 2017. Soil salinity and water quality. Routledge.

Chylek, P., Li, J., Dubey, M., Wang, M., Lesins, G., 2011. Observed and model simulated 20th century Arctic temperature variability: Canadian earth system model CanESM2. Atmospheric Chemistry and Physics Discussions 11, 22893-22907.

Cicek, N., Erdogan, M., Yucedag, C., Cetin, M., 2022. Improving the Detrimental Aspects of Salinity in Salinized Soils of Arid and Semi-arid Areas for Effects of Vermicompost Leachate on Salt Stress in Seedlings. Water, Air, & Soil Pollution 233, 1-9.

CIESIN, 2005. Gridded Population of the World Version 3 (GPWv3), Palisades NY, Socioeconomic Data and Applications Center (SEDAC), Columbia University.

Clemmens, A., El-Haddad, Z., Strelkoff, T., 1999. Assessing the potential for modern surface irrigation in Egypt. Transactions of the ASAE 42(4), 995.

Combalicer, E.A., Lee, S.H., Ahn, S., Kim, D.Y., Im, S., 2008. Modeling water balance for the small-forested watershed in Korea. KSCE Journal of Civil Engineering 12, 339-348.

Condon, M., Kriens, D., Lohani, A., Sattar, E., 2014. Challenge and response in the Indus Basin. Water Policy 16, 58-86.

Connor, J., Schwabe, K., King, D., Villacampa Esteve, Y., Brebbia, C., Prats Rico, D., 2008. Irrigation to meet growing food demand with climate change, salinity and water trade. Second international conference on sustainable irrigation management, Alicante, 2008. WIT Press, pp. 43-52.

Connor, J.D., Schwabe, K., King, D., Knapp, K., 2012. Irrigated agriculture and climate change: the influence of water supply variability and salinity on adaptation. Ecological Economics 77, 149-157.

Connor, R., 2015. The United Nations world water development report 2015: water for a sustainable world. UNESCO publishing.

Corwin, D.L., 2021. Climate change impacts on soil salinity in agricultural areas. European Journal of Soil Science 72, 842-862.

CRS, P., 2017. District wise crops final estimates data book 2016-17. Directorate of Agriculture, Crop Reporting Service, Punjab, Pakistan, Lahore. http://www.amis.pk/Agristatistics/DistrictWise/2016-17.pdf. (accessed:16 May, 2020).

D'Urso, G., Menenti, M., Santini, A., 1999. Regional application of one-dimensional water flow models for irrigation management. Agricultural Water Management 40, 291-302.

Dagès, C., Voltz, M., Lacas, J.-G., Huttel, O., Negro, S., Louchart, X., 2008. An experimental study of water table recharge by seepage losses from a ditch with intermittent flow. Hydrological Processes: An International Journal 22, 3555-3563.

Datta, K., De Jong, C., 2002. Adverse effect of waterlogging and soil salinity on crop and land productivity in northwest region of Haryana, India. Agricultural Water Management 57(3), 223-238.

de Loë, R., Bjornlund, H., Villacampa Esteve, Y., Brebbia, C., Prats Rico, D., 2008. Irrigation and water security: the role of economic instruments and governance. Second international conference on sustainable irrigation management, Alicante, 2008. WIT Press, pp. 35-42.

De Pascale, S., Dalla Costa, L., Vallone, S., Barbieri, G., Maggio, A., 2011. Increasing water use efficiency in vegetable crop production: from plant to irrigation systems efficiency. HortTechnology 21, 301-308.

de Vos, A., Bruning, B., van Straten, G., Oosterbaan, R., Rozema, J., van Bodegom, P., 2016. Crop salt tolerance under controlled field conditions in The Netherlands, based on trials conducted at Salt Farm Texel. Salt Farm Texel.

de Vries, T.T., Anwar, A.A., 2015. Equitable canal water allocation. World Environmental and Water Resources Congress 2015, pp. 736-744.

de Wit, C.T., 1958. Transpiration and crop yields. Versl. Landbouwk. Onderz. 64. 6.

Dehghanisanij, H., Oweis, T., Qureshi, A.S., 2006. Agricultural water use and management in arid and semi-arid areas: current situation and measures for improvement. Annals of Arid Zone 45(2), 1-24.

Dench, W.E., Morgan, L.K., 2021. Unintended consequences to groundwater from improved irrigation efficiency: Lessons from the Hinds-Rangitata Plain, New Zealand. Agricultural Water Management 245, 106530.

Deng, X.-P., Shan, L., Zhang, H., Turner, N.C., 2006. Improving agricultural water use efficiency in arid and semiarid areas of China. Agricultural water management 80, 23-40.

Dennis, H.a.N.W.T., 2002. Precision Irrigation in South Africa. Internation Farm Management Congress, Wageningen, The Netherland, http://ageconsearch.umn.edu/bitstream/7023/4/cp02de01.pdf.

Devia, G.K., Ganasri, B.P., Dwarakish, G.S., 2015. A review on hydrological models. Aquatic procedia 4, 1001-1007.

DGA, 2011. Punjab Irrigated Agriculture Productivity Improvement Project. Directorate General Agriculture. PC1, Lahore, Punjab http://http://www.ofwm.agripunjab.gov.pk/pipip (accessed 15 January, 2020).

Doherty, J., 1994. PEST: a unique computer program for model-independent parameter optimisation. Water Down Under 94: Groundwater/Surface Hydrology Common Interest Papers; Preprints of Papers, p. 551.

Doorenbos, J., Kassam, A., 1979. Yield response to water. Irrigation and drainage paper 33, 257.

Dougherty, T., Hall, A., 1995. Environmental impact assessment of irrigation and drainage projects. Food & Agriculture Org.

Dregne, H.E., Mojallali, H., 1969. Salt-fertilizer-specific ion interactions in soil.

Droogers, P., Bastiaanssen, W., 2002. Irrigation performance using hydrological and remote sensing modeling. Journal of Irrigation and Drainage Engineering 128, 11-18.

Droogers, P., Bastiaanssen, W., Beyazgül, M., Kayam, Y., Kite, G., Murray-Rust, H., 2000. Distributed agro-hydrological modeling of an irrigation system in western Turkey. Agricultural Water Management 43, 183-202.

Dziegielewski, B., 2003. Strategies for managing water demand. Water Resources Update 126, 29-39.

Esmaili, E., Kapourchal, S.A., Malakouti, M.J., Homaee, M., 2008. Interactive effect of salinity and two nitrogen fertilizers on growth and composition of sorghum. Plant Soil Environ 54, 537-546.

Esteve, Y.V., and, C.A.B., Rico, D.P., 2008. Sustainable Irrigation Management, Technologies and Policies II. WIT Press Southhampton, Boston, UK.

Fan, X., Pedroli, B., Liu, G., Liu, Q., Liu, H., Shu, L., 2012. Soil salinity development in the yellow river delta in relation to groundwater dynamics. Land Degradation & Development 23, 175-189.

FAO, 2011. AQUASTAT Transboundary River Basins – Indus River Basin.Food and Agriculture Organization of the United Nations (FAO). Rome, Italy. http://www.fao.org/nr/Water/aquastat/basins/indus/indus-CP_eng.pdf.

FAO, 2015. Pakistan Water Resources. Food & Agriculture Organization of the United Nations.

Farooq, O., 2013. Pakistan economic survey 2012-13: Agriculture. Ministry of Finance, Islamabad, Pakistan.

Feddes, R., Kowalik, P., Zaradny, H., 1978. Simulation model of the water balance of a cropped soil. *Simulation Monograph*. PUDOC, Wageningen, The Netherlands, p. 189.

Feddes, R.A., 1971. Water, heat and crop growth. H. Veenman en Zonnen NV; Institute for Land and Water.

Feddes, R.A., 1985. Crop water use and dry matter production: state of the art. ICW technical bulletin new series. ICW.

Feddes, R.A., 2007. Assessing crop water productivity from field to regional scale under a changing climate. ICID. Pavia, Italy.

Feinerman, E., Yaron, D., Bielorai, H., 1982. Linear crop response functions to soil salinity with a threshold salinity level. Water Resources Research 18, 101-106.

Ferguson, W., Hedlin, R., 1963. Effect of soluble salts on plant response to and absorption of phosphorus. Canadian Journal of Soil Science 43, 210-218.

Fernández, J., Alcon, F., Diaz-Espejo, A., Hernandez-Santana, V., Cuevas, M., 2020a. Water use indicators and economic analysis for on-farm irrigation decision: A case study of a super high density olive tree orchard. Agricultural Water Management 237, 106074.

Fernández, J., Alcon, F., Diaz-Espejo, A., Hernandez-Santana, V., Cuevas, M., 2020b. Water use indicators and economic analysis for on-farm irrigation decision: A case study of a super high density olive tree orchard. Agricultural Water Management, 106074.

Ferrer-Alegre, F., Stockle, C., 1999. A model for assessing crop response to salinity. Irrigation Science 19, 15-23.

Ferrer, F., Stockle, C., 1996. A model for assessing crop response and water management in saline conditions. Water Reports (FAO).

Flexas, J., Galmés, J., Gallé, A., Gulías, J., Pou, A., Ribas-Carbo, M., Tomàs, M., Medrano, H., 2010. Improving water use efficiency in grapevines: potential physiological targets for biotechnological improvement. Australian Journal of Grape and Wine Research 16, 106-121.

Flörke, M., Schneider, C., McDonald, R.I., 2018. Water competition between cities and agriculture driven by climate change and urban growth. Nature Sustainability 1, 51-58.

Foster, S., Pulido-Bosch, A., Vallejos, Á., Molina, L., Llop, A., MacDonald, A.M., 2018. Impact of irrigated agriculture on groundwater-recharge salinity: a major sustainability concern in semi-arid regions. Hydrogeology Journal 26, 2781-2791.

Gagnon, S., Singh, B., Rousselle, J., Roy, L., 2005. An application of the statistical downscaling model (SDSM) to simulate climatic data for streamflow modelling in Québec. Canadian Water Resources Journal 30, 297-314.

Garg, N., Hassan, Q., 2007. Alarming scarcity of water in India. Current Science 93(7), 932-941.

Gérardeaux, E., Sultan, B., Palaï, O., Guiziou, C., Oettli, P., Naudin, K., 2013. Positive effect of climate change on cotton in 2050 by CO 2 enrichment and conservation agriculture in Cameroon. Agronomy for sustainable development 33, 485-495.

Ghassemi, F., Jakeman, A.J., Nix, H.A., 1995. Salinisation of land and water resources: human causes, extent, management and case studies. CAB international.

Ghazavi, R., Moosavian, S.M.M., 2017. Investigation of Climate Anomalies using the Statistical Downscaling Model (SDSM) in Tabas.

Gilmartin, D., 1994. Scientific empire and imperial science: Colonialism and irrigation technology in the Indus Basin. Journal of Asian Studies 53, 1127.

Gleeson, T., Wada, Y., Bierkens, M.F., Van Beek, L.P., 2012. Water balance of global aquifers revealed by groundwater footprint. Nature 488, 197-200.

Goldfarb, R.S., Adams, A.V., 1960. Pakistan - Indus Basin Multi-Purpose Project - Negotiations 04. Records of the South Asia Regional Office (WB IBRD/IDA SAR).

GoP, 2009. Agriculture Statistics of Pakistan 2008-09. Ministry of Food and Agriculture, Economic Wing, Islamabad Governament of Pakistan.

Grafton, R.Q., Williams, J., Perry, C.J., Molle, F., Ringler, C., Steduto, P., Udall, B., Wheeler, S., Wang, Y., Garrick, D., 2018. The paradox of irrigation efficiency. Science 361, 748-750.

Gupta, S., Deshpande, R., 2004. Water for India in 2050: first-order assessment of available options. Current science 86, 1216-1224.

Habib, Z., 2021. Water availability, use and challenges in Pakistan-Water sector challenges in the Indus Basin and impact of climate change. Food & Agriculture Org.

Haj-Amor, Z., Bouri, S., 2019. Use of HYDRUS-1D–GIS tool for evaluating effects of climate changes on soil salinization and irrigation management. Archives of Agronomy and Soil Science.

Hamid, A., Mahmood, K., Mahmood, S., 2000. Farmer organization's potential for reducing waterlogging and salinity through improved equity and reliability of irrigation water: Evidence from Hakra 4-R Distributary in Southern Punjab.

Hanks, R., 1974. Model for predicting plant yield as influenced by water use. Agronomy journal 66, 660-665.

Hashmi, M.Z., Shamseldin, A.Y., Melville, B.W., 2011. Comparison of SDSM and LARS-WG for simulation and downscaling of extreme precipitation events in a watershed. Stochastic Environmental Research and Risk Assessment 25, 475-484.

Hassan, N.A., Drew, J.V., Knudsen, D., Olson, R.A., 1970. Influence of soil salinity on production of dry matter and uptake and distribution of nutrients in barley and corn: I. Barley (Hordeum vulgare L.) 1. Agronomy Journal 62, 43-45.

Hassanli, A.M., Ahmadirad, S., Beecham, S., 2010. Evaluation of the influence of irrigation methods and water quality on sugar beet yield and water use efficiency. Agricultural Water Management 97, 357-362.

Hewitt, K., 2011. Glacier change, concentration, and elevation effects in the Karakoram Himalaya, Upper Indus Basin. Mountain Research and Development 31, 188-200.

Hoffman, G., Rhoades, J., Letey, J., Fang, S., 1990. Salinity management. Management of Farm Irrigation Systems. American Society of Agricultural Engineers, St. Joseph, MI. 1990. p 667-715, 17 fig, 9 tab, 15 ref.

Hoffman, G.J., 2006. An evaluation of irrigation and salinity research programs along the River Murray, Australia. Cooperative Research centre for irrigation futures, viewed.

Hoffman, G.J., Van Genuchten, M.T., 1983. Soil properties and efficient water use: Water management for salinity control. Limitations to efficient water use in crop production, 73-85.

Horneck, D.A., Ellsworth, J.W., Hopkins, B.G., Sullivan, D.M., Stevens, R.G., 2007. Managing salt-affected soils for crop production.

Hossain, M.S., 2019. Present scenario of global salt affected soils, its management and importance of salinity research. Int. Res. J. Biol. Sci 1, 1-3.

Howell, T.A., 2003. Irrigation efficiency. Encyclopedia of water science 467, 500.

Howell, T.A., Stewart, B.A., 2003. The Irrigation Efficiency, Encyclopedia of water science. Marcel Dekker.

Hu, Y., Maskey, S., Uhlenbrook, S., 2013. Downscaling daily precipitation over the Yellow River source region in China: a comparison of three statistical downscaling methods. Theoretical and applied climatology 112, 447-460.

Huang, G., Hoekstra, A.Y., Krol, M.S., Jägermeyr, J., Galindo, A., Yu, C., Wang, R., 2020. Water-saving agriculture can deliver deep water cuts for China. Resources, conservation and recycling 154, 104578.

Hurd, B.H., Callaway, M., Smith, J., Kirshen, P., 2004. Climatic change and us water resources: from modelled watershed impacts to national estimates JAWRA Journal of the American Water Resources Association 40, 129-148.

Hussain, I., Hussain, Z., Sial, M.H., Akram, W., Farhan, M., 2011. Water balance, supply and demand and irrigation efficiency of Indus Basin. Pakistan Economic and Social Review, 13-38.

Hussain, I., Sakthivadivel, R., Amarasinghe, U., Mudasser, M., Molden, D., 2003. Land and water productivity of wheat in the western Indo-Gangetic plains of India and Pakistan: A comparative analysis. IWMI.

Ibrakhimov, M., Park, S., Vlek, P.L., 2004. Development of groundwater salinity in a region of the lower Amu-Darya River, Khorezm, Uzbekistan. Agriculture in Central Asia: Research for Development. Proceedings of a Symposium held at the American Society of Agronomy Annual Meetings at Indianapolis, Indiana, USA, ICARDA, Aleppo, Syria, pp. 56-75.

Iglesias, A., Garrote, L., Flores, F., Moneo, M., 2007. Challenges to manage the risk of water scarcity and climate change in the Mediterranean. Water resources management 21, 775-788.

Ijaz, M., Nawaz, M., Ali, H., Hussain, M., Chattha, M.U., Nawaz, A., Hussain, S., Ahmad, S., 2019. Advanced Production Technologies of Oilseed Crops. Agronomic Crops. Springer, pp. 313-334.

Ikram, F., Afzaal, M., Bukhari, S., Ahmed, B., 2016. Past and future trends in frequency of heavy rainfall events over Pakistan. Pakistan Journal of Meteorology Vol 12.

Ines, A.V., Honda, K., Gupta, A.D., Droogers, P., Clemente, R.S., 2006. Combining remote sensing-simulation modeling and genetic algorithm optimization to explore water management options in irrigated agriculture. agricultural water management 83, 221-232.

Irshad, M., Eneji, A., Yasuda, H., 2008. Comparative effect of nitrogen sources on maize under saline and non-saline conditions. Journal of Agronomy and Crop Science 194, 256-261.

Işık, M.F., Sönmez, Y., Yılmaz, C., Özdemir, V., Yılmaz, E.N., 2017. Precision irrigation system (PIS) using sensor network technology integrated with IOS/Android application. Applied Sciences 7, 891.

Israelsen, O.W., Blaney, H.F., 1946. Water application efficiencies in irrigation. US Department of Agriculture, Soil Conservation Service, Research.

Jehangir, W.A., Masih, I., Ahmed, S., Gill, M.A., Ahmad, M., Mann, R.A., Chaudhary, M.R., Qureshi, A.S., Turral, H., 2007. Sustaining crop water productivity in rice-wheat systems of South Asia: A case study from the Punjab, Pakistan. IWMI.

Jehangir, W.A., Mudasser, M., Mahmood-ul-Hassan, A., 1998. Multiple uses of irrigation water in the Hakra 6-R, Distributary Command Area, Punjab, Pakistan. IWMI.

Jehangir, W.A., Murray-Rust, H., Masih, I., Shimizu, K., 2002. Sustaining Crop and Water Productivity in Irrigated Rice-Wheat Systems. Workshop on Rice-Wheat Systems in Pakistan, p. 49.

Jensen, M.E., 1967. Evaluation Irrigation Efficiency. Journal of the Irrigation and Drainage Division 93, 83-98.

Jensen, M.E., 2007. Beyond irrigation efficiency. Irrigation Science 25, 233-245.

Jhorar, R., Van Dam, J., Bastiaanssen, W., Feddes, R., 2004. Calibration of effective soil hydraulic parameters of heterogeneous soil profiles. Journal of Hydrology 285, 233-247.

Jolly, I., Williamson, D., Gilfedder, M., Walker, G., Morton, R., Robinson, G., Jones, H., Zhang, L., Dowling, T., Dyce, P., 2001. Historical stream salinity trends and catchment salt balances in the Murray–Darling Basin, Australia. Marine and Freshwater Research 52, 53-63.

Jones, H.G., 2004. Irrigation scheduling: advantages and pitfalls of plant-based methods. Journal of experimental botany 55(407), 2427-2436.

Jurriëns, R., Mollinga, P., Wester, P., 1996. Scarcity by design: Protective irrigation in India and Pakistan.

Kahlown, M.A., Azam, M., 2002. Individual and combined effect of waterlogging and salinity on crop yields in the Indus basin. Irrigation and Drainage: The journal of the International Commission on Irrigation and Drainage 51, 329-338.

Kahlown, M.A., Iqbal, M., Skogerboe, G.V., Rehman, S., 1998. Waterlogging, salinity and crop yield relationships. Fordwah Eastern Sadiqia (south) Irrigation and Drainage Project. Mona reclamation experimental project (MREP) and International irrigation management institute (IIMI), Pakistan. IIMI Report No. R-73.

Kalnay, E., Kanamitsu, M., Kistler, R., Collins, W., Deaven, D., Gandin, L., Iredell, M., Saha, S., White, G., Woollen, J., 1996. The NCEP/NCAR 40-year reanalysis project. Bulletin of the American meteorological Society 77, 437-472.

Kamyab-Talesh, F., Mostafazadeh-Fard, B., Vazifedoust, M., Navabian, M., Shayannejad, M., 2015. Evaluation and simulation of crops yield under different soil and irrigation water salinities using swap model. Advances in Environmental Biology, 335-346.

Katerji, N., 1995. Crop response to saline water stress: empirical and mecanistic approaches. Comptes Rendus de l'Academie d'Agriculture de France (France).

Katerji, N., Van Hoorn, J., Hamdy, A., Mastrorilli, M., 2003. Salinity effect on crop development and yield, analysis of salt tolerance according to several classification methods. Agricultural water management 62, 37-66.

Keating, B.A., Carberry, P.S., Hammer, G.L., Probert, M.E., Robertson, M.J., Holzworth, D., Huth, N.I., Hargreaves, J.N., Meinke, H., Hochman, Z., 2003. An overview of APSIM, a model designed for farming systems simulation. European journal of agronomy 18, 267-288.

Kendy, E., Zhang, Y., Liu, C., Wang, J., Steenhuis, T., 2004. Groundwater recharge from irrigated cropland in the North China Plain: case study of Luancheng County, Hebei Province, 1949–2000. Hydrological Processes 18, 2289-2302.

Khan, A., Iqbal, N., Ashraf, M., Sheikh, A.A., 2016. Groundwater investigations and mapping in the upper Indus plain. Pakistan Council of Research in Water Resources (PCRWR).

Khan, M.N., Hassnain Shah, A.A., Abassi, S.S., 2013. Characterization and water productivity of irrigated farms at project site Fateh Jang: a case study. Int. Res. J. Social Sci 2, 6-12.

Khorsandi, F., Anagholi, A., 2009. Reproductive compensation of cotton after salt stress relief at different growth stages. Journal of Agronomy and Crop Science 195, 278-283.

Kijne, J.W., 1996. Water and salinity balances for irrigated agriculture in Pakistan. IWMI.

Kijne, J.W., Barker, R., Molden, D.J., 2003. Water productivity in agriculture: limits and opportunities for improvement. Cabi.

Kirby, M., Ahmad, M.-u.-D., 2022. Can Pakistan achieve sustainable water security? Climate change, population growth and development impacts to 2100. Sustainability Science, 1-14.

Konar, M., Dalin, C., Hanasaki, N., Rinaldo, A., Rodriguez-Iturbe, I., 2012. Temporal dynamics of blue and green virtual water trade networks. Water Resources Research 48.

Konikow, L.F., Kendy, E., 2005. Groundwater depletion: A global problem. Hydrogeology Journal 13, 317-320.

Kooij, S.v.d., Zwarteveen, M., Boesveld, H., Kuper, M., 2013. The efficiency of drip irrigation unpacked. Agricultural Water Management 123, 103-110.

Kour, R., Patel, N., Krishna, A.P., 2016. Climate and hydrological models to assess the impact of climate change on hydrological regime: a review. Arabian Journal of Geosciences 9, 1-31.

Kristvik, E., Kleiven, G.H., Lohne, J., Muthanna, T.M., 2018. Assessing the robustness of raingardens under climate change using SDSM and temporal downscaling. Water Science and Technology 77, 1640-1650.

Kroes, J., van Dam, J., 2003. Reference Manual SWAP; version 3.0. 3. Alterra.

Kroes, J., Van Dam, J., Groenendijk, P., Hendriks, R., Jacobs, C., 2008. SWAP version 3.2: Theory description and user manual. Alterra Wageningen, The Netherlands.

Kroes, J.G., Van Dam, J.C., Bartholomeus, R.P., Groenendijk, P., M, H., Hendriks, R., Mulder, H.M., Supit, I., Van Walsum, P.E.V., Jacobs, C., 2017. SWAP version 4. Theory description and user manual. Alterra.

Kumar, R., Kumar, M., Farooq, Z., Dadhich, S.M., 2017. Evaluation of models and approaches for effective rainfall in irrigated agriculture–An overview. Journal of Soil and Water Conservation 16, 32-36.

Laghari, A.N., Vanham, D., Rauch, W., Gelfan, A., 2012. The Indus basin in the framework of current and future water resources management. Hydrology & Earth System Sciences 16, 1063.

Laghari, K., Qasim, Lashari, B.K., Memon, H.M., 2010. Water Use Efficiency of Cotton and Wheat Crops at Various Management Allowed Depletion in Lower Indus Basin. Mehran university research journal of engineering & technology 29(4), 661-672.

Latif, M., 2007. Spatial productivity along a canal irrigation system in Pakistan. Irrigation and Drainage 56, 509-521.

Latif, M., Ahmad, M.Z., 2009. Groundwater and soil salinity variations in a canal command area in Pakistan. Irrigation and Drainage: The journal of the International Commission on Irrigation and Drainage 58, 456-468.

Latif, M., Haider, S.S., Rashid, M.U., 2016. Adoption of high efficiency irrigation systems to overcome scarcity of irrigation water in Pakistan. Proc. Pak. Acad. Sci. B Life Environ. Sci 53(4), 243-252.

Latif, M., Pomee, M.S.S., 2003. Impacts of institutional reforms on irrigated agriculture in Pakistan. Irrigation and drainage systems 17, 195-212.

Läuchli, A., Epstein, E., 1990. Plant responses to saline and sodic conditions. Agricultural salinity assessment and management 71, 113-137.

Lecina, S., Playán, E., Isidoro, D., Dechmi, F., Causapé, J., Faci, J.M., 2005. Irrigation evaluation and simulation at the Irrigation District V of Bardenas (Spain). Agricultural Water Management 73(3), 223-245.

Lenzen, M., Moran, D., Bhaduri, A., Kanemoto, K., Bekchanov, M., Geschke, A., Foran, B., 2013. International trade of scarce water. Ecological Economics 94, 78-85.

Letey, J., Dinar, A., Knapp, K.C., 1985. Crop-water production function model for saline irrigation waters. Soil Science Society of America Journal 49, 1005-1009.

Letey, J., Hoffman, G.J., Hopmans, J.W., Grattan, S.R., Suarez, D., Corwin, D.L., Oster, J.D., Wu, L., Amrhein, C., 2011. Evaluation of soil salinity leaching requirement guidelines. Agricultural water management 98, 502-506.

Liaqat, U.W., Awan, U.K., McCabe, M.F., Choi, M., 2016. A geo-informatics approach for estimating water resources management components and their interrelationships. Agricultural Water Management 178, 89-105.

Liaqat, U.W., Choi, M., Awan, U.K., 2015. Spatio-temporal distribution of actual evapotranspiration in the Indus Basin Irrigation System. Hydrological processes 29, 2613-2627.

Lovenstein, H., Lantinga, R., Rabbinge, R., Van Keulen, H., 1995. Principles of Production Ecology: Text of course F 300-001. Fig 8, 121.

Lunin, J., Gallatin, M., 1965. Salinity-Fertility Interactions in Relation to the Growth and Composition of Beans. I. Effect of N, P, and K 1. Agronomy Journal 57, 339-342.

Maas, E., 1990. Crop salt tolerance. In'Agricultural salinity assessment and management', KK Tanji. ASCE Manuals and Reports on Engineering practice.

Maas, E.V., Grattan, S., 1999. Crop yields as affected by salinity. Agricultural drainage 38, 55-108.

Maas, E.V., Hoffman, G.J., 1977. Crop salt tolerance–current assessment. Journal of the irrigation and drainage division 103(2), 115-134.

Macneil, M., 2018. Overcoming the “paradox” of irrigation efficiency. International Food Policy Research Institute https://www.ifpri.org/blog/overcoming-%E2%80%9Cparadox%E2%80%9D-irrigation-efficiency-0#:~:text=However%2C%20there%20is%20a%20paradox,water%20available%20for%20other%20purposes. Access on 02/05/2022.

Mahadevan, I., 2006. Agricultural terms in the Indus Script. Journal of Tamil Studies 70, 64-76.

Mahar, G.A., Zaigham, N.A., 2010. Identification of climate changes in the lower indus basin, sindh, pakistan. Journal of Basic & Applied Sciences 6.

Majeed, A., Stockle, C.O., King, L.G., 1994. Computer model for managing saline water for irrigation and crop growth: preliminary testing with lysimeter data. Agricultural water management 26, 239-251.

Malhotra, S., 1982. Warabandi system and its infrastructure. Central Board of Irrigation and Power New Delhi, India.

Malik, A., Tayyab, H., Ullah, A., Talha, M., 2021. Dynamics of salinity and land use in Punjab Province of Pakistan. Pak J Agric Res 34, 16-22.

Mancosu, N., Snyder, R.L., Kyriakakis, G., Spano, D., 2015. Water scarcity and future challenges for food production. Water 7, 975-992.

Maqsood, L., Khalil, T.M., 2013. A review of direct and indirect implications of laser land leveling as agriculture resource conservation technology in Punjab province of Pakistan. 2013 IEEE Global Humanitarian Technology Conference (GHTC). IEEE, pp. 349-354.

Marlet, S., Bouksila, F., Bahri, A., 2009. Water and salt balance at irrigation scheme scale: A comprehensive approach for salinity assessment in a Saharan oasis. Agricultural Water Management 96, 1311-1322.

McCartney, M., Rex, W., Yu, W., Uhlenbrook, S., von Gnechten, R., 2022. Change in Global Freshwater Storage. IWMI Working Paper 202.

McCartney, M., Sullivan, C., Acreman, M.C., McAllister, D., 2001. Ecosystem impacts of large dams. Background paper 2.

McRae, D., Roth, G., Bange, M., 2007. Climate change in cotton catchment communities–a scoping study. Cotton Catchment Communities CRC.

Mearns, L.O., 2009. Methods of downscaling future climate information and applications. White Paper. National Center for Atmospheric Research. Retrieved from www ….

Meier, J., Zabel, F., Mauser, W., 2018. A global approach to estimate irrigated areas–a comparison between different data and statistics. Hydrology and Earth System Sciences 22, 1119-1133.

Miao Q, S.H., Li R, 2017. Modernizing Surface Irrigation and Land Levelling in Hetao with Application of the Decision Support Systems SADREG. Irrigation & Drainage Systems Engineering 6(3), 1-8.

Michel, A.A., 1967. The Indus rivers: A study of the effects of partition. Yale University Press New Haven.

Minacapilli, M., Agnese, C., Blanda, F., Cammalleri, C., Ciraolo, G., D'Urso, G., Iovino, M., Pumo, D., Provenzano, G., Rallo, G., 2009. Estimation of actual evapotranspiration of Mediterranean perennial crops by means of remote-sensing based surface energy balance models. Hydrology and Earth System Sciences 13, 1061-1074.

Minhas, P., Sharma, D., Khosla, B., 1990. Mungbean response to irrigation with waters of different salinities. Irrigation science 11, 57-62.

Mohammad, G., 1964. Waterlogging and salinity in the Indus Plain: a critical analysis of some of the major conclusions of the Revelle Report. The Pakistan Development Review, 357-403.

Mohan Reddy, J., 2013. Design of level basin irrigation systems for robust performance. Journal of irrigation and drainage engineering 139(3), 254-260.

Molden, D., 1997. Accounting for water use and productivity. Iwmi.

Molden, D., 2013. Water for food water for life: A comprehensive assessment of water management in agriculture. Routledge.

Molden, D., Murray-Rust, H., Sakthivadivel, R., Makin, I., 2003. A water-productivity framework for understanding and action. Water productivity in agriculture: Limits and opportunities for improvement. Cabi, International Water Management Institute, Colombo, Sri Lanka, pp. 1-18.

Molden, D.J., Gates, T.K., 1990. Performance measures for evaluation of irrigation-water-delivery systems. Journal of irrigation and drainage engineering 116, 804-823.

Molz, F.J., 1981. Models of water transport in the soil-plant system: A review. Water resources research 17, 1245-1260.

Monteith, J.L., 1965. Evaporation and environment. Symposia of the society for experimental biology. Cambridge University Press (CUP) Cambridge, pp. 205-234.

Moriasi, D.N., Arnold, J.G., Van Liew, M.W., Bingner, R.L., Harmel, R.D., Veith, T.L., 2007. Model evaluation guidelines for systematic quantification of accuracy in watershed simulations. Transactions of the ASABE 50, 885-900.

Mostafazadeh-Fard, B., Mansouri, H., Mousavi, S.-F., Feizi, M., 2009. Effects of different levels of irrigation water salinity and leaching on yield and yield components of wheat in an arid region. Journal of irrigation and drainage engineering 135(1), 32-38.

Msangi, J.P., 2014. Managing water scarcity in Southern Africa: Policy and strategies. Combating water scarcity in Southern Africa, 21-41.

Mu, Q., Zhao, M., Running, S.W., 2011. Improvements to a MODIS global terrestrial evapotranspiration algorithm. Remote sensing of environment 115, 1781-1800.

Mualem, Y., 1976. A new model for predicting the hydraulic conductivity of unsaturated porous media. Water Resour. Res 12(3), 513-522.

Mudasser, M., Hussain, I., Aslam, M., 2001. Constraints to land-and water productivity of wheat in india and pakistan: A comparative analysis. International Water Management, Colombo, Sri Lanka.

Muhammad Aamer, Q.J., Ghulam Mustafa, S. Mahmood, 2015. Soil Fertility Management for Sustainable Agriculture: A case Study of District Bahalnagar, Pakistan. Journal of Natural Sciences Research 5, No. 19, 2015.

Mukherjee, A., Saha, D., Harvey, C.F., Taylor, R.G., Ahmed, K.M., Bhanja, S.N., 2015. Groundwater systems of the Indian Sub-Continent. Journal of Hydrology: Regional Studies 4, 1-14.

Mundorff, M.J., Carrigan Jr, P., Steele, T., Randall, A., 1976. Hydrologic evaluation of salinity control and reclamation projects in the Indus Plain, Pakistan--A summary. US Govt. Print. Off.

Mustafa, D., Wrathall, D., 2011. Indus basin floods of 2010: Souring of a Faustian bargain? Water Alternatives 4.

Narayanamoorthy, A., 2009. Drip and sprinkler irrigation in India: Benefits, potential and future directions. India's water future: Scenarios and issues. Strategic Analyses of National River Linking Project of India. Series 2, 253-266.

Narayanamurthy, S., 1985. Methods for improving canal regulation in Northwest India. New Delhi Office, World Bank. Duplicated.

NGWA, N.G.A., 2016. Facts about global groundwater usage. National Ground Water Association, http://www.ngwa.org/Fundamentals/Documents/globalgroundwater-use-fact-sheet. pdf.

Nielsen, D., Th. Van Genuchten, M., Biggar, J., 1986. Water flow and solute transport processes in the unsaturated zone. Water resources research 22, 89S-108S.

Noorka, I.R., 2011. Sustainable rural development and participatory approach by on-farm water management techniques. Sustainable Agricultural Development. Springer, pp. 139-146.

Noory, H., Van Der Zee, S., Liaghat, A.-M., Parsinejad, M., Van Dam, J., 2011. Distributed agro-hydrological modeling with SWAP to improve water and salt management of the Voshmgir Irrigation and Drainage Network in Northern Iran. Agricultural Water Management 98, 1062-1070.

Nury, A.H., Sharma, A., Marshall, L., Mehrotra, R., 2019. Characterising uncertainty in precipitation downscaling using a Bayesian approach. Advances in Water Resources 129, 189-197.

Nuttall, J., Brady, S., Brand, J., O'Leary, G., Fitzgerald, G., 2012. Heat waves and wheat growth under a future climate. Aust. Soc. Agron. The 16th Australian Agronomy Conference: Climate Change. Available at: http://www.regional.org.au/au/asa/2012/climate-change/8085_nuttalljg.htm. Accessed 26/02/2022, pp. 14-18.

O'Mara, G.T., Duloy, J.H., 1984. Modeling efficient water allocation in a conjunctive use regime: The Indus Basin of Pakistan. Water Resources Research 20, 1489-1498.

Oster, J., 1994. Irrigation with poor quality water. Agricultural water management 25, 271-297.

Oster, J., Letey, J., Vaughan, P., Wu, L., Qadir, M., 2012. Comparison of transient state models that include salinity and matric stress effects on plant yield. Agricultural Water Management 103, 167-175.

Pang, X., Letey, J., 1998. Development and evaluation of ENVIRO-GRO, an integrated water, salinity, and nitrogen model. Soil Science Society of America Journal 62, 1418-1427.

PBS, 2017. Pakistan Bureau of Statistics Population Census-2017. Pakistan. http://www.pbs.gov.pk/content/population-census.

Peña-Arancibia, J.L., Stewart, J.P., Kirby, J.M., 2021. Water balance trends in irrigated canal commands and its implications for sustainable water management in Pakistan: Evidence from 1981 to 2012. Agricultural Water Management 245, 106648.

Pereira, L.S., Oweis, T., Zairi, A., 2002. Irrigation management under water scarcity. Agricultural water management 57, 175-206.

Perry, C., Steduto, P., Karajeh, F., 2017. Does improved irrigation technology save water?

Peter, J.R., 2004. Participatory irrigation management. Participatory Irrigation Management (PIM) Newsletter 6, 1-13.

Phuong, N.M., Schappacher, M., Sikora, A., Ahmad, Z., Muhammad, A., 2015. Real-time water level monitoring using low-power wireless sensor network. Embedded World Conference. Nuremberg, Germany, pp. 24-26.

Pielke Sr, R.A., Wilby, R.L., 2012. Regional climate downscaling: What's the point? Eos, Transactions American Geophysical Union 93, 52-53.

Playán, E., Mateos, L., 2006. Modernization and optimization of irrigation systems to increase water productivity. Agricultural water management 80, 100-116.

Qadir, M., Sharma, B.R., Bruggeman, A., Choukr-Allah, R., Karajeh, F., 2007. Non-conventional water resources and opportunities for water augmentation to achieve food security in water scarce countries. Agricultural water management 87, 2-22.

Quiggin, J., Adamson, D., Chambers, S., Schrobback, P., 2010. Climate change, uncertainty, and adaptation: the case of irrigated agriculture in the Murray–Darling Basin in Australia. Canadian Journal of Agricultural Economics/Revue canadienne d'agroeconomie 58, 531-554.

Qureshi, A., 2014. Conjunctive Water Management in the Fixed Rotational Canal System: A Case Study from Punjab Pakistan. Irrigat Drainage Sys Eng 3(122), 1-6.

Qureshi, A., 2016. Perspectives for bio-management of salt-affected and waterlogged soils in Pakistan. Agroforestry for the Management of Waterlogged Saline Soils and Poor-Quality Waters. Springer, pp. 97-108.

Qureshi, A.L., Gadehi, M.A., Mahessar, A.A., Memon, N.A., Soomro, A.G., Memon, A.H., 2015. Effect of drip and furrow irrigation systems on sunflower yield and water use efficiency in dry area of Pakistan. Am. Eurasian J. Agric. Environ. Sci 15, 1947-1952.

Qureshi, A.S., 2011. Water management in the Indus basin in Pakistan: challenges and opportunities. Mountain Research and Development 31, 252-260.

Qureshi, A.S., Fatima, A., 2012. Sustaining irrigated agriculture for food security: a perspective from Pakistan. On the Occasion of World Water Day.

Qureshi, A.S., Gill, M.A., Sarwar, A., 2010. Sustainable groundwater management in Pakistan: challenges and opportunities. Irrigation and Drainage 59, 107-116.

Qureshi, A.S., McCornick, P.G., Qadir, M., Aslam, Z., 2008. Managing salinity and waterlogging in the Indus Basin of Pakistan. Agricultural Water Management 95, 1-10.

Qureshi, A.S., Perry, C., 2021. Managing water and salt for sustainable agriculture in the Indus Basin of Pakistan. Sustainability 13, 5303.

Qureshi, A.S., Shah, T., Akhtar, M., 2003. The groundwater economy of Pakistan. IWMI.

Qureshi, R., Ashraf, M., 2019. Water security issues of agriculture in Pakistan. PAS Islamabad Pak 1, 41.

Raeisi, L.G., Morid, S., Delavar, M., Srinivasan, R., 2019. Effect and side-effect assessment of different agricultural water saving measures in an integrated framework. Agricultural Water Management 223, 105685.

Raes, D., Munoz, G., 2009. The ETo Calculator. Reference Manual Version 3.

Ragab, R., 2002. A holistic generic integrated approach for irrigation, crop and field management: the SALTMED model. Environmental Modelling & Software 17, 345-361.

Ragab, R., Prudhomme, C., 2002. Sw—soil and Water: climate change and water resources management in arid and semi-arid regions: prospective and challenges for the 21st century. Biosystems engineering 81(1), 3-34.

Rahimtoola, A., 1965. Power development in West Pakistan. Electronics and Power 11, 370-373.

Raine, S., Meyer, W., Rassam, D., Hutson, J.L., Cook, F., 2007. Soil–water and solute movement under precision irrigation: knowledge gaps for managing sustainable root zones. Irrigation Science 26(1), 91-100.

Raine, S.R., Meyer, W., Rassam, D., Hutson, J., Cook, F., 2005. Soil-water and salt movement associated with precision irrigation systems-research investment opportunities.

Rawlins, S., 1973. Principles of managing high frequency irrigation. Soil Science Society of America Journal 37, 626-629.

Raza, A., Khanzada, S., Ahmad, S., Afzal, M., 2012a. Improving water use efficiency for wheat production in Pakistan. Pakistan Journal of Agriculture: Agricultural Engineering Veterinary Sciences (Pakistan).

Raza, A., Zaka, M., Khurshid, T., Nawaz, M., Ahmed, W., Afzal, M., 2020. Different irrigation systems affect the yield and water use efficiency of kinnow mandarin (Citrus Reticulata Blanco.). JAPS: Journal of Animal & Plant Sciences 30.

Raza, S.A., Ali, Y., Mehboob, F., 2012b. Role of agriculture in economic growth of Pakistan.

Reddy, K., Robana, R., Hodges, H.F., Liu, X., McKinion, J.M., 1998. Interactions of CO2 enrichment and temperature on cotton growth and leaf characteristics. Environmental and Experimental Botany 39, 117-129.

Reddy, V.R., Reddy, P.P., 2005. How participatory is participatory irrigation management? Water users' associations in Andhra Pradesh. Economic and political Weekly, 5587-5595.

Revelle, R., 1964. Report on land and water development in the Indus Plain. The White House--Department of Interior Panel on Waterlogging and Salinity in West Pakistan.

Rhoades, J., 1990. Overview. Diagnosis of salinity problems and selection of control practices. ASCE, NEW YORK, NY,(USA), 1990., 18-41.

Riahi, K., Grübler, A., Nakicenovic, N., 2007. Scenarios of long-term socio-economic and environmental development under climate stabilization. Technological Forecasting and Social Change 74, 887-935.

Riahi, K., Krey, V., Rao, S., Chirkov, V., Fischer, G., Kolp, P., Kindermann, G., Nakicenovic, N., Rafai, P., 2011. RCP-8.5: exploring the consequence of high emission trajectories. Climatic Change 109, 33-57.

Rijsberman, F.R., 2006. Water scarcity: Fact or fiction? Agricultural water management 80, 5-22.

Ringler, C., Anwar, A., 2013. Water for food security: challenges for Pakistan. Water International 38, 505-514.

Ritchie, J., Alagarswamy, G., 1989. Genetic coefficients for CERES models. Modeling the growth and development of sorghum and pearl millet. Ed. by Virmani, SM, Tandon, HLS, and G. Alagarswamy. Research Bullettin, 27-29.

Rizwan, M., Bakhsh, A., Li, X., Anjum, L., Jamal, K., Hamid, S., 2018. Evaluation of the impact of water management technologies on water savings in the lower chenab canal command area, Indus River Basin. Water 10(6), 681.

Rodrigues, G.C., Pereira, L.S., 2009. Assessing economic impacts of deficit irrigation as related to water productivity and water costs. Biosystems engineering 103, 536-551.

Rosegrant, M.W., Cai, X., Cline, S.A., 2002. World water and food to 2025: dealing with scarcity. Intl Food Policy Res Inst.

Running, S.W., Mu, Q., Zhao, M., Moreno, A., 2017. MODIS global terrestrial evapotranspiration (ET) product (NASA MOD16A2/A3) NASA earth observing system MODIS land algorithm. NASA: Washington, DC, USA.

Ryden, J., Syers, J., 1975. Rationalization of ionic strength and cation effects on phosphate sorption by soils. Journal of Soil Science 26, 395-406.

Sadoff, C.W., Grey, D., 2002. Beyond the river: the benefits of cooperation on international rivers. Water policy 4, 389-403.

Sajjad Ali, M., 2013. The natural refuge policy for Bt cotton (Gossypium L.) in Pakistan–a situation analysis. Acta Agrobotanica Vol. 66 (2), 2013: 3–12.

Sánchez, N., Martínez-Fernández, J., Calera, A., Torres, E., Pérez-Gutiérrez, C., 2010. Combining remote sensing and in situ soil moisture data for the application and validation of a distributed water balance model (HIDROMORE). Agricultural Water Management 98, 69-78.

Sanchis-Ibor, C., García-Mollá, M., Avellà-Reus, L., 2017. Effects of drip irrigation promotion policies on water use and irrigation costs in Valencia, Spain. Water Policy 19(1), 165-180.

Santoso, H., 2003. Towards an integrated model for assessing the effects of changes in climate and land use patterns on the quantity and variability of river flows in indonesia. The University of Waikato.

Scheierling, S.M., Young, R.A., Cardon, G.E., 2006. Public subsidies for water-conserving irrigation investments: Hydrologic, agronomic, and economic assessment. Water Resources Research 42.

Scherer, T.F., Seelig, B., Franzen, D., 1996. Soil, water and plant characteristics important to irrigation.

Sepahvand, A., Singh, B., Sihag, P., Nazari Samani, A., Ahmadi, H., Fiz Nia, S., 2021. Assessment of the various soft computing techniques to predict sodium absorption ratio (SAR). ISH Journal of Hydraulic Engineering 27, 124-135.

Shafeeque, M., Cheema, M.J.M., Sarwar, A., Hussain, M.W., 2016. Quantification of groundwater abstraction using SWAT model in Hakra branch canal system of Pakistan. Pakistan Journal of Agricultural Sciences 53.

Shah, T., 1988. Externality and equity implications of private exploitation of ground-water resources. Agricultural Systems 28, 119-139.

Shahani, W.A., Kaiwen, F., Memon, A., 2016. Impact of laser leveling technology on water use efficiency and crop productivity in the cotton-wheat cropping system in Sindh. International Journal of Research Granthaalayah 4(2), 220-231.

Shahid, M.A., Chauhdary, J.N., Usman, M., Qamar, M.U., Shabbir, A., 2022. Assessment of Water Productivity Enhancement and Sustainability Potential of Different Resource Conservation Technologies: A Review in the Context of Pakistan. Agriculture 12, 1058.

Shahid, S.A., Abdelfattah, M.A., Taha, F.K., 2013. Developments in soil salinity assessment and reclamation: innovative thinking and use of marginal soil and water resources in irrigated agriculture. Springer Science & Business Media.

Shahid, S.A., Zaman, M., Heng, L., 2018. Introduction to soil salinity, sodicity and diagnostics techniques. Guideline for salinity assessment, mitigation and adaptation using nuclear and related techniques. Springer, pp. 1-42.

Shambat, S., 1980. The Effects of Electrolyte Concentration and Sodium Adsorption Ratio on Phosphate Retension by Soil.

Sharma, B., Amarasinghe, U., Xueliang, C., de Condappa, D., Shah, T., Mukherji, A., Bharati, L., Ambili, G., Qureshi, A., Pant, D., 2013. The Indus and the Ganges: river basins under extreme pressure. Water, Food and Poverty in River Basins. Routledge, pp. 40-68.

Sharma, D.K., Singh, A., 2017. Current trends and emerging challenges in sustainable management of salt-affected soils: a critical appraisal. Bioremediation of salt affected soils: an Indian perspective. Springer, pp. 1-40.

Sharma, D.L., Moghe, V., Mathur, C., 1968. Salinity and alkalinity problem and fertility status of soils of Pali district (Rajasthan). J. Indian Soc. Soil Sci 16, 263-269.

Shelia, V., Hansen, J., Sharda, V., Porter, C., Aggarwal, P., Wilkerson, C.J., Hoogenboom, G., 2019. A multi-scale and multi-model gridded framework for forecasting crop production, risk analysis, and climate change impact studies. Environmental Modelling & Software 115, 144-154.

Shrestha, A.B., Wagle, N., Rajbhandari, R., 2019. A review on the projected changes in climate over the Indus Basin. Indus River Basin, 145-158.

Shrivastava, P., Parikh, M., Sawani, N., Raman, S., 1994. Effect of drip irrigation and mulching on tomato yield. Agricultural Water Management 25, 179-184.

Silberstein, R., 2006. Hydrological models are so good, do we still need data? Environmental Modelling & Software 21, 1340-1352.

Šimůnek, J., Suarez, D., Sejna, M., 1996. The UNSATCHEM software package for simulating the one-dimensional variably saturated water flow, heat transport, carbon dioxide production and transport, and multicomponent solute transport with major ion equilibrium and kinetic chemistry. Version 2.0. Rep. 141. US Salinity Lab., Riverside, CA. -.

Šimunek, J., Van Genuchten, M.T., Šejna, M., 2012. HYDRUS: Model use, calibration, and validation. Transactions of the ASABE 55, 1263-1274.

Singh, 2005. Water productivity analysis from field to regional scale. Integration of crop and soil modeling, remote sensing and geographical information. PhD Thesis, Wageningen University, The Netherlands. http://www.gcw.nl.

Singh, A., Chhabra, R., Abrol, I., 1979. Effect of fluorine and phosphorus applied to a sodic soil on their availability and on yield and chemical composition of wheat. Soil Science 128, 90-97.

Singh, K., Gajri, P., Arora, V., 2001. Modelling the effects of soil and water management practices on the water balance and performance of rice. Agricultural Water Management 49, 77-95.

Singh, R., Jhorar, R., Van Dam, J., Feddes, R., 2006a. Distributed ecohydrological modelling to evaluate irrigation system performance in Sirsa district, India II: Impact of viable water management scenarios. Journal of Hydrology 329, 714-723.

Singh, R., Kroes, J., Van Dam, J., Feddes, R., 2006b. Distributed ecohydrological modelling to evaluate the performance of irrigation system in Sirsa district, India: I. Current water management and its productivity. Journal of Hydrology 329, 692-713.

Singh, R., van Dam, J.C., Feddes, R.A., 2006c. Water productivity analysis of irrigated crops in Sirsa district, India. Agricultural Water Management 82, 253-278.

Smedema, L.K., Shiati, K., 2002. Irrigation and salinity: a perspective review of the salinity hazards of irrigation development in the arid zone. Irrigation and drainage systems 16(2), 161-174.

Smets, S., Kuper, M., Van Dam, J., Feddes, R., 1997. Salinization and crop transpiration of irrigated fields in Pakistan's Punjab. Agricultural Water Management 35, 43-60.

Smith, M., 1992. CROPWAT: A computer program for irrigation planning and management. Food & Agriculture Org.

Smith, R., 2011. Review of precision irrigation technologies and their applications. University of Southern Queensland.

Smith, R., Hancock, N., 1986. Leaching requirement of irrigated soils. Agricultural water management 11, 13-22.

Smith, R.J., Baillie, J.N., McCarthy, A.C., Raine, S.R. & Baillie, C.P., 2010. Review of Precision Irrigation Technologies and their Application. University of Southern Queensland, National Centre for Engineering in Agriculture Publication 1003017/1, USQ, Toowoomba,Australia, p. 104.

Solomon, S., 2007. The physical science basis: Contribution of Working Group I to the fourth assessment report of the Intergovernmental Panel on Climate Change. Intergovernmental Panel on Climate Change (IPCC), Climate change 2007 996.

Soncini, A., Bocchiola, D., Confortola, G., Bianchi, A., Rosso, R., Mayer, C., Lambrecht, A., Palazzi, E., Smiraglia, C., Diolaiuti, G., 2015. Future hydrological regimes in the upper indus basin: A case study from a high-altitude glacierized catchment. Journal of Hydrometeorology 16, 306-326.

Sood, A., Smakhtin, V., 2015. Global hydrological models: a review. Hydrological Sciences Journal 60, 549-565.

Sparks, A.H., 2018. nasapower: a NASA POWER global meteorology, surface solar energy and climatology data client for R. Journal of Open Source Software 3, 1035.

Spitters, C., Keulen, H.v., Van Kraalingen, D., 1989. A simple and universal crop growth simulator: SUCROS87. In R. Rabbinge, S. A. Ward, & H. H. van Laar (Eds.), Simulation and systems management in crop protection. Pudoc, Wageningen, Netherland, pp. 147-181. (Simulation monographs). Pudoc. https://edepot.wur.nl/171923.

Steduto, P., Hsiao, T.C., Raes, D., Fereres, E., 2009. AquaCrop—The FAO crop model to simulate yield response to water: I. Concepts and underlying principles. Agronomy Journal 101, 426-437.

Stocker, T., Qin, D., Plattner, G.-K., Tignor, M., Allen, S., Boschung, J., Nauels, A., Xia, Y., Bex, V., Midgley, P., 2014. Summary for policymakers.

Stone, P., Nicolas, M., 1994. Wheat cultivars vary widely in their responses of grain yield and quality to short periods of post-anthesis heat stress. Functional Plant Biology 21, 887-900.

Stutley, C., Kalavakonda, V., Jansen, J.G.P., 2018. A Feasibility Study: Assessing the Potential for Large-Scale Agricultural Crop and Livestock Insurance in Punjab province, Pakistan. The World Bank. http://documents.worldbank.org/curated/en/906921547616572396/pdf/133553-WP-P162446-PUBLIC-Punjab-Crop-Insurance-Web.pdf.

Supit, I., 1994. System description of the WOFOST 6.0 crop simulation model implemented in CGMS. Theory and algorithms. Joint Research Centre, European Commission, Luxembourg, p. 146.

Tahir, A.A., Chevallier, P., Arnaud, Y., Ahmad, B., 2011. Snow cover dynamics and hydrological regime of the Hunza River basin, Karakoram Range, Northern Pakistan. Hydrology and Earth System Sciences 15, 2275-2290.

Tahir, Z., Habib, Z., 2001. Land and water productivity: Trends across Punjab canal commands. IWMI.

Talukder, A., Gill, G., McDonald, G., Hayman, P., Alexander, B., Dove, H., Culvenor, R., 2010. Field evaluation of sensitivity of wheat to high temperature stress near flowering and early grain set. 15th ASA Conference, pp. 15-19.

Tanji, K.K., 1990. Nature and extent of agricultural salinity. Agricultural salinity assessment and management, 71-92.

Tanji, K.K., Kielen, N.C., 2002. Agricultural drainage water management in arid and semi-arid areas. FAO, Roma (Italia).

Tanjii, K.K., 1990. Agricultural salinity assessment and management.

Taylor, K.E., Stouffer, R.J., Meehl, G.A., 2012. An overview of CMIP5 and the experiment design. Bulletin of the American meteorological Society 93, 485-498.

Taylor, S.A., Ashcroft, G.L., 1972. Physical edaphology. The physics of irrigated and nonirrigated soils.

Thomas, J.R., Langdale, G., 1980. Ionic Balance in Coastal Bermudagrass Influenced by Nitrogen Fertilization and Soil Salinity 1. Agronomy Journal 72, 449-452.

Thomson, A.M., Calvin, K.V., Smith, S.J., Kyle, G.P., Volke, A., Patel, P., Delgado-Arias, S., Bond-Lamberty, B., Wise, M.A., Clarke, L.E., 2011. RCP4. 5: a pathway for stabilization of radiative forcing by 2100. Climatic change 109, 77-94.

Thornton, P., Herrero, M., 2010. The inter-linkages between rapid growth in livestock production, climate change, and the impacts on water resources, land use, and deforestation. World Bank Policy Research Working Paper Series, Vol.

Ullah, Z., Ullah, R., Ali, M., Junaid, M., 2016. Performance evaluation of diesel and electric operated tube wells irrigation system in sub-tropical conditions. Pure and Applied Biology 5, 142.

Usman, M., 2012. Apparent and real water productivity for cotton-wheat zone of Punjab, Pakistan. Pak. J. Agri. Sci 49(3), 357-363.

Uysal, Ö.K., Atış, E., 2010. Assessing the performance of participatory irrigation management over time: A case study from Turkey. Agricultural water management 97, 1017-1025.

Van Bakel, P., Kselik, R., Roest, C., Smit, A., 2009. Review of crop salt tolerance in the Netherlands. Alterra, Wageningen-UR.

van Dam, J., Feddes, R., 2000. Numerical simulation of infiltration, evaporation and shallow groundwater levels with the Richards equation. Journal of Hydrology 233, 72-85.

van Dam, J., Singh, R., Bessembinder, J., Leffelaar, P., Bastiaanssen, W., Jhorar, R., Kroes, J., Droogers, P., 2006. Assessing options to increase water productivity in irrigated river basins using remote sensing and modelling tools. Water resources development 22, 115-133.

van Dam, J.C., Groenendijk, P., Hendriks, R.F., Kroes, J.G., 2008. Advances of modeling water flow in variably saturated soils with SWAP. Vadose Zone Journal 7, 640-653.

van Dam, J.C., Huygen, J., Wesseling, J.G., Feddes, R.A., Kabat, P., Walsum, v.P.E.V., Groenendijk, P., Diepen, v.C.A., 1997. Theory of SWAP version 2.0; Simulation of water flow, solute transport and plant growth in the Soil-Water-Atmosphere-Plant environment. DLO Winand Staring Centre, Wageningen, Netherland.

van Genuchten, M.T., 1980. A closed-form equation for predicting the hydraulic conductivity of unsaturated soils. Soil science society of America journal 44(5), 892-898.

Van Genuchten, M.T., Cleary, R., 1979. Movement of solutes in soil: Computer-simulated and laboratory results. Developments in soil science. Elsevier, pp. 349-386.

Van Genuchten, M.T., Gupta, S., 1993. A reassessment of the crop tolerance response function. Journal of the Indian Society of Soil Science 41, 730-737.

van Ittersum, M.K., Leffelaar, P.A., Van Keulen, H., Kropff, M.J., Bastiaans, L., Goudriaan, J., 2003. On approaches and applications of the Wageningen crop models. European Journal of Agronomy 18, 201-234.

van Schilfgaarde, J., Bernstein, L., Rhoades, J.D., Rawlins, S.L., 1974. Irrigation management for salt control. Journal of the Irrigation and Drainage Division 100, 321-338.

Van Vuuren, D.P., Den Elzen, M.G., Lucas, P.L., Eickhout, B., Strengers, B.J., Van Ruijven, B., Wonink, S., Van Houdt, R., 2007. Stabilizing greenhouse gas concentrations at low levels: an assessment of reduction strategies and costs. Climatic change 81, 119-159.

Van Vuuren, D.P., Edmonds, J., Kainuma, M., Riahi, K., Thomson, A., Hibbard, K., Hurtt, G.C., Kram, T., Krey, V., Lamarque, J.-F., 2011a. The representative concentration pathways: an overview. Climatic change 109, 5-31.

Van Vuuren, D.P., Edmonds, J.A., Kainuma, M., Riahi, K., Weyant, J., 2011b. A special issue on the RCPs. Climatic Change 109, 1-4.

Van Vuuren, D.P., Stehfest, E., den Elzen, M.G., Kram, T., van Vliet, J., Deetman, S., Isaac, M., Goldewijk, K.K., Hof, A., Beltran, A.M., 2011c. RCP2. 6: exploring the possibility to keep global mean temperature increase below 2 C. Climatic change 109, 95-116.

Varela-Ortega, C., Sagardoy, J.A., 2002. Analysis of irrigation water policies in Syria: current developments and future options. International Conference on Irrigation Water Policies: Micro and Macro Considerations'. Agadir, Morocco, pp. 15-17.

Vasileiadou, E., Heimeriks, G., Petersen, A.C., 2011. Exploring the impact of the IPCC Assessment Reports on science. Environmental Science & Policy 14, 1052-1061.

Vazifedoust, M., 2007. Development of an agricultural drought assessment system: integration of agrohydrological modelling, remote sensing and geographical information.

Vazifedoust, M., Van Dam, J., Feddes, R.A., Feizi, M., 2008. Increasing water productivity of irrigated crops under limited water supply at field scale. Agricultural water management 95(2), 89-102.

W. Ahmad, Y.N., M.H. Zia, K. Mahmood, A. Ashraf, N. Ahmad, M. Salim and M.A. Shakir, 2017. Soil Fertility Atlas of Pakistan: The

Punjab Province. FAO, Islamabad, Pakistan.

Wada, Y., Van Beek, L.P., Van Kempen, C.M., Reckman, J.W., Vasak, S., Bierkens, M.F., 2010. Global depletion of groundwater resources. Geophysical research letters 37.

Wagan, S., Memon, Q., Wagan, T., Memon, I., Wagan, Z., 2015. Economic analysis of laser land leveling technology water use efficiency and crop productivity of wheat crop in Sindh, Pakistan. Journal of Environment and Earth Science 5(15), 21-25.

Wagenet, R., Hutson, J., 1989. Leaching estimation and chemistry model: a process based model of water and solute movement, transformations, plant uptake, and chemical reactions in the unsaturated zone. Continuum, Vol2 (version2). Ithaca, NY: Centre of Environmental Research, Cornell University.

Wallender, W.W., Tanji, K.K., 2011. Agricultural salinity assessment and management. American Society of Civil Engineers (ASCE).

Wanders, N., Karssenberg, D., Bierkens, M., Van Dam, J., De Jong, S., 2012. Using high-resolution soil moisture modelling to assess the uncertainty of microwave remotely sensed soil moisture products at the correct spatial and temporal support. EGU General Assembly Conference Abstracts, p. 5338.

Wang, J., Li, J., Li, Y., 2019. Evaluating the necessity of supplementary irrigation in Songnen Plain of Northeast China using a distributed agro-hydrological model. 2019 ASABE Annual International Meeting. American Society of Agricultural and Biological Engineers, p. 1.

Waqas, M.M., Shah, S.H.H., Awan, U.K., Waseem, M., Ahmad, I., Fahad, M., Niaz, Y., Ali, S., 2020. Evaluating the Impact of Climate Change on Water Productivity of Maize in the Semi-Arid Environment of Punjab, Pakistan. Sustainability 12, 3905.

Ward, C., Darghouth, S., 2006a. Reengaging in agricultural water management: policy and institutional options for decision makers. Agricultural and Rural Development notes ; no. 3, Washington, D.C: World Bank Group.

Ward, C., Darghouth, S., 2006b. Reengaging in agricultural water management: policy and institutional options for decision makers.

Water, U., 2003. Water for People, Water for Life. United Nations World Water Development Report. Paris: UNESCO Division of Water Sciences.

Watto, M.A., Mugera, A.W., 2016. Groundwater depletion in the Indus Plains of Pakistan: imperatives, repercussions and management issues. International Journal of River Basin Management 14, 447-458.

Webber, H., Martre, P., Asseng, S., Kimball, B., White, J., Ottman, M., Wall, G.W., De Sanctis, G., Doltra, J., Grant, R., 2017. Canopy temperature for simulation of heat

stress in irrigated wheat in a semi-arid environment: A multi-model comparison. Field Crops Research 202, 21-35.

Wesseling, J., Feddes, R.A., 2006. Assessing crop water productivity from field to regional scale. Agricultural Water Management 86, 30-39.

Wilby, R.L., Dawson, C.W., 2007. SDSM 4.2-A decision support tool for the assessment of regional climate change impacts. User manual 94.

Wilby, R.L., Dawson, C.W., Barrow, E.M., 2002. SDSM—a decision support tool for the assessment of regional climate change impacts. Environmental Modelling & Software 17, 145-157.

Williams, A., White, N., Mushtaq, S., Cockfield, G., Power, B., Kouadio, L., 2015. Quantifying the response of cotton production in eastern Australia to climate change. Climatic Change 129, 183-196.

Williams, A.A., McRae, D., Kouadio, L., Mushtaq, S., Davis, P., 2019. Cotton and climate change. Agroclimatology, 343.

Willmott, C.J., 1982. Some comments on the evaluation of model performance. Bulletin of the American Meteorological Society 63, 1309-1313.

Winston, H.Y., Yang, Y.-C., Savitsky, A., Alford, D., Brown, C., 2013. The Indus basin of Pakistan: The impacts of climate risks on water and agriculture. World bank publications.

Woldegebriel, E., 2011. Salt accumulation under Drip-Irrigation in Turkey:A case study on salt accumulation simulation Using SWAP model under drip irrigation in the Gediz basin. International Land and Water Management. Wageningen University, the Netherlands, pp. vi, 42. https://library.wur.nl/WebQuery/theses/directlink/2018918.

Wollenweber, B., Porter, J., Schellberg, J., 2003. Lack of interaction between extreme high-temperature events at vegetative and reproductive growth stages in wheat. Journal of Agronomy and Crop Science 189, 142-150.

Wolters, W., 1992. Influences on the efficiency of irrigation water use.

Wolters, W., Bhutta, M., 1997. Need for Integrated Irrigation and Drainage Management: Example from Pakistan.

Woodruff, J., Ligon, J., Smith, B., 1984. Water Table Depth Interaction with Nitrogen Rates on Subirrigated Corn 1. Agronomy Journal 76, 280-283.

Wösten, J., Lilly, A., Nemes, A., Le Bas, C., 1998. Using existing soil data to derive hydraulic parameters for simulation models in environmental studies and in land use planning. Report.

Xie, X.-H., Cui, Y.-L., 2010. Distributed hydrological modeling of irrigation water use efficiency at different spatial scales. Advances in Water Science 21, 681-689.

Xu, X., Huang, G., Zhan, H., Qu, Z., Huang, Q., 2012. Integration of SWAP and MODFLOW-2000 for modeling groundwater dynamics in shallow water table areas. Journal of Hydrology 412, 170-181.

Xu, X., Li, J., Tolson, B.A., 2014. Progress in integrating remote sensing data and hydrologic modeling. Progress in Physical Geography 38, 464-498.

Xue, J., Ren, L., 2016. Evaluation of crop water productivity under sprinkler irrigation regime using a distributed agro-hydrological model in an irrigation district of China. Agricultural Water Management 178, 350-365.

Xue, J., Ren, L., 2017. Assessing water productivity in the Hetao Irrigation District in Inner Mongolia by an agro-hydrological model. Irrigation Science 35, 357-382.

Yasin, H.Q., Akram, M.M., Tahir, M.N., 2021. High Efficiency Irrigation Technology As a Single Solution for Multi-Challenge: A Case of Pakistan. Water, Climate Change, and Sustainability, 185-196.

Yeo, A., 1998. Predicting the interaction between the effects of salinity and climate change on crop plants. Scientia Horticulturae 78, 159-174.

Yuan, C., Feng, S., Huo, Z., Ji, Q., 2019. Simulation of saline water irrigation for seed maize in arid northwest China based on SWAP model. Sustainability 11(16), 4264.

Zaman, M., Shahid, S.A., Heng, L., 2018. Guideline for salinity assessment, mitigation and adaptation using nuclear and related techniques. Springer Nature.

Zhang, L., Xu, Y., Meng, C., Li, X., Liu, H., Wang, C., 2020. Comparison of statistical and dynamic downscaling techniques in generating high-resolution temperatures in China from CMIP5 GCMs. Journal of Applied Meteorology and Climatology 59, 207-235.

Zhongming, Z., Linong, L., Xiaona, Y., Wangqiang, Z., Wei, L., 2009. Water resources across Europe—confronting water scarcity and drought.

Zhou, T., Wu, P., Sun, S., Li, X., Wang, Y., Luan, X., 2017. Impact of future climate change on regional crop water requirement—A case study of Hetao Irrigation District, China. Water 9, 429.

Zhu, X., Chikangaise, P., Shi, W., Chen, W.-H., Yuan, S., 2018. Review of intelligent sprinkler irrigation technologies for remote autonomous system. International Journal of Agricultural & Biological Engineering 11.

Zwart, S.J., Bastiaanssen, W.G., 2004. Review of measured crop water productivity values for irrigated wheat, rice, cotton and maize. Agricultural water management 69(2), 115-133.

Appendices

Appendix A: Supporting material for chapter 4

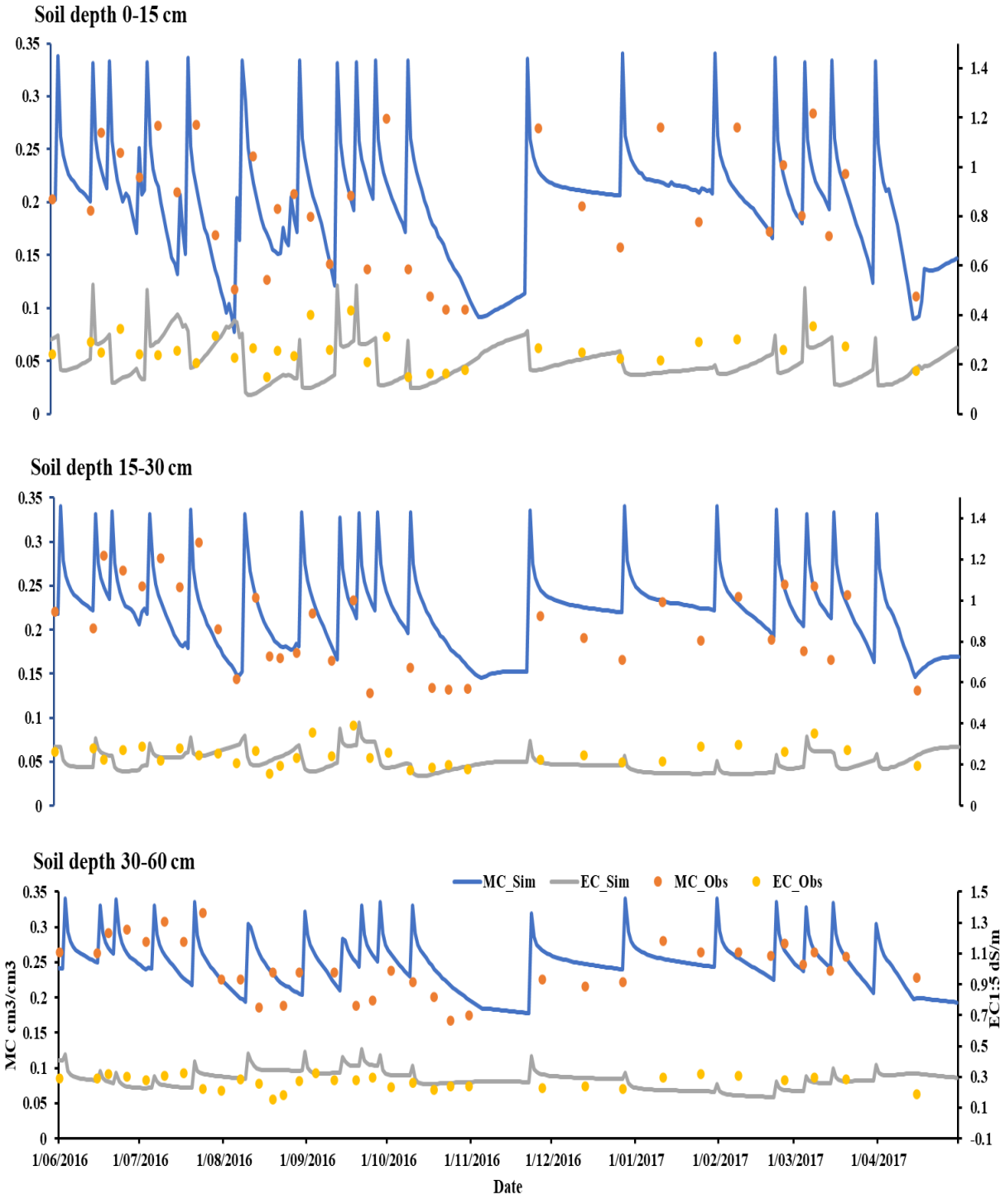

Figure A.1: The observed and simulated soil moisture and salinity profile at a local farmer field CW1 under cotton-wheat cultivation in Hakra canal command, Punjab Pakistan.

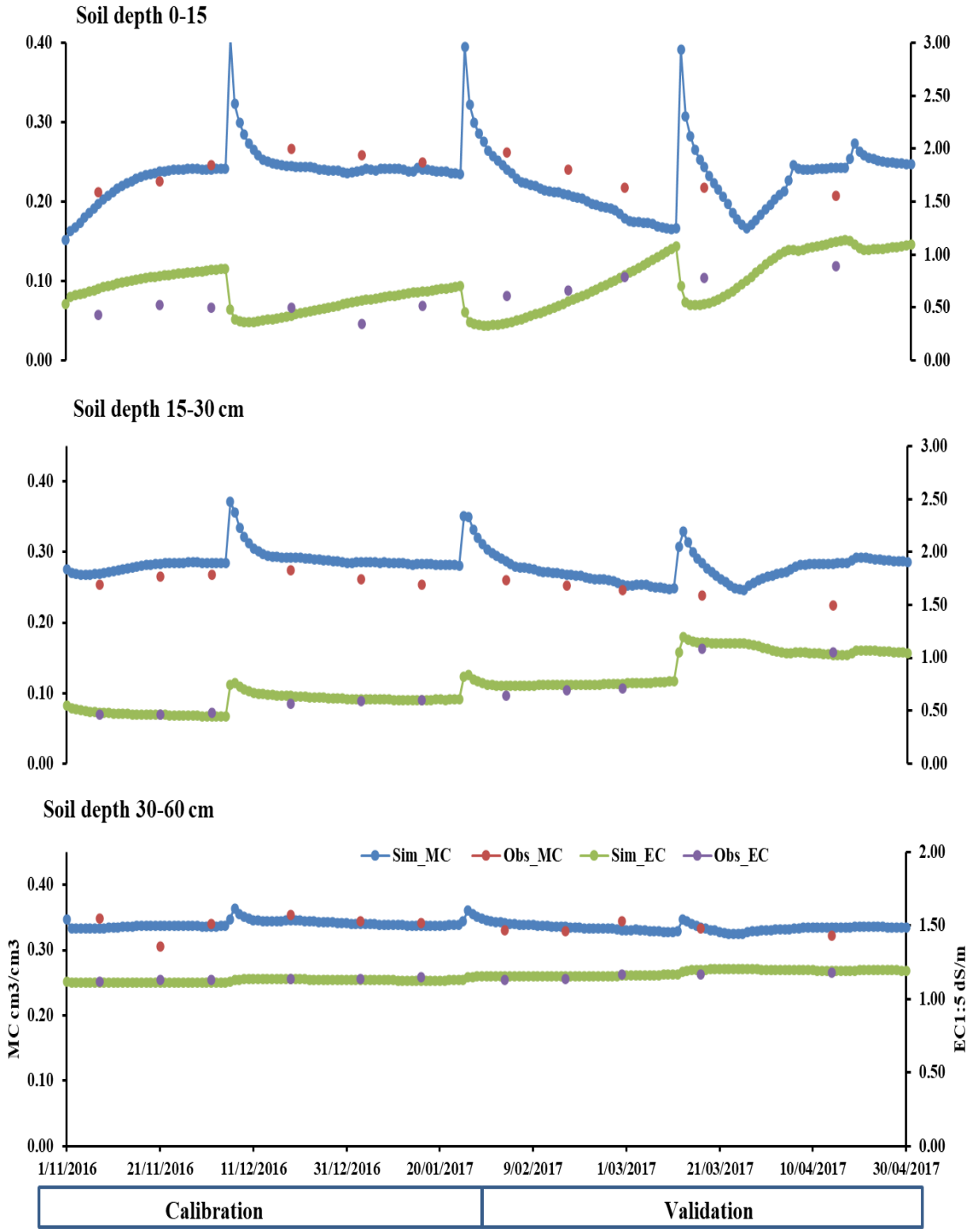

Figure A.2: The observed and simulated soil moisture and salinity profile at a local farmer field RW1 under rice-wheat cultivation in Hakra canal command, Punjab Pakistan.

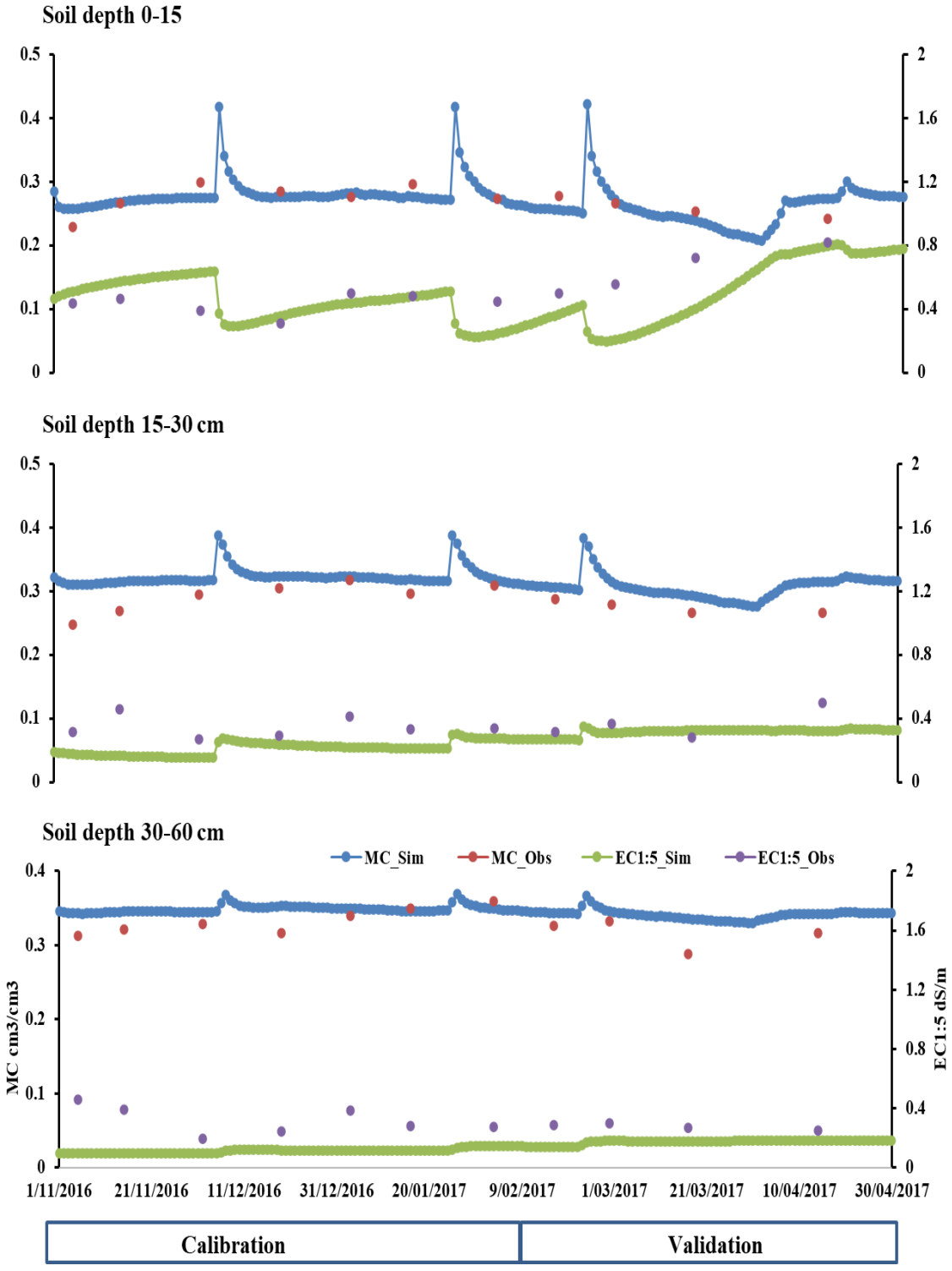

Figure A.3: The observed and simulated soil moisture and salinity profile at a local farmer field RW2 under rice-wheat cultivation in Hakra canal command, Punjab Pakistan.

Appendix B: Supporting material for chapter 5

Table B.1: SWAP simulated soil water and salt balance components for 10 years (2007-2017) simulation of Cotton-Wheat crops under 'business-as-usual' reference (baseline) irrigation scenario in Hakra canal command, Punjab Pakistan.

Season	*Water and Salt balance/WP*	2007-08	2008-09	2009-10	2010-11	2011-12	2012-13	2013-14	2014-15	2015-16	2016-17	Average	*CV*
Kharif (Cotton) Season from May 2016 to November 2016	*Rain(mm)*	245	189	195	183	460	194	227	201	322	98	**231**	**0.42**
	Irrigation (mm)	1100	1100	1100	1100	1100	1100	1100	1100	1100	1100	**1100**	**0.00**
	E_p *(mm)*	357	333	336	370	372	360	356	366	340	350	**354**	**0.04**
	T_p *(mm)*	742	756	778	665	639	684	673	734	776	794	**724**	**0.08**
	T (mm)	670	680	706	596	578	649	642	683	716	735	**665**	**0.08**
	T_a/T_p *(mm)*	0.90	0.90	0.91	0.90	0.90	0.95	0.95	0.93	0.92	0.93	**0.92**	**0.02**
	ET_a *(mm)*	**775**	**781**	**796**	**685**	**684**	**736**	**734**	**791**	**799**	**818**	**760**	**0.06**
	Q_{bot} *(mm)*	-681	-466	-502	-554	-834	-512	-580	-504	-605	-335	**-557**	**-0.24**
	ΔW *(mm)*	-110	44	-1	46	43	47	15	7	19	47	**16**	**3.04**
	IC_i *(mg cm^2)*	73	73	73	73	73	73	73	73	73	73	**73**	**0.00**
	C_{bot} *(mg cm^2)*	-86	-73	-74	-85	-99	-65	-60	-65	-81	-45	**-73**	**-0.21**
	ΔC *(mg cm^2)*	-13	0	-1	-12	-26	8	13	8	-8	28	**-0.38**	**-40.40**
	Cotton seed yield (kg ha^{-})[1]	2927	2395	2756	2762	2990	4069	3422	3428	2386	2643	**2978**	**0.18**
	WP_{ET} *(kg m^{-3})*	**0.38**	**0.31**	**0.35**	**0.40**	**0.44**	**0.55**	**0.47**	**0.43**	**0.30**	**0.32**	**0.39**	**0.20**
	WP_{Irr} *(kg m^{-3})*	**0.27**	**0.22**	**0.25**	**0.25**	**0.27**	**0.37**	**0.31**	**0.31**	**0.22**	**0.24**	**0.27**	**0.18**
Rabi (Wheat) Season from December 2016 to April 2017	*Rain(mm)*	35	55	7	51	28	104	65	99	47	17	**51**	**0.63**
	Irrigation (mm)	490	490	490	490	490	490	490	490	490	490	**490**	**0.00**
	E_p *(mm)*	179	216	216	180	163	174	178	186	181	193	**186**	**0.09**
	T_p *(mm)*	299	237	272	250	259	215	240	285	299	297	**265**	**0.11**
	T (mm)	288	232	261	245	254	211	235	280	293	288	**259**	**0.11**
	T_a/T_p *(mm)*	0.96	0.98	0.96	0.98	0.98	0.98	0.98	0.98	0.98	0.97	**0.98**	**0.01**
	ET_a *(mm)*	**351**	**315**	**322**	**318**	**321**	**282**	**304**	**353**	**357**	**350**	**327**	**0.08**
	Q_{bot} *(mm)*	-203	-211	-200	-218	-210	-312	-243	-224	-201	-197	**-222**	**-0.16**
	ΔW *(mm)*	-29	19	-25	4	-13	-1	7	12	-22	-40	**-9**	**-2.22**
	IC_i *((mg cm^2)*	31	31	31	31	31	31	31	31	31	31	**31**	**0.00**
	C_{bot} *((mg cm^2)*	-24	-32	-30	-29	-12	-46	-33	-35	-27	-37	**-30**	**-0.30**
	ΔC *((mg cm^2)*	7	0	2	2	20	-15	-1	-4	4	-6	**1**	**10.01**
	Wheat yield (kg ha^{1})	5676	6692	3552	5989	4959	5916	6172	5782	6403	5923	**5707**	**0.16**
	WP_{ET} *(kg m^{-3})*	**1.62**	**2.13**	**1.10**	**1.88**	**1.55**	**2.10**	**2.03**	**1.64**	**1.80**	**1.69**	**1.75**	0.18
	WP_{Irr} *(kg m^{-3})*	1.16	1.37	0.73	1.22	1.01	1.21	1.26	1.18	1.31	1.21	**1.17**	0.16

The symbols *E* is evaporation, *T* is transpiration *ET* is evapotranspiration, *Q* is percolation, ΔW change in water storage, *I* is irrigation, *C* is solute concentration, ΔC is change in solute concentration, *WP* is water productivity. Subscripts *p* is potential, *a* is actual, *bot* is bottom, *ET* is evapotranspiration, *Irr* is irrigation.

Appendix C: Supporting material for chapter 6

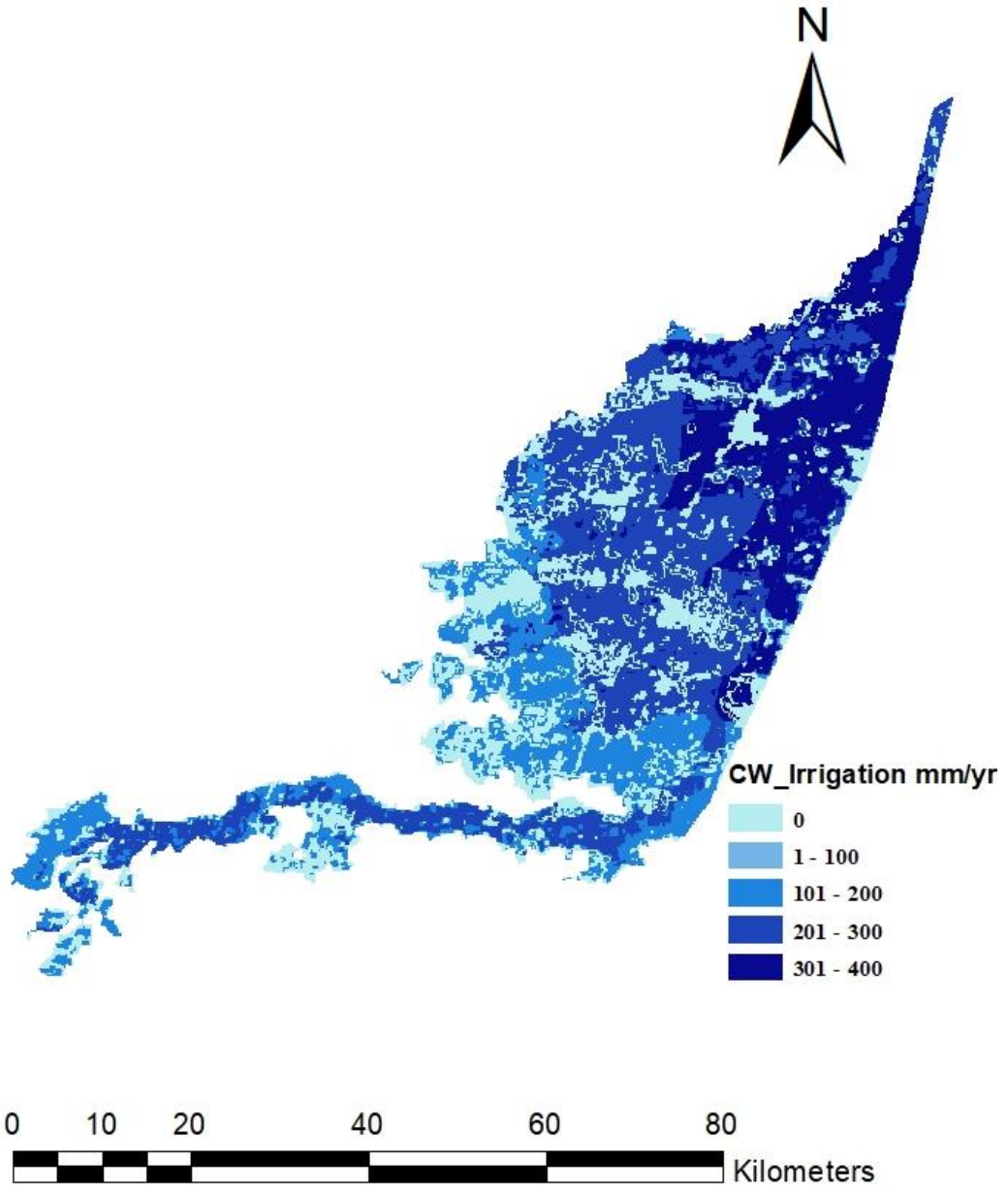

Figure C.1: Canal irrigation across all the simulation units of HBC command during agricultural year 2016-2017.

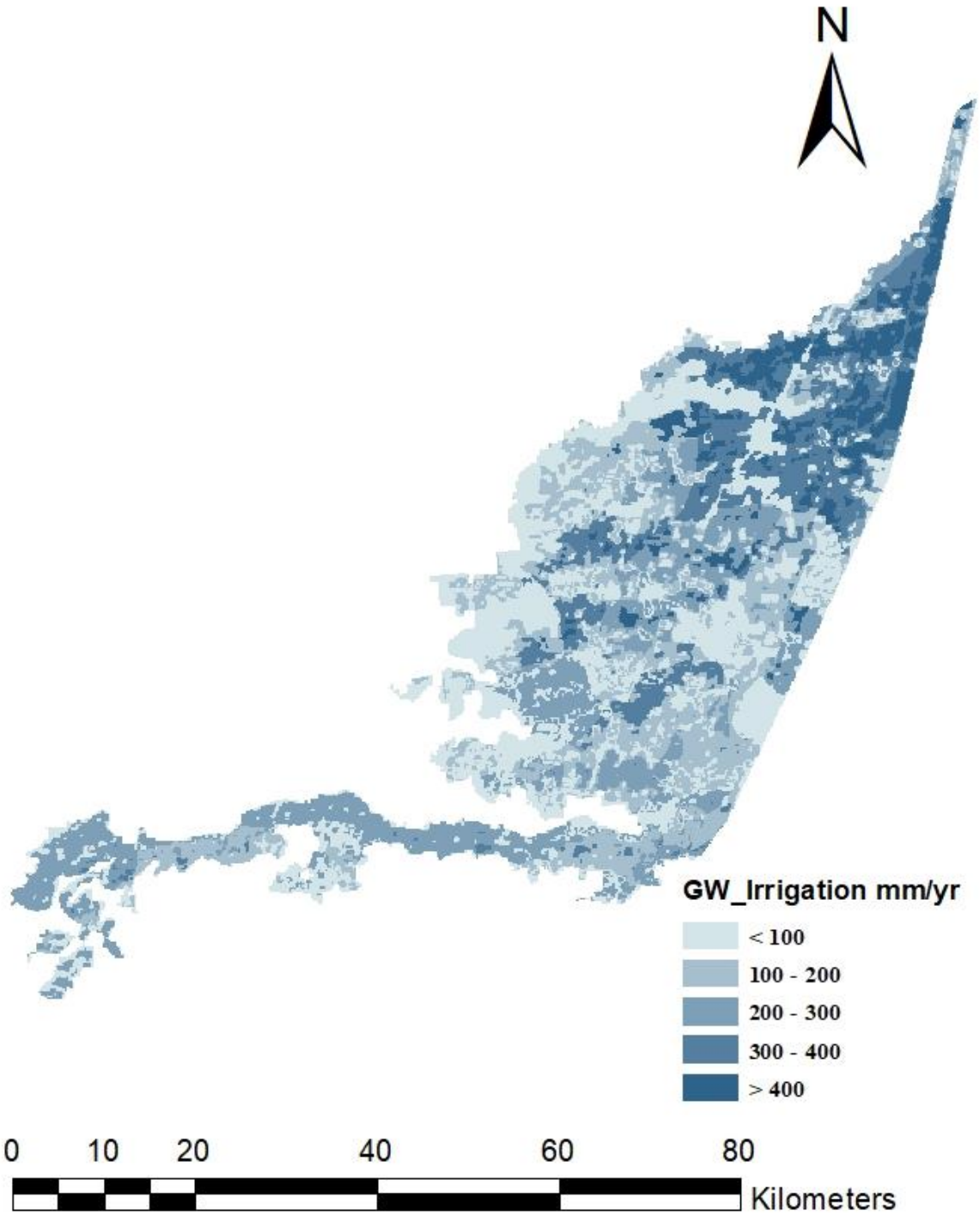

Figure C.2: Groundwater irrigation across all the simulation units of HBC command during agricultural year 2016-2017.

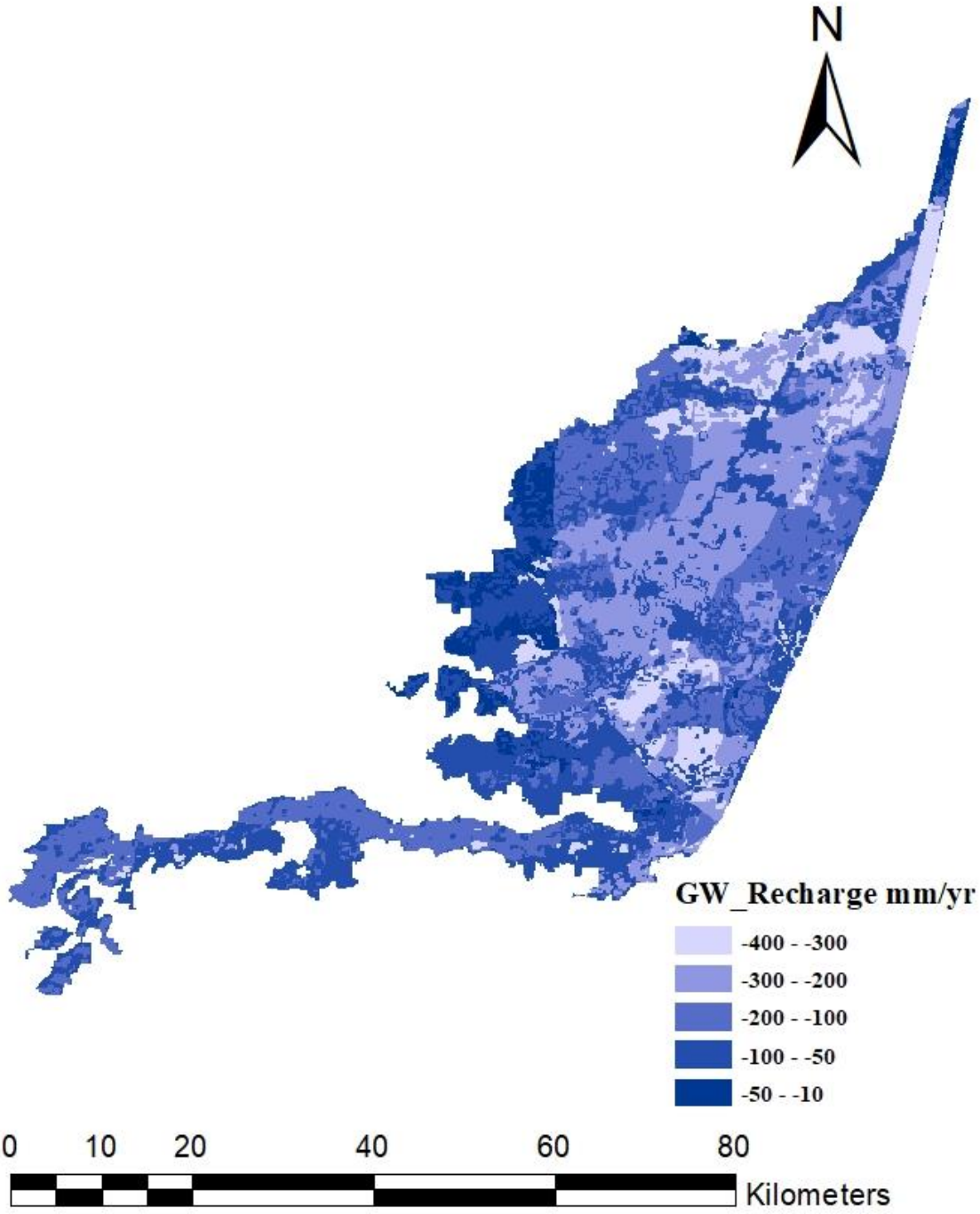

Figure C.3: SWAP simulated groundwater recharge across all the simulation units of HBC command during the agricultural year 2016-2017

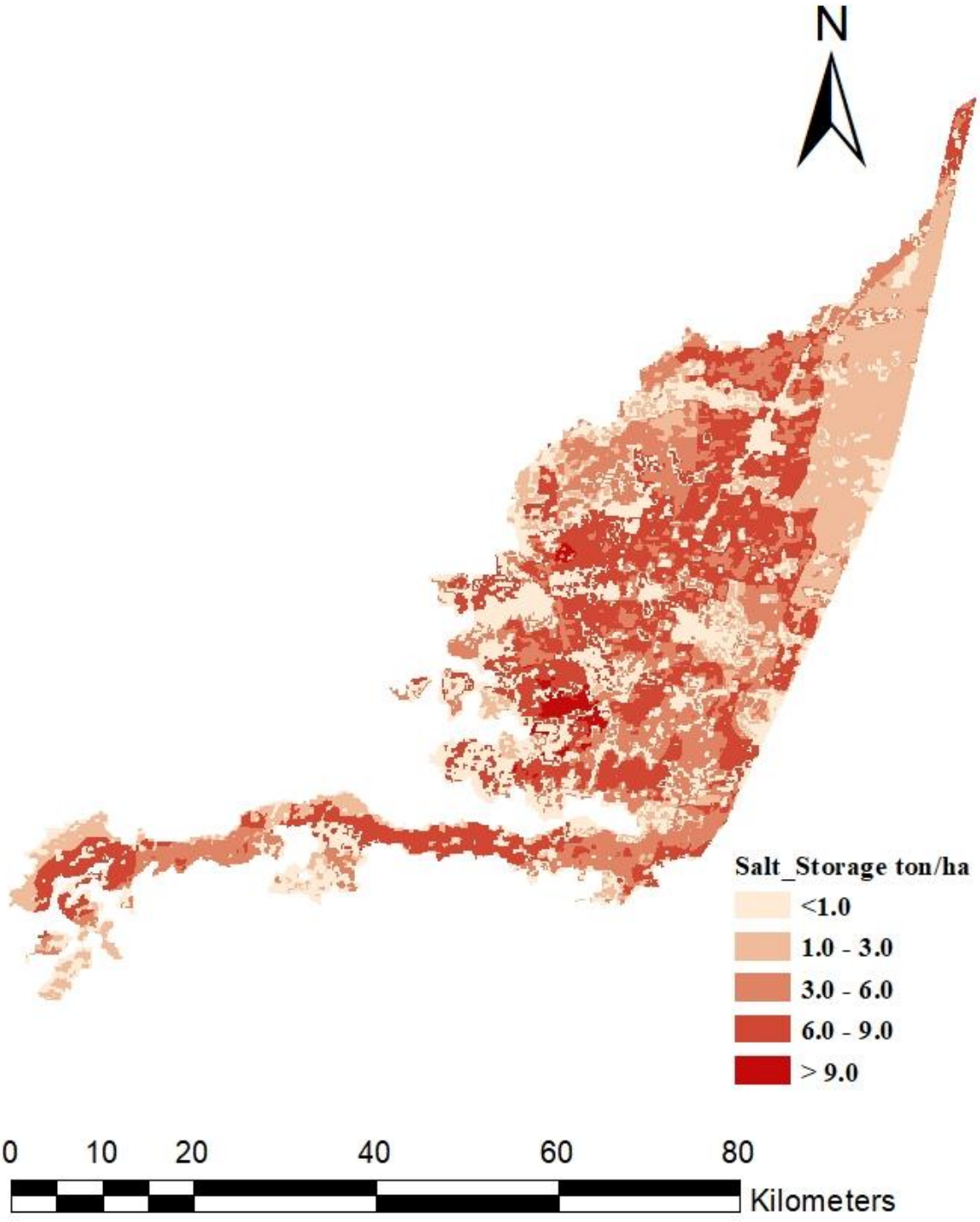

Figure C.4: SWAP Simulated salt storage across all the simulation units of HBC command during agricultural year 2016-2017

Appendix D: Supporting material for chapter 7

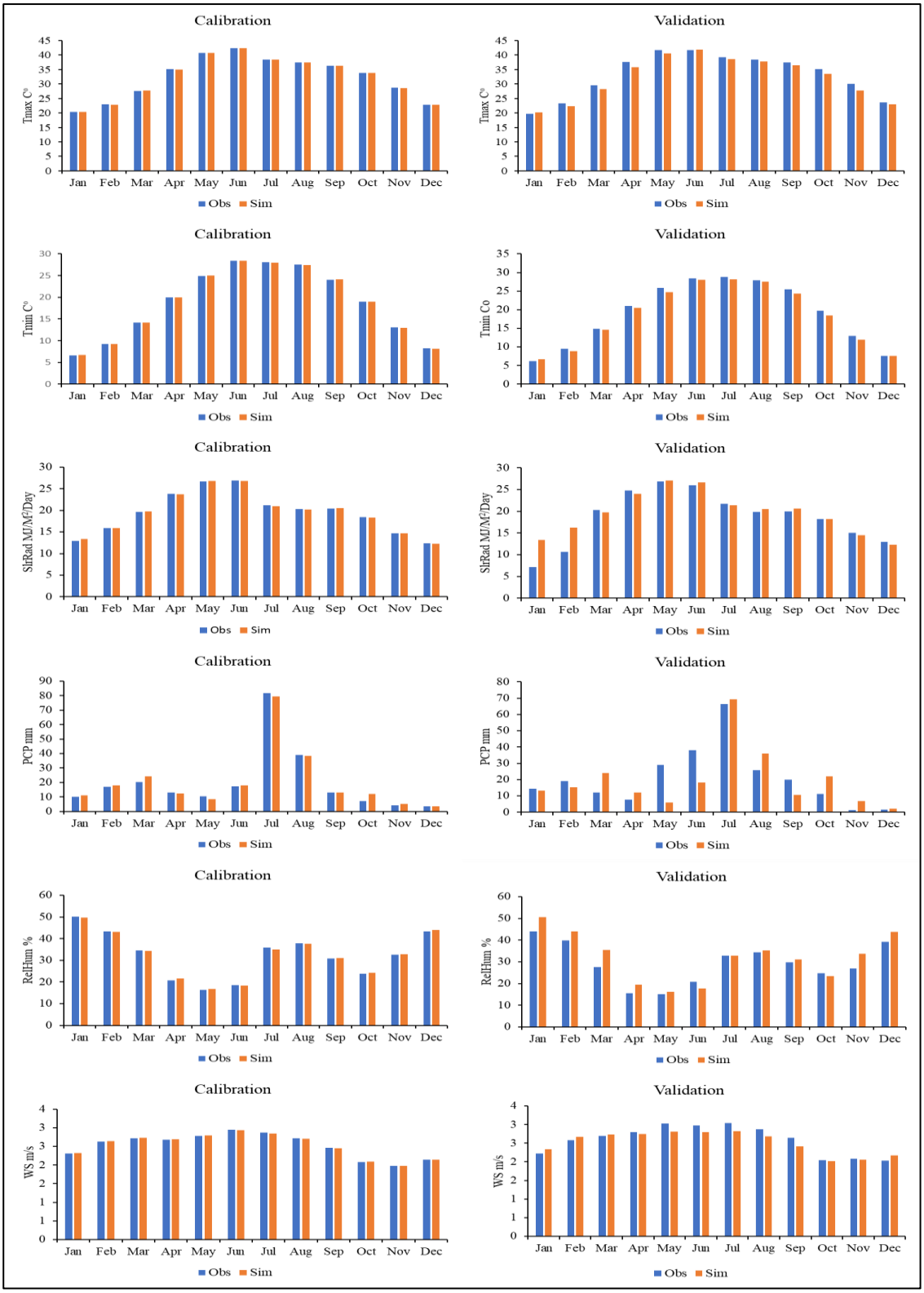

Figure D.1: Comparison of the mean monthly observed and simulated climate variables in Hakra branch canal command for the calibration (1979-1995) and validation (1996-2005) period.

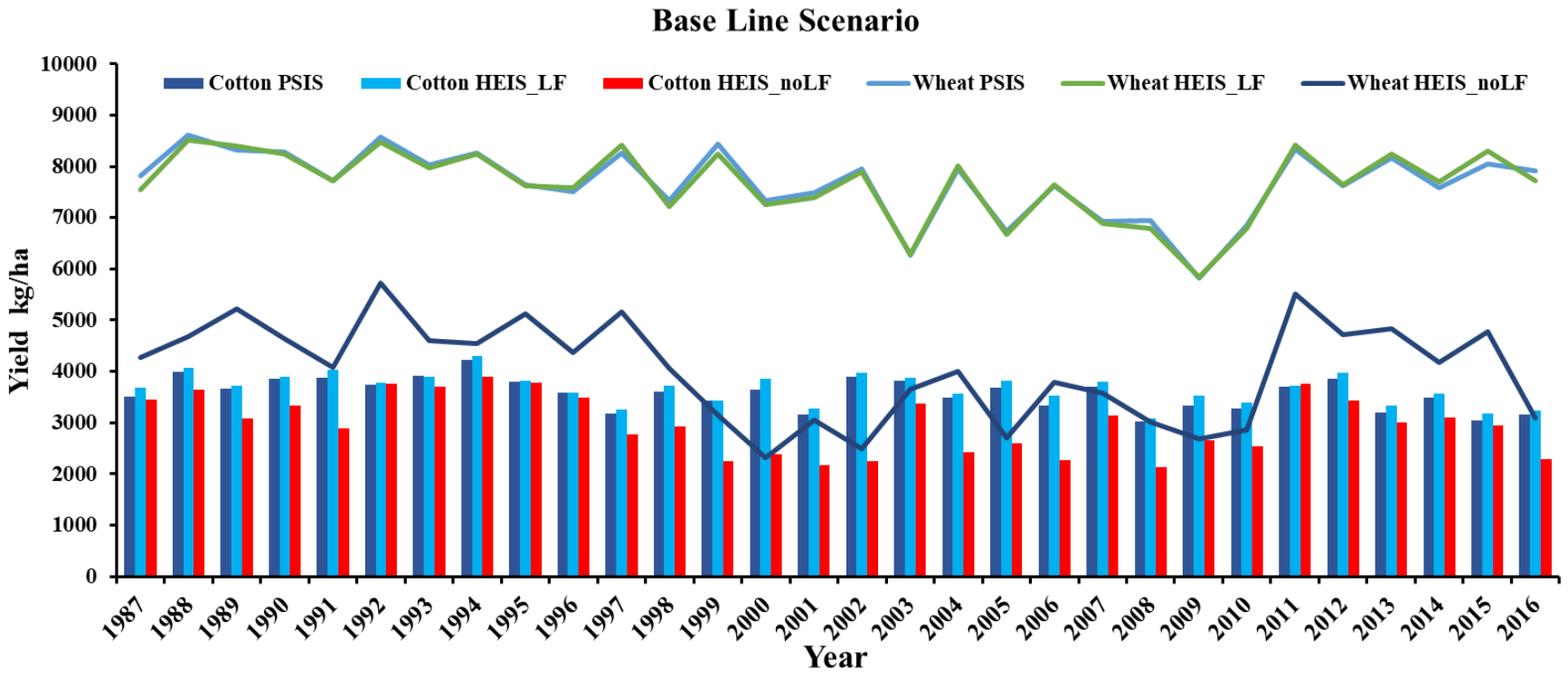

Figure D.2: SWAP simulated water- and salt-limited crop yields (cotton-wheat) under base line scenario (1987-2017) with different irrigation systems in HBC command, Punjab Pakistan.

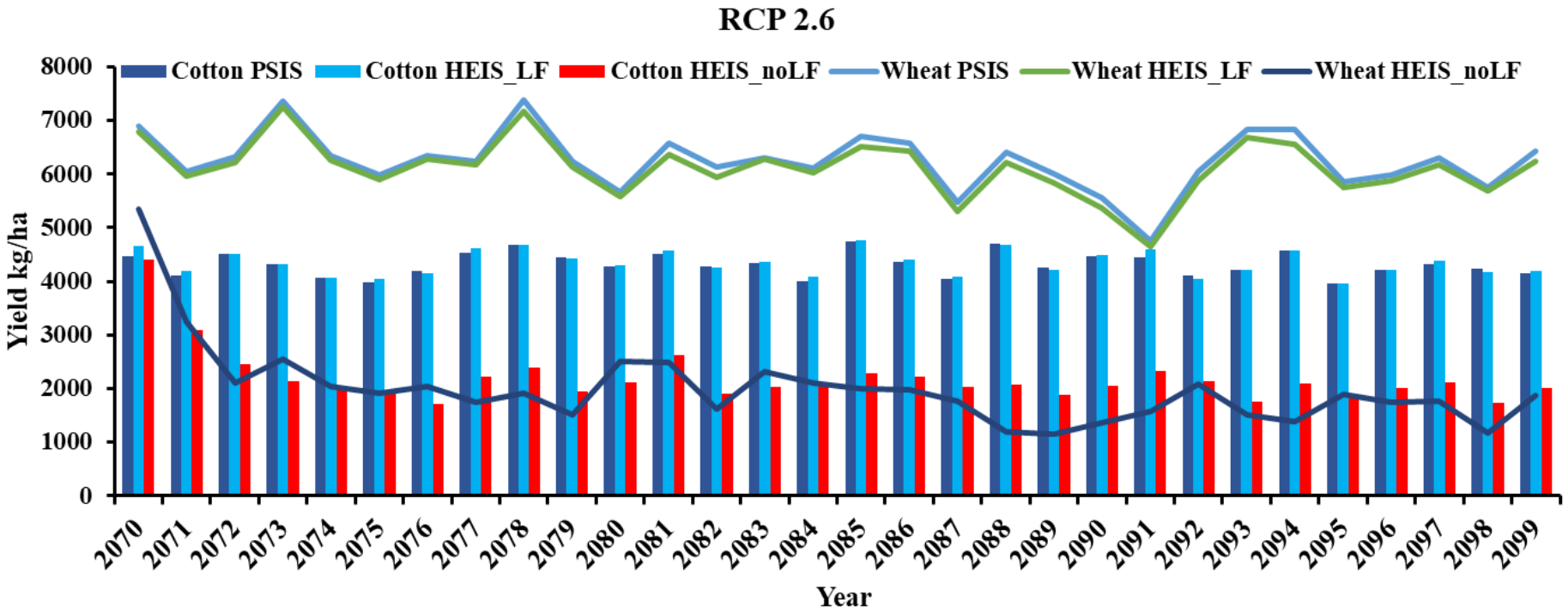

Figure D.3: SWAP simulated water- and salt-limited crop yields (cotton-wheat) under potential climate change scenario RCP 2.6 (2070-2099) with different irrigation systems in HBC command, Punjab Pakistan.

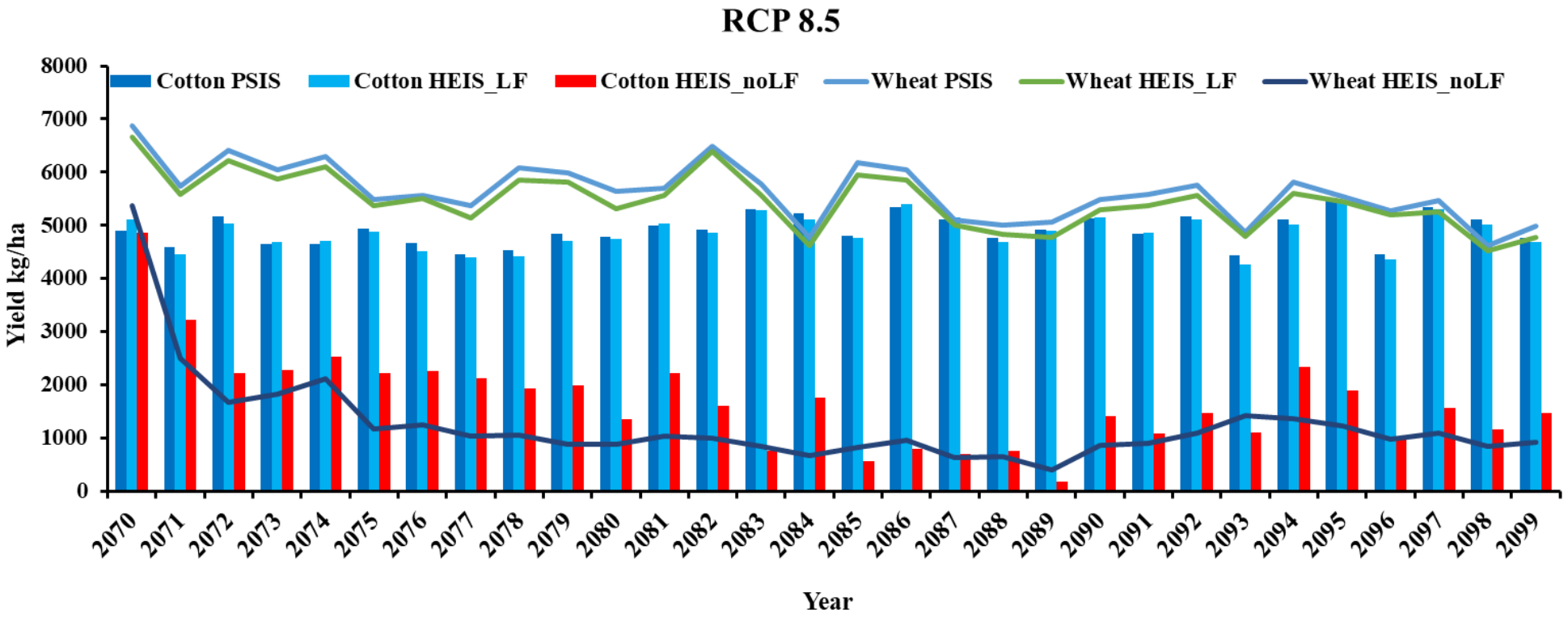

Figure D.4: SWAP simulated water- and salt-limited crop yields (cotton-wheat) under potential climate change scenario RCP 8.5 (2070-2099) with different irrigation systems in HBC command, Punjab Pakistan.

Appendix E: Programming codes

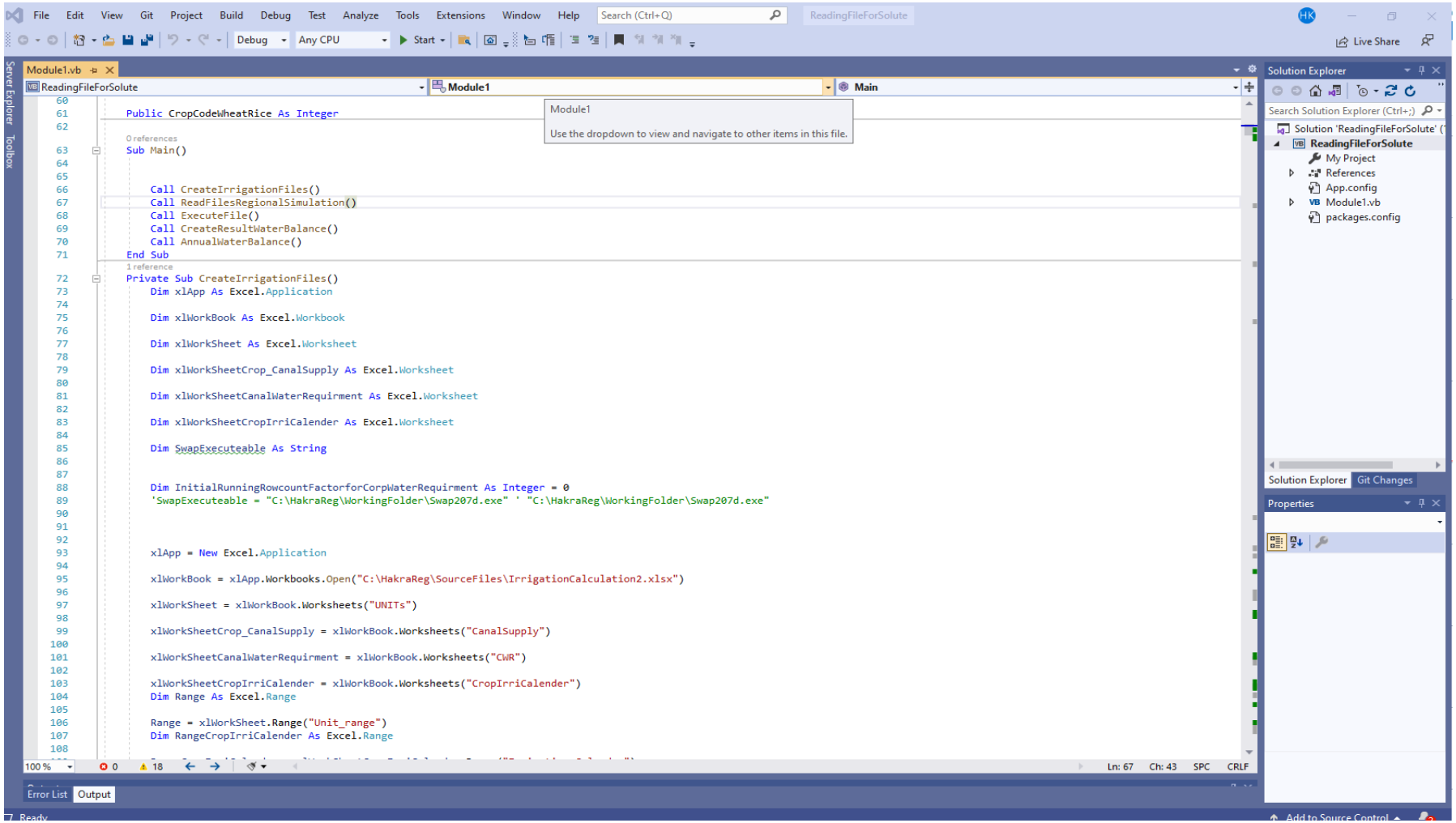

Figure E.1: Part of Visual Basic.Net program used in chapter 6 for running the SWAP in batch for all the simulation units.

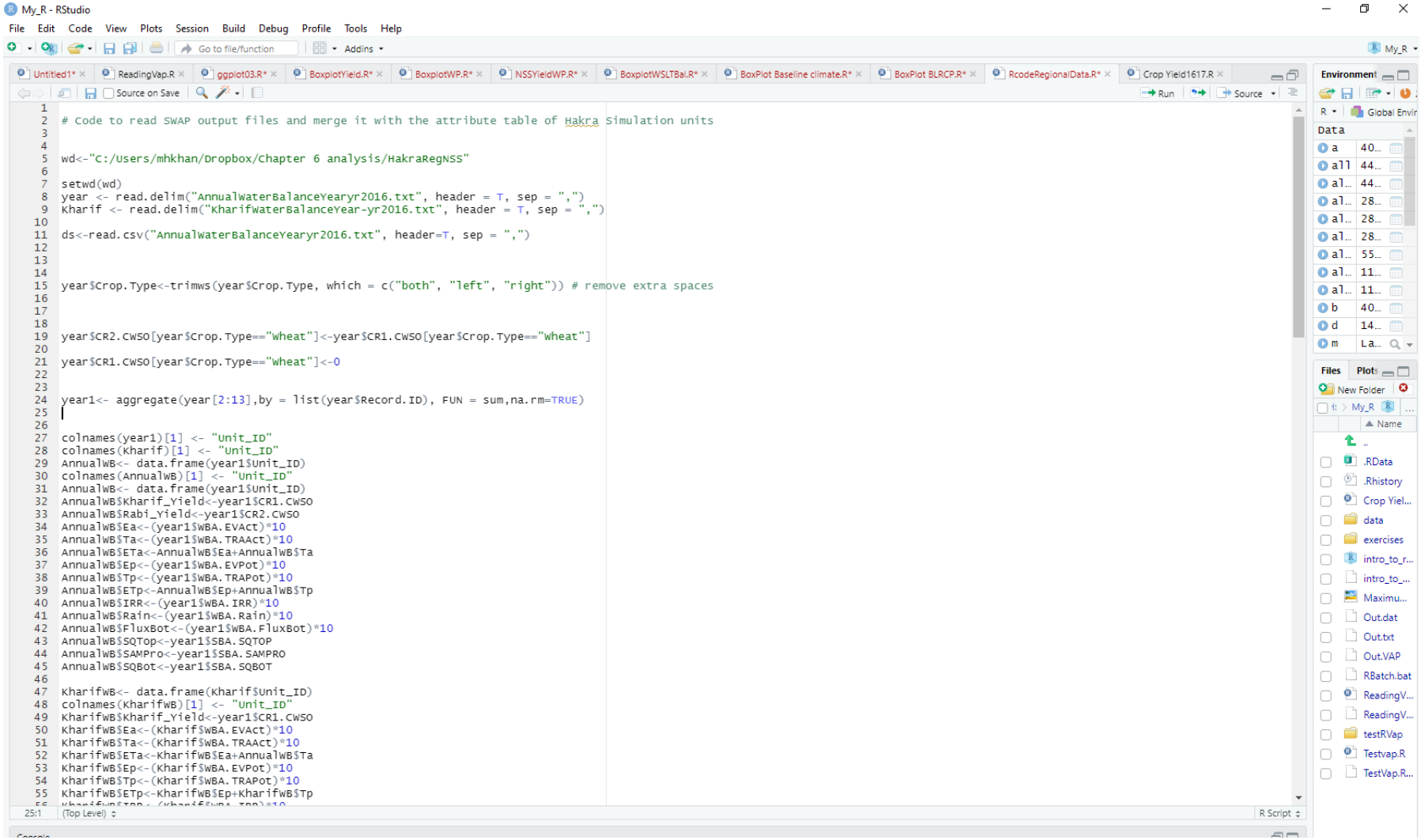

Figure E.2: Part of R code used in chapter 6 for analysis of SWAP output files and joining with attribute data of all the simulation units.

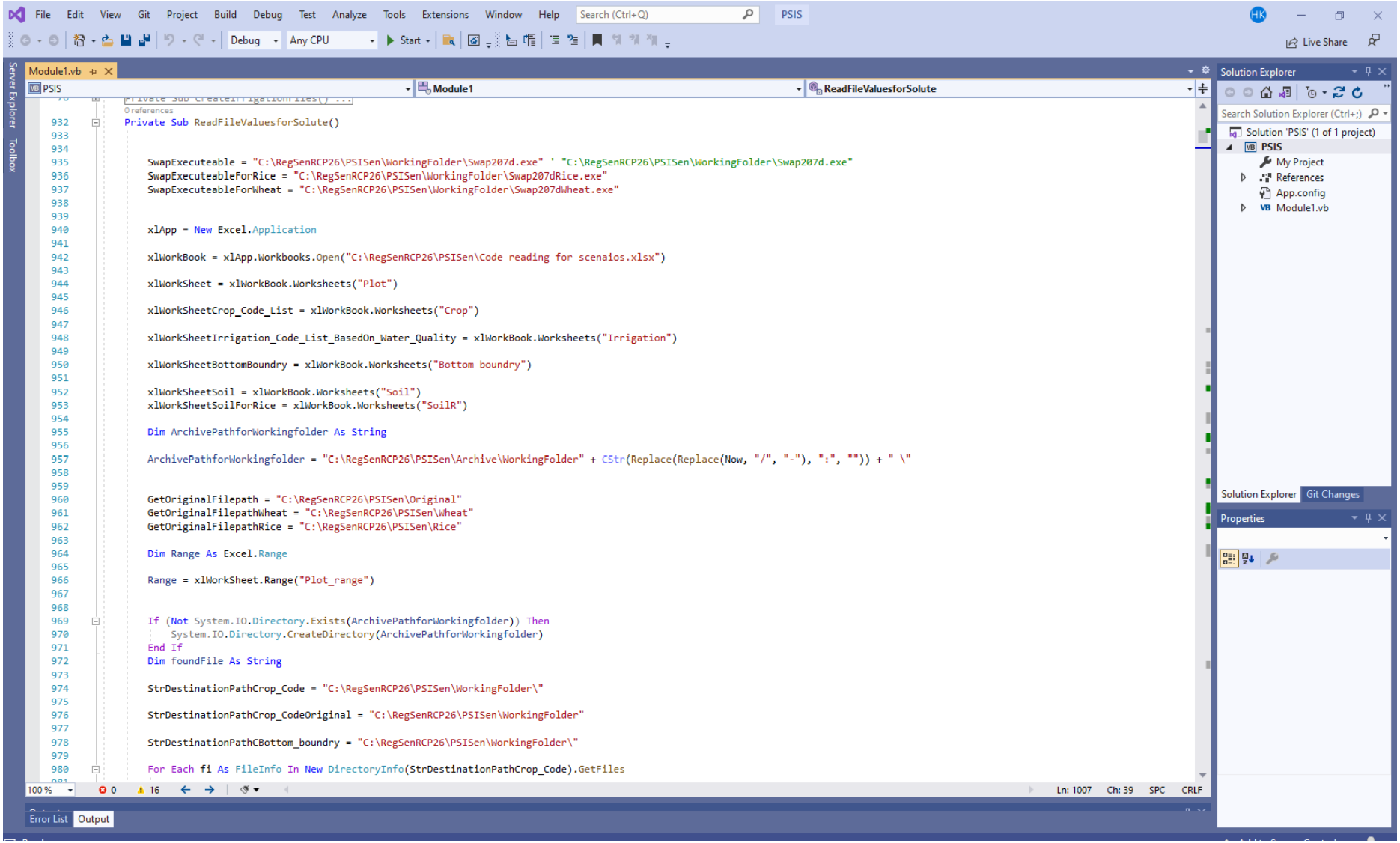

```
Private Sub ReadFileValuesforSolute()


    SwapExecuteable = "C:\RegSenRCP26\PSISen\WorkingFolder\Swap207d.exe" ' "C:\RegSenRCP26\PSISen\WorkingFolder\Swap207d.exe"
    SwapExecuteableForRice = "C:\RegSenRCP26\PSISen\WorkingFolder\Swap207dRice.exe"
    SwapExecuteableForWheat = "C:\RegSenRCP26\PSISen\WorkingFolder\Swap207dWheat.exe"


    xlApp = New Excel.Application

    xlWorkBook = xlApp.Workbooks.Open("C:\RegSenRCP26\PSISen\Code reading for scenaios.xlsx")

    xlWorkSheet = xlWorkBook.Worksheets("Plot")

    xlWorkSheetCrop_Code_List = xlWorkBook.Worksheets("Crop")

    xlWorkSheetIrrigation_Code_List_BasedOn_Water_Quality = xlWorkBook.Worksheets("Irrigation")

    xlWorkSheetBottomBoundry = xlWorkBook.Worksheets("Bottom boundry")

    xlWorkSheetSoil = xlWorkBook.Worksheets("Soil")
    xlWorkSheetSoilForRice = xlWorkBook.Worksheets("SoilR")

    Dim ArchivePathforWorkingfolder As String

    ArchivePathforWorkingfolder = "C:\RegSenRCP26\PSISen\Archive\WorkingFolder" + CStr(Replace(Replace(Now, "/", "-"), ":", "")) + " \"


    GetOriginalFilepath = "C:\RegSenRCP26\PSISen\Original"
    GetOriginalFilepathWheat = "C:\RegSenRCP26\PSISen\Wheat"
    GetOriginalFilepathRice = "C:\RegSenRCP26\PSISen\Rice"

    Dim Range As Excel.Range

    Range = xlWorkSheet.Range("Plot_range")


    If (Not System.IO.Directory.Exists(ArchivePathforWorkingfolder)) Then
        System.IO.Directory.CreateDirectory(ArchivePathforWorkingfolder)
    End If
    Dim foundFile As String

    StrDestinationPathCrop_Code = "C:\RegSenRCP26\PSISen\WorkingFolder\"

    StrDestinationPathCrop_CodeOriginal = "C:\RegSenRCP26\PSISen\WorkingFolder"

    StrDestinationPathCBottom_boundry = "C:\RegSenRCP26\PSISen\WorkingFolder\"

    For Each fi As FileInfo In New DirectoryInfo(StrDestinationPathCrop_Code).GetFiles
```

Figure E.3: Part of Visual Basic.Net program used in regional scale scenario simulation of chapter 7.

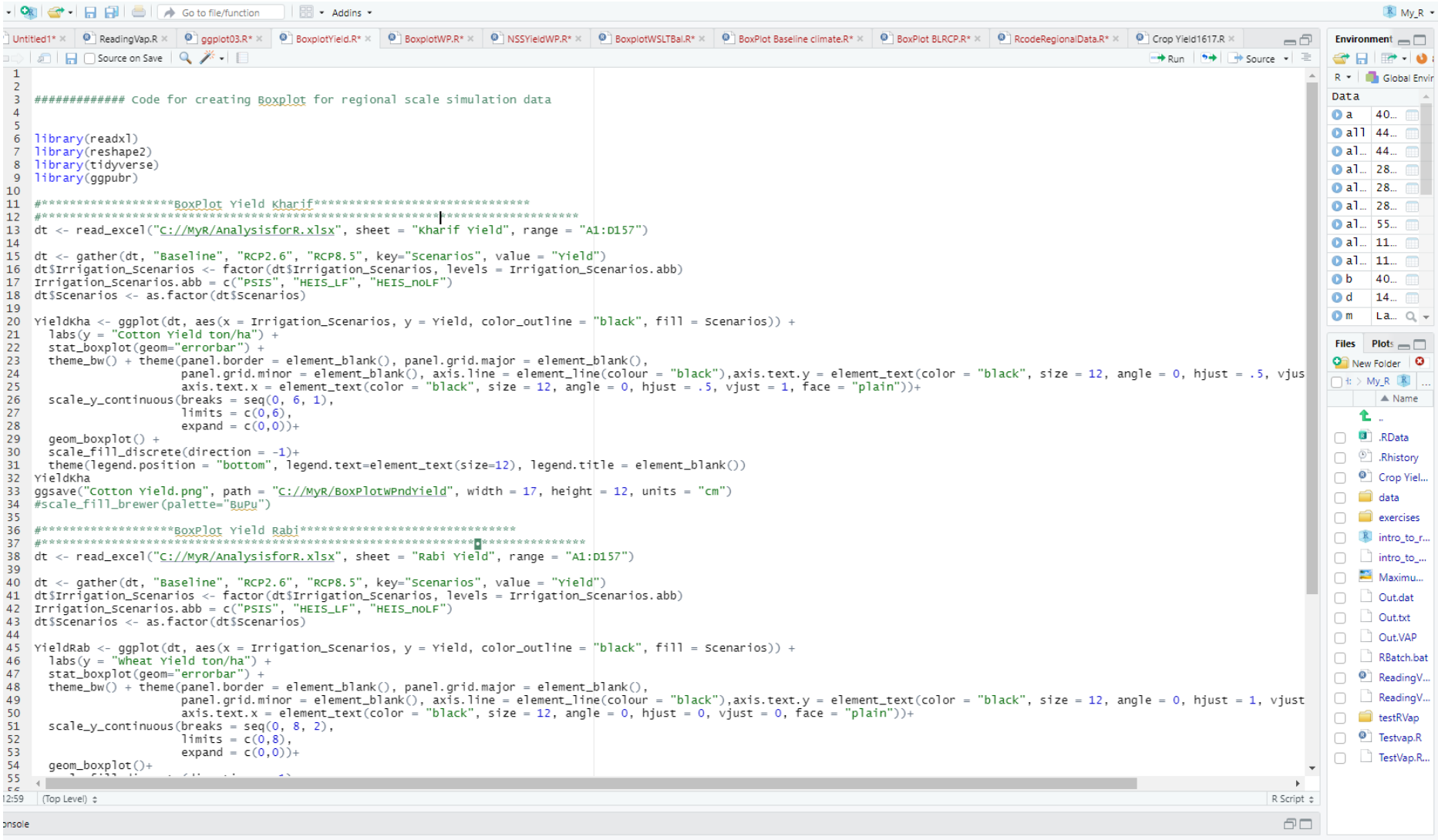

```
############ Code for creating Boxplot for regional scale simulation data


library(readxl)
library(reshape2)
library(tidyverse)
library(ggpubr)

#******************BoxPlot Yield Kharif*******************************
#**********************************************************************
dt <- read_excel("C://MyR/AnalysisforR.xlsx", sheet = "Kharif Yield", range = "A1:D157")

dt <- gather(dt, "Baseline", "RCP2.6", "RCP8.5", key="Scenarios", value = "Yield")
dt$Irrigation_Scenarios <- factor(dt$Irrigation_Scenarios, levels = Irrigation_Scenarios.abb)
Irrigation_Scenarios.abb = c("PSIS", "HEIS_LF", "HEIS_noLF")
dt$Scenarios <- as.factor(dt$Scenarios)

YieldKha <- ggplot(dt, aes(x = Irrigation_Scenarios, y = Yield, color_outline = "black", fill = Scenarios)) +
  labs(y = "Cotton Yield ton/ha") +
  stat_boxplot(geom="errorbar") +
  theme_bw() + theme(panel.border = element_blank(), panel.grid.major = element_blank(),
                     panel.grid.minor = element_blank(), axis.line = element_line(colour = "black"),axis.text.y = element_text(color = "black", size = 12, angle = 0, hjust = .5, vjus
                     axis.text.x = element_text(color = "black", size = 12, angle = 0, hjust = .5, vjust = 1, face = "plain"))+
  scale_y_continuous(breaks = seq(0, 6, 1),
                     limits = c(0,6),
                     expand = c(0,0))+
  geom_boxplot() +
  scale_fill_discrete(direction = -1)+
  theme(legend.position = "bottom", legend.text=element_text(size=12), legend.title = element_blank())
YieldKha
ggsave("Cotton Yield.png", path = "C://MyR/BoxPlotWPndYield", width = 17, height = 12, units = "cm")
#scale_fill_brewer(palette="BuPu")

#******************BoxPlot Yield Rabi*******************************
#**********************************************************************
dt <- read_excel("C://MyR/AnalysisforR.xlsx", sheet = "Rabi Yield", range = "A1:D157")

dt <- gather(dt, "Baseline", "RCP2.6", "RCP8.5", key="Scenarios", value = "Yield")
dt$Irrigation_Scenarios <- factor(dt$Irrigation_Scenarios, levels = Irrigation_Scenarios.abb)
Irrigation_Scenarios.abb = c("PSIS", "HEIS_LF", "HEIS_noLF")
dt$Scenarios <- as.factor(dt$Scenarios)

YieldRab <- ggplot(dt, aes(x = Irrigation_Scenarios, y = Yield, color_outline = "black", fill = Scenarios)) +
  labs(y = "Wheat Yield ton/ha") +
  stat_boxplot(geom="errorbar") +
  theme_bw() + theme(panel.border = element_blank(), panel.grid.major = element_blank(),
                     panel.grid.minor = element_blank(), axis.line = element_line(colour = "black"),axis.text.y = element_text(color = "black", size = 12, angle = 0, hjust = 1, vjust
                     axis.text.x = element_text(color = "black", size = 12, angle = 0, hjust = 0, vjust = 0, face = "plain"))+
  scale_y_continuous(breaks = seq(0, 8, 2),
                     limits = c(0,8),
                     expand = c(0,0))+
  geom_boxplot()+
```

Figure E.4: Part of R code used for plotting the simulation output data in chapter 7

MASSEY UNIVERSITY
TE KUNENGA KI PŪREHUROA
UNIVERSITY OF NEW ZEALAND

GRADUATE RESEARCH SCHOOL

STATEMENT OF CONTRIBUTION DOCTORATE WITH PUBLICATIONS/MANUSCRIPTS

We, the student and the student's main supervisor, certify that all co-authors have consented to their work being included in the thesis and they have accepted the student's contribution as indicated below in the Statement of Originality.

Student name:	Muhammad Hamed Khan
Name and title of main supervisor:	Dr. Ranvir Singh (Associate Professor)
In which chapter is the manuscript/published work?	Chapter 5
What percentage of the manuscript/published work was contributed by the student?	

Describe the contribution that the student has made to the manuscript/published work:

> 90% - conceptual design, methods and materials - fieldwork and modelling analysis, results and discussion; and preparation and revisions of the manuscript.

Please select one of the following three options:

	The manuscript/published work is published or in press Please provide the full reference of the research output:
	The manuscript is currently under review for publication Please provide the name of the journal: Irrigatiob Science
	It is intended that the manuscript will be published, but it has not yet been submitted to a journal

Student's signature:	Muhammad Hamed Khan Digitally signed by Muhammad Hamed Khan Date: 2022.12.21 19:12:05 +13'00'	Main supervisor's signature:	Ranvir Singh Digitally signed by Ranvir Singh DN: cn=Ranvir Singh, c=NZ, o=Massey University, ou=Environmental Sciences, email=R.Singh@massey.ac.nz Date: 2022.12.22 22:39:21 +13'00'

This form should be placed at the beginning of each relevant thesis chapter.